

**CATION DYNAMICS AND STRUCTURAL PHASE  
TRANSITIONS IN  
TRIS [ALKYLAMMONIUM] HALOGENO BISMUTHATES  
A PROTON MAGNETIC RESONANCE STUDY**

**A Thesis submitted  
for the award of the Degree of**

**Doctor of Philosophy**


**By**


**P.K.RAJAN**

**SCHOOL OF PHYSICS  
UNIVERSITY OF HYDERABAD  
HYDERABAD - 500 134, INDIA  
APRIL 1994**

## CERTIFICATE

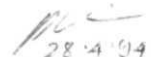
This is to certify that the work reported in this thesis has been carried out by Mr. P.K. Rajan, under my supervision and it is his bonafide work. The work is original and has not been submitted for any other degree of this or any other university.

  
(Prof. V.S.S. Sastry)  
Thesis Supervisor

  
Dean  
School of Physics  
University of Hyderabad.

## DECLARATION

I hereby declare that the work reported in this thesis has been carried out by me independently in the School of Physics, University of Hyderabad, under the supervision of Prof. V.S.S. Sastry. I also declare that this work is original and has not formed the basis for the award of any degree, diploma, fellowship, associateship or similar title of any University or Institution.



28.4.94  
(P.K. Rajan)

Date: 28.4.94  
Place: Hyderabad

# I thank....

Perhaps expressing one's sense of gratitude towards such a large number of people who contributed to the making of this thesis in such a small space is more tricky than writing this thesis itself. Nevertheless I shall make my humble attempt in doing so.

## I thank

Prof. V.S.S. SASTRY who is not only my supervisor but also my teacher and friend. I thank him for all the time and effort he has spared to guide me, the patience he exercised while dealing with me, the joy of learning he instilled in me and also for his inimitable smile and sense of humour. He has been more than a guide and one of the very good human beings I have ever met and I am privileged to have associated myself with him all these years.

Dr. K. Venu for the kind of help he has extended to me and the keen interest he evinced in this work and words seem too powerless to express my sense of gratitude to him for all the kind help he provided. I thank him for making me realize the importance of maintaining a cool head even in the extreme of crises.

The Dean, School of physics for providing me the much needed facilities to carry out this work and I also thank all the erstwhile Deans, faculty of the department who all happened to be my beloved teachers too, and I express my sense of gratitude to all of them who provided me an opportunity to feel the magic of physics within my own limited abilities. I thank them all for providing such a warm atmosphere and made me feel that the School is a home away from home.

Mr. B. Jagadeesh, my friend and colleague, for putting up with my moods which are more unpredictable than the weather! I thank him for all the support extended during this work, both physical and moral.

All my other lab-mates and colleagues who helped me throughout in one way or the other. I thank them for pointing out my limitations at the appropriate time and showed that there is a lot to learn in every walk of life.

A special word of thanks is in order to my dear friends and colleagues Mr. Loganathan and Ms. Kavita Vemuri for putting in a lot of hard work in the preparation of this thesis. Thanks to them for their sense of humour and happy attitude towards life which lifted up many of my otherwise depressing days.

I thank all my dear friends who made my stay in this campus such a wonderful experience and many a times helped me to pull out of my bad moods. I should specially thank my close friends Nirmal Kumar and what he extended to me in way of help is too subtle to express in few words, Arun Kumar who always made me feel confident about myself. I also thank them for the relentless hardwork they have spared in the preparation of the thesis.



This work would not have been realizable but for the selfless and untiring support given by my parents Mr. P.S. Kuppuswamy and Mrs. P.K. Saroja , my brothers Mr. P.K. Vijayasathy, Mr. P.K. Sowmyanarayanan and my beloved sister Ms. P.K. Shoba and all other members of my family.

I thank Dr. K.V. Reddy, P.S.O., of C.I.L., for his kind cooperation and generous support with the C.I.L. facilities and I also thank all the C.I.L. staff for extending their cooperation during this work. My thanks are also to the staff of central workshop and the office staff of School of Physics for the help they extended during this work. I thank the administration of University of Hyderabad for providing me the opportunity to carry out this work. Finally, I thank the Council for Scientific and Industrial Research, INDIA and the University Grants Commission, INDIA, for kindly providing me financial assistance during my Ph.D work.

# CONTENTS

	Preface	i-viii
<b>SECTION A</b>	Nuclear Magnetic Resonance and Relaxation — An Introduction	-
<b>SECTION B</b>	Relaxation Measurements	
	(B-1) Methodology of Experiments	41
	(B-2) Pulsed NMR Spectrometer	61
	(B-3) Instrumentation and Automation	67
<b>SECTION C</b>	NMR Investigations on tris (alkylammonium) nonahalogeno dibismuthates	
	(C-1) Review of $A_3M_2X_9$ compounds	102
	Relaxation and Resonance studies on $[(CH_3)_{4-n}N]_3M_2X_9$ (n = 0 to 4; $M = Bi$ ; $X = Cl, Br$ )	
	(C-2) $[(CH_3)_4N]_3Bi_2Cl_9$ and $[(CH_3)_4N]_3Bi_2Br_9$	125
	(C-3) $[(CH_3)_3NH]_3Bi_2Cl_9$ and $[(CH_3)_2NH_2]_3Bi_2Cl_9$	158
	(C-4) $(CH_3NH_3)_3Bi_2Cl_9$	190
	(C-5) $(NH_4)_3Bi_2Cl_9$ and $(NH_4)_3Bi_2Br_9$	204
	(C-6) Relaxation and Resonance studies on $[(C_2H_5)_4N]_6Bi_8Cl_{30}$	217
	(C-7) Conclusions	231
	contd. ...	

APPENDIX I	Microprograms for the Microprocessor based pulse programmer	241
APPENDIX II	Software for interfacing and automation	242
APPENDIX III	Programs for processing and analysis of data	243

## P R E F A C E

Nuclear Magnetic Resonance has come a long way from the time of **its** inception in becoming a powerful and versatile experimental tool for Physicists, Chemists, and Biologists alike to probe structure at a microscopic level, and more rewardingly, to report on different molecular dynamic processes. The advent of FT-NMR techniques has opened new areas of investigations which were hitherto not quite amenable to experimental techniques. NMR Imaging has become an important application of a basic idea developed in physics in the recent times. Measurements on different spin relaxation rates, which can be carried out even with simpler experimental methodologies (using pulsed NMR instruments, for example) are one of the most powerful methods of investigation, especially of solids, to throw valuable light on the dynamic processes, often important in our understanding of many other physical phenomena, structural phase transitions in solids being one of them. The spin-lattice relaxation time ( $T_1$ ) of a probe nucleus depends not only on the **configuration** of the molecular group in which this probe is situated and the crystal structure of the solid, but also, even more sensitively, on the motional state of these groups. The existence and its relative importance of a given type of motion, like reorientation or vibration, of a given molecular group is in turn dependent on the temperature as well as on the potential barriers such a group experiences in its surroundings due to the inter molecular interactions in the solid. Owing to this delicate coupling of **the** spin probe with its dynamic environment, investigation of relaxation rates as a function of temperature and resonance (**Larmor**) frequency can be profitably used to distinguish and report on the type of the different

inequivalence, correlation times, and activation energies with the help of appropriate molecular dynamic models. On the other hand, linewidth and second moment ( $M_2$ ) measurements provide complementing and confirmatory information on these processes, which crucially helps to check the validity of the microscopic model proposed on the basis of the relaxation information.

The systems investigated in the present study, tris(alkylammonium) halogeno bismuthates, belong to a family of solids with the general formula  $[(CH_3)_n N]^+ M_2X_9$ , where n varies from 0 to 4, M is a metal atom belonging to the Group V elements, but predominantly Sb and Bi, and X is a halogen atom like Cl, Br or I. These complex solids are formed by an

3-

infinite network of the  $M_2X_9$  anions and alkylammonium cations are situated in cavities within these layers, undergoing reorientational motions. These solids exhibit order-disorder type structural phase transitions, and due to the sensitive dependence of the dynamics of the cation on the structural and dynamic properties of the solid, such a phase transition will observably affect the dynamic state of the cations. Therefore to investigate the dynamic properties of these cations it is ideal to use proton as the NMR probe and manifestation of such transitions are then expected to be reflected as subtle and characteristic changes in resonance and relaxation parameters of the spin probe. With these objectives a systematic study of both Antimony and Bismuth substituted solids of above family was undertaken using proton magnetic resonance measurements in this laboratory. The work presented in this thesis concerns the spin-lattice relaxation time ( $T_1$ ) and second moment ( $M_2$ ) measurements on tris(alkylammonium) halogeno bismuthates with proton as the NMR probe, the measurements being made as a function of temperature and Larmor frequency. Since results on the Antimony

substituted compounds were readily available, this thesis presents a comparative picture of both Bi and Sb substituted compounds where ever possible apart from a discussion on Bismuth substituted compounds themselves. The measurements were made on a home-made automated pulsed-NMR spectrometer with the necessary supporting instrumentation having been developed as a part of this research project.

The thesis consists of three sections A, B and C. Section-A is dedicated to the discussion of the necessary theoretical ideas to interpret the results being presented later. A detailed discussion of Bloembergen-Purcell-Pound theory (BPP, in short) is provided. Further, outline of the general method of deriving the appropriate expression for the spin-lattice relaxation rate taking into account the relevant dynamic processes of a given cationic group is presented, the detailed models appropriate to the different cations being presented in later sections along with the results of measurements on each compound.

Section-B concerns the experimental details and is divided into three parts. Sub-section B-1 describes the methodology of pulsed NMR experiments, and of measurements of spin lattice relaxation time ( $T_1$ ), spin-spin relaxation relaxation time ( $T_2$ ) and second moment of resonance absorption line ( $M_2$ ). Sub-section B-2 includes a brief description of the pulsed NMR spectrometer used. The author's contribution towards the upgradation of this instrument forms the content of sub-section B-3, and this includes a description of a microprocessor based pulse programmer which was developed as part of such an upgradation, the hardware and software details of the effort to automate the experiments by interfacing with a personal computer in the GPIB and RS-232-C environments, as well as the instrumentation effort to make the spectrometer compatible to

carry out other interesting measurements (like translational diffusion using spin echoes under pulsed field gradients).

In Section-C the results of investigations on tris(alkylammonium) halogeno bismuthates are presented, and these results are analyzed based on suitable theoretical models. This section begins with a brief survey of the properties of A M<sub>2</sub>X family of compounds (sub-section C-1). The geometrical and bonding considerations which lead to the unique structures of these compounds are discussed in some detail, and is followed by a brief overview of the results of measurements by various physical techniques on tris(alkylammonium) halogeno metallates. The utility and relevance of a NMR study on these systems, in the light of the information presented, is then highlighted.

Sub-section (C-2) contains the results of T and M measurements on the compounds [(CH<sub>3</sub>)<sub>4</sub>N]<sub>3</sub>Bi<sub>2</sub>Cl<sub>9</sub> and [(CH<sub>3</sub>)<sub>4</sub>N]<sub>3</sub>Bi<sub>2</sub>Br<sub>9</sub>. T<sub>1</sub> data show the presence of structural phase transitions at 151K and 183K, respectively, in these compounds as confirmed by other physical measurements. Formation of T minima due to the isotropic reorientation of the tetramethylammonium cation is seen in both these compounds, and also, T minima due to the reorientation of the methyl groups about their C axes are also observed. To analyze the T data the theoretical model of Albert et al., (1972) is discussed in detail. Analysis of data in these compounds show the presence of dynamically inequivalent methyl groups and such a presence is a reflection of the considerable amount of structural disorder present in these compounds. Second moment measurement on these compounds as a function of temperature corroborates the model used to analyze T data but there is no signature of the phase transitions on M<sub>2</sub> data on these compounds. Further, analysis of T data strongly suggests

the possibility of additional structural phase transitions at about 91K in  $[(CH_3)_4N]_3 Bi_2Cl_9$  and 120K in  $[(CH_3)_4N] Bi_2Br_9$ .

Results of T and M measurements on  $[(CH_3)_2NH]_3 Bi_2Cl_9$  and  $[(CH_3)_2NH] BiCl$  and their analysis form sub-section (C-3). These compounds contain cations which are more asymmetric than above, and they have preferred triad and diad axes of rotation. T data on  $[(CH_3)_2NH] Bi_2Cl_9$  show the effect of isotropic reorientation of the dimethylammonium cation in the form of a minimum around 400 K but such a minimum is not seen below 400 K in the case of  $[(CH_3)_3NH]_3 Bi_2Cl_9$ , even though its presence is suggested by the T data.  $[(CH_3)_3NH]_3 Bi_2Cl_9$  shows the possibility of a structural phase transition at 300K whereas  $[(CH_3)_2NH] BiCl$  shows a discontinuity in the T data at 152K, suggesting a structural phase transition. In both these compounds the signature of a structural phase transition at lower temperatures (around 100K) is detected by the NMR measurements (125 K in  $[(CH_3)_3NH]_3 Bi_2Cl_9$  and 78 K in  $[(CH_3)_2NH] BiCl$ ). Theoretical models taking into account the triad and diad axis reorientations as well as the internal motions (methyl group dynamics) of these cations are presented in this section, and the T. data are thus analyzed for trimethylammonium and dimethylammonium group dynamics. The compound  $[(CH_3)_2NH] BiCl$  exhibits an increased degree of structural inequivalence as evidenced by the observed dynamic inequivalence of trimethylammonium cations as well as the methyl groups. On the other hand, analysis of T data in  $[(CH_3)_2NH] Bi_2Cl_9$  shows the presence dynamic inequivalence only among the methyl groups but not in dimethylammonium groups.

Sub-section (C-4) is devoted to the discussion of T. and M. measurements on the compound  $(CH_3)_2NH] BiCl$ . M data at the highest



temperature of measurement ( $\approx 400$  K) in this compound show the presence of isotropic reorientation among all the cations. Four structural phase transitions are reported in this system using other physical techniques (385K, 349K, 247K and 200K) and  $M$  data show the signature of all the four transitions. At 385K  $M$  shows a slight increase which suggests an increase in the interproton distance in this compound. Around 349K, 249K and 200K,  $M$  data show stepwise increase as we go down the temperature from 385K and the values of the different plateaus suggest that there are three dynamically inequivalent methylammonium cations. It appears that the isotropic reorientation of each of one of them gets frozen by NMR line width time scales at 349K, 249K and 200K, respectively and the reorientation of these ions about their 3-fold C-N axis finally becomes dominant. The magnetization recovery in this compound shows marked non-exponential behaviour and is therefore fitted to a two exponential model and the corresponding relaxation times are calculated ( $T_1$  and  $T_{1\text{slow}}$ ).  $T_1$  data show discontinuities at the respective transition temperatures and below 150K the non-exponentiality of the magnetization recovery disappears.  $T_1$  values seem to decrease monotonically with decreasing temperature below 150K, and the activation energy estimated from this portion suggests that the methylammonium cations may be undergoing uncorrelated C reorientations about their C-N axis.

$(\text{NH}_4)_3\text{Bi}_2\text{Cl}_9$  and  $(\text{NH}_4)\text{BiBr}_6$  are two of the ammonium substituted compounds of this family which provide interesting contrast with the other compounds as there are no internal dynamics possible with these cations.  $M$  measurements on  $(\text{NH}_4)_3\text{Bi}_2\text{Cl}_9$  show that the cations are undergoing rather fast reorientations and  $T_1$  data show a maximum like structure. Interestingly, above 250K  $T_1$  values at 8 MHz are smaller than those at 5 MHz. Analysis of the data shows that such a non-BPP type

behaviour may be caused by the cross relaxation of the protons through the quadrupolar levels of Cl nucleus in this compound.  $(\text{NH}_4)_2\text{Bi}_2\text{Br}_8$  shows an entirely different picture where T data show the formation of an usually expected minimum due to the isotropic reorientation of the  $\text{NH}_4^+$  cations, and at 250K a structural phase transition is observed as a slope change in the T data. The activation energy above this temperature is found to be about 7 kJ/mole, whereas below this temperature it is close to 18 kJ/mole, thereby showing the increased amount of hindrance to the cation dynamics. These discussions form sub-section (C-5).

It has been observed that Bismuth has a tendency to cluster with other atoms or halogens to form large clusters leading to compounds with novel anions having reasonable amount of free space for the cations to undergo reorientations. One such system is  $[(\text{C}_2\text{H}_5)_4\text{N}]_3\text{Bi}_8\text{Cl}_{30}$  having the anion  $\text{Bi}_8\text{Cl}_{30}^{3-}$ , and this provides an interesting contrast to all the others discussed above. Sub-section (C-6) describes the results of T and M measurements on this compound and includes a discussion on suitable theoretical model taking into account the dynamics of the tetraethylammonium cation. A phase transition is reported at 241 K and near this temperature both T and M data show its signature. Analysis of T data shows the presence of a wide distribution of correlation times of the methyl group reorientations, and the analysis of T data in the observed range of temperature shows the presence of at least four dynamically inequivalent methyl groups.

Sub-section (C-7) provides a comprehensive survey of the results we have obtained from these investigations on tris(alkylammonium) halogeno bismuthates, and also a comparison with those of the Antimony substituted compounds of this family. The discussion brings out the role of Bismuth

in causing an increased amount of structural inequivalence (structural disorder) in these compounds as reflected by the presence of increased amount of inequivalence among the different groups, in comparison with the Antimony substituted compounds. A comparison of dynamic parameters above and below the phase transitions in the **tetramethylammonium** substituted compounds shows that at their respective transition temperatures the correlation times of these motions reach, rather curiously, a particular value. Conclusions based on the present investigations on these compounds are summarized as the last part of this section.

Appendix - I of the thesis provides the listing of some of the assembly level programmes which are used for generation of different pulse sequences using the microprocessor based pulse programmer. Appendix - II gives programmes specific to the present work which are developed to automate the spectrometer in the **GPIB** and **RS-232-C** environment. Finally, Appendix - III provides the list of programmes which are developed in different programming languages (**BASICA** and **ASYST**) for analysis and display of data and graphics and a sample listing of some of the important programmes.

*SECTION A*

*NUCLEAR MAGNETIC RESONANCE  
AND RELAXATION*

*AN INTRODUCTION*

# SECTION A

## PART 1

### NUCLEAR MAGNETIC RESONANCE AND RELAXATION

#### - AN INTRODUCTION

#### BASIC NMR THEORY

When a nucleus with spin  $I$  is placed in a static magnetic field of strength  $H$ , the interaction Hamiltonian is given by

$$(A-1.1) \quad \mathcal{H}_Z = - \vec{\mu} \cdot \vec{H}_0$$

referred to as the Zeeman Hamiltonian. Here,  $\vec{\mu}$  is the magnetic moment operator for the spin  $I$ , given by

$$(A-1.2) \quad \vec{\mu} = \gamma \hbar \vec{I}$$

Let the direction of the applied magnetic field  $H$  be chosen as the  $Z$ -axis. Then the expression (A-1.1) can be written as

$$(A-1.3) \quad \mathcal{H}_Z = -\gamma \hbar H_0 I_Z$$

The Zeeman interaction creates  $(2I+1)$  distinct levels of energy with values given by  $-\gamma \hbar H m$ , where  $m$  is the magnetic quantum number. The energy difference between any two adjacent levels is given by

$$\Delta E = \gamma \hbar H_0$$

At thermal equilibrium, the number of spins occupying different energy levels is given by the **Maxwell -Bo ltzmann** distribution. If  $N$  is the total number of spins in the system, then the number of spins present in the energy level denoted by  $m$  is

$$N_I = N \exp \left( \frac{-\gamma \hbar H_0 m_I}{kT} \right)$$

In this expression,  $T$  is the lattice temperature and here lattice implies all the translational, rotational and vibrational degrees of freedom of the nuclei. Focusing our attention on a spin 1/2 probe like proton, the spin ensemble is described by two levels of energy and the population in the higher and lower energy states, (which we shall refer to as -1/2 and +1/2 states respectively) are given by  $N^0 = N \exp(\gamma \hbar H / 2kT)$  and  $N^0 = N \exp(-\gamma \hbar H / 2kT)$ . These expressions show that there is an excess of spins in the lower energy state at any given finite temperature  $T$ .

When a sinusoidally oscillating magnetic field at the frequency  $\omega = \gamma H_0$  is applied in the XY plane, this field couples the two levels and causes transition of spins between these levels. Owing to the excess population of nuclei in the lower energy state, there is a net absorption of energy from such an oscillating field. This happens because of the fact that, the rate at which spins get transferred from +1/2 to -1/2 is greater than the rate at which the spins go from -1/2 to 1/2 state.

In order for the spins to achieve their thermal equilibrium the spin

subsystem will have to interact with all other degrees of freedom (called lattice). If such is not the case, for example, an application of even a weak resonant continuous r.f. perturbation would have led to an eventual equalization of populations (saturation). The interactions among the spins modulated in time due to the motional processes provide the connection between the spin and the lattice degrees of freedom and hence serve as relaxation mechanisms, which try to maintain the equilibrium population difference. Two cases here can be identified. In the first case, which forms the basis of CW-NMR experiments, the amplitude of the applied field is maintained at a sufficiently low value as to avoid saturation of the spin system. Here, the rate at which the energy is absorbed from the applied field is equal to the rate at **which** this energy is dissipated by the competing relaxation process and the spin system is said to be maintained in a **near-equilibrium** state. In the second case, which forms the basis for the so-called **pulsed-NMR** experiments, the amplitude of the applied field is deliberately made large so that within a time interval in which the relaxation effects are negligible, the spin system is disturbed away from equilibrium (saturation being one such state) and the perturbing field is subsequently removed to allow the system to relax back to its thermal equilibrium. This time evolution is monitored to measure the relevant relaxation times.

The molecules (or atoms) in which the nuclei are situated act as carriers of these nuclei and these are subjected to all the translational, rotational and vibrational motions experienced by the carrier molecules (carrier atoms), **which are** random functions of time. The presence of all other spins causes a local magnetic field at any

given spin, and owing to the above mentioned motional processes this local field fluctuates in time. The component of this fluctuating field perpendicular to the Z-axis can in principle cause transition between the levels and this serves as the path through which spin-lattice relaxation takes place. The inherent dependence of these thermally activated processes on temperature makes the relaxation times too a function of temperature, and measurement of the relaxation times as a function of temperature thus, in principle, provides an opportunity to investigate the dynamic processes present in the system and their relation to other interesting physical phenomena.

As an alternative to the quantum mechanical description of the spin system, a semi-classical description can be given, by which it is more convenient to visualize the evolution of the spins in the presence of the magnetic fields. Let us consider a single spin with a magnetic moment given by  $\mu$  in the presence of an applied magnetic field H. The time rate of change of  $\mu$  is given by

$$(A-1.6) \quad d\mu/dt = \mu \times (\gamma H)$$

Equation (A-1.6) shows that the vector  $\mu$  is moving in a direction perpendicular to the plane containing  $\mu$  and H. This corresponds to the precession of the vector  $\mu$  about the applied field's direction and if H is constant in time,  $\mu$  subtends a constant angle  $\theta$  about H and it describes a cone about H, known as Larmor precession. If the applied field is along the Z-direction, the Z-component of the magnetic moment is independent of time but X and Y components are time dependent, from eqn.



(A-1.6). This time evolution of  $\mu$  is as seen from the laboratory frame and it will be convenient to transform into a reference frame which rotates with an angular velocity  $\Omega$ . It can be shown that the time rate of change of  $\vec{\mu}$  in such a rotating frame can be written as

$$(A-1.7) \quad \delta\mu/\delta t = (1 \times (yH + f_i))$$

Comparing eqns. (A-1.6) and (A-1.7) it is seen that the time evolution of the magnetic moment in the rotating frame is described by an equation similar to that in the lab frame, provided we visualize the net field felt by  $\mu$  to be equal to  $(H - \hbar/\gamma)$ . If we assume that the field  $H$  is time independent and it is along the  $Z$ -axis, denoted by  $H$ , we can rewrite (A-1.7) as

$$(A-1.8) \quad \delta\vec{\mu}/\delta t = \mu \times \gamma(H + \Omega/\gamma)$$

Now, if we choose the frequency of the rotating frame as  $f_i = -\gamma H$ , then in such a frame the time rate of change of  $\mu$  is zero, and therefore in this frame the magnetic moment is static. The frequency  $-\gamma H$ , which we shall denote by  $\omega$ , is called the Larmor frequency [Slichter, 1978].

Treating  $\mu$  as the quantum mechanical operator for the magnetic moment, the expectation value of  $\mu$  can be expressed as the sum of the expectation values of the three components, namely,

$$(A-1.9) \quad \langle \vec{\mu} \rangle = \hat{i} \langle \mu_x \rangle + \hat{j} \langle \mu_y \rangle + \hat{k} \langle \mu_z \rangle$$

It can be shown that the expectation value of this magnetic moment operator  $\mu$  obeys a rate equation, similar to (A-1.6), namely,

$$(A-1.10) \quad d\langle\mu\rangle/dt = \langle n \rangle \times \gamma H$$

and the X and Y components of the expectation values,  $\langle\mu_x\rangle$  and  $\langle\mu_y\rangle$ , are oscillating functions of time with a frequency  $\omega = \gamma H$  and Z component of  $\mu$ ,  $\langle\mu_z\rangle$ , is independent of time [Slichter, 1978] and these are in accordance with the classical description of the magnetic moment in the presence of the static field H.

Let us suppose that an alternating magnetic field  $H(t) = H \cos \omega t$  is applied along the X-axis. Such an alternating field can be broken into two circularly rotating components denoted by  $H_R$  and  $H_L$ .  $H_L$  rotates about the Z-axis with an angular frequency  $\omega$  and  $H_R$  rotates with an angular frequency  $-\omega$ . When  $\omega$  is made close to  $\omega_0$ ,  $H_L$  will rotate in the same sense as the moment  $\mu$  and  $H_R$  will rotate in the opposite direction. Thus, we can assume that the effect of  $H_R$  in causing any observable change in the time evolution of  $\mu$  is negligible. We shall rewrite  $H_R$  by the expression

$$(A-1.11) \quad \vec{H}_R = \vec{H}_1 = H_1 (\hat{i} \cos \omega t + \hat{j} \sin \omega t)$$

In the presence of H and the rotating field  $H(t)$ , the rate of change of  $\mu$  is given by

$$(A-1.12) \quad d\vec{\mu}/dt = \vec{\mu} \times \gamma (\vec{H}_0 + \vec{H}_1(t))$$

In the rotating frame, in the presence of  $H(t)$ , the time evolution of can be described by the equation

$$(A-1.13) \quad \delta \vec{\mu} / \delta t = \vec{\mu} \times [\hat{k}(\omega + \gamma H_0) + \gamma \hat{i} H_1]$$

It is seen that the time dependence <sup>of</sup>  $H_1$  is removed in this rotating frame, since in the lab frame  $H$  also rotates with the same angular frequency  $\omega$  as that of the rotating frame. When  $\omega = -\gamma H$ , which is also called the resonance condition, the Z-axis magnetic field in the rotating field becomes zero (A-1.13), and the only non-zero field in this frame is  $H$ , which is static. Thus, at resonance, in the rotating frame, the magnetic moment  $\mu$  precesses about this static field  $H$  which is in the XY-plane. The angular frequency of such a precession is given by  $\omega = \gamma H$ . In a time interval  $t$ , the spin will precess by an angle  $\theta = \gamma H t$ . Now, if we choose  $t_w$  in such a way that  $\theta_w$  is equal to  $n/2$  radians and if  $\vec{u}$  was along the Z-direction at time  $t = 0$ , then at  $t=t$ , the magnetic moment would have been tilted by  $90^\circ$  and it will be in the XY plane. The restricted application of the rotating field  $H$  for a short interval of time  $t$  is called a pulse and the pulse corresponding to  $\theta = n/2$  is called the "90 degree pulse" or the "n/2 pulse". Similarly a "n pulse" can be applied such that at the end of  $t$  the magnetic moment is along the -Z direction, if it was kept initially along the +Z direction. The magnetic moment after a n/2 pulse precesses about the static field  $H$  in the laboratory frame, and if an inductance coil is kept in the XY-plane such a precession causes a time dependent change in the magnetic flux of the coil which induces an e.m.f. and this is the standard method of

detecting NMR signals in pulsed NMR experiments. In the quantum mechanical description the expectation value, in the rotating frame, of the Z-axis magnetic moment  $\mu$  can be shown to be [Slichter, 1978]

$$(A-1.14) \quad \langle \mu_z(t) \rangle = \langle \mu_z(0) \rangle \cos \gamma H_1 t$$

where  $\langle \mu_z(0) \rangle$  is the expectation value of the Z-axis magnetic moment time  $t = 0$  and we assume here that the magnetic moment is aligned along the Z-axis at time  $t = 0$ .

The description given so far was confined to an isolated nucleus with a magnetic moment  $\mu$ . When we have an ensemble of spins we can define a net magnetization  $M$  for this ensemble, given for non-interacting spins by

$$(A-1.15) \quad \vec{M} = \sum_i \vec{\mu}_i$$

The azimuthal angle  $\phi_i$  of all the individual spins will be randomly distributed and thus the summation of the component of magnetic moments in the XY plane will be zero, and thus the macroscopic magnetization **will** have only a non-zero component along the Z-axis denoted by  $M$ , though the individual magnetic moments  $\mu_i$  can have non-vanishing components in the XY plane. The assumption of such a random distribution of  $\phi_i$  is called the random phase approximation. Thus, in the presence of a static magnetic field  $H$  in an ensemble of spins, there will be a net magnetization  $M$  which is static and lies along the direction of this field.

Bloch's phenomenological equations depict the time evolution of the macroscopic magnetization in the presence of the applied fields and the relaxation processes, and introduces the relaxation times  $T_1$  and  $T_2$ . These equations are given by,

$$(A-1.16a) \quad \frac{dM_z}{dt} = \gamma (\vec{M} \times \vec{H})_z - \frac{M_z - M_0}{T_1}$$

$$(A-1.16b) \quad \frac{dM_x}{dt} = \gamma (\vec{M} \times \vec{H})_x - \frac{M_x}{T_2}$$

$$(A-1.16c) \quad \frac{dM_y}{dt} = \gamma (\vec{M} \times \vec{H})_y - \frac{M_y}{T_2}$$

In the above expressions,  $T_1$  is the spin-lattice relaxation time which is the characteristic time associated with the dissipation of excess energy of the spin system to the lattice. After a  $\pi/2$  pulse is applied, the magnetization  $M$  is tipped onto the XY plane. But, this corresponds to a non-equilibrium condition among the spins, since at equilibrium we expect no net magnetization in XY plane, in the absence of a field component in this plane. Thus, the spin system loses this excess coherence built in the XY plane eventually, and the characteristic time constant associated with the decay of this coherence is the spin-spin relaxation time  $T_2$ . Now, in order to use these macroscopic relaxation processes to investigate the microscopic dynamics, a suitable theoretical framework is needed providing a connection of  $T_1$  and  $T_2$  to dynamic variables.

The Bloembergen-Purcell-Pound theory (BPP theory) is one of the

important microscopic theories which provides such a connection and the present investigations are based on it. It may be mentioned in passing that other comprehensive microscopic theories of relaxation are also available in literature, for example, Kubo and Tomita's linear response theory, Bloch-Wangsness-Redfield theory and Hebel-Slichter's theory of nuclear relaxation. In what follows, we shall discuss in detail, the BPP theory and its application to relaxation in solids.

### **Bloembergen-Purcell-Pound theory :**

In the following discussion let us consider only the simple case of spin-1/2 particles unless otherwise specified and take note of the assumptions thereof.

1. The total Hamiltonian of the physical system is of the general type

where  $\mathcal{H}$  is contribution to the total Hamiltonian from the system alone expressed in terms of the spin degrees of freedom,  $\mathcal{H}$  is the lattice part of the total Hamiltonian, and  $\mathcal{H}$  expresses the coupling between the spin system and the lattice.

2. The lattice reservoir is assumed to be of infinite thermal capacity because of which even when the spin system exchanges energy with the lattice, the lattice remains at a constant temperature  $T$ .
3. In the high-temperature approximation, the energy difference between the spin levels is assumed to be much smaller than  $kT$ .

4. In comparison to  $\mathcal{H}$   $\mathcal{H}$  is quite small and a second order perturbation calculation can be used to calculate the lattice induced transitions between the different levels of  $\mathcal{H}$ .
5.  $\mathcal{H}$  is assumed to be a random operator with vanishing ensemble average and the correlation function  $\langle \mathcal{H}(t') \mathcal{H}(t'+\tau) \rangle$  is assumed to be stationary. This function is characterized by a correlation time  $T$ .
6. Since a perturbation theory is to be applied, the observation time  $t$  has to be much larger than the correlation time  $T$  of the lattice fluctuations.
7. On the time scale of the NMR probe these random processes are assumed to be Markovian (with no memory effects), leading to time independent relaxation rates.

Let us consider  $N$  spins in a rigid lattice subjected to a strong Zeeman field  $H$  applied in  $z$ -direction and an oscillating field  $H \cos \omega t$  applied in the  $xy$ -plane. The total Hamiltonian of this system can be written as,

$$(A-1.17) \quad \mathcal{H}_{\text{tot}} = \mathcal{H}_Z + \sum_{r, \mathbf{I}} \mathcal{H}_r(t) + \mathcal{H}_L * \mathcal{H}_{SL}$$

Here  $\mathcal{H}_{\text{rf}}$  is given by  $-M \cdot H_1 \cos \omega_0 t$ . Let us define  $\langle r$  as the density matrix over the spin variables for the ensemble of the  $N$  spins. Denoting the

spin states by  $|+\rangle$  and  $|-\rangle$ , the probability of occupation of the  $|+\rangle$  or  $|-\rangle$  energy level is given by  $\sigma_+$  or  $\sigma_-$  where,

$$(A-1.18) \quad \sigma_{\pm} = \frac{\langle i | \sigma_{\pm} | i \rangle}{1} = \frac{\exp(-\beta E_{\pm})}{\sum_k \exp(-\beta E_k)}$$

where  $\beta=1/kT$  and  $i$  is  $+$  or  $-$ . Thus the populations in  $|+\rangle$  and  $|-\rangle$  levels are given by

$$(A-1.19) \quad N_+ = N \sigma_+ ; \quad N_- = N \sigma_-$$

The applied r.f. field causes transition between the two energy levels and let  $W_+$  and  $W_-$  denote the transition probability per unit time induced by the applied field for a transition from  $|+\rangle$  to  $|-\rangle$  and  $|-\rangle$  to  $|+\rangle$ , respectively. There exists a competing relaxation process mediated by the interaction among the spins which tries to restore the change in the population difference caused by the applied r.f. field, and the transition probability per unit time associated with this process be denoted by  $P_+$  and  $P_-$ . Now the rate of change of population in each level is given by the equations

$$(A-1.20) \quad \frac{dN_+}{dt} = -N_+ (W_+ + P_+) + N_- (W_- + P_-)$$

$$(A-1.21) \quad \frac{dN_-}{dt} = -N_- (W_- + P_-) + N_+ (W_+ + P_+)$$

The transition probability per unit time due to the applied field is given by the formula



$$(A-1.22) \quad W_{+-} = \frac{2\pi}{\hbar} \left| \langle \pm 1/2 | \mathcal{H}_{r.f.} | \mp 1/2 \rangle \right|^2 \rho_\nu$$

It is clear that the probability for the downward and upward transition is the same and thus we shall denote this probability as  $W$ , dropping the indices. Thus equations (A-1.20) and (A-1.21) can now be written as

$$(A-1.23) \quad dN_+/dt = - (N_+ - N_-)W - N_+P_{+-} + N_-P_{-+}$$

$$(A-1.24) \quad dN_-/dt = + (N_+ - N_-)W - N_-P_{-+} + N_+P_{+-}$$

from which it can be derived that

$$(A-1.25) \quad dn/dt = -2Wn - \frac{n-n_0}{T_1}$$

with the definitions

$$n \equiv (N_+ - N_-) \quad ; \quad n_0 \equiv N \frac{P_{-+} - P_{+-}}{P_{-+} + P_{+-}}$$

$$\text{and} \quad 1/T_1 \equiv P_{+-} + P_{-+}$$

Equation A-1.25 shows that for a system with a very weak spin lattice coupling, or for a case where  $W \gg 1/T$ , the population difference will eventually go to zero and this condition is the saturation condition. It can also be seen that after the perturbing field is removed the population difference reaches its equilibrium value  $n_0$  given by the

relaxation equation

$$(A-1.26) \quad n = n_0 [1 - \exp(-t/T)]$$

which also gives the time evolution of the net magnetization  $M$  as it is proportional to the population difference  $n$ . Analogous relation can also be derived from the **Bloch's** equations and the simple picture given so far is able to connect to the macroscopic **Bloch's** equations.

The spin-lattice relaxation time  $T$ , introduced as the inverse of the transition rates induced by the molecular motions, now has to be connected to the microscopic dynamics in the system. We shall do it by considering an explicit form of  $\mathcal{H}$  which will be treated as a perturbation on the Zeeman Hamiltonian  $\mathcal{H}$ . In fact, spin-spin relaxation time,  $T$ , which we have seen to be the time constant for the magnetization decay in the  $xy$ -plane, is derived naturally to be the inverse of the linewidth of the Zeeman levels, from the above calculation.

Let us consider the dipole-dipole interaction summed over all the spins, given by

$$(A-1.27) \quad \mathcal{H}_{SL} = (1/2) \sum_i \sum_j \gamma_i \hbar \vec{I}_i \cdot \left( \frac{\gamma_j \hbar \vec{I}_j}{r_{ij}^3} - \frac{3 \gamma_j \hbar \vec{r}_{ij} (\vec{r}_{ij} \cdot \vec{I}_j)}{r_{ij}^5} \right)$$

where  $\vec{r}_{ij}$  is the internuclear vector of any two spins  $i$  and  $j$ , and  $\gamma$  refers to the gyromagnetic ratio of the respective spins. Let

(A-1.28)

$$\mathcal{H}_{SL} = \sum_{j>i} V_{ij}$$

where  $V_{ij}$  is given by

(A-1.29)

$$V_{ij} = \gamma^2 \hbar^2 r_{ij}^{-3} (A+B+C+D+E+F)$$

and

$$\begin{aligned} A &= I_{zi} I_{zj} (1-3\cos^2\theta_{ij}) \\ B &= -1/4 [(I_{xi}-iI_{yi})(I_{xj}+iI_{yj}) + (I_{xi}+iI_{yi})(I_{xj}-iI_{yj})] (1-3\cos^2\theta_{ij}) \\ C &= -3/2 [(I_{xi}+iI_{yi})I_{zj} + (I_{xj}+iI_{yj})I_{zi}] \\ &\quad \sin\theta_{ij} \cos\theta_{ij} \exp(-i\phi_{ij}) \exp(i\gamma H_o t) \\ D &= -3/2 [(I_{xi}-iI_{yi})I_{zj} + (I_{xj}-iI_{yj})I_{zi}] \\ &\quad \sin\theta_{ij} \cos\theta_{ij} \exp(i\phi_{ij}) \exp(-i\gamma H_o t) \\ E &= -3/4 (I_{xi}+iI_{yi})(I_{xj}+I_{yj}) \sin^2\theta_{ij} \exp(-2i\phi_{ij}) \exp(2i\gamma H_o t) \\ F &= -3/4 (I_{xi}-iI_{yi})(I_{xj}-I_{yj}) \sin^2\theta_{ij} \exp(2i\phi_{ij}) \exp(-2i\gamma H_o t) \end{aligned}$$

In a rigid lattice, each spin experiences a static field which is different from the applied field  $H$  due to the presence of the neighbouring spins. Since the distribution of spins in the  $+1/2$  and  $-1/2$  states in the neighbourhood of any given spin varies from site to site, this "local field" also varies from spin to spin. The average of the local field distribution can therefore be expressed as [Bloembergen et al., 1948]

$$(A-1.30) \quad \langle H_{loc}^2 \rangle_{AV} = (1/3) \gamma^2 \hbar^2 I(I+1) \sum_j (1-3\cos^2\theta_{ij})^2 \times r_{ij}^{-6}$$

and the mean square deviation in frequency units of the energy level is given by

$$(A-1.31) \quad \langle \Delta\omega^2 \rangle_{AV} = \gamma^2 \langle H_{loc}^2 \rangle_{AV}$$

Eqn.(A-1.31) gives an expression for the broadening of the resonance line caused by the local field distribution. Term B, which contains the  $I$  and  $I_-$  operators in pairs, will cause a simultaneous flip of the two spins  $i$  and  $j$  in the opposite directions. This term thus imposes a finite lifetime on a given spin whether it is in the  $|+\rangle$  or  $|-\rangle$  state, and thus this also contributes to the broadening of the energy levels. Now the contribution of this term to the linewidth can be included in the expression for  $\langle \Delta\omega \rangle$  in the form of a numerical factor and taking this also into account the total broadening caused by term A and term B are given by

$$(A-1.32) \quad [\langle \Delta\omega^2 \rangle_{AV}]^{1/2} = (1/T_2) = (3/2) \gamma^2 \hbar [I(I+1)/3]^{1/2} \times \left( \sum_{i \neq j} (1-3\cos^2\theta_{ij})^2 \times r_{ij}^{-6} \right)^{1/2}$$

The spin-spin relaxation time is the shortest in a rigid lattice since the coupling between the spins is strong in the absence of motions and this aids in dissipating the coherence in XY plane more efficiently. It can be shown that lattice motions lead to a time averaging of terms A

and B thereby reducing the linewidth of the resonance line, known as "motional narrowing". In principle, the spin-lattice relaxation process which couples the two levels of energy also contributes to the broadening of the lines [Bloembergen et al., 1948].

#### Spin-Lattice relaxation process:

From eqns. (A-1.28) and (A-1.29), it is seen that terms C and D are capable of coupling the spin levels differing in  $m$  by  $\pm 1$  and terms E and F couple spin levels differing in their  $m$  by  $\pm 2$ . When motions are present, these terms are modulated in time and they lead to the spin-lattice relaxation. At a finite temperature, motions are present in a system because a finite amount of energy is available to all the lattice degrees of freedom. Normally such thermally activated dynamic processes are random functions of time. These dynamic processes modulate the spatial co-ordinates  $(r., \theta., \phi.)$  of any given spin randomly in time. Thus, the space part of the terms in the Hamiltonian given in eqn.(A-1.24) are random functions of time. Defining the space dependent terms in the Hamiltonian for some arbitrary test nucleus (i) due to its interactions with a specific j, as

$$(A-1.33(a)) \quad F_{0j} = (1-3\cos^2\theta_{ij})r_{ij}^{-3}$$

$$(A-1.33(b)) \quad F_{1j} = \sin\theta_{ij}\cos\theta_{ij} \exp(i\phi_{ij})r_{ij}^{-3}$$

$$(A-1.33(c)) \quad F_{2j} = \sin^2\theta_{ij} \exp(2i\phi_{ij})r_{ij}^{-3}$$

it may be noted that in the presence of isotropic stochastic motions these terms are averaged to zero. The processes are then characterized by the two-time correlation functions. These correlations are quantified by a correlation time  $T$ , which is an average time interval over which the magnitude of the function has not changed appreciably. We can define the autocorrelation function of  $F(t)$  as

$$(A-1.34) \quad \langle F(t) F^*(t+\tau) \rangle_{AV} = K(t, \tau)$$

where the average is over the entire ensemble of spins. Assuming that these randomly modulated processes in time are stationary and Markovian the autocorrelation function becomes

$$(A-1.35) \quad K(\tau) = \langle F(t) F^*(t) \rangle_{AV} \exp(-|\tau|/\tau_c)$$

The spectral density function for  $K(\tau)$  is given by

$$(A-1.36) \quad J(\nu) = \int_{-\infty}^{\infty} K(\tau) \exp(i\nu\tau) d\tau$$

and since  $K(\tau)$  is real and even,  $J(\nu)$  is also real and even. Let us define the spectral density functions  $J_0(\nu)$ ,  $J_1(\nu)$  and  $J_2(\nu)$  by

$$(A-1.37.a) \quad \langle \Sigma |F_{0j}|^2 \rangle_{AV} = \int_{-\infty}^{\infty} J_0(\nu) d\nu$$

$$(A-1.37.b) \quad \langle \Sigma |F_{1j}|^2 \rangle_{AV} = \int_{-\infty}^{\infty} J_1(\nu) d\nu$$

$$(A-1.37.c) \quad \langle \Sigma |F_{2j}|^2 \rangle_{AV} = \int_{-\infty}^{\infty} J_2(\nu) d\nu$$

The transition probability per unit time caused by these lattice **fluctuations**, in the case of spin 1/2 particles, can be computed as

$$(A-1.38) \quad P = (9/16)\gamma^4 \hbar^2 [J_1(\nu) + J_2(2\nu)]$$

Though the probability for upward and downward transitions are the same, the overall transition probability for  $!+>$  to  $!->$  transition and  $!->$  to  $:+>$  transition has to be weighted by the respective **Boltzmann** factors as required by the principle of detailed balance, from which

$$(A-1.39) \quad N_+ P_{+-} = N_- P_{-+},$$

where

$$(A-1.40) \quad P_{+-} = P \exp(-\gamma \hbar H_0 / 2kT) ; P_{-+} = P \exp(+\gamma \hbar H_0 / 2kT)$$

Though this condition is strictly valid only under thermal equilibrium, as long as  $kT \gg \gamma \hbar H$ , this condition can be assumed to be valid even if the spin system is not in thermal equilibrium with the lattice. Therefore, in the high temperature approximation, equation (A-1.40) can be written as

$$(A-1.41) \quad P_{+-} \cong P [1 - (\gamma \hbar H_0 / 2kT)] ; P_{-+} \cong P [1 + (\gamma \hbar H_0 / 2kT)]$$

Recalling equations (A-1.23) through (A-1.25), in the absence of the perturbing r.f. field we can write,

$$(A-1.42) \quad \frac{dn}{dt} = 2N_-P_{-+} - 2N_+P_{+-}$$

$$(A-1.43) \quad \frac{dn}{dt} = (N+n)P_{+-} - (N-n)P_{-+}$$

Defining the equilibrium population difference  $n = N\gamma\hbar H / kT$  under the high temperature approximation and substituting the appropriate expression for  $P_{-}$  and  $P_{+}$  from equation (A-1.41), we can express the rate at which the population difference between the two energy levels changes in time as

$$(A-1.44) \quad \frac{dn}{dt} = 2P_0(n_0 - n)$$

from which we see that the spin population difference attains its equilibrium value by following a simple exponential law with a characteristic time constant given by

$$(A-1.45) \quad T_1 = 1/2P_0$$

Thus the general formula for the spin-lattice relaxation time in the case of spin-1/2 particles can be written as

$$(A-1.46) \quad (1/T_1) = (9/8)\gamma^4\hbar^2 [J_1(\nu) + J_2(2\nu)]$$

From (A-1.35) the spectral density function can be expressed in a general form as



$$(A-1.47) \quad J(\nu) = \langle F(t)F^*(t) \rangle_{AV} [\tau_c / (1 + \omega^2 \tau_c^2)]$$

with  $\omega = 2\pi\nu$ . Thus, the spin-lattice relaxation time can be expressed in terms of the spectral density functions as

$$(A-1.48) \quad 1/T_1 = (9/8) \cdot 4\hbar^2 \left[ \langle F_1(t)F_1^*(t) \rangle_{AV} \frac{\tau_c}{1 + \omega^2 \tau_c^2} + \langle F_2(t)F_2^*(t) \rangle_{AV} \frac{4\tau_c}{1 + 4\omega^2 \tau_c^2} \right]$$

#### Effect of motions on the linewidth:

The equation for the spin-spin relaxation time  $T_2$ , expressed in (A-1.32) is for the rigid lattice and we should reconsider this equation in **the** presence of the molecular motions. Clearly, the space dependent term in equation (A-1.32) must be replaced by its ensemble average and from the definition of  $J(\nu)$  given in equation (A-1.37a), **this** ensemble average can be written as

$$(A-1.49) \quad \langle \sum_{ij} [(1-3\cos^2\theta_{ij}(t))r_{ij}^{-3}(t)]^2 \rangle_{AV} = \int J_o(\nu) d\nu$$

Taking into account the effect of motion, equation (A-1.32) can be modified to express the spin-spin relaxation time as [Bloembergen **et al.**, 1948]

$$(A-1.50) \quad 1/T_2 = 3/2 \gamma^2 \hbar [I(I+1)/3]^{1/2} \left[ \int J_0(\nu) d\nu \right]^{1/2}$$

The time modulation of the terms C to F limits the lifetime of the spins in any given energy state and this also contributes to the broadening of the line. In principle, the broadening of the line due to this effect also should be included in determining the overall broadening of the line but in solids where the spin-lattice relaxation time  $T_1$  is much larger than the spin-spin relaxation time  $T_2$  this effect is negligible. Using equation (A-1.35) we can rewrite equation (A-1.50) as

$$(A-1.51) \quad 1/T_2 = 3/2 \gamma^2 \hbar [I(I+1)]^{1/2} \left[ |F_0|^2 \int \frac{\tau_c d\nu}{1 + 4\pi\nu^2 \tau_c^2} \right]^{1/2}$$

The limits of the above integral have to be restricted to  $(-1/\pi T_1, 1/\pi T_1)$  as terms A and B will represent secular perturbations only when the contribution from  $J(\nu)$  is confined to the components which are within the actual width caused by the perturbation. It can be seen that equation (A-1.51) can be recast into

$$(A-1.52) \quad (1/T_2)^2 = C_1 \tan^{-1} (2\tau_c/T_2)$$

by evaluating the integral within the above said limits. The constant  $C_1$  contains the **prefactors** shown in equation (A-1.51) apart from the value

2

of  $|F_0|$  for the specific case. The general dependence of the spin-spin relaxation time on the correlation time  $T_2$  can be seen from (A-1.52), which shows that for very small  $T_2$ ,  $1/T_2$  is proportional to  $\tau_c$  and with

increasing  $T$ ,  $T$  decreases. In fact when  $x/T \approx 1$ ,  $T$  reaches its asymptotic value of  $T'$  where  $T'$  is the spin-spin relaxation time corresponding to the rigid-lattice line width, and  $T$  remains at that value with further increase in  $\tau$ . Therefore it is seen that the presence of thermally activated motions decreases the linewidth as the line broadening terms get time averaged to a smaller value, and this is referred to as motional narrowing.

#### Homogeneous and Inhomogeneous broadening:

An important distinction needs to be made in the way the A term and B term contribute to the line broadening. In one case the broadening of the spectral line arises due to the spatial distribution of the spins aligned either parallel or antiparallel to the Zeeman field since this makes the local field felt by any nucleus to be different from site to site and this broadening effect is referred to as inhomogeneous broadening. Term A corresponds to this kind of broadening effect. It is also to be noted that the inherent inhomogeneity present in the Zeeman field also contributes to the inhomogeneous broadening. On the other hand, the finite transition probability provided by the term B for the mutual flipping of a spin pair contributes to the line broadening by making the life time of any given spin pair in their respective energy levels finite. This effect is felt to be the same in intensity on an average by any given spin pair and does not depend on the spatial distribution of any quantity, leading to homogeneous broadening. This difference between term A and B is also brought out by the fact that, even if the spins are not identical, the local field distribution will remain as it was for the

case of identical spins, but term B will not be able to cause the mutual spin-flip between any two non-identical nuclei as this transition does not conserve the total energy of the spin system. Thus its contribution to the broadening by way of limiting the lifetime of the spins in their respective energy states will not be present. An imaginative experiment reported by BPP brings out this difference clearly and this is referred to as the "hole burning" experiment. In recording the absorption spectrum in the frequency domain, the **Zeeman** field is scanned slowly between two limiting values with a fixed frequency r.f. field and for each quasi-static value of the Zeeman field the absorption is detected as a change in the susceptibility of the sample coil. Instead, if the Zeeman field is fixed at some value within the absorption curve and the r.f. power at a particular frequency within this time is made sufficiently large and after some time if the absorption curve is traced in the regular manner, a "hole" is created in the absorption curve, corresponding to the value of the field value where it was held constant for some time if the line is inhomogeneously broadened. This is because in the case of an inhomogeneously broadened absorption line, only a pocket of spins among all experience a total Zeeman field equal to the value at which the field was locked and only these spins are saturated with prolonged exposure to the r.f. radiation. When the scan of the field is resumed the spin pocket corresponding to this **Zeeman** field does not have any excess spin in the lower energy state and thus shows zero absorption intensity for this value of  $H$ . If the line was homogeneously broadened

o

on the other hand, the increased intensity of r.f. field would have saturated all the spins in the system, as, **on an average all the spins in** the system experience a Zeeman field of a given value and as consequence

one would observe the entire absorption line to saturate. Thus burning a hole in the spectral line is a clear confirmation of the **inhomogeneous** broadening present in the system.

To summarize, BPP theory provides the necessary expressions for the spin-lattice and spin-spin relaxation time constants expressed in terms of the microscopic variables by treating the dipolar interaction **Hamiltonian** as a perturbation on the **Zeeman Hamiltonian**. Part of this **Hamiltonian** accounts for the broadening of the energy levels and the **time** dependence of this Hamiltonian brought about by molecular motions leads to spin-lattice relaxation in the system. Since molecular motions are thermally activated, they are stochastic processes in time and they are characterized by a correlation time  $T_c$ , and it is shown that  $T_1$  and  $T_2$  depend on  $T_c$ . The correlation function, being a measure of the randomness of the dynamics concerned, is dependent on temperature and a systematic observation of spin-lattice and spin-spin relaxation times as a function of temperature provides us with the necessary qualitative and quantitative information on all the relevant dynamic processes.

BPP theory is valid within the purview of the assumptions made in the beginning and its treatment is **semiclassical** to the extent **that the** spin **part of** the dipolar Hamiltonian is treated as quantum mechanical whereas the space part is treated as due to strictly classical random variables. This is enabled by **the** fact that the dipolar Hamiltonian is expressible as

$$(A-1.53) \quad \mathcal{H}_{SL} = (1/2) \sum_j \sum_k \sum_{q=-2}^2 A_{jk}^{(q)} F_{jk}^{(q)}$$

where  $A$  -s are the spin functions expressed exclusively in terms of the spin operators, whereas  $F$  , -s, the lattice functions, are expressed in terms of the lattice variables  $r, \theta$  and  $\phi$ , which are the ones to pick up the random correlation brought about by the thermal motions. For instance, in Bloch-Wangsness-Redfield theory, this problem is treated differently in that the entire spin system is represented in terms of its density matrix which is subject to both the necessary ensemble and quantum mechanical averaging. But all these microscopic theories address to the general problem of arriving at a rate equation similar to the macroscopic equations of Bloch, from which the respective relaxation rates are naturally derived.

#### Method of Moments by Van Vleck:

In pulsed experiments, we saw that if a perturbing r.f. field whose frequency is equal to  $\gamma H$  is applied suddenly then the magnetization  $M$  precesses about this field  $H$  and it subtends an angle  $90^\circ$  with respect to this perturbing field. In contrast, if we apply a very weak, oscillating field with a variable frequency  $\omega$  scanned slowly through the spectral region it can be shown that under adiabatic fast passage conditions the magnetization  $M$  is always aligned along an effective field

$$H_{\text{eff}} = \sqrt{H^2 + \left(\frac{\omega}{\gamma}\right)^2}$$

(which is equal to  $\{H^2 + [(\omega/\gamma) - H]^2\}^{1/2}$ ) and this is the basis of the CW experiments [Abragam, 1970; Slichter, 1978]. Here the magnetization induced by the applied field  $H$  along X-axis is given by

$$(A-1.54) \quad M_x = H_1 [\chi'(\omega) \cos \omega t + \chi''(\omega) \sin \omega t]$$

where  $\chi'$  and  $\chi''$  define the susceptibility of the inductance coil containing the sample. The complex part of the susceptibility  $\chi''$  is proportional to the rate of absorption of r.f. energy by the spin system and the real part  $\chi'$  gives the dispersion due to the sample, and these are related through Kramers-Krönig equations [Abragam, 1970]. By defining a quantum mechanical operator  $M$  corresponding to the X-axis magnetization, a density operator  $\rho$  for the ensemble of spins in the sample, and a correlation function  $G(t)$ , one can derive an expression for the complex part of the susceptibility  $\chi''$  as [Abragam, 1970, chap.IV]

$$(A-1.55) \quad \chi''(\omega) = \frac{\omega V}{kT} \frac{1}{(2I+1)} \int_0^{\infty} \cos \omega t' G(t') dt'$$

Here,  $G(t) = \frac{\text{trace}(M(t)M)}{X}$  and  $M(t) = e^{i\mathcal{H}t} M e^{-i\mathcal{H}t}$ .  $\mathcal{H}$  corresponds to the equilibrium Hamiltonian, prior to the application of the perturbing field in the XY plane. Expanding  $G(t)$ ,  $\chi''$  can be expressed as

$$(A-1.56) \quad \chi'' = \frac{2\pi}{(2I+1)} \frac{\omega V}{4kT} \sum'_{n,n'} |\langle n | M_X | n' \rangle|^2$$

where the summation is taken only over states which differ in energy  $|E_n - E_{n'}| = \hbar\omega$ . It is desirable to know  $M_X(t)$  so that the complex susceptibility can then be calculated. From the definition of  $\chi''(\omega)$ , it is clear that the complex susceptibility is proportional to the shape function or absorption curve  $f(\omega)$ . With the presence of dipolar interaction  $M(t)$  obeys the rate equation (Heisenberg picture)

$$(A-1.57) \quad (1/i) dM_X/dt = [\mathcal{H}_Z, M_X(t)]$$

and in the interaction picture,

$$(A-1.58) \quad (1/i) \, d\tilde{M}_x/dt = [e^{-i\mathcal{H}_0 t} \mathcal{H}_1 e^{i\mathcal{H}_0 t}, \tilde{M}_x]$$

where  $M$  is given by  $(e^{-i\mathcal{H}_0 t} M e^{i\mathcal{H}_0 t})$ . Choosing a set of basis states of  $\mathcal{H}$ , labelled as  $|E_o s\rangle$ , where  $s$  is the quantum number to distinguish between the various states of the same energy  $E_o$ , we can write equation (A-1.58) in the matrix form as

$$(A-1.59)$$

$$(1/i) \frac{d}{dt} \langle E_o s | \tilde{M}_x | E_o' s' \rangle = \sum_{E_o'' s''} [e^{-i(E_o - E_o'')t} \langle E_o s | \mathcal{H}_1 | E_o'' s'' \rangle \langle E_o'' s'' | \tilde{M}_x | E_o' s' \rangle] \\ - [e^{-i(E_o'' - E_o')t} \langle E_o s | \tilde{M}_x | E_o'' s'' \rangle \langle E_o'' s'' | \mathcal{H}_1 | E_o' s' \rangle]$$

From (A-1.58), we see that in the absence of the perturbation  $\mathcal{H}$ ,  $dM/dt$  is zero and thus with the inclusion of a small perturbation like  $\mathcal{H}$ , the variation of  $M_x$  must be slow, so, it is reasonable to assume that in equation (A-1.59), terms for which  $E_o' \neq E_o''$  or  $E_o \neq E_o''$  contribute a negligible amount to the above summation for small  $\mathcal{H}$ . Thus (A-1.59) can be rewritten as,

$$(A-1.60)$$

$$(1/i) \frac{d}{dt} \langle E_o s | \tilde{M}_x | E_o' s' \rangle = \sum_{s''} [\langle E_o s | \mathcal{H}_1 | E_o s'' \rangle \langle E_o s'' | \tilde{M}_x | E_o' s' \rangle] \\ - [\langle E_o s | \tilde{M}_x | E_o s'' \rangle \langle E_o s'' | \mathcal{H}_1 | E_o' s' \rangle]$$

This is equivalent to considering only those terms in the  $\mathcal{H}$  which are secular with respect to the Zeeman Hamiltonian  $\mathcal{H}$ . This implies that



the truncated dipolar Hamiltonian which includes only the terms A and B must be included in the above equation and let this truncated Hamiltonian be denoted by  $\mathcal{H}'$ . Thus, solving for  $M$  and in turn solving for  $\chi$  which is proportional to the shape function translates into finding out all the eigen states for the Hamiltonian,

$$(A-1.61) \quad \hbar(\mathcal{H}_2 + \mathcal{H}_1') = \sum_j \mathcal{H}_2^j + \sum_{j < k} \gamma^2 \hbar^2 \frac{A_{jk} + B_{jk}}{r_{jk}^3}$$

The problem of finding the shape function leads to finding the complete set of eigen states of the Hamiltonian  $\mathcal{H} = \mathcal{H} + \mathcal{H}_1'$ , and since  $\mathcal{H}'$  does not commute with  $\mathcal{H}$  it is not possible to solve this problem exactly. Therefore, only certain statistical properties of the shape function can at best be estimated, involving only traces of relevant operators over these eigen states. In such a case a convenient method to calculate such moments of the distribution function, due to Van Vleck [1948], is very appropriate.

Definition:

For an absorption curve which is represented by a normalized symmetric function  $f(\omega)$  with a maximum at  $\omega = \omega_0$ , the  $n$  moment is defined by

$$(A-1.62) \quad M_n = \int (\omega - \omega_0)^n f(\omega) d\omega$$

If  $f(\omega)$  is symmetric about  $\omega_0$  all odd moments vanish. The shape function  $f(\omega)$  is related to the correlation function  $G(t)$  by

$$(A-1.63) \quad f(\omega) = \frac{1}{\pi A} \int_0^{\infty} G(t) \cos \omega t \, dt$$

and conversely,

$$(A-1.64) \quad G(t) = \frac{2}{\pi A} \int_0^{\infty} f(\omega) \cos \omega t \, d\omega$$

Here  $A$  is given by the normalization of the function  $f(\omega)$ .  $M(t)$  is given by  $M(t) = e^{-\mathcal{H}t}$  where,  $\mathcal{H}$  is given by

$$(A-1.65) \quad \mathcal{H}(t) = \mathcal{H}_2 + \mathcal{H}_1'$$

Substitution of this definition leads to

$$(A-1.66) \quad G_1(t) \cos \omega_0 t = \frac{2}{\pi A} \int_{-\omega_0}^{\infty} f(\omega_0 + u) \cos(\omega_0 + u)t \, du,$$

where  $G(t)$  is called the reduced correlation function, given by

$$(A-1.67) \quad G_1(t) = \text{tr} \{ e^{i\mathcal{H}_1' t} M_X e^{-i\mathcal{H}_1' t} \}$$

Let us also define  $h(u) = f(\omega_0 + u)$  and utilizing the fact that the shape function is a sharp enough line, one can show that

$$(A-1.68) \quad G_1(t) = \frac{2}{\pi A} \int_{-\infty}^{\infty} h(u) \cos ut \, du$$

and the various even moments of the absorption curve are defined by

$$(A-1.69) \quad M_{2n} = \int_{-\infty}^{\infty} h(u) u^{2n} du$$

Expanding  $G(t)$ ,

$$(A-1.70) \quad G_1(t) = \frac{2}{\pi A} \int_{-\infty}^{\infty} h(u) \left[ 1 + \frac{u^2 t^2}{2!} + \dots \right] du$$

$$(A-1.71) \quad = \frac{2}{\pi A} \left[ \int h(u) du + \frac{t^2}{2!} \int u^2 h(u) du + \dots \right]$$

$$(A-1.72) \quad = \frac{2}{\pi A} \left[ A + \frac{t^2}{2!} M_2 + \frac{t^4}{4!} M_4 + \dots \right]$$

Thus the function  $G(t)$  can be derived to different **approximations** by including more terms. From the definition of  $G(t)$ , the moments can also expressed as,

$$(A-1.73) \quad M_{2n} = (-1)^n (1/2) \pi A \left( \frac{d^{2n} G_1(t)}{dt^{2n}} \right)_{t=0}$$

It can be shown that at  $t = 0$

$$(A-1.74) \quad \frac{d^p G_1(t)}{dt^p} = (i)^p \text{tr} \left( \underbrace{[\mathcal{H}_1', [\mathcal{H}_1', [\dots, [\mathcal{H}_1', M_x] \dots]]}_{p \text{ times}} M_x \right)$$

The advantage of the method of moments is the fact that the trace in the above given formula is independent of the specific basis set within the

vector space in which one evaluates them. Thus one can evaluate the moments in a representation where the values of  $\mathbf{m}_J = \mathbf{I}_J^J$  of the individual spins are good quantum numbers, thus circumventing the insoluble problem of finding all the eigen states  $|n\rangle$  of the total **Hamiltonian**.

From the above the second and fourth moments can be expressed for instance as

$$(A-1.75) \quad M_2 = - \text{tr} \{ [\mathcal{H}_1', I_x]^2 \} / \text{tr} \{ I_x^2 \}$$

and

$$(A-1.76) \quad M_4 = \text{tr} \{ [\mathcal{H}_1', [\mathcal{H}_1', I_x]]^2 \} / \text{tr} \{ I_x^2 \}$$

From (A-1.75) and (A-1.76) it can be deduced that any interaction which commutes with  $I_x$  does not contribute to the second or the fourth moment and in fact such a term in the Hamiltonian will not contribute to the higher order moments as well.

Expression for M :

Substituting the appropriate expression for the truncated Hamiltonian given by (A-1.65) in terms of A and B, the second moment of the absorption curve for a crystalline lattice is derived to be

$$(A-1.77) \quad M_2 = (3/4) \gamma^4 \hbar^2 I(I+1) \sum_k \frac{(1-3\cos^2\theta_{jk})}{r_{jk}^6}$$

For a polycrystalline compound which has a uniform angular distribution of crystallites in space,  $M_2$  is given by

$$(A-1.78) \quad M_2 = (3/5) \gamma^4 \hbar^2 I(I+1) \sum \frac{1}{r_{jk}^6}$$

These are the well known Van Vleck's formulae for the second moment. From (A-1.75) and (A-1.76) it can be deduced that any interaction which commutes with  $I_x$  does not contribute to the moments. Since  $M_2$  varies as  $1/r$ , it is sufficient to consider the nearest neighbours in evaluating the lattice sum, and one can calculate  $M_2$  knowing the specific information on a given crystal structure. For instance, in the case of a simple cubic lattice and a **polycrystalline** compound,  $M$  is given by

$$(A-1.79) \quad M_2 = 5.1 \gamma^4 \hbar^2 I(I+1) \frac{1}{d^6}$$

where  $d$  is the lattice constant.

Since the moments are derived from the absorption curve, they should essentially reflect the dependence of the lineshape on temperature or changes in dynamic environment. The moments for any given system can be experimentally obtained by recording the absorption spectrum **in** the frequency domain and numerically calculating the moments adapting the

definition given in (A-1.62). Calculation of second moment as a function of temperature is a popular scheme to observe the effects of motions in solids, and  $M$  values reflect the onset of different dynamic processes, both qualitatively and quantitatively, as a function of temperature. Starting from a sufficiently high temperature where the motions are very rapid, progressive cooling of the sample may lead to freezing of different motions in a specific sequence, and  $M_2$  measured as a function of temperature develops a step like structure for every motion which undergoes a linewidth transition given by the condition  $\omega T = 1$  where  $\omega$ , is the dipolar linewidth of the absorption curve. Another advantage of measuring  $M$  to observe the dynamical changes is the fact that  $M_2$  is a very sensitive function of the shape function values which are far away from the central frequency of the absorption curve, and small changes in the lineshape which may not reflect to a great extent in the linewidth will also affect  $M_2$  considerably. In some favourable cases, knowledge of  $M_2$  provides with the information about the inter-nuclear distances also, and in fact by measuring  $M$  in a single crystal, Van Vleck formula can be conveniently used to estimate the inter nuclear distances.

#### Relaxation in Solids :

Here we shall attempt to provide a general scheme to adapt the results of BPP theory to the case of solids. The expression for the spin-lattice relaxation rate (spin-1/2 particles) is given by

$$(A-1.80) \quad 1/T_1 = (9/8) \gamma^4 h^2 \left[ \langle |F_1|^2 \rangle_{AV} \frac{\tau_c}{1 + \omega^2 \tau_c^2} + \langle |F_2|^2 \rangle_{AV} \frac{4\tau_c}{1 + 4\omega^2 \tau_c^2} \right]$$

Normally, the dynamics in the solids are thermally activated and these Arrhenius processes have temperature dependent  $\tau$  given by

$$(A-1.81) \quad \tau_c = \tau_o \exp (E_a/kT)$$

where  $E$  is the activation energy associated with this process. A random fluctuation, especially in a solid, can be thought of as a jump process where a given molecular group jumps from one equivalent orientation to another. In a solid all the atoms are subjected to the electrostatic potentials created by the presence of the next of the atoms, and a given orientation in which a molecule exists is its "equilibrium" **configuration**. But, conducive to the overall structure of the solid, a molecule may have more than one such "equilibrium" orientation but it costs energy for the molecule to change itself from one such orientation to the other as it has to cross a hindering potential barrier. The size of the potential barrier the molecular group may have to overcome depends on the surrounding molecular groups at a given site. Depending on the availability of kinetic energy to the rotational, vibrational and translational degrees of freedom, the molecule may reorient from one equilibrium position to another frequently or rarely, and the correlation

time in this context can be thought of as the average dwell time in a given equilibrium orientation. Considering all such processes being inherently stochastic, the probability of occupancy quantified by such 'dwell' times can be expressed by eqn. (A-1.81). In this context,  $E$  is the hindering potential a given group has to overcome and  $\tau$  is a prefactor formally corresponding to the correlation time at infinite temperature ( $T$  indicates the extent to which the molecular group couples with the available thermal energy spectrum or phonons).

Often, the problem of arriving at an expression for the spin-lattice relaxation rate is reduced to finding out the ensemble average of the lattice functions  $F_i$ . In view of the present investigations on the reorientational dynamics of groups like  $(\text{CH}_3)_4\text{N}^+$ ,  $(\text{CH}_3)_3\text{NH}^+$ ,  $(\text{CH}_3)_2\text{NH}_2^+$ ,  $(\text{CH}_3)\text{NH}$ ,  $\text{NH}$  and  $\text{CH}$ , one focuses on molecular dynamics of symmetric groups in solids.

Such random motions in molecular solids with symmetric groups often involve discrete rotational motion about different symmetric axes, and so the problem of performing such ensemble averages corresponds in solids to building suitable stochastic models taking care of these motions over the intermolecular potential barriers. All these molecular groups have one or more axes of symmetry about which "reorientation" or a "rotational jump" can take place between a few well defined positions. For instance, in the case of  $\text{CH}_3$  groups, there is one 3-fold axis of symmetry and the  $\text{CH}_3$  group has three well defined positions at which the potential felt by the molecule is minimum. The hindering potential that the molecule has to overcome to jump from one position to the other is then given by the



activation energy E (Eqn. A-1.81).

Depending on the complexity of a given molecular group we can have reorientation of the group as a whole as well as internal reorientations within the molecule of smaller constituent groups. A typical example is that of the trimethylammonium cation where reorientation of the entire cation takes place about the triad axis passing through the N-H bond, and methyl group reorientations about their 3-fold axes about the bond connecting the C and N atoms can also take place. For this kind of groups, where the number of orientations are limited, we can assign an occupational probability  $p$  for a given pair of positions "ij" and our intention is to consider a given pair of nuclei at a time. We also note that it is the modulation of the dipolar interaction among each individual pairs of spins that is responsible for the relaxation.

We can write a rate equation for the probability of each possible pair of sites and it can be shown that this rate consists of an inward flux into the given site ij which is proportional to the occupational probabilities of the other pairs, and has an outward flux which is proportional to the occupational probability of pair ij itself. An illustrative form of such an equation can be given as

$$(A-1.82) \quad \frac{dp_{ij}}{dt} = -R^{ij} p_{ij} + \sum_{\substack{lm \\ \neq ij}} R^{lm} p_{lm}$$

Here, R refers to the rate of reorientation of given rotational jump

process and in principle R can contain the sum of reorientational rates corresponding to some internal motions mentioned above. By symmetry considerations the number of these equations can be restricted and by a proper recombination of variables, these coupled equations can be separated and solved. Even without getting into the finer details, the functional form of these equations suggest that the probabilities are going to be **exponentially** decaying functions of time with the **preexponential** factors given by the combination of the relevant reorientation rates.

Once we are equipped with the solution to these rate equations, it is in principle simple to connect these probabilities to the relaxation rates. From BPP theory, it is established that the relaxation rate is given by

$$(A-1.83) \quad 1/T_1 = (9/8) \gamma^4 \hbar^2 [J_1(\omega) + J_2(2\omega)]$$

$$(A-1.84) \quad J^\mu(\omega) = \int_{-\infty}^{\infty} G^\mu(t) e^{i\omega t} dt$$

where  $G(t)$  is the correlation function of the relevant lattice function  $F$  given by  $\langle F_{ij}^\mu(0) F_{ij}^\mu(\tau) \rangle_{AV}$ . In the present case this average corresponds to the averaging of the function  $F$  over all the possible equivalent sites  $ij$ . It can be stated as

$$(A-1.85) \quad G^\mu(\tau) = \sum_{ij} \langle F_{ij}^{\mu*} F_{ij}^\mu(\tau) \rangle_{AV}$$

Now for each  $ij$ , we can show that

$$(A-1.86) \quad \langle F_{ij}^{\mu*}(0) F_{ij}^{\mu}(\tau) \rangle = \sum_{lm} F_{ij}^{\mu*}(0) P_{lm} F_{lm}^{\mu}(0)$$

and thus we can substitute the expressions for  $P_{lm}$ 's we have obtained into the above equation.

With the relevant crystal structure data on a given molecular group, we can actually evaluate terms like  $|F_{lm}|^2$ , or  $F_{ij}^* F_{lm}$ , in equation (A-1.86) to get the necessary relaxation constants. What we have outlined here is a brief summary of a general procedure for the computation of the relaxation rate in the case of symmetric molecular group reorientations applicable to the type of solids we have investigated. In latter sections, relevant dynamic models are discussed in order to obtain formulae for spin lattice relaxation rates appropriate for the particular type of molecular groups studied thereof.

## REFERENCES

(A-1.1) ABRAGAM A., " The Principles of Nuclear Magnetism", *Oxford University Press*, 1970

(A-1.2) BLOEMBERGEN N., E.M. PURCELL AND R.V. POUND, *Phys.Rev.*, 73, (1948) 679

(A-1.3) SLICHTER C.P., "Principles Magnetic Resonance" *Springer-Verlag*, 1978

(A-1.4) Van Vleck J.H., *Phys.Rev.*, 74, (1948) 1168

*SECTION B*

*RELAXATION MEASUREMENTS*

# SECTION B

## PART 1

### METHODOLOGY OF EXPERIMENTS

#### METHODOLOGY :

In general, NMR experiments are of two types: continuous wave type (CW) and pulsed measurements. CW-NMR experiments correspond to measurements in the frequency domain where absorption and/or dispersion spectra are recorded as a function of Larmor frequency  $\omega$ . Pulsed-NMR experiments are performed in the time domain where the recovery of the macroscopic magnetization from a non-equilibrium value, specifically created by a chosen set of r.f. irradiation pulses, is recorded as a function of time. Each has its advantages as well as drawbacks. However, data in both the domains are related by the Fourier transform, and this fact is exploited in the FT-NMR techniques.

#### CW-EXPERIMENTS - PRINCIPLE OF OPERATION

The imaginary part of the magnetic susceptibility ( $\chi''$ ) at resonance frequencies is connected with resonance absorption of energy by the nuclear spins. while the real part is related to the frequency dispersion. CW experiments are mostly aimed at obtaining the absorption spectrum. In an experiment, this is detected as the change in  $x''$  of an inductance coil L in which the sample is kept, while scanning the resonance condition commonly by slowly varying the quantizing field H. In crossed-coil type spectrometers an induced e.m.f. in an inductance

coil kept in the XY-plane perpendicular to the irradiating coil is detected and is proportional to  $g(\omega)$ , the absorption shape function. In single coil detection schemes, the resonant absorption of energy is detected as a change in the output level of a limited oscillator. In both techniques, a modulating field parallel to the Z-axis is applied to facilitate efficient signal detection and processing. The frequency of the modulating field,  $\omega_m$ , is chosen to be few order of magnitudes less than the Larmor frequency, and the carrier frequency  $\omega$  can be filtered out after detection with the help of a low pass filter.

The rate at which the Zeeman field can be scanned is restricted by the "adiabatic fast passage" condition [Abragam, 1970]

$$(B-1.1) \quad 1/T_1 \ll (1/H_1) |dH_0/dt| \ll \gamma H_1$$

and this condition is satisfied in the case of solids, where  $T \ll T_1$ . The intensity of the irradiating r.f. should also be kept at a low enough level to avoid 'saturation'. This condition can be expressed by

$$(B-1.2) \quad \gamma^2 H_1^2 T_1 T_2 \ll 1$$

The amplitude of the modulating field too is restricted by the adiabatic fast passage condition

$$(B-1.3) \quad \omega_m H_m \ll \gamma H_1^2$$

In order to calculate the second moment,  $M$ , the derivative spectrum obtained due to phase sensitive detection is integrated numerically to

generate the absorption curve and the  $M$  is computed by using the relation

$$(B-1.4) \quad M_2 = \frac{\int_0^{\infty} (\Delta\omega)^2 f(\omega) d\omega}{\int_0^{\infty} f(\omega) d\omega}$$

In practice, the integral needs to be replaced by a suitable summation to a very good approximation.

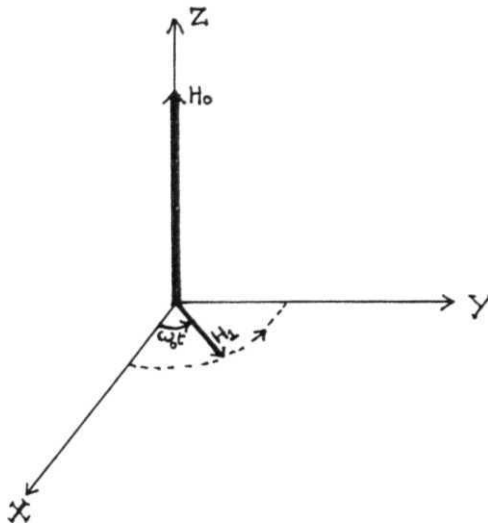
#### PULSED EXPERIMENTS - PRINCIPLE OF OPERATION :

The basic principle in these experiments is to create a chosen non-equilibrium state for the magnetic state of the spin subsystem, and then observe, through suitable coupling to the measuring apparatus, the relaxation of the spins to their equilibrium state, in the absence of external r.f. fields. In practice, such an observation involves coupling to the **magnetization** components perpendicular to the applied static field and the resultant signal is called the free induction decay (FID).

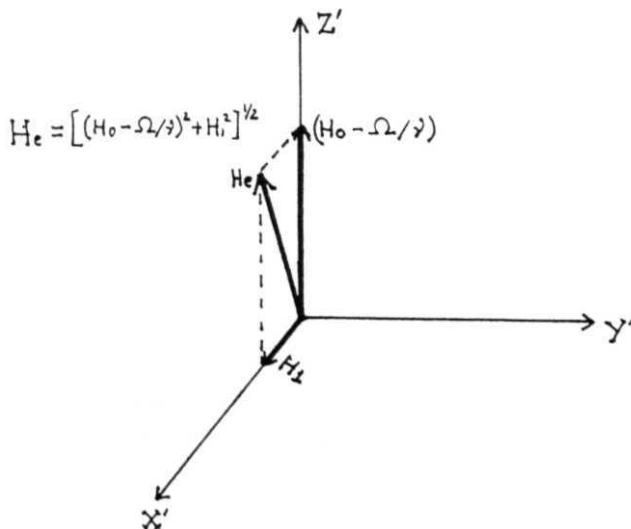
The methodology of the pulsed NMR experiment is appreciated in a more lucid fashion by considering a description of the dynamics of the **magnetization** in the laboratory and "rotating" frames. In the laboratory frame, a static **Zeeman** field  $H$  is applied along the Z-direction and an oscillating r.f. field is applied along, say, the X-axis, at the **Larmor** frequency  $\gamma H$ . This field can be decomposed into right **circularly** polarized and **left** circularly polarized components (Fig. B-1.1a).

Now, **if** we transform from the lab frame to a frame of reference

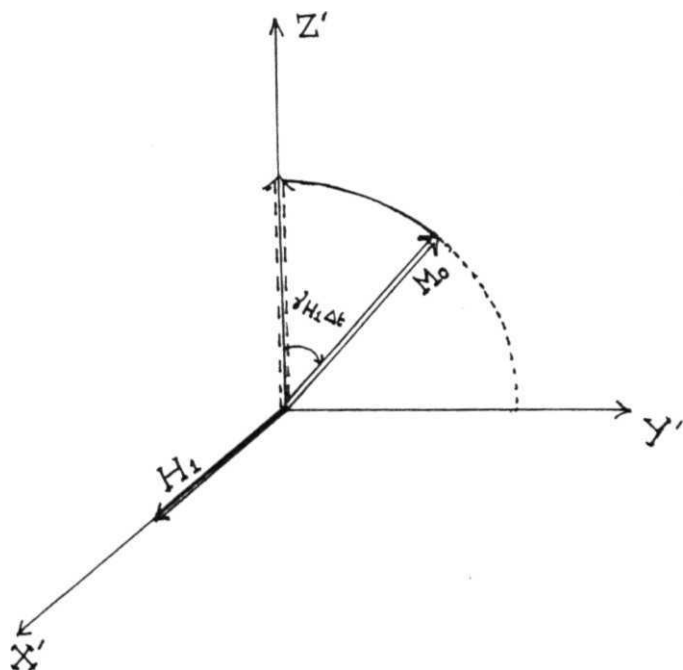




{B - 1.1a) Diagram showing the static field  $H_0$  and rotating field



— 1.16) Diagram showing the effective field in a frame rotating with angular velocity  $\Omega$  about Z-axis in the laboratory frame.



(B - 1.2) Diagram showing the tipping of the magnetization  $M_0$  about the field  $H_1$  in the rotating frame.

rotating with an angular velocity  $\Omega$  about the Z-axis, the Z-axis magnetic field in this rotating frame is given by  $(H - \Omega/\gamma)$  and the magnetic moment of any given spin experiences in this frame an effective field  $H_e = (H_0 - \Omega/\gamma)\mathbf{k} + H_1\mathbf{i}$  (Fig. B-1.1b). Now, when  $\Omega = \gamma H_0$ , the effective field in this frame is given by  $H_1\mathbf{i}$  alone and this corresponds to the resonance condition. Thus, at resonance, the magnetic moment in the rotating frame experiences a static field  $H_1$  in the XY-plane, along X-axis. For an ensemble of non-interacting spins, a macroscopic magnetization  $\mathbf{M}$  is present along the Z-axis, which is the sum of the Z-components of the individual magnetic moments. This magnetization tips by an angle  $\gamma H_1 \Delta t$  in an interval of time  $\Delta t$  about this field (Fig. B-1.2). The time for which the field  $H_1$  is applied can be so chosen that  $\Delta\theta = \gamma H_1 \Delta t = \pi/2$ , and after this interval the magnetization  $\mathbf{M}$  will be in the XY-plane, along the Y-axis. This corresponds to the populations in the two levels of energy becoming equal as evidenced by the absence of a net Z-axis magnetization. The r.f. pulse applied for this characteristic time to tip  $\mathbf{M}$  by an angle  $\pi/2$  is called the  $\pi/2$  pulse. If this time interval is doubled, the magnetization precesses all the way to the -Z direction, and then this pulse is referred to as the  $\pi$ -pulse. This condition corresponds to the inversion of the equilibrium populations between the two energy levels.

The free induction decay is recorded as an observable emf induced in a pick up coil due to the time dependent (rotating at  $\omega$ , and irreversibly decaying to zero due to T process) magnetization. Normally the same inductance coil is used both for irradiation and subsequent detection, and a typical FID at this stage would be a decaying (exponentially) sinusoid.

## Measurement of the spin-lattice relaxation time $T_1$ :

By recording the growth of the longitudinal magnetization to its equilibrium value  $M$  progressively in time, the relaxation time  $T$  can be calculated. Such monitoring of  $M$  can be achieved in different ways, and some of the popular schemes are discussed below.

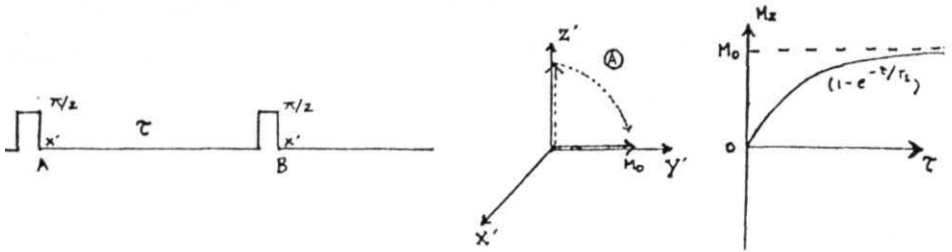
### 1. Saturation recovery sequence: ( $n/2 - T - n/2 \dots$ )

This is the simplest of all the three sequences. It contains a preparation  $n/2$  pulse which is followed by 'detection'  $n/2$  pulse after a time interval  $T$  (Fig. B-1.3a). Assuming that the spin system is at equilibrium to begin with, the first  $n/2$  pulse tilts the magnetization  $M$  on to the **XY-plane** thereby creating the non-equilibrium condition. If we wait for time  $T$  after this pulse, then the Z-axis magnetization  $M$  would have grown to a non-zero value and when the second  $n/2$  pulse is applied at this point, it tilts the ambient magnetization on to the XY-plane which induces an FID in the inductance coil.

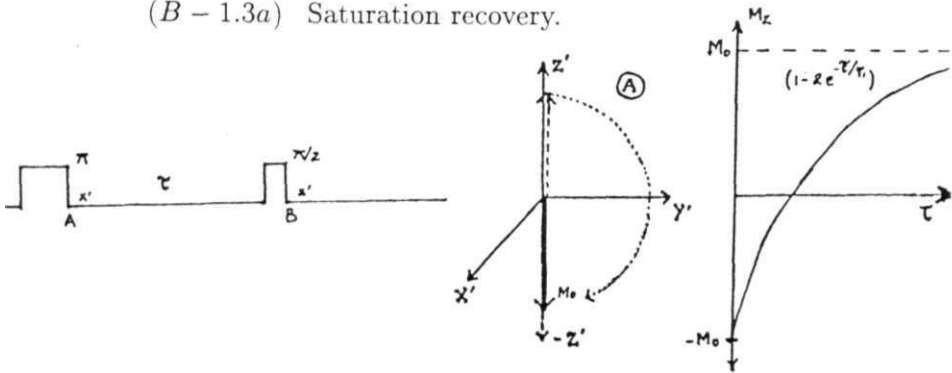
From Bloch equations it is seen that

$$(B-1.5) \quad M_z = M_0 (1 - e^{-\tau/T_1})$$

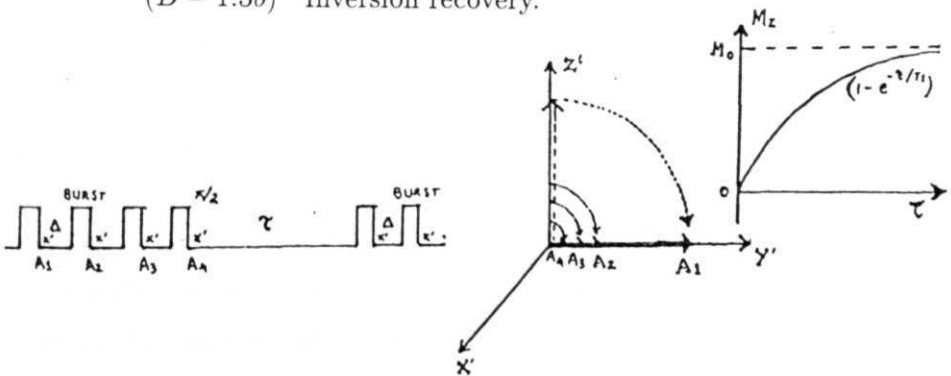
for the initial condition  $M = 0$  at  $\tau = 0$ , and describes the growth of magnetization with  $T$  with the above pulse sequence.



(B - 1.3a) Saturation recovery.



(B - 1.3b) Inversion recovery.



(D - 1.3c) Saturation burst.

## 2. Inversion Recovery sequence : ( $\pi$ - T - $n/2$ )

This sequence is shown schematically in (Fig.B-1.3b). The preparation pulse is a  $n$  pulse and this causes the magnetization  $M$  to be inverted to the  $-Z$  direction. A time delay  $T$  is applied and the magnetization would have evolved in the  $Z$ -direction from  $-M$  to a larger value in this time, which is followed by a  $n/2$  detection pulse which gives rise to an FID whose amplitude depends on the value of  $M$  after its recovery from  $-M$  in an interval of time  $x$ . Thus plotting the magnetization  $M$  as a function of  $x$ , the delay time, we get an exponential recovery whose time constant is  $T$ . If we solve the  $Z$ -component of Bloch's equations with an initial condition that at  $T=0$ ,  $M_z = -M_0$ , we get,

$$(B-1.6) \quad M_z = M_0 (1 - 2e^{-x/T_1})$$

Fitting the set of  $(x, M)$  pairs to this equation will enable us to calculate  $T$ . In order to ensure that we satisfy the initial condition, namely  $M = -M$  at  $x = 0$ , we must allow enough time to elapse after a given pulse sequence so that the magnetization will recover back to its equilibrium value  $M$  and the application of a  $n$  pulse will make  $M = -M$  at time  $x = 0$ . In an actual measurement, the sequence with a given  $x$  itself is repeated several times to average out the baseline noise and to improve the signal to noise ratio (S/N) of the FID.

### 3. Saturation Burst or Saturation Comb sequence :

$$(n/2 - A - n/2 - \dots - A - n/2) - x - (\text{Burst}) - \dots$$

This sequence is improvement over the saturation recovery method. The primary drawback of that method was the error incurred due to, either incorrect pulse width or the r.f. field inhomogeneity. This problem is taken care of in this method by the repeated application of  $n/2$  - pulses separated by time  $A$ , where  $A$  is chosen so that,  $T < A \ll T$  . Even in the presence of the above mentioned problems, after repeated application of sufficient number of these pulses, the magnetization along Z-axis is made zero exactly. This bunch of  $n/2$  pulses are referred to as the "saturation burst" or "saturation comb". After the application of a given comb, a time delay  $\tau$  is inserted after which another burst is applied. As in the case of saturation recovery method, the burst serves a dual purpose in that, the first  $n/2$  pulse of a given burst acts as the detection pulse, apart from the burst itself acting as a preparation sequence. Measurement of  $M$  as a function of  $x$  provides us a recovery curve, which is fitted to equation (B-1.5) and  $T$  is thus calculated.

Saturation burst sequence incorporates some of the advantages of both the previously described sequences. It does not put heavy load on the transmitter, as the duty cycle is kept at a low value by the inherent delay time  $x$  used in the experiment, which is always larger than the duration of the burst. Long waiting times are avoided as each burst prepares the spin system in its initial condition. But it does not match the dynamic range of  $M$  available in the inversion recovery sequence. The

relevant schematic diagram of this sequence is provided in Figure (B-1.3c).

An interesting and useful spin-off of the inversion-recovery method is the 'fly-by' measurement of  $T$  using the zero-crossing method. From equation (B-1.6), it can be seen that  $M$  becomes zero when

$$(B-1.7) \quad \tau_{\text{zero}} = T_1 \ln 2$$

If we can find out the time delay  $\tau$  for which the magnetization is zero along the Z-direction, from that information,  $T$  can be estimated. But this method is not as accurate as the other methods due to the inherent ambiguities present in measuring the zero-crossover time delay  $T_{\text{zero}}$ , but this is quite a useful technique in situations where a necessity for quick succession of measurements of  $T$  may arise.

The methods given here are the widely used schemes. Numerous other methods are also reported in literature and these methods aim at improving the sensitivity of the measuring technique as well as reduce the experimental time involved [Canet et al., 1975; Freeman et al., 1971; Heatley, 1973; Edzes, 1975; Sezginer et al., 1991; Moore et al., 1993]. Very useful tips and elaborate discussions are available on these matters, in the treatise by Fukushima and Roeder (1981).

#### **Measurement of spin-spin relaxation time $T_2$ :**

The rate of decay of the FID depends not only on the spin-spin relaxation time but also on the broadening caused by the Zeeman field



inhomogeneity. Thus, the time constant determined from the FID is to be denoted as  $T_2^*$  while the true spin-spin relaxation time as  $T_2$ , and these two are related by

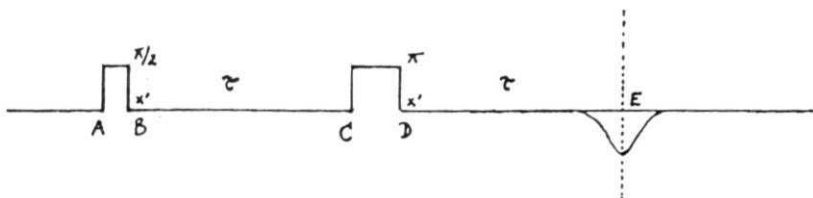
$$(B-1.8) \quad 1/T_2^* = 1/T_2 + \gamma \Delta H$$

where  $\gamma \Delta H$  is the broadening of the line caused by the field inhomogeneity.

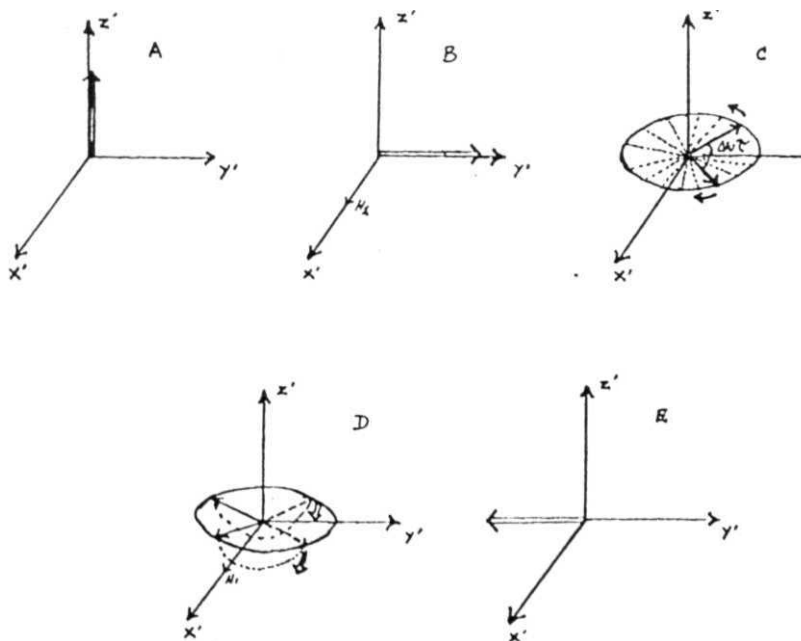
#### Spin Echoes :

When a  $\pi/2$  pulse is applied,  $M$  is tipped on to the XY-plane.  $M$  precesses in the XY-plane about Z-axis. Due to inhomogeneity in the d.c. field as well as in local fields within the sample, different pockets of spins experience different Larmor frequencies and thus the total magnetization, which comprises of the magnetic moment of these different pockets, phase out to zero. Even though the macroscopic magnetization  $M$  become zero in the XY-plane, the magnetization within the pockets of spin which experience a reasonably homogeneous field ( $H + \Delta H$ ) takes more time to decay truly irreversibly to zero, which is of the order of the true spin-spin relaxation time  $T_2$ . Suppose that these defocused spin pockets are refocused by some means, the non-zero magnetic moment in each spin pocket will add up to give a total non-zero magnetization in the XY-plane once again, and the reappearance of the magnetization in the XY-plane is observable as the spin-echo. This fact was demonstrated by Hahn in his famous paper [Hahn, 1950], in which he has shown that two  $\pi/2$  pulses applied in succession with an interval of time  $T$  separating them produces after time  $\tau$  from the second pulse a non-zero magnetization, which is

the Hahn echo. An echo essentially looks like two FID-s superimposed back to back. The more widely used Hahn-echo sequence, which consists of a  $n/2$  pulse followed by a  $n$  pulse after time  $\tau$  is given in Fig.(B-1.4a). It is much easier to form Hahn echoes in liquids as their  $T_2$ 's are large. One can understand the formation of echoes by looking at the evolution of the magnetization in the rotating frame as follows (Fig.B-1.4b). We shall use primed symbols ( $X',Y',Z'$ ) to denote the directions in the rotating frame. Let us assume that in the  $Z'$ -direction there is a net magnetization  $M_z(A)$ . After the  $\pi/2$  pulse is applied along the  $X'$  direction, the magnetization is tipped on to the  $Y'$  axis (B). Now, if we allow for some time  $\tau$  to elapse, because of the static field inhomogeneity, different spin pockets having different Larmor frequencies begin to dephase in the  $XY$ -plane (C). Spins which experience a Larmor frequency greater than  $\omega$  ( $\omega + \Delta\omega$ , say) rotate in one direction with an angular velocity  $\Delta\omega$  and spins which are slower i.e. whose Larmor frequency is less than  $\omega$  move in the opposite direction. After x, a  $\pi$ -pulse is applied along  $X'$  direction and this makes the various spin pockets to precess about the field along  $X'$  direction by an angle  $n$ . For the sake of clarity, in Fig.(B-1.4b), the magnetization of only two spin pockets are shown whose Larmor frequencies are away from  $\omega$  by equal amounts  $\pm\Delta\omega$ . Now, if one waits for the time  $x$  after the pulse, the spin pockets refocus on to the  $Y'$  axis and this net magnetization gives a spin echo (E). Now, to measure  $T_2$ , we can record the echo amplitude for increasing  $\tau$ -values and a plot of the echo amplitude versus  $\tau$ -values is an exponential decay with a time constant given by  $T_2$ .



(B — 1.4a) Hahn echo sequence.



{B - 1.46) Echo formation in stages in rotating frame.

### Carr-Purcell Sequence :

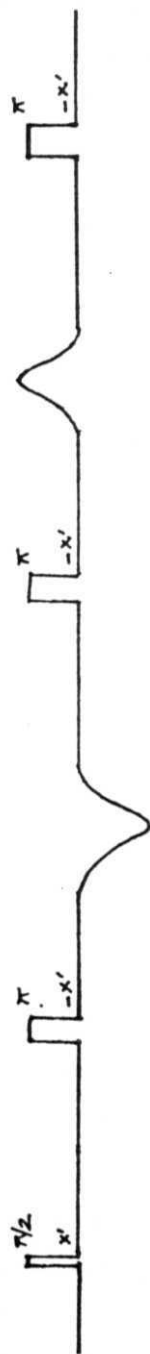
In this sequence [Carr et al., 1954] a train of  $\pi$  pulses are applied along  $-X'$  direction at intervals  $x$ ,  $3\tau$ ,  $5\tau$ ,... etc. after the first  $n/2$  pulse, applied in the  $X'$  direction and echoes will form at the intervals  $2x$ ,  $4x$ ,  $6x$  and so on. Because the refocusing pulses are applied along  $-X'$  direction, the echoes form along  $Y'$  and  $-Y'$  direction alternatively. This method has the advantage that unlike Hahn sequence, a single application of this sequence will give us the entire echo amplitude decay envelope from which  $T_2$  can be measured readily. But this method still suffers from the limitation that, if the  $n$  pulses are not exact in their width, the cumulative error on the echo amplitude leads to a smaller measured value of  $T_2$ . This problem can be taken care of by phase shifting the adjacent  $n$  pulses by  $180^\circ$ . The Carr-Purcell sequence is shown in **Fig. (B-1.5a)**.

### Carr-Purcell-Meiboom-Gill sequence (CPMG) :

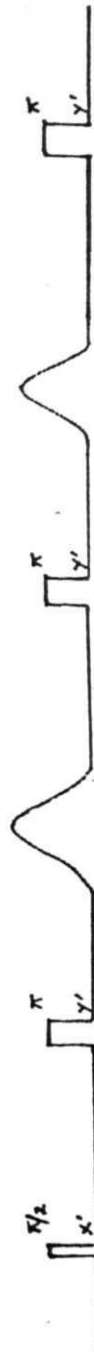
A simple modification to the CP (Carr-Purcell) sequence is to apply all the refocusing pulses along  $Y'$  direction after applying the preparation  $\pi/2$  pulse along the  $X'$  direction (Fig. B-1.5b). In this way all the echoes form along the  $Y'$  direction and the sequence with this modification is known as the CPMG sequence [Meiboom et al., 1958]. This sequence can be used for signal enhancement of the echo also.

### **Measurement of Diffusion Coefficient :**

It was shown by Hahn and later by Carr and Purcell that the



(B - 1.5a) Carr-Purcell sequence.



(B - 1.5b) CPMG sequence.

formation of spin echoes can provide us very useful information on the translational diffusion in liquids [Hahn, 1950; Carr et al., 1954]. In the Hahn echo sequence, as  $\tau$  is made very large, the decay of the echo amplitude is not only determined by the spin-spin relaxation process but the **self-diffusion** of the nuclei also contribute to this decay. This can be understood in the following way. Let us consider a case when diffusion is not present. In this case, after the preparation pulse, in time  $T$  a given spin pocket with a Larmor frequency  $(\omega + \Delta\omega)$  would have dephased by an angle  $\Delta\omega\tau$  or we can say that this spin pocket has a phase  $\Delta\omega\tau$ , in the rotating frame. After the refocusing pulse, in time  $T$ , this spin pocket accumulates the same phase  $\Delta\omega\tau$  but in the opposite direction and at the end of  $\tau$  s the net phase of this spin pocket is zero. This is true of all such spin pockets and therefore all of them coincide at the same point to give rise to the echo of the maximum amplitude. But when diffusion is present, during the time interval  $\tau$ , the spins move from a region of a given Larmor frequency to a region of another frequency, and thus as the time elapses there will be a change in the phase of any given spin pocket as the quantity  $\Delta\omega$  itself is time dependent. Thus the phase accumulated by a given spin pocket before and after the  $n$  pulse are no longer same, because of which a complete refocusing of the spin pockets does not take place at the end of  $T$  s after the  $n$  pulse.

Effect of diffusion on spin echoes can be quantitatively understood by suitably modifying the Bloch equations. [Torrey, 1956]. It can be shown that the effect on the echo amplitude in the case of a Hahn echo sequence is different from that of the Carr-Purcell echo sequence. The Bloch equation modified suitably to include the effect of translational diffusion is given by

$$(B-1.9) \quad \frac{\partial \vec{M}(\vec{r}, t)}{\partial t} = \gamma (\vec{M} \times \vec{H}(\vec{r}, t)) - \frac{(M_x i' + M_y j')}{T_1} - \frac{(M_z - M_0) k'}{T_2} + D \nabla^2 \vec{M}$$

2.

and the term  $D \nabla^2 \vec{M}$  represents the contribution to the rate of change of the macroscopic magnetization  $\vec{M}$  due to the presence of diffusion and  $D$  is the "diffusion coefficient". Let  $H_x = H_y = 0$  and the Z-component of the magnetic field will be the applied field which changes from one point to other and this variation of the  $H_z$  can be expressed as

$$(B-1.10) \quad H_z = H_0 + (\vec{G} \cdot \vec{r})$$

where  $H_0$  is an average value of the Zeeman field and  $G$  is the field gradient. Substituting this expression in equation (B-1.9) and writing  $\vec{m} = \vec{M} + i\vec{M}$ , the modified Bloch's equation can be written as

$$(B-1.11) \quad \partial \vec{m} / \partial t = i\omega_0 \vec{m} - \vec{m} / T_2 - i\gamma (\vec{G} \cdot \vec{r}) \vec{m} + D \nabla^2 \vec{m}$$

and introducing  $\psi(\vec{r}, t)$  by the relation  $\vec{m} = \psi \exp(i\omega_0 t - t/T_2)$  this equation modifies to

$$(B-1.12) \quad \partial \psi / \partial t = -i\gamma (\vec{G} \cdot \vec{r}) \psi + D \nabla^2 \psi$$

We can look at the solution of equation (B-1.12) in the light of Carr-Purcell sequence or Hahn sequence and we shall do the first in this case. In the case of Carr-Purcell sequence,  $n$  pulses are applied at intervals  $\tau, 3\tau, 5\tau, \dots (2n-1)\tau$  and the echoes form at intervals  $2\tau, 4\tau, 6\tau, \dots 2n\tau$  and so on. Assuming that the  $n$  pulses are phase shifted by  $90^\circ$  with respect to the preparation  $n/2$  pulse, for an interval  $(2n-1)\tau$  to

$(2n+1)T$ , the solution  $\psi$  of (B-1.12) in the absence of the diffusion term is given by

$$(B-1.13) \quad \psi = A \exp\{-i\gamma(G.r)(t-2n\tau)\}$$

and the influence of the term  $D \nabla^2 \psi$  can be seen as making the amplitude  $A$  time dependent. Substituting this solution back in (B-1.12), we get the following equation for the rate of change of  $A$

$$(B-1.14) \quad dA/dt = -AD\gamma^2 G^2 (t-2n\tau)^2$$

and integrating this equation within the interval  $(2n-1)\tau$  to  $(2n+1)\tau$ , we get

$$(B-1.15) \quad A\{(2n+1)\tau\} = A\{(2n-1)\tau\} \exp\{-(2/3)D\gamma^2 G^2 \tau^3\}$$

from which it can be deduced that

$$(B-1.16) \quad A\{2n\tau\} = A(0) \exp\{-(2/3)D\gamma^2 G^2 \tau^3 n\}$$

and  $A(0)$  is the amplitude of the unattenuated echo at time  $x = 0$ . The attenuation of the echo amplitude at the time  $t=2nx$  is

$$(B-1.17) \quad A(t) = A(0) \exp\{-(1/3)D\gamma^2 G^2 \tau^2 t\}$$

In contrast to this result, the attenuation of the echo amplitude in the case of a Hahn echo sequence can be shown to be [Abragam, 1970]



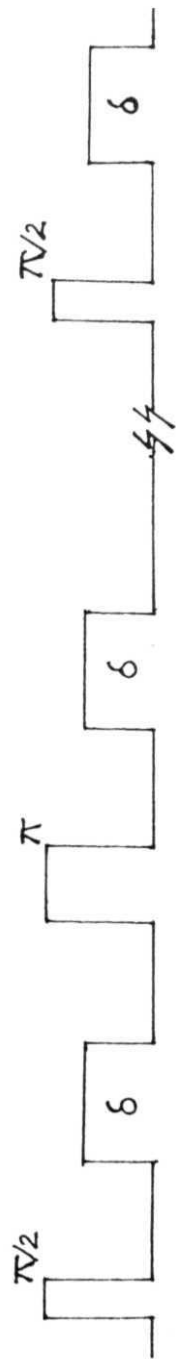
$$(B-1.18) \quad A(t) = A(0) \exp \{-(1/12)D\gamma^2 G^2 t^3\}$$

One can see from these equations that the effect of diffusion on the amplitude of a Carr-Purcell echo train is seen as an exponential decay as a function of the observation time  $t$ . But in the Hahn echo sequence, the echo amplitude is attenuated by the factor whose functional dependence on the observation time  $t$  is  $\exp(-t^3)$ . By a careful measurement of the echo amplitude attenuation and a prior knowledge of the field gradient  $G$ , the Hahn echo sequence can be used as an excellent method for the measurement of the self-diffusion coefficient  $D$ . In a typical diffusion measurement scheme, the echo attenuation due to the translation of the spins is exploited selectively, by imposing on the static Zeeman field  $H$  a linear static field gradient  $G$  along the  $Z$ -direction and using formulae like (B-1.18), the diffusion coefficient  $D$  is calculated. In these experiments, it is assumed that the field gradient  $G$  which is inherent in the static field is much smaller compared to the applied field gradient  $G$ . The sensitivity of the measuring technique depends on the highest gradient one can produce and also on how long the observation time interval  $t$  can be. The former is limited by the instrumentation being employed and the latter by the spin lattice relaxation time of the given sample. Currently, self-diffusion measurement using NMR has become a vast and active field of research in itself and one can find excellent reviews in literature like the one by Karger and others [Karger et.al., 1988].

As a part of the present work, a diffusion measurement set up has been developed by the author by augmenting the existing home-built pulsed NMR spectrometer suitably and the instrumentation details are given in Part-3 of this section (sub-section B-3). The setup is designed to make

it possible to measure diffusion coefficients in liquids and liquid crystals. Liquid crystals are interesting anisotropic systems in which the spin-spin relaxation time is much smaller than it is in the case of liquids owing to the strong unaveraged dipolar interactions among nuclei.

There are certain difficulties in making diffusion measurement on this kind of systems using the above mentioned methods. First of all, due to strong spin-spin interaction in these compounds, it is tough to form the spin echoes. Secondly, these systems have high viscosity and it is expected that the diffusion coefficient is relatively small in these systems. This puts a high demand on the largest field gradient one can create, as can be seen from the attenuation factor given in equations (B-1.15) and (B-1.16). It can also be observed that the time of observation has to be made as large as possible to enhance the sensitivity of the measurement and this is restricted by the order of  $T$  in the compound. To take care of the first problem, line narrowing techniques are employed like Magic Angle Spinning (MAS) and there are other multiple pulse techniques which selectively average out the dipolar interaction and make the  $T$  longer. It is difficult to create d.c. field gradients of very large values, but high field gradients in a pulsed manner can be sustained for small intervals of time (of the order of a few hundred  $\mu\text{s}$ ). One can analyze the effect of these pulsed field gradients on the echo amplitudes and derive an expression for the attenuation factor from which the diffusion coefficient may be calculated [Karger et al., 1988]. It can be said that most of the spin echo techniques to study diffusion in various systems are all Pulsed Field Gradient (PFG) techniques. The first ever PFG technique was that of Stejskal and Tanner, and the pulse sequence is provided in Fig. (B-1.6)



(B - 1.6) Stejskal-Tanner sequence.

[Stejskal et al., 1965). This is a simple sequence in that, apart from the Hahn sequence, two field gradient pulses in between the  $n/2$  and  $n$  pulses are inserted, and the amplitude of the echo which forms at  $2T$  is monitored as a function of either the duration of the gradient pulses or the strength of the pulses. The echo attenuation factor is given by

$$(B-1.19) \quad \Psi = \exp [-\gamma^2 D \delta^2 g^2 (\Delta - (1/3)\delta)]$$

Here,  $g$  is the strength of the field gradient pulse and  $\delta$  is the duration of the pulse and  $\Delta$  is the time interval separating the two gradient pulses.

PFG techniques also have their own limitations. The fast rising field gradient pulses may create eddy currents in the NMR probe body and reflections from the pole caps of the magnets also cause residual field gradients which may persist for a considerable amount of time. Any mismatch in the gradient pulse amplitudes leads to attenuation of the echo amplitude which may be construed as due to the diffusion effect. Various other pulse schemes are available in literature which tend to correct these problems [Meerwall et al., 1989; Murday, 1973 Holz et.al., 1991; Price, 1991; Heink et.al., 1991]. There are methods reported to circumvent specific difficulties pertaining to the systems studied thereof. For instance the scheme suggested by Karlick and Lowe addresses the problem of large background fields created in powdered samples of considerable bulk susceptibility and circumvents this problem [Karlick et al., 1980]. Novel schemes of measuring diffusion using RF field gradients is reported [Canet et.al., 1989]. Techniques are suggested for measurement of transverse relaxation rates as well as diffusion

parameters in a fast manner [ Moore et al., 1993]. Some of the other methods are available in the following references [Counsell, 1993; Latour et.al., 1993; Merril, 1993]. Apart from the new methods of measurements, considerable importance is given to the interpretation of the results as well as theoretical modeling of diffusion processes, in literature [ Brooklevinson et al., 1993; Murad et al., 1993; Araujo et al., 1993]. The field of diffusion measurements in micellar, porous and polymeric systems as well as biological systems is a rapidly expanding one and especially diffusion studies in systems with restricted and fractal geometries offers understanding of several new concepts and potential applications as well. As, discussing about the finer details of this interesting branch of NMR spectroscopy is beyond the scope the present work, the reader is referred to the above said articles for further details.

## REFERENCES

- (B-1.1) ABRAGAM A., "The Principles of Nuclear Magnetism", *Oxford University Press*, (1970)
- (B-1.2) ARAUJO C.D., A.L.McKAY, K.P. WHITALL AND J.R.T. HAILEY, *J.Magn.Reson. (B)*, **101**, (1993) 248
- (B-1.3) BROOKLEVINSON E.T. AND A.V. ZAKHAROV, *Europhys.Lett.*, **22**, (1993) 439
- (B-1.4) CANET D. AND G.C. LEVY AND I.R. PEAT, *J.Magn.Reson.*, **18**, (1975) 199
- (B-1.5) CARR H.Y. AND E.M. PURCELL, *Phys.Rev.*, **94**, (1954) 630
- (B-1.6) CANET D., B. DITTER, A. BELMAJDOUB, J. BRONDEAU, J.C. BOUBEL AND K. ELBAYED, *J.Magn.Reson.*, **81**, (1989) 1
- (B-1.7) COUNSELL C.J.R., *J.Magn.Reson.(B)*, **101**, (1993) 28
- (B-1.8) EDZES H.T., *J.Magn.Reson.*, **17**, (1975) 301
- (B-1.9) FREEMAN R. AND H.D.W. HILL, *J.Chem.Phys.*, **54**, (1971) 3367
- (B-1.10) FUKUSHIMA E. AND S.B.W. ROEDER, "Experimental Pulse NMR - A Nuts and Bolts Approach", *Addison-Wesley Pub.Co., Inc.*, **1981**
- (B-1.11) HAHN E.L., *Phys.Rev.*, **80**, (1950) 580
- (B-1.12) HEATLEY F., *Faraday Trans. II*, **69**, (1973) 831
- (B-1.13) HEINK W. . *Z. Phys.Chem.*, **170**, (1991) 199
- (B-1.14) HOLZ M., *J.Magn.Reson.*, **92**, (1991) 115
- (B-1.15) KARGER J., H. PFEIFER AND W. HEINK, " Principles and Application of Self-Diffusion Measurements by Nuclear Magnetic Resonance", *Advances in Magnetic Resonance*, **VOL.12**, *Academic Press*, 1988
- (B-1.16) KARLICEK AND I.J. LOWE, *J.Magn.Reson.*, **37**, (1980) 75
- (B-1.17) LATOUR L.L, L.M. LI AND C.H. SOTAK, *J.Mang. Reson. (B)*, **101**, (1993) 72

- (B-1.18) MEIBOOM S. AND D. GILL, *Rev.Sci.Instrum.*, 29, (1958) 688
- (B-1.19) MERRIL M.R. , *J.Magn.Reson. (A)*, 103, (1993) 223
- (B-1.20) MOORE J.R., K.R. METZ, *J.Magn.Reson.(A)*, 101, (1993) 84
- (B-1.21) MURAD S., P. RAVI, J.G. POWLES, *J.Chem.Phys.*, 98, (1993) 9771
- (B-1.22) MURDAY J.S., *J.Magn.Reson.* , 10, (1973) 111
- (B-1.23) PRICE U.S., *J.Magn.Reson.* , 94, (1991) 133
- (B-1.24) SEZGINER A., R.L. KLEINBERG, M. FUKUHARA AND L. LATOUR,  
*J.Magn.Reson.* , 92, (1991) 504
- (B-1.25) STEJSKAL E.O., J.E. TANNER, *J.Chem.Phys.*, 42, (1965) 288
- (B-1.26) TORREY H.C., *Phys.Rev.* , 104, (1956) 563
- (B-1.27) VON MEERWALL E. AND M. KAMAT, *J.Magn.Reson.* , 83, (1989) 309

## SECTION B

### PART 2

#### PULSED NMR SPECTROMETER

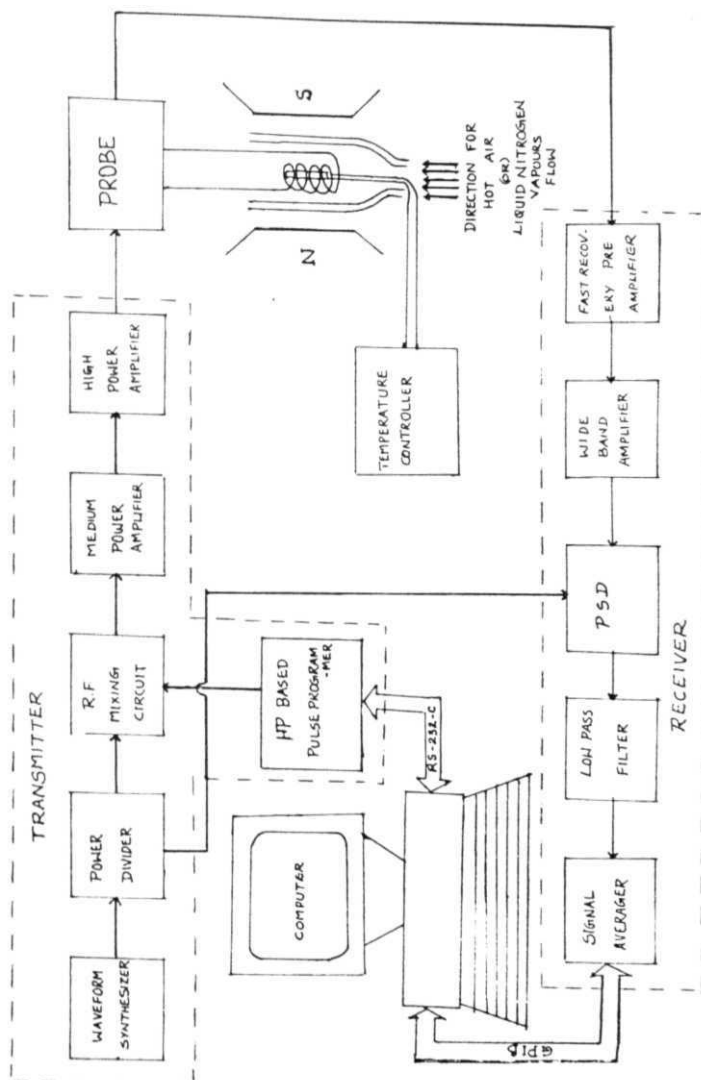
This section contains a brief description of the pulsed NMR spectrometer, employed for measurements in the current work. The details of the construction of various units and their functions are found elsewhere [Venu, 1988].

Fig.(B-2.1) provides a block diagram of the pulsed NMR spectrometer. The spectrometer can be broadly divided into the transmitter, the NMR probe and receiver. The transmitter has to generate the appropriate pulsed r.f. radiation and amplify it to typically 100s of volts and deliver it to the NMR probe. The probe is a matching network made of passive elements L, C and R, and the sample is kept inside the inductance coil. At resonance, the impressed voltage is multiplied several-fold and the nuclei are subject to a high voltage r.f. field. The receiver picks up the very weak signal from the NMR coil, and amplifies it in stages, to be detected by the phase sensitive detector and processed through the low pass filter. Finally, the signal is routed to a signal averager, which averages the signal for improved signal to noise (S/N) ratio.

#### *Transmitter:*

1. **Waveform synthesizer** : This provides the continuous sinusoidal voltage at the required Larmor frequency. Output voltage of this





(B - 2.1) Block diagram of the pulsed NMR spectrometer.

unit is few hundreds of millivolts which is gated by appropriate pulse sequence and amplified. A **WAVETEK** make frequency synthesizer (model No. 2500A) is used here, which has a range of frequencies from 0.2 MHz to 1100 MHz.

2. The power divider : This splits the input from the waveform synthesizer into two parts and routes one to the r.f. mixing circuit and the other to the PSD for detection purposes.
3. Pulse Programmer : This unit generates the required pulse sequences. A detailed description of the  $\mu$ P-based pulse programmer developed as a part of this work is postponed till the next sub-section (B-3). In a simple minded configuration to perform T experiments, the pulse programmer consists of a master clock, two pulse generators and one delay generator. In the case of inversion recovery sequence, the master clock provides the repetition rate of the pulse sequence. For saturation burst, the master clock is not needed as the delay generator produces the trigger at the required repetition rate to the first pulse generator and the output is used to gate the second generator which is in free running mode. This produces a burst of pulses and the number of them in a burst can be modified with the help of the gating pulse and the rate of generation of the second pulse generator. The delay generator is BNC model 7010 and the pulse generators are BNC 8010.

4. **RF mixing circuit** : For this, double balanced mixers manufactured by Mini Circuits company are used. A current driver circuit is fabricated to bias the the DBMs, by this method ON/OFF ratio better than 80 dB is achieved [McLachlan, 1982].

5. **Power amplifier (two stages)** :

- Medium power amplifier of ENI make (model no. 310L) is used, which has a gain of 50 dB and has a bandwidth of 250 kHz to 110 MHz.
- High power amplifier is a home built circuit with a 3E29 dual tetrode tube, providing a gain of 10.

*Probe :*

Two designs of home built probes were employed. One is the series resonance probe [W.G. Clark, 1973]. **The** other is a parallel resonance circuit. The parallel resonance circuit has the facility to change the Q factor and has wider bandwidth than the series resonance circuit.

*Receiver:*

1. **Pre-Amplifier** : The preamplifier must have the ability to recover from the overload due to the transmitter pulse and it should also be able to provide reasonable gain to pick up the weak NMR signal. Two commercial units were used : MATEC 252 and

MATEC 253. Model 252 is tunable over a range of 0.5 MHz to 25 MHz and has an overall gain of 30 dB. Model 253 is a wide band amplifier with a bandwidth of 0.5 MHz to 40 MHz having an overall gain of 20 dB.

2. **Wide-band amplifier** : The signal output from the preamp stage is further amplified by this unit. Commercial unit of MATEC make, model No. 625 with a bandwidth of 2 to 200 MHz is used.
3. **Phase Sensitive Detector** : Reference from the power divider is taken in and multiplied with the incoming signal to detect the signal selectively at the Larmor frequency and the phase information is also kept intact. A Hewlett-Packard make DBM is used.
4. **Low Pass filter** : Recovers the FID envelope and filters out all unwanted higher frequencies. This is a home-built  $\pi$ -section filter.
5. **Signal Averager** : A TEKTRONIX make model 2230 signal averager is employed to collect the FID signals sequentially and average out the random noise and thereby improve S/N ratio.

### *Temperature Control :*

Home made P.I.D. circuit using calibrated **Chromel-Alumel** as the sensor, provided good temperature control up to  $\pm 0.5$  K. A gas flow type cryostat is used. For low temperature work liquid nitrogen vapours are needed while high temperature work utilizes dry air.

#### REFERENCES

- (B-2.1) CLARK W.G. AND J.A. McNEIL, *Rev.Sci.Instrum.*, 44, (1973) 843
- (B-2.2) McLACHLAN L.A., *J.Magn.Reson.* , **47**, (1982) 490
- (B-2.3) VENU K. , Ph.D thesis, *University of Hyderabad*, 1987

## SECTION B

### PART 3

#### *INSTRUMENTATION AND AUTOMATION*

The basic pulsed-NMR spectrometer was described in the previous section (B-2). The flexibility, versatility and ultimately the utility of the instrument depends on the design of the pulse programmer. The existing instrument uses, as mentioned earlier, two pulse generators coupled through a digital delay generator. The limitation of such an arrangement include restriction to only two pulse sequences, necessity for only manual operation of the delay generator and the lack of facility for automatic data collection synchronous with such a pulse sequencer. In this connection, the fabrication of a microprocessor ( $\mu P$ ) based pulse programmer overcoming some of the above problems, and interfacing of the spectrometer to a PC for automatic execution of the experiment are the author's efforts to upgrade the instrument. One of the useful byproducts of such an exercise has been the demonstration of the flexibility of the arrangement to perform, in principle, diffusion measurements with a fairly complex rf and field gradient pulses. This aspect of the instrumentation has been taken up more as a logical extension of the effort to upgrade the facility available to the author.

This Section discusses in two parts, the general pattern of pulse programming including the present work of the author, as well as interfacing of the different subunits to a PC, through GPIB/RS-232-C buses.

## PULSE PROGRAMMERS - A OVERVIEW

The utility of the pulse programmer depends on the flexibility of the instrument, and in order to appreciate various considerations in attempting its design, it is useful to list all the relevant features, as expected from **experimenter's** point of view.

- (i) It should generate pulses of variable widths through independent channels at TTL levels (typically 1  $\mu\text{sec}$  pulses on the lower side and few milliseconds on the higher side for NMR purposes).
- (ii) It generate variable delays between any two pulses. For most of the simple experiments, a resolution of, say, 100  $\mu\text{sec}$  in the delay time is adequate. The demand on the total range of delay required is sometimes more stringent.
- (iii) The pulse programmer should generate adequate number of triggering and gating pulses to serve various other units like the power amplifier, signal averager etc.
- (iv) It should have flexible scheme of pulse mixings and provide a desired pulse sequence in a given channel.

The programmer should have a flexible user-interface for changing the various settings as **well as** triggering the **generator into** action.



There are a variety of methods reported in literature, for the implementation of pulse programming, each one of them having a unique design philosophy pointed towards a particular set of objectives and requirements of a given spectrometer, Majority of the pulse programmers can be categorized into four broad groups :

1. Single purpose hardware PP-s (or) hardwired PP-s
2. Hardware PP-s with flexible hardware control
3. Hardware PP-s with software control
4. Software pulse generators

1. The first category of pulse programmers are hardwired circuits, designed for a specific pulse sequence. The early models of pulse programmers were of this type [e.g.: Lind, 1972; Franconiet.al., 1970; Shenoy et.al., 1976], and obviously these are not flexible enough for modern purposes.
2. The next generation of PP-s are the hardwired programmers with control capability implemented through hardware [Lind, 1972; Taylor et.al., 1974; Conway et.al., 1977; Aducci et.al., 1977; Lalanne et.al., 1970; Shenoy et.al., 1976; Ellet et.al., 1971] This category of PP-s **are** also known as modular programmers since several modules each with a specific task are combined together to generate the required pulse sequences. The respective modules have facilities to reorganize the parameters and thus a hardware-based flexible control **is** possible in these systems. Typically the modules are divided into

the clock module, a series of pulse channel modules and a control module. The clock module has a master clock which may be operating within a frequency range of 10-20 MHz and this module provides the clock inputs to the pulse channels, sets the repetition rate of a given pulse sequence being generated which is achieved through a separate counter -timer circuit in-built and important of all, should start the pulse sequence. The pulse channel modules have the capability to produce pulses of variable width and the width variation may be done in an analog fashion using trigger pulses and **monostable** circuits or it may be digitally produced with help of a dedicated counter. The clock input from the clock module provides with counting rate and that determines the resolution of the pulse width generation. Other counters within this module, set the delay between pulses and a start trigger for the next pulse channel module in the series. In this type of programmers, invariably, the user interface is through thumb wheel switches or rotary switches. For a fairly complicated pulse sequence, the number of thumb wheels to be operated becomes unmanageable.

3. To alleviate these problems, hardware pulse programmers with software control were designed, and here the parameters, connected with a given pulse sequence, are programmable through a **μP-based** circuitry or a **μP-based** development board, the parameters of the experiments being stored in memory. Essentially, the **μP** replaced the cumbersome process of changing thumb wheel settings to set different parameters. The basic organization of this programmer is similar to

that of a microcomputer. We can identify the memory unit, the control logic circuitry and address counter. The data and instructions are stored in the memory, and the control and logic circuitry reads a given data from the location pointed by the address counter. Several authors have adopted this approach of software controlled hardware pulse generators [Ellet et.al., 1971; Matson, 1977; Aducci et.al., 1979; Mohr et.al., 1983; Ader et.al., 1978; Hale et.al., 1986; Saint-Jalmes et.al., 1982]. One finds slight differences in these approaches also. In one system, only the timing data is stored in the memory but not the instructions. A hardwired program selects these values sequentially to generate a particular sequence [Lapray et.al., 1976]. Some of them have the looping characteristic in built, such that, a burst of identical pulses can be produced [Caron et.al., 1978]. Aducci et.al., have used a Motorola M6802  $\mu$ P with few peripheral chips like the 4K EPROM, 2K RAM and a console connected to the  $\mu$ P via a serial interface controller chip M6850 and this configuration provides the necessary software support to a microprogrammable logic system called the sequencer and these two units are connected via parallel I/O port controller M6820. All the necessary information about the pulse sequence is stored in the RAM of the microprocessor and the actual generation of the levels, widths, etc. are implemented by the sequencer [Aducci et.al., 1979]. An excellent review on the various kinds of pulse programmers is available [Geiger et.al., 1980].

The last category of pulse programmers are the so called "software"

pulse generators. Here the time delay between pulses is essentially generated by the finite execution time of the program and this fact is used in the form of setting up "software counters" to count the necessary delay [Wright et.al., 1973; Huang et.al., 1977]. In some cases, instead of the execution time of instruction providing the delay, the computer clock gives a hardware interrupt to the CPU after the required amount of delay time, and thus a gating pulse synchronous with the interrupt is generated. In all the methods, except the last one, a dedicated, somewhat complex logic circuitry is needed to generate a pulse sequence, and a  $\mu$ P based system or a micro computer is inevitable to provide the necessary user interface. However, these PP-s have the unique advantage that almost any kind of pulse sequence can be produced with minimal hardware support from outside. Since the pulse programming is effected by the microcomputer, other useful functions of the computer like data collection and manipulation is integrated with the pulse programming.

The pulse programmer developed as part of the current work belongs to the last category. It is built around a stand-alone microprocessor development board which is interfaced via RS-232-C serial interface bus to a PC . Such an interface provides the following flexibility, namely, the pulse programmer can function either in the "slave" mode by receiving all relevant information connected with any pulse sequence from the PC or it can use the relevant pulse sequence data already stored by the user in its own memory and function independently.

## The 8085 based Pulse Programmer :

### SPECIFICATIONS

LOGIC AND CONTROL	Based on INTEL $\mu$ PD-8085 chip.
USER INTERFACE	Hex-pad input and 7 segment display
CONTROL LOGIC	Internal - Software delay counter External - using $\mu$ PD-8253
INTERFACES	Parallel Interface - using PPI 8255 Serial Interface - USART 8251
PULSE WIDTH GENERATION	Using 74123 buffered monostable circuit and buffered OR gates 7432
PULSE WIDTH CONTROL	Continuous variation with 10 turn potentiometer.
PULSE WIDTH RANGE	1.5 $\mu$ s to 100 $\mu$ s
DELAY RANGE	23 $\mu$ s to = 100 s
ERROR IN DELAY	$\leq 0.2 \%$
SYSTEM CLOCK FREQUENCY	3 MHz

## PULSE SEQUENCES GENERATED

1. Simple single pulse sequence with a variable time period

2. Inversion recovery sequence

$$(\pi - \tau - \pi/2) -- 5T_1 --$$

3. Saturation Burst sequence

$$(\pi/2 - \Delta - \pi/2 - \Delta - \dots) -- (\pi/2 - \Delta - \pi/2 - \Delta - \dots) --$$

4. Jeener-Brokaert sequence for  $T_{1D}$  measurements

$$(\pi/2 - \Delta - \pi/4 - \tau - \pi/4) -- \dots$$

5. Spin locking Sequence for  $T_{1\rho}$  measurements

$$(\pi/2 - P_{\text{spin-lock}}) -- \dots$$

4. Hahn echo sequence

$$(\pi/2 - \tau - \pi) -- 5T_1 --$$

5. CPMG sequence

$$(\pi/2 - \tau - \pi - 2\tau - \pi -) -- 5T_1 --$$

6. Stejskal - Tanner sequence ( $P_g \Rightarrow$  gradient pulse trigger)

$$(\pi/2 - \Delta - P_g - (\tau - \Delta) - \pi - \Delta - P_g) -- 5T_1$$

7. Liquid crystal sequence

*(all these pulse sequences are provided in Fig.B-3.1 and Fig.B-3.2)*

Note; 1. Appropriate trigger pulses are provided for the digitizer and amplifier units.

2. Upgradation to any other pulse sequence requires minimal effort as the available codes can be combined suitably to generate a given sequence.

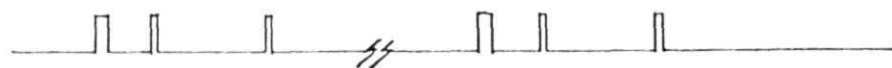
INVERSION RECOVERY



SATURATION BURST



JEENER · BROKAERT



CPMG



STEJSKAL · TANNER



— 3.1) Simple pulse sequences.



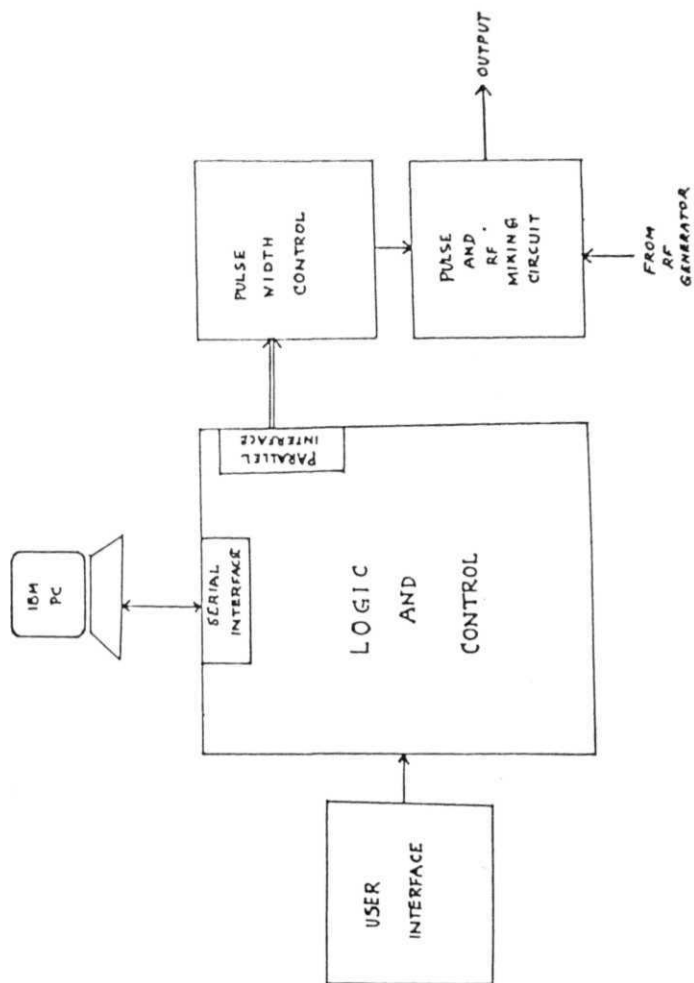


OTHER FEATURES : # Cassette interface for hardcopy of  
assembly codes  
# CRT Monitor and ASCII keyboard  
included - Monitor code provided  
# EPROM Assembler-Disassembler of 8085  
instruction set included  
# EPROM recorder available on board -  
for hardcopy backup of codes

The Block diagram in Fig.(B-3.3) gives a simple representation of the pulse programmer, and the pulse programmer is based on a minimal number of modular units, resulting in a simple construction.

#### LOGIC AND CONTROL UNIT :

All the information regarding the pulse sequence is processed in this module. This includes the CPU ( $\mu$ PD-8085) with its memory, the programmable timer/counter (IC 8253) and a few other passive components. Necessary information on the sequence generation is stored in the memory as data and the algorithm which generates a given pulse sequence is stored in the form of relevant 8085 instruction sets in the memory. In one method, where the sequence is entirely software driven, appropriate delay loops are executed within the program when the code is initialized and executed. The sequence can also be generated with the help of  $\mu$ PD-8253. The appropriate number corresponding to the delay to be



(B - 3.3) Block diagram of pulse programmer.

generated is loaded in the counter/counters of the 8253 and at the end of the delay counting, a hardware interrupt is sent to the CPU for a trigger pulse generation. With this method, we can achieve a better resolution for the delay increment.

#### USER INTERFACE:

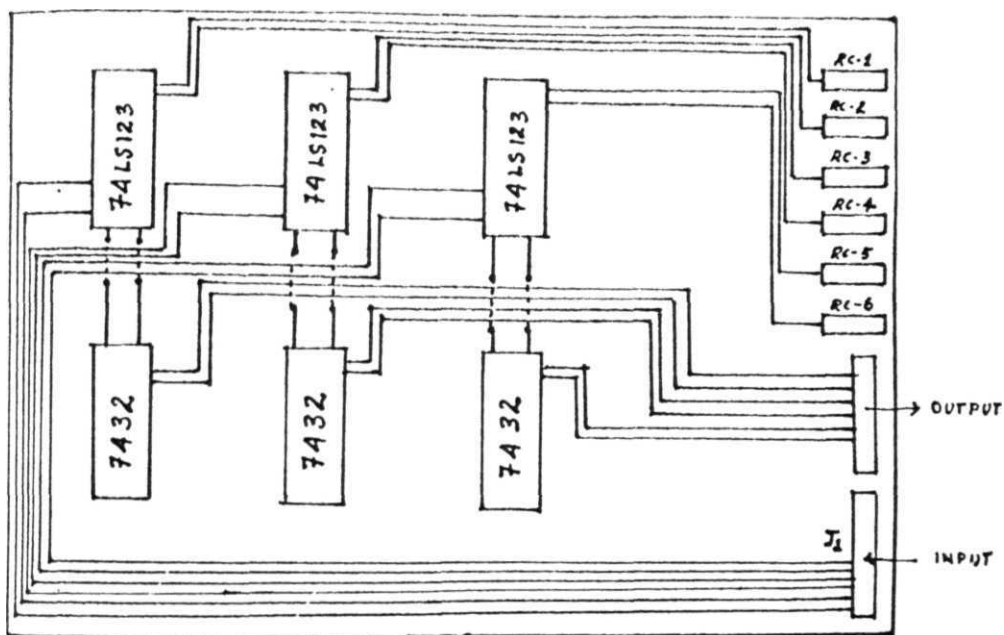
A set of "hexadecimal keys", along with some utility functions (like selection of the desired memory location or relocation of the contents of a set of locations to some other memory area), are available on the development board for the user to interact with the  $\mu$ P-system and a seven segment LED display is also provided. Both these functions are controlled by  $\mu$ PD-8279-5 keyboard/display controller.

#### PARALLEL INTERFACE :

The parallel port of the  $\mu$ PD system is controlled by the programmable peripheral interface (PPI),  $\mu$ PD-8255. The data and control registers are accessible by the host CPU and appropriate trigger pulses at the end of the necessary delay generation is sent through the output ports of 8255 to the pulse width control unit, where the appropriate pulse widths can be set.

## PULSE WIDTH CONTROL :

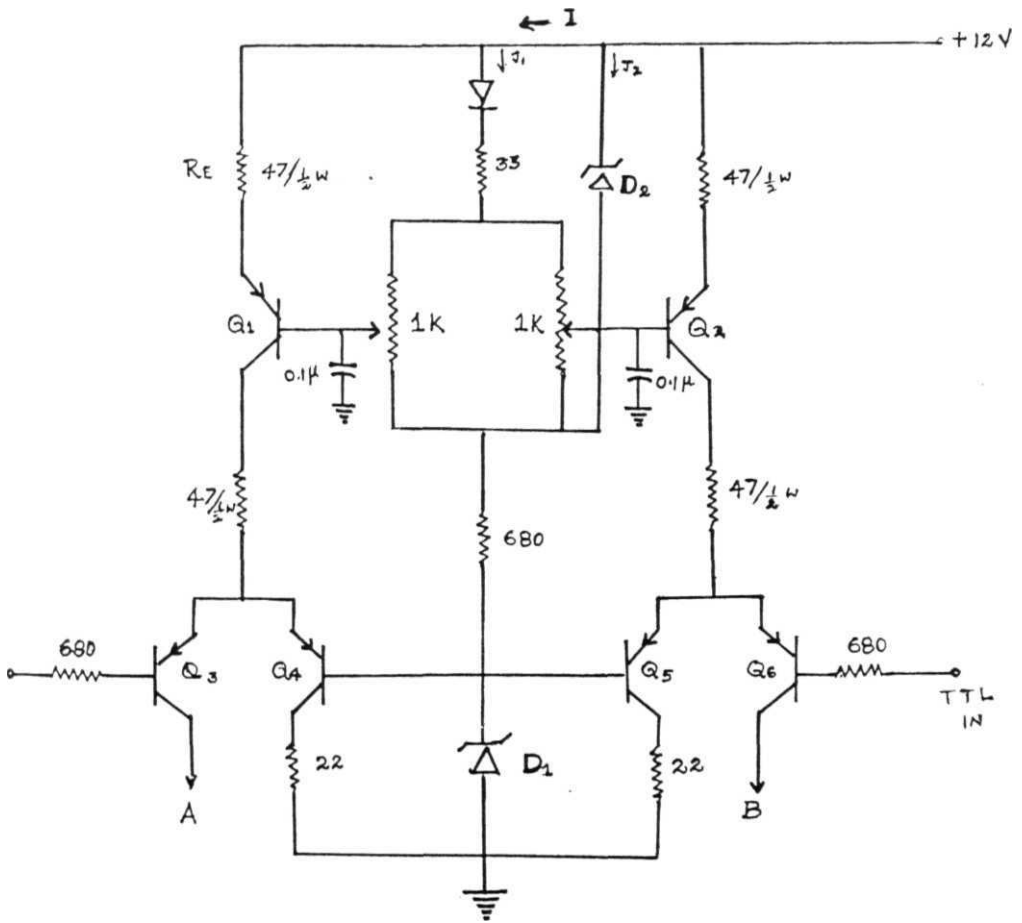
The schematic diagram of the circuitry in pulse width controller is provided in Fig (B-3.4). The task of the pulse width controller is to receive appropriate trigger pulses from the Logic and Control Unit and generate pulses of variable width. It is made of three 74LS123 buffered monoshot circuits which provides six independent channels, and the outputs at each of these channels are further buffered through the OR gates 7432. The OR gate circuits are also used to do the pulse mixing within the pulse programmer itself, for some simple two pulse sequences. Appropriate trigger pulses generated at the parallel port of the Logic and Control Unit is routed into the pulse width controller with help of the edge connector J . These pulses trigger the array of buffered monoshot **circuits**, and for each trigger input a pulse is generated whose width can be varied by a variable RC combination. In principle, by choosing a set of capacitors C, we can generate the desired large range of pulse widths. But in the present system, we have chosen a fixed value of C with a variable R provided by a 10-turn trimpot to achieve a maximum pulse width of 100  $\mu$ sec. The circuit has in built d.c. power supply for all the ICs. The whole circuit is housed in a sturdy metal casing and the outputs are brought out through BNC connectors, so that the desired pulses can be sent to the respective inputs in the spectrometer.



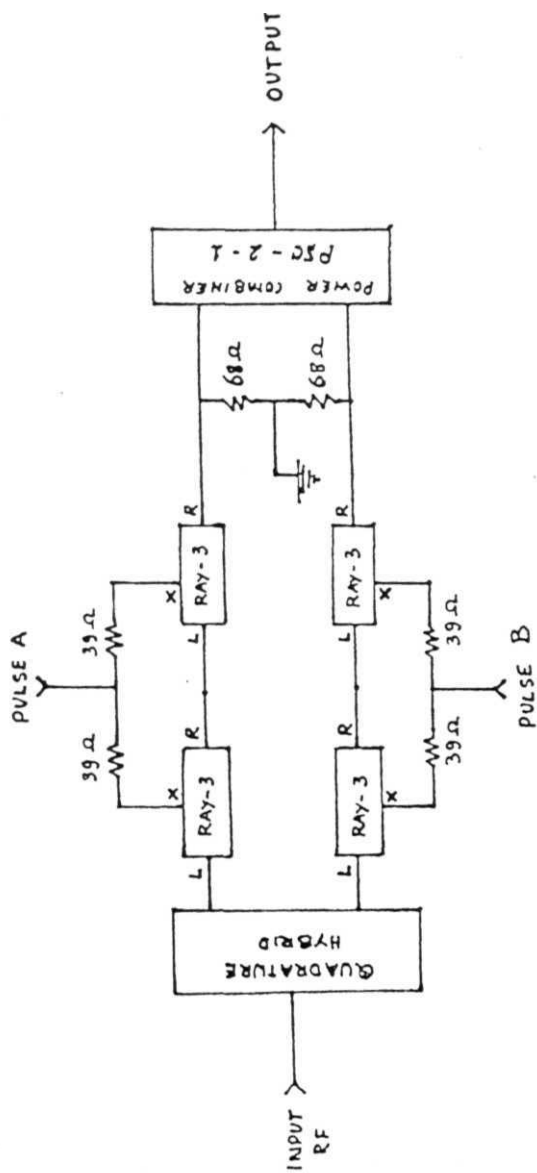
(B - 3.4) Schematic representation of pulse width controller circuit.

## PULSE AND RF MIXING CIRCUIT :

After the pulse sequence is generated, the pulses are used to gate r.f. voltages which are later amplified to high levels to be applied to the NMR probe and this module provides such an r.f. mixing facility. It consists of a combination of double balanced mixers and power combiners (Mini Circuits) (Fig.B-3.6) and a current driver circuit [ McLachlan, 1982] which is used to bias the double balanced mixers for the best ON/OFF ratio (a 80 dB) and the circuit diagram of the current driver circuit is shown in Fig.(B-3.5). In Fig.(B-3.6) we have shown two independent channels of mixers, but as can be made out from the figure this configuration can be extended to any number of independent channels of r.f. mixing, in a very simple way. The TTL pulses from the pulse sequencer is fed into the current driver circuit (Fig.B-3.5) and by adjusting the variable  $1K\Omega$  resistors, the mixing characteristics can be optimized. The outputs like A and B are fed into the DBM module (Fig. B-3.6) and the r.f. is fed to the input "L". The quadrature hybrid unit is shown to indicate the option that, if phase shifting of  $90^\circ$  is needed between two pulses, r.f. outputs of phase  $0^\circ$  and  $90^\circ$  can be tapped from this unit and mixed with the individual pulses. For such applications, these individual pulses are not mixed initially in the pulse width control unit and they are generated separately on individual channels and later mixed with the r.f. in the pulse and r.f. mixing unit, and this feature is taken care of by the appropriate program.



3.5) Current driver circuit to bias the Double Balanced Mixers.



(B - 3.6) Block diagram of pulse and r.f. mixing configuration.

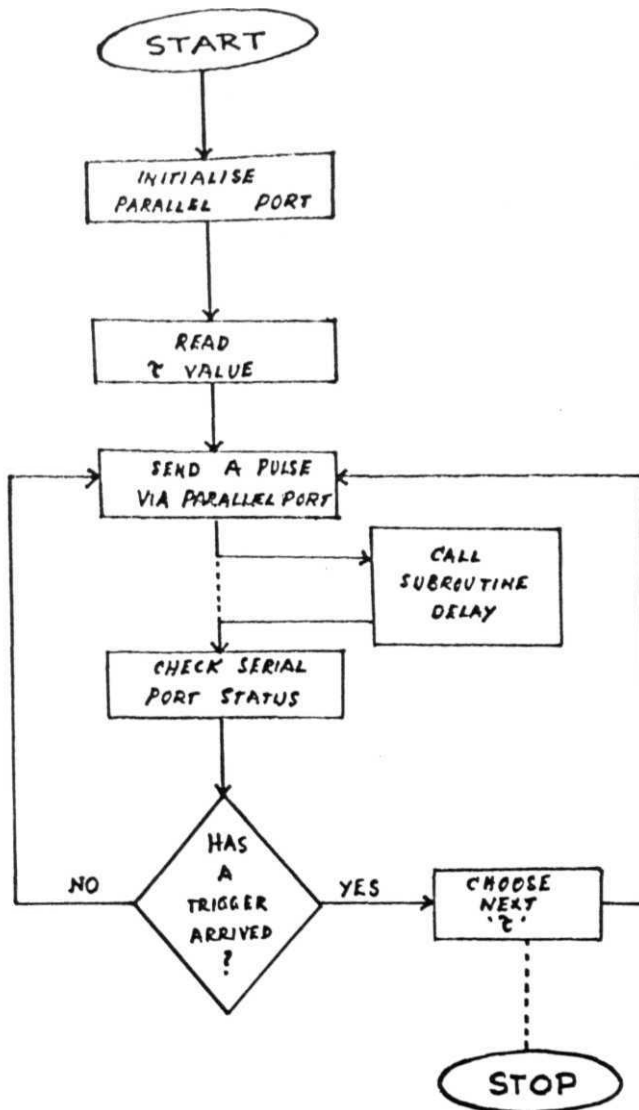


## SERIAL INTERFACE :

The serial interface provides the necessary interlink between the pulse programmer and an IBM PC-AT, which is being used as the master controller for the entire environment. All the assembly codes developed for the  $\mu$ PD controller are interfaced with other application programs written in BASICA language in the IBM PC-AT, such that, pulse generation is performed independently by the  $\mu$ PD programmer but it is synchronized with the other instruments in the spectrometer by communicating with the PC through the serial interface. In fact, with a small boot strap code loaded in the  $\mu$ P programmer, the entire assembly code pertaining to a particular pulse sequence can be loaded on to the memory of the  $\mu$ P from the PC-AT via the serial port. The serial port is built around the  $\mu$ PD-8251, which is also programmable from the host CPU. It has the maximum baud rate of 9600 but since data throughput need not be very high for the occasional control messages or information to be exchanged between the computer and  $\mu$ P-programmer, we have programmed it to operate at a low baud rate of 300. For such a small rate, hand shake is not necessary with the computer and this makes the wiring as well as the programming much simpler. In this configuration itself we have found the interface to work without any problems.

It may be instructive at this juncture to look at some programs for generation of some specific pulse sequences. Few of these programs are provided in Appendix-I. For each program a flow-diagram is given tracing the logic of the program, and the corresponding assembly program is

provided next to it. Considering, for example, the simple problem of generating a single pulse sequence, the corresponding flow diagram is given in Fig.(B-3.7). The flow-chart is self explanatory and the steps given in the flow chart are implemented in the form an assembly program derived from the instruction set of 8085, and this programme is provided in (Appendix I). With this program, the PP generates the pulse sequence with a set of tau values stored in specified locations of memory. The pulse sequence is generated ad infinitum and advancing from one tau value to other is done through an interrupt communicated to the processor by the master controller, which is the PC, via the serial port. Here the delay is generated in a separate subroutine. Division of the programs into such general modules is quite desirable, as such routines with general applicability can be readily adopted into other programs where similar functions may be needed. Several other programs were developed as a part of developing the pulse programmer, and a sample of some important programs are all provided in **Appendix-I**. The programs provided in the appendix are all recorded on cassette for a hard-copy storage. These programs can be either retrieved from the cassette and loaded onto the appropriate memory locations and executed, or they can be loaded by the master controller, the IBM PC-AT, via the serial interface also. Separate BASICA codes are developed, to interface the  $\mu P$  to the PC via the serial communication interface and these programs are provided in **APPENDIX-II**, and are discussed under the heading 'SOFTWARE' in the text, later.



(B - 3.7) Flow diagram of one pulse sequence.

# AUTOMATION

The need for automation of a group of instruments like the pulsed NMR spectrometer for control of the experiment, unaided data collection, besides analysis and display of data etc., is well recognized. But one of the major challenges in achieving this task seems to be to interface different kinds of measuring instruments and make them transfer data/information among them in a reliable fashion. Initially, different manufacturers were defining their own standards of communication and interface between their own instruments so that it was not possible to interface any two arbitrarily chosen commercial instruments for data communication. With the advent of "General Purpose Interface Bus" (GPIB) defining an industry standard for the connection of various measuring instruments and computers, such interfacing of different instruments was made possible.

## FEATURES OF GPIB :

The GPIB environment is basically made of instruments which are classified as Talkers, Listeners and Controllers. Talkers are those which only transmit data, Listeners are those which only receive data and the Controller is both a Talker and Listener, and further it controls all the activities in the bus. For a given Controller there can be a total of 15 devices, Talkers and Listeners put together. Each device is connected to the other or to the Controller with an IEEE cable whose maximum length can be 2m only. The recommended standard says

that the total length of the cable must not exceed 20 meters within the entire environment.

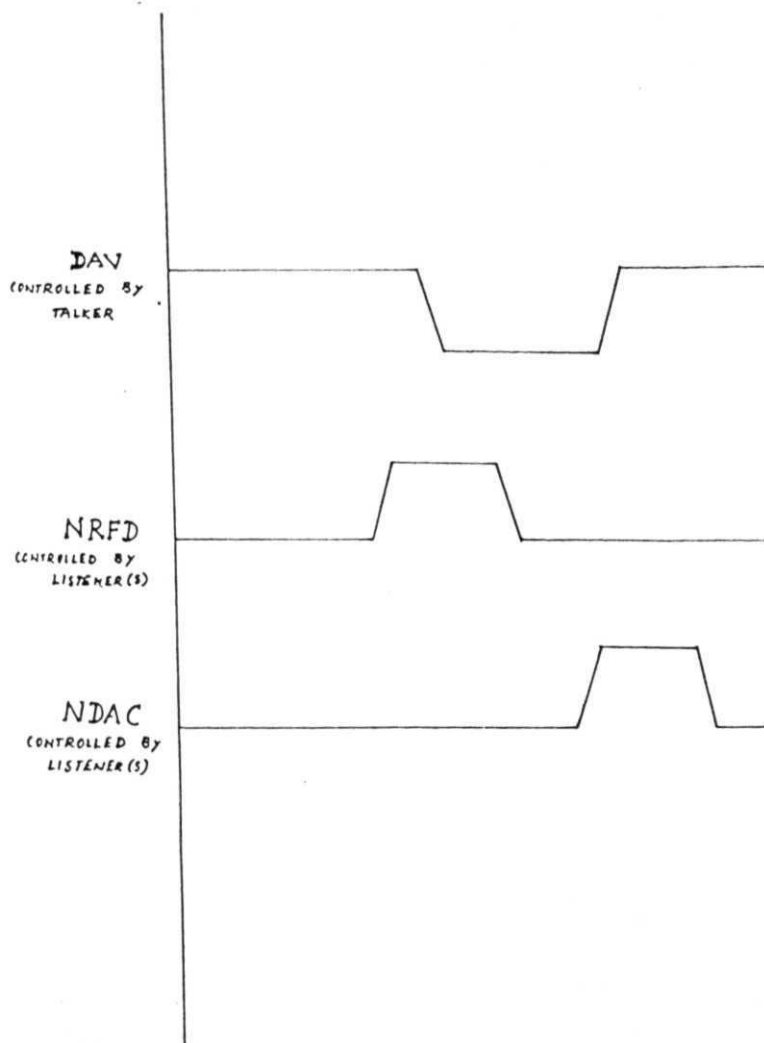
Each device is assigned a **"primary address"** and this address can either be set by dip switches on instruments or one can set the address using software commands sent to the instrument. It is the Controller which decides which device should transmit or "talk" and which are all the devices which ought to receive the message or "listen". There can be more than one Listener in the environment but only one instrument is allowed to be a Talker at a given time. The GPIB is a 24 line bus with 8 dedicated lines for data transfer (contrast the fact that this type of data transfer is bit parallel byte serial in comparison to the serial interface which is bit serial byte serial). It has 3 hand shake lines and 5 bus management lines. It is important to note that all the lines in GPIB are active LOW. This means that, to assert a signal on a given line a device has to make that line 0 V from 5 V.

#### HANDSHAKE PROTOCOL :

For a reliable data transfer a handshake protocol is needed in the GPIB environment and this facility is provided. A handshake protocol is nothing but an exchange of electrical pulses via dedicated conducting lines between instruments to provide a synchronization of the instruments with one another, for data transfer. Normally a handshake protocol needs at least two lines out of which one is an input and the other is an output line. The device can place a signal on the output

line and wait for acknowledgement from the other device. The moment such an acknowledgement is received, the handshake, for **this simple** purpose, is complete. After this, successful data **transfer can take** place on the bus. The handshake lines in the case of GPIB are DAV (Data Valid), NRFD (Not Ready For Data), NDAC (Not Data ACcepted). The complete handshake sequence for one data byte is shown in Fig.(B-3.8). DAV is the signal controlled by the active bus Talker. It is used to communicate the state of the bus data lines. When this signal is low, the data on the data lines is valid and have had time to settle to the correct logic levels. NRFD is the signal that the active Listeners use to hold off transmission of a byte until all are ready to receive. NDAC is the signal used by the active Listeners to force the Talker to hold data on the data lines until all active Listeners have had time to accept the information. The sequence of events shown in Fig.(B-3.8) for the bus handshake is simple:

1. NRFD goes high, signifying that all Listeners are ready for the next piece of data.
2. The Talker recognizes this by placing the data on the data bus and driving DAV low after waiting for the data to settle.
3. **Listeners** acknowledge by driving NRFD low.
4. When all of the Listeners have acquired the data, they allow NDAC to go high, signifying their acceptance.
5. The Talker then releases DAV to end its part of the handshake.
6. The Listeners then pull NDAC low to prepare for the next bus transaction.



- 3.8) Handshake protocol in GPIB.

## THE BUS MANAGEMENT LINES :

To manage the GPIB environment, the Controller sends several commands to all the devices and these commands can be divided into uniline commands and multiline commands. The uniline commands are simply signals ascertained on the dedicated lines of the bus management. The uniline commands or functionalities of the bus management lines can be seen as follows :

1. **ATN** (Attention) - The ATN line is one of the important management lines. The state of the ATN line determines whether Controller information on the data is to be considered data or a multiline command as described below.
2. **IFC** (Interface Clear) - Setting the IFC line true (low) causes the bus to go to a known state.
3. **REN** (Remote Enable) - Setting the REN line low sends the REN command. This sets up instruments on the bus for remote operation.
4. **EOI** (End or Identify) - The EOI line is used to send the end signal which usually terminates a multi-byte transfer sequence.
5. **SRQ** (Service Request) - The SRQ line is set low by a device when it requires service from the Controller.



One of the important features available in the GPIB standard is the serial polling function. When an instrument or instruments request(s) attention of the Controller, the Controller begins a Serial Polling sequence and gets a status word from each of the instruments which had requested for service. Depending on the information available in the status word, the Controller takes necessary action.

#### MULTILINE COMMANDS :

The multiline commands are sent by the Controller on the data bus by ascertaining the ATN line. These commands can be further divided into Universal, Addressed and Unaddressed groups.

##### *Universal Commands*

**LLO** (Local Lockout) - This command is used to lock out front panel controls on devices so equipped.

**DCL** (Device Clear) - After a DCL is sent, instrumentation equipped to implement the command will revert to a known state. Usually, instruments return to their power up conditions.

**SPE** (Serial Poll Enable) - The SPE command is the first step in the serial polling sequence, which is used to determine which instrument has requested service with the SRQ command.

**SPD** (Serial Poll Disable) - The SPD command is sent by the Controller to remove all instrumentation on the bus from the serial poll mode.

### *Addressed Commands*

Addressed commands are multiline commands that must be preceded by a listen command derived from the device's primary address before the instrument will respond. Only the addressed device will respond to each of these commands.

1. **SDC** (Selective Device Clear) - The SDC command performs essentially the same function as the DCL command except that only the addressed device will respond. Instruments usually return to their default conditions when the SDC command is sent.
2. **GTL** (Go to Local) - The GTL command is used to remove instruments from the remote mode of operation. Also, front panel control operation will usually be restored, if the LLO command was previously sent.
3. **GET** (Group Execute Trigger) - The GET command is used to trigger devices to perform a specific action that depends on device configuration. Although GET is considered to be an addressed command, many devices respond to GET without being addressed.

### *Unaddressed Commands*

The two unaddressed commands are used by the Controller to remove

all Talkers and Listeners from the bus simultaneously. ATN is low when these multiline commands are asserted.

1. **UNL** (Unlisten) - All Listeners are removed from the bus at once when the UNL command is placed on the bus.
2. **UNT** (Untalk) - The Controller sends the **UNT** command to clear the bus of any Talkers.

Apart from these specific commands, there are other addressed commands which are MLA (My Listen Address), MTA (My Talk Address) and these commands are derived from the primary addresses of the devices.

After looking at the various commands, we can see the typical way by which the Controller will be able to coordinate a byte transfer and in the case of service request, how the Controller carries out a serial poll of all the devices. For data transfer, the Controller first sends an IFC command to clear the bus and asserts the REN line to place the devices in remote operation. After this, UNL and UNT commands are placed on the data bus by asserting the ATN line, and the Controller then places the MTA for the specific device, by placing one by one the MLA command for all the Listeners. During these commands the ATN is line is still asserted. After completion of the task, the Controller unasserts ATN line. Now, the Talker and Listener(s) communicate to transfer data. At the end of all data transfer, the Talker is configured to assert the EOI line, which tells **the** Controller that the transaction is complete

and thus the Controller places the UNT and UNL commands on the line and thus the bus is ready for the next set of data transfer.

When devices have requested for service by asserting the SRQ line, the Controller enters into serial polling in the following way.

1. The Controller sets the ATN line true.
2. The SPE (serial poll enable) command is placed on the bus by the Controller.
3. A device on the bus is addressed to talk.
4. The instrument then places its status byte on the bus to be read by the Controller. The ATN line is made false at this point.
5. The Controller then sets the ATN line low and places SPD (serial poll disable) on the bus to end the serial polling sequence.
6. Steps 3 to 5 are repeated for all the other devices.

#### Device Dependent Commands :

All the commands, discussed so far pertain to the basic control of the bus. Now in order to provide a facility by which the Controller can communicate with a specific device, certain "device dependent commands" are **needed**. Device dependent commands are string of characters sent by the Controller to a particular device as data. The device interprets such a string as a command and performs a specific function. As examples we can consider two instruments, like the TEKTRONIX 2230 digitizer/signal averager and the **Keithley** 195A digital multimeter. In

the case of the 2230 system, when a string of characters given by "CH1?" is sent on the data bus, the scope responds by placing on the data bus the following information "CH1 VOL:<nl>, COU:AC". The string "CH1?" is interpreted by the digitizer as a query as to what are the current settings in channel 1 of the scope and sends a reply back to the Controller indicating that the VOLTS/DIV setting is n1 and the coupling is AC. In the case of DMM 195A, a string like "R1X" will be interpreted as a command to set the resistance measurement range. Thus, different instruments treat different sets of characters as device dependent commands. As of now, there is no accepted industry standard for the format of device dependent commands but some manufacturers like TEKTRONIX have defined their own Codes and Formats Standard for device dependent commands. Few examples from this standard are considered below.

Each command has what is called a "header" and this header is as self explanatory as possible for the function it performs.

example :                   INIT

a command which initializes the scope. A header may have an "argument" also which is to be separated from the header with a space.

example :                   SAVEREF REF4

When argument itself requires another argument, the two arguments are

separated by a colon.

example :                   ACQ REP:SAMPLE

Where the header has multiple arguments, the arguments (or argument pairs, if the argument has its own argument) must be separated by commas, such as

example :                   DAT ENC:BIN,CHA:CH2

Multiple commands can be put in one line and each command can be separated from the other with a semicolon.

example :                   DAT ENC:BIN,CHA:CH1;WFMPRE

Here DAT is the header of first command which has multiple arguments and WFMPRE **is** the header of another command.

#### GPIB PROGRAMMING IN IBM-PC ENVIRONMENT :

Though stand alone GPIB Controllers are available from commercial sources, integrating the ability of a GPIB Controller into a computer has obvious advantages. Apart from the controlling ability, the computer's computational and programming power can be put to good use. Standard circuit boards called "Add on" cards are available which can be connected to one of the expansion slots of the IBM-PC, which makes the

PC **function** as a GPIB Controller. Some of the standard cards available in the market are the PC-II and PC-IIA cards manufactured by National Instruments Inc. In the **configuration** implemented for the present work, a National Instruments PC-II card was used. This card is treated as any other peripheral device attached to the computer and a device driver need be placed in the **configuration** table of the computer before booting. The manufacturer provides the necessary device driver and also a high-level language interface program, and by far the most popular high level language being used for this purpose is BASICA. The flexibility of BASICA to perform even machine level operations with ease and the impressive graphics manipulation capabilities makes it one of the ideal languages for GPIB programming. Device drivers in other languages like PASCAL and C are also available.

*The BASICA programme :*

Appendix - II gives the listing of some of the programs developed to control and perform experiments in the GPIB environments along with the  $\mu$ P-based pulse programmer. Every BASICA - GPIB program has a declaration block and in fact this is provided as a separate file along **with the driver**. In the programs listed, one normally finds this declaration block to be from statements 1 to 6. This declaration block loads a machine level routine known as the "BIB.M" into specific location of the system RAM and this works in cooperation with the BASICA interpreter. This routine acts as the translator between the BASICA statement calls and the machine level language driver. Before one

attempts to write a program, one configures a table of the GPIB environment with a utility called `IBCONF.EXE`. This utility allows one to specify, for each device, all its important characteristics starting from the primary address of the device. Thus, the table gives a realistic information to the device driver about what the devices are, which are connected in the bus. The device driver is made of a number of routines, each one performing a specific task of I/O or control between the Controller and the device(s). The manual gives a complete listing of all the routines. Depending on the level of operation, these routines can also be divided into categories. With the group of routines at the lowest level, we can perform some of the bus management tasks like setting the REN line, for instance. At the highest level, certain routines just take the BASICA variables as operands, which are either used to send a string of data to a device or receive data from a device and the routine takes care of all the handshake formalities and other control tasks to complete the communication automatically.

Immediately after the declaration statements, the functions `IBFIND` are executed which return into the integer variables like `BRD%`, the so called device descriptors, which are derived from the primary address of each device. Even the GPIB board has to be accessed via `IBFIND` and a device descriptor value is returned in the variable `BRD%`. After the device descriptors are assigned to each device on the bus, all the functions are accessed through the basica `CALL` statements and each of these statements have two parameters. The first one is the device descriptor of the particular instrument we are accessing, and the second



one will be either a string variable (e.g. `CMD$`) or a numerical variable (e.g. `v%`), which will be taken as the argument for the subroutine functions. The string variable will normally contain the device dependent command strings. For instance, to write a command like "CH1? VOL" onto the 2230, we assign this string to a variable called `CMD$`, say, and we execute

```
CALL IBWRT (SCOPE%,CMD$)
```

The function then completes the task of placing the string on the bus to be read by the scope. Here `SCOPE%` contains the device descriptor for the TEK 2230 scope. After this function call if we execute

```
CALL IBRD (SCOPE%,ANSS$)
```

the response to the previously sent query will be read into the variable `ANSS`. It is a remarkable fact that just to perform I/O between devices, these are the only two function calls needed.

#### ERROR CAPTURE AND STATUS MONITORING :

When a reasonably complex program is developed with many devices on the bus, it is desirable to have some error capture and status monitoring facilities and the handler provides this facility. For the execution of each function, a status variable `IBSTA%` is updated. Each bit in the `IBSTA%` variable being set or reset conveys a specific

condition in the bus. For example, if the data transfer is successfully completed, then the eighth bit is set. If a device has requested for service by asserting the SRQ line, the 12th bit in **IBSTA%** is set. If an error has occurred, then the 15th bit of this variable is set. The program should be coded in such a way that, after finding an error condition, it must go and examine another variable called the **IBERR%**. Each bit in **IBERR%** conveys a specific error, which occurred in the bus. It may be worth mentioning that some of the Controllers provide the facility that the SRQ assertion can be brought into the BASICA program as a hardware interrupt using the "ON PEN ..." statement. Such a facility is implemented in PC-IIA, for instance. Another feature implemented with the handler or driver is the auto-serial polling facility by initiating which the program can be made to automatically poll the devices at regular intervals and collect the status bytes from the respective devices into appropriate variables.

Some of the programs are provided in the **Appendix-II**. The subunits are configured, and programs are developed such that even in the absence of the  $\mu$ P based pulse programmer, standard experiments like T measurements can be carried out **with** all the units entirely under the GPIB environment, provided of course they are all GPIB compatible (**Appendix -II**). One can further develop other useful programs performing different tasks, like retrieving waveforms from the digital storage oscilloscope onto disk files and performing signal averaging to improve the **S/N ratio**, etc. The GPIB facility developed **by the author** has been used successfully in other applications like automation of a Field

Cycling NMR spectrometer and pulsed NQR spectrometer, in the same laboratory.

#### SOFTWARE DEVELOPMENT

Apart from the programs developed in specific reference to the pulse programmer development and the automation environment, an integrated approach was taken to write several other programs to analyze the data collected from specific experiments and provide outputs of them in presentable formats. A list of program names and their categorization are provided in Appendix - III.

The software which was developed as part of this work can thus be categorized under three broad headings. They are:

1. 8085 - Assembly programming
2. BASICA language programming
3. ASYST language programming

Programmes of first type are presented in Appendix-I. BASICA programs are of two types. The first type pertains to the programming for automation of the spectrometer. The second contains programs to extract  $T_1$  values from the magnetization recovery data from standard experiments like the inversion recovery or saturation burst, and also non-linear least square **fit** programs to fit the  $T_1$  data as a function of temperature to a specific microscopic model. These programs were written using the grid and gradient search algorithms. A group of programs **were**

also written to do simple manipulation of data like sorting of a data file and to plot the data in desired formats. Finally, the third type of programs written in the ASYST scientific programming language. ASYST is a commercial software which is made of compact scientific subroutines and it has the complete structure as that of any other programming language. Examples of these programs are available in **Appendix-III**. We have written programs in ASYST programming environment also, to fit our T data to the microscopic models. Because, it borrows all the salient features of the important programming languages like, FORTRAN, PASCAL and **BASICA**, the ASYST code is very compact and very quick in running. It works on an IBM compatible PC-AT with 512 Kbytes of base memory and with a math coprocessor like the INTEL 80287.

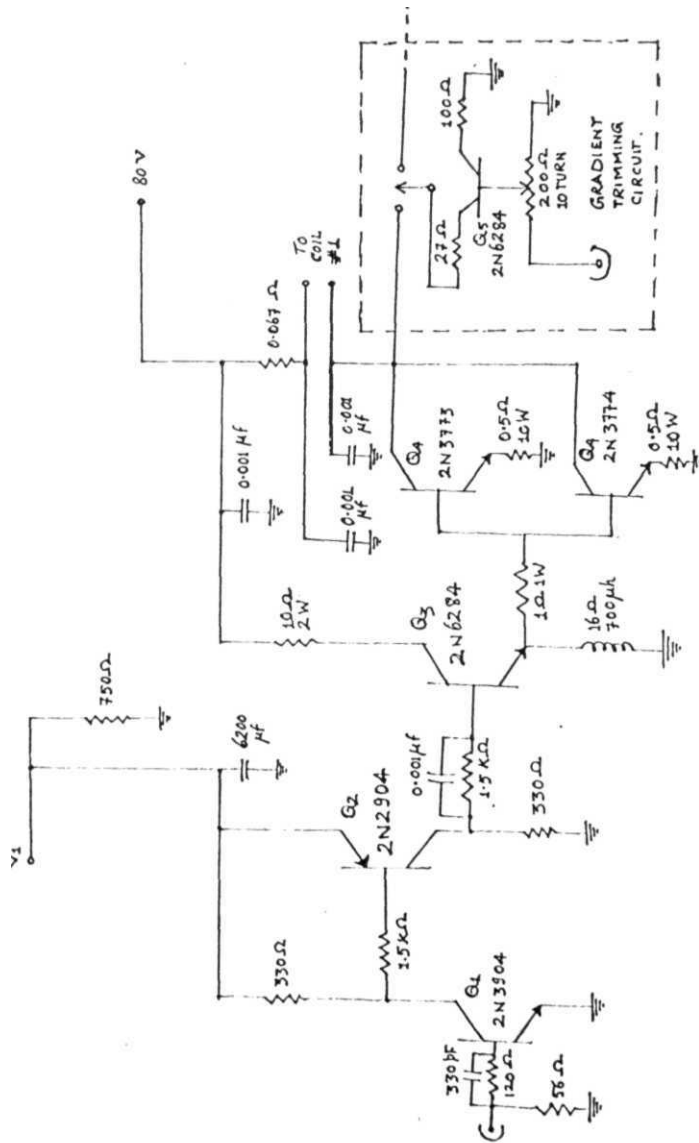
With this effort by the author on the development of a software controlled pulse programmer and different types of programs to control the experiment, collect and process data, as well as analyze and display relaxation measurements, the available pulsed NMR instrument could be upgraded to perform an automated experiment **with** reasonable flexibility and convenience in one environment.

## D I F F U S I O N      M E A S U R E M E N T

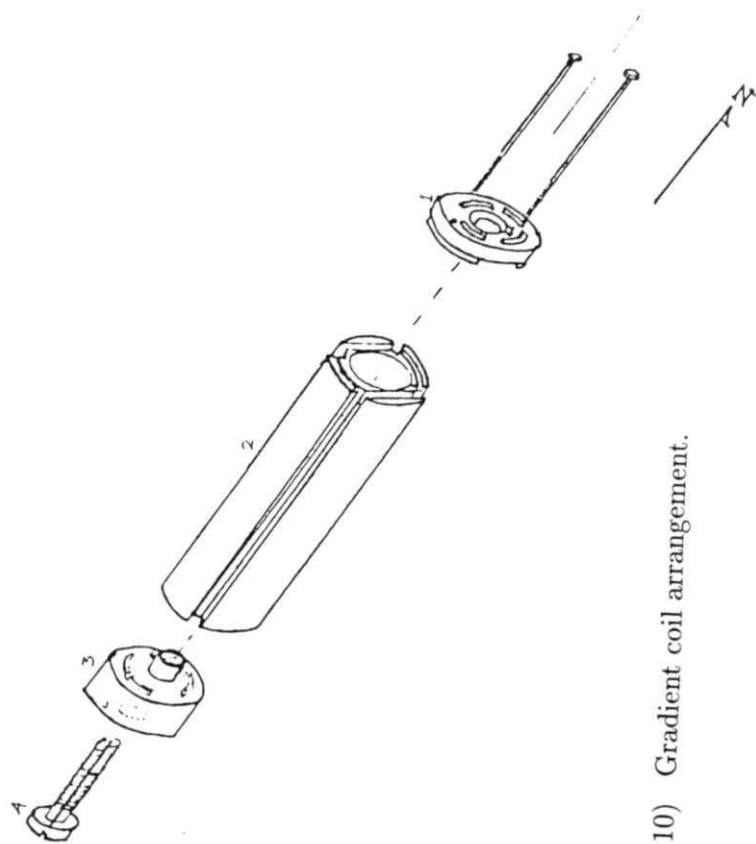
As a part of developing assembly level programs for somewhat involved pulse sequences also, programs are developed to effect measurements on translational diffusion based on nuclear spin echo modulations in the presence of pulsed field gradients, (including the

sequence for measurements in liquid crystals [Blinc et al., 1971; Zupancic et al., 1974]). In the process, the necessary hardware (like field gradient coils, power driver etc.) is also fabricated.

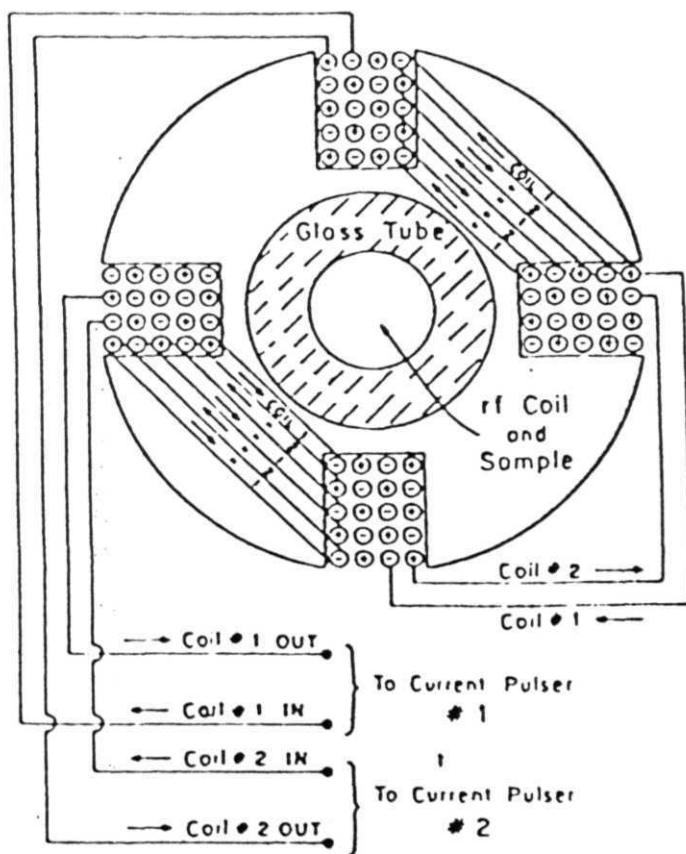
For generating large field gradients to enhance the sensitivity of the diffusion apparatus, a circuit which can send large pulses of current to a pair of Helmholtz coils were needed. For this purpose, we have adopted the electrical and mechanical design reported by Karlicek and Lowe [Karlicek et.al., 1980], which was originally intended for diffusion measurements in solids with large bulk susceptibility. Fig.(B-3.9) shows the circuit diagram of one of the two current pulsers, which are used in the generation of large magnetic field gradients. Fig.(B-3.10) shows the gradient coil arrangement used to generate the gradients across the sample and Fig.(B-3.11) provides a view of the cross-section of this arrangement. It consists of a cylindrical Teflon former in which, four vertical grooves of 1.5 mm width and 2.5 mm depth are made, which are at 90 to each other. About 20 turns of two independent set of wires (SWG 33) are wound in the opposite directions into the grooves so that, d.c. or pulsed field gradients in the opposite senses can be obtained from these two sets of coils, when appropriate d.c. or current pulses are applied to them. The teflon former has a cylindrical hole coaxial to the axis of the cylinder and its inner diameter is 6 mm. A support glass tube is inserted into this hole in which the sample is kept with the r.f. coil wound on it. Standard signals have been tested in the presence of these field gradient pulses. Applying a field gradient modifies the FID as well as the spin echoes,



(B - 3.9) Current pulser circuit for diffusion apparatus.



(B - 3.10) Gradient coil arrangement.



(B - 3.11) Cross section of gradient coil.



and the signal takes the shape of a Bessel function, approximately. The distance between the adjacent nodes of the wiggles gives us an estimate of the field gradient strength [Murday, 1973]. Our preliminary measurement on water and benzene showed that, we could get a field gradient of about 250 Gauss/cm with an application of 3 Amps of d.c. current.

The d.c. sources used for pulsing the current in the circuit are an array of batteries used in automobiles. The circuit (Fig.B-3.9) consists of an inverting amplifier formed by  $Q_1$  and  $Q_2$  and a Darlington type current amplifier made up of  $Q_3$  and  $Q_4$ . The bias to the Darlington configuration can be varied and in effect the current delivered to the helmholtz coils can be varied by adjusting the bias of the inverting amplifier configuration  $V$ . The input  $I$  is only to trigger the pulser to turn the inverting amplifier on and this is derived from the source of the pulse programmer. Thus it can be seen that the pulse amplifier is operated in its extreme operating regions, namely the cut-off and saturation regions. This circuit was fabricated and tested successfully.

Now it remains to apply the relevant pulse sequence to different systems to measure diffusion coefficients and calibrate the unit for optimal performance. Since the pulse programmer is readily equipped with the necessary pulse sequences to measure diffusion coefficients, both in liquids (like the CPMG and Stejskal and Tanner sequence), as well as liquid crystals (the liquid crystal sequence, refer to Fig.(B-3.2)), the above arrangement is in principle ready for use. However, necessary

effort is still required to standardize and calibrate this set-up for regular diffusion measurements.

## REFERENCES

- (B-3.1) ADER R.E., A.R. LEPLY AND D.C. SONGCO, *J.Magn.Reson.*, 29, (1978) 105
- (B-3.2) ADUCCI D.J., P.A. HORNING AND D.R. TORGESON, *Rev.Sci.Instrum.*, 48, (1977) 661
- (B-3.3) ADUCCI D.J. AND B.C. GERSTEIN, *Rev.Sci.Instrum.*, 50, (1979) 1403
- (B-3.4) BLINC R., V. DIMIC, J. PIRS, M. VILFAN AND I. ZUPANCIC, *Mol.Cryst. Liq.Cryst.*, 14, (1971) 97
- (B-3.5) CARON F. AND R.F. HERZOG, *J.Magn.Reson.*, 31, (1978) 357
- (B-3.6) CONWAY J.L. AND R.M. COTTS, *Rev.Sci.Instrum.*, 48, (1977) 656
- (B-3.7) ELLET J.D. jr., M.G. GIBBY, U. HAEBERLEN, L.M. HUBER, M. MEHRING, PINES A. AND J.S. WAUGH, *Adv.Magn.Res.*, 5, (1971) 117
- (B-3.8) FRANCONI C. AND M. TERENCE, *Rev.Sci.Instrum.*, 41, (1970) 456
- (B-3.9) GEIGER A. AND M. HOLZ, *J.Phys.E : Sci.Instrum.*, 13, (1980) 697
- (B-3.10) HALE M.E., H. PEEMOELLER AND R.A. SHARP, *Rev.Sci. Instrum.*, 57, (1986) 689
- (B-3.11) HUANG S.G. AND M.T. ROGERS, *Chem. Instrum.*, 8, (1977) 17
- (B-3.12) KARLICEK AND I.J. LOWE, *J.Magn.Reson.*, 37, (1980) 75
- (B-3.13) LALANNE P. AND S. ELETR, *Rev.Sci.Instrum.*, 41, (1970) 71
- (B-3.14) LAPRAY C., A. BRIGUET, J.C. DUPLAN AND J. DELMAN, *J.Magn.Reson.*, 23, (1976) 129
- (B-3.15) LIND A.C., *Rev.Sci.Instrum.*, 43, (1972) 1800
- (B-3.16) MATSON G.B., *J.Magn.Reson.*, 25, (1977) 477
- (B-3.17) McLACHLAN L.A., *J.Magn.Reson.*, 47, (1982) 490
- (B-3.18) MOHR G.A. AND C.M. EDWARDS, *Rev.Sci. Instrum.*, 54, (1983) 1238

- (B-3.19) MURDAY J.S., *J.Magn.Reson.* , 10, (1973) 111
- (B-3.20) SAINT-JALMES H. AND Y. BARJHOUX, *Rev.Sci.Instrum.*, 53, (1982) 1
- (B-3.21) SHENOY R.K., J. RAMAKRISHNA AND R. SRINIVASAN, *J.Phys. E: Sci.Instrum.*, 9, (1976) 779
- (B-3.22) TAYLOR D.G., S. BOOTH AND P.S. ALLEN, *J.Phys.E: Sci.Instrum.*, 7, (1974) 105
- (B-3.23) WRIGHT D.A. AND M.T. ROGERS, *Rev.Sci.Instrum.*, 44, (1973) 1189
- (B-3.24) ZUPANCIC I., M. VILFAN, M. SENTJURC, M. SCHARA, F. PUSNIK, J. PIRS AND R. BLINC, *Liquid Crystals and Ordered Fluids*, vol.2, Plenum Press, (1974) 525

*SECTION C*

*NMR INVESTIGATIONS ON*  
**TRIS (ALKYLAMMONIUM)**  
**NONAHALOGENO DIBISMUTHATES**

## SECTION C

### PART 1

#### REVIEW OF $A_3M_2X_9$ COMPOUNDS

**Alkylammonium** halogeno **bismuthates** investigated in this study have the general formula  $[(CH_3)_nNH]_3Bi_2X_9$ , where  $n$  varies from 0 to 4 and  $X$  is Cl, Br and I and belong to a general family  $[(CH_3)_{4-n}NH]_3M_2X_9$ , where  $M$  can be Bi or Sb. The structure of these compounds shows considerable variety (1-D chains, 2-D layers etc.) and the nature of cations as well as the specific halogen in the compound are known to play an important role in determining the structure of these compounds [Jakubas et al., 1990a]. Investigations using different physical techniques show that the cations are situated in the free space available between layers of anions and that they exhibit reorientational motion. The order-disorder type structural phase transitions most of these compounds exhibit are found to be related to such reorientational motions of the cations. Proton NMR measurement is one of the powerful techniques to investigate the structural and dynamic properties of these compounds, and the results of such resonance and relaxation investigations are presented in the following sections. This section begins with a brief survey of some interesting related aspects of  $A_3M_2X_9$  compounds based on investigations using other physical techniques.

#### BONDING AND STRUCTURAL CONSIDERATIONS :

A lkyl ammonium substituted compounds belonging to the  $A_3M_2X_9$  family

exhibit different structural **configurations** but their important common characteristic is that each anion is strongly bonded to its immediate neighbours and such cooperative bonding leads to chain and layer structures of the anions with infinite expanse, though such formations are not unique to the  $A_3M_2X_9$  family alone. The formation of different structures in these compounds are determined by many factors including the type of bonding between the atoms and geometrical and space filling considerations in an infinite lattice, among others. The detailed understanding of such structures and the different factors which govern their formation is a subject of study in structural chemistry. To appreciate these factors in the context of the  $A_3M_2X_9$  family, we shall look at some ideas related to the bonding among atoms and some basic aspects of formation of solids from this point of view.

#### Bonding among atoms :

Out of the different types of bonding schemes found in molecules some important ones relevant for the present purpose are outlined below :

- (i) One of the commonly encountered bonds is the ionic bond or the polar bond. This bond forms between charged atoms or groups of atoms. The ionic bonds form between highly electropositive and electronegative elements.
- (ii) The next important type is the covalent bond, formed by the sharing of two electrons by the bonding partners. It is observed that this kind of bond is most favourably formed in the case of elements which do not differ greatly in their electronegativity.

(iii) Metallic bonds form a separate class found in metals and alloys.

Here, there **is** a complete **delocalization** of some of the valence electrons, unlike the covalent bonds.

(iv) In forming a crystal, the weak inter atomic forces due to Van der Waal's interactions play a dominant role and there are many cases where groups of atoms are held together by such forces.

(v) Another important class of bonds are the hydrogen bonds, which are special cases of Van der Waal type bonds. Hydrogen bonds form mostly between elements of strong electronegativity. The bond is formed between two like, or unlike, atoms via the hydrogen atom like  $N \dots H \dots O$ ,  $O \dots H \dots O$ . In most cases, the lone electron pair in the atoms being bonded develops a dipole moment which interacts with H to form the hydrogen bond, and depending on the directional property of the bonding orbitals of the lone electron pair the directional property of the hydrogen bond is determined.

(vi) **Co-ordination** bonds form between metal atoms and non-metallic elements where the non-metallic element donates both its bonding electrons to the metal and a bond is formed between them.

Often, more than one type of bonding may be present in a molecule. For example, in the case of  $A_n M_m X_q$  compounds, the bonds within the cation and anion are covalent while the bonding between the anions and cations **is** essentially **ionic** in character. But in the case of **alkylammonium** substituted compounds in  $A M X$  family, the bonding between the cation



and anion complexes are not so strong as in the case of ionic bonds, as is evidenced by the free reorientations that the cations are able to undergo in the interstitial spaces formed by the anionic complexes. In some of the  $A_2M_2X$  compounds, both metal-metal interaction as well as covalent bonding may be simultaneously present and an example in this case is the compound  $K_2WCl$

#### Geometric and Topological considerations :

The formation of any given compound is determined by a limited number of possible ways in which a group atoms can be arranged in space, apart from energy and symmetry considerations. For instance, in the formation of a compound like  $MX$  where the atoms do not lie on the same line, the  $M - X$  and  $X - X$  distance and the interbond angle  $\angle X - M - X$  are all related to one another, so that these can assume only a limited range of values restricting the kind of structures in which  $MX$  can exist. Such geometric considerations are applicable from the simple example given above to complex molecules as well, which explains the existence of only a limited number of types of structures for a given chemical composition of the compound. The structures of majority of solids can be derived from certain fundamental set of forms in three dimensions called polyhedra and certain basic forms in two dimensions called nets. Whereas polyhedra are closed structures, nets have infinite expanse.

Polyhedra are geometrical shapes assumed by compounds in three dimensions and the constituent atoms are situated at the vertices of these structures. The nearest neighbours of an atom in a molecule,

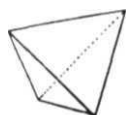
complex ion, or crystal, define a *polyhedral coordination group*, the number of vertices of which defines the coordination number of the atom. Normally, any given polyhedra is a closed structure made up of polygon faces like triangles, squares, hexagons, and so on. Among all types of polyhedra the tetrahedron and the octahedron are the most prevalently occurring structures in solids because, for these structures, the vertices represent the most symmetrical arrangement of four or six points around a central point. When a crystal is described in terms of coordination polyhedra around the cations, it becomes a system of polyhedra joined together by sharing vertices, edges, or faces. There are five basic polyhedra called "regular polyhedra", denoted by the names tetrahedron, cube, pentagonal dodecahedron, octahedron and icosahedron. There are also other three-dimensional structures derivable from these basic structures and they are called "semi-regular polyhedra". Any given compound is formed as a combination of these fundamental structures only and these are shown in Fig. (C-1.1).

Plane nets are arrangement of atoms in a 2-D plane with each point connected to a given number of neighbouring atoms. All the basic forms of plane nets are shown in Fig.(C-1.2). Any kind of layered structure in a compound falls into one of these types.

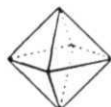
#### CLASSIFICATION OF CRYSTALS :

With the restricted type of bondings possible among atoms and the geometrical and topological constraints present in the formation of a given compound, all crystals can be classified in two and **three** dimensions in a particular way. Such a **classification** of crystals is

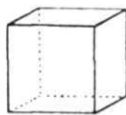
# *Polyhedra and Nets*



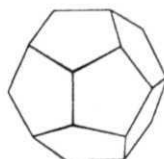
Tetrahedron  
4



Octahedron  
6



Cube  
8

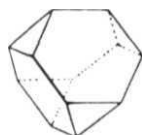


Pentagonal dodecahedron  
20



Icosahedron  
12

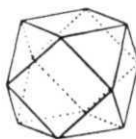
(a)



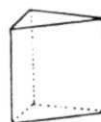
Truncated  
tetrahedron  
12a



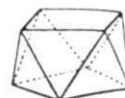
Truncated  
octahedron  
24



Cuboctahedron  
12b

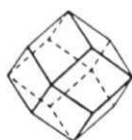


Trigonal  
prism  
6a

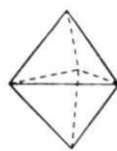


Square  
antiprism  
8a

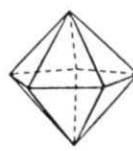
(b)



Rhombic  
dodecahedron (14)

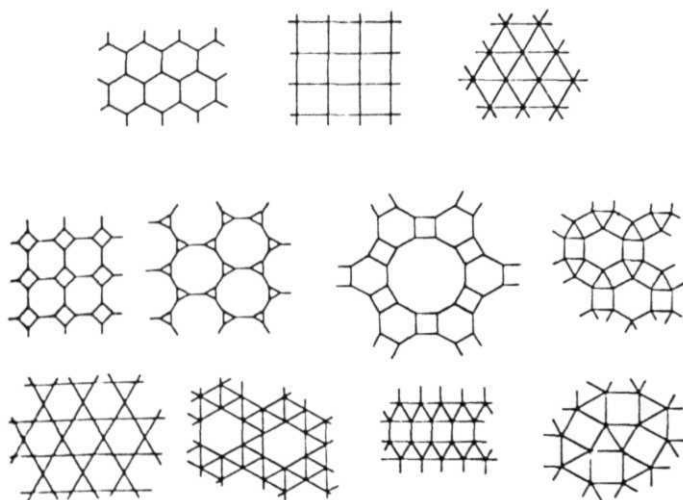


Trigonal  
bipyramid (5)  
(c)



Pentagonal  
bipyramid (7)

(C - 1.1) Regular and semi-regular polyhedra.

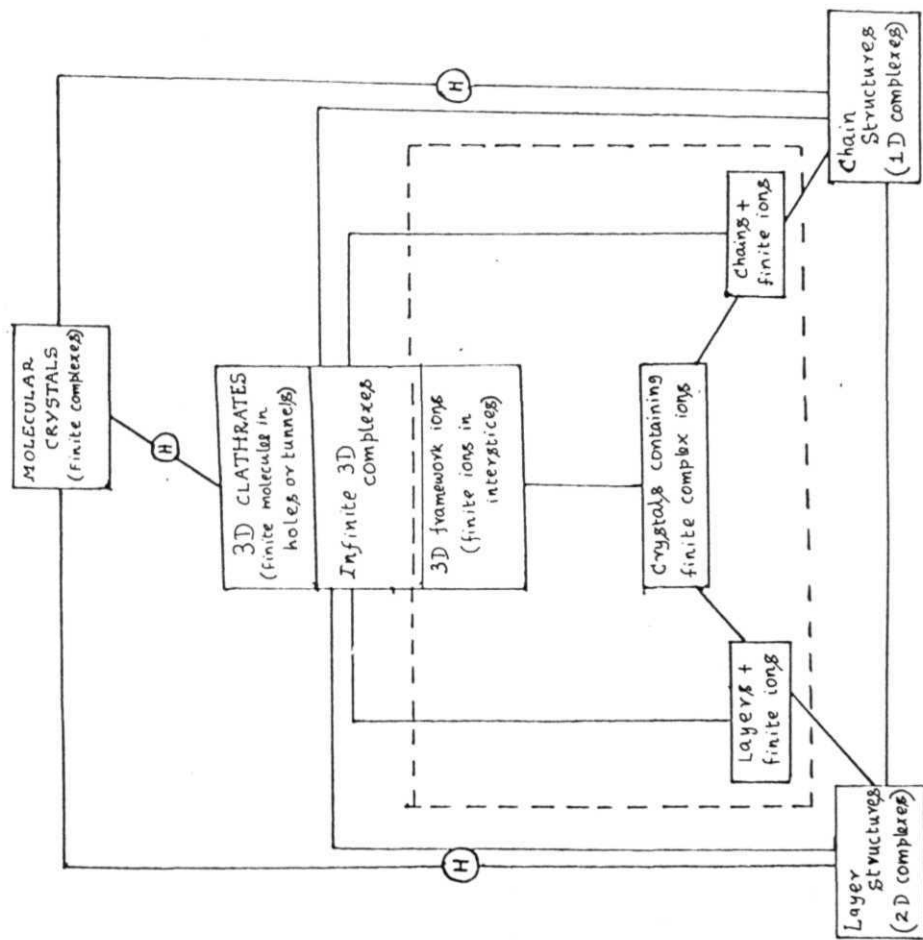


(C - 1.2) Regular and semi-regular plane nets.

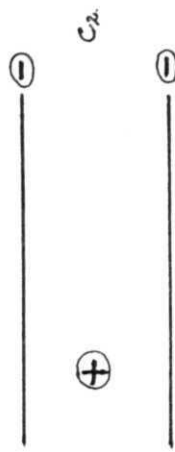
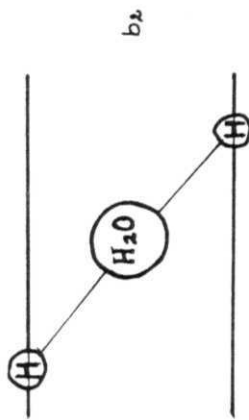
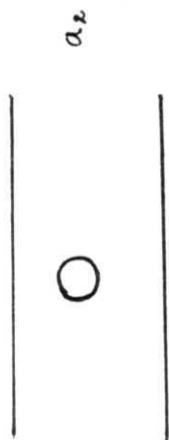
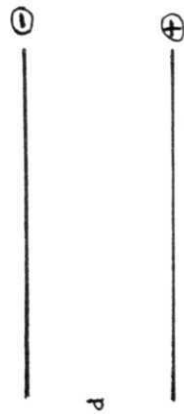
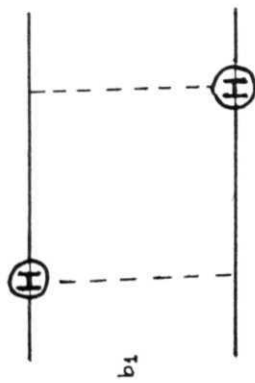
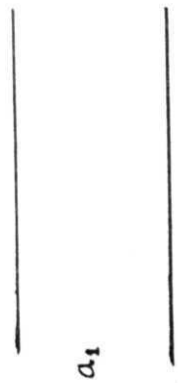
provided in the form of a chart in Fig.(C-1.3) [Wells, 1975]. The four groups listed within the dotted box are closely related types of ionic structures, all of which involve two distinct kinds of charged units. These are finite one-, two- and three- dimensional **ions** in addition to discrete ions (usually **monatomic**). The lines joining different structures marked with the letter **H** indicate that one form can be derived from the other through the formation of hydrogen bonds.

The different groups which can be considered under layered structures are represented **diagrammatically** in Fig.(C-1.4). Each class is denoted by symbols like a , b , etc. In the kind of compounds denoted by (a ), identical layers repeat after one another in a direction perpendicular to the individual layers and these are held together by Van der Waal's bonds. In (b ) of compounds, layers are held together by hydrogen bonds formed in between the layers. In (a ) type of crystals, a guest molecule is found in between identical layers and it is to be noted that the layers are electrically neutral in character as also is the molecular group in between the layers. In the type of compounds denoted by (b ), some foreign molecule like H<sub>2</sub>O is found in the interleaving layers, through which hydrogen bond is formed between layers. (c ) contains identical layers which are charged and this charge is neutralized by the oppositely charged group found in the interstitial site. Finally, (d) type compounds have layers of two different kinds alternating, and these layers are also of opposite charges. The electrostatic attraction between the layers stabilizes the structure.

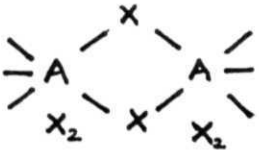
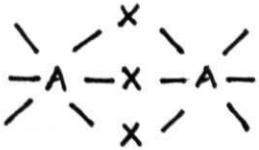
The different one dimensional chain structures feasible are illustrated in Fig.(C-1.5). Complexes which exhibit chain structures



(C - 1.3) The Chart giving all the possible structural forms in solids.



(C - 1.4) Diagrammatic representation of layered structures.

TYPE OF CHAIN	NEUTRAL MOLECULE	INFINITE ION
$\begin{array}{c} -A-X-A-X- \\   \quad \quad   \\ X \quad \quad X \end{array}$	$SeO_2$	$(BO_2)_n^{n-}$ in $CaB_2O_4$
$\begin{array}{c} -A-X-A-X- \\   \quad \quad   \\ X_2 \quad \quad X_2 \end{array}$	$SO_2; AuF_3$	$(SiO_3)_n^{2n-}; (PO_3)_n^{n-}$
$\begin{array}{c} -A-X-A-X- \\   \quad \quad   \\ X_4 \quad \quad X_4 \end{array}$	$BiF_5$	$(AlF_5)_n^{2n-}$
	$NbI_4$	$(HgCl_4)_n^{2n-}$
	$ZrI_3; Cs_3O$	$(N_3Cl)_n^{n-}$ in $CsN_3Cl_3$

(C - 1.5) Chart of chain structures with examples.



contain groups,  $AX_n$ ,  $AX_m$ ,  $AX$  sharing one or more X atoms.

Among the  $A M_n X$  compounds, and specifically those having the alkylammonium groups as their cations, the tetramethylammonium substituted compounds belong to the category where the discrete cations with a finite charge are found in the interstitial sites of the anionic structure, and these cations balance the charge on the framework. A large number of trimethylammonium and dimethylammonium halogenometallates belong either to the category c or to b where there is hydrogen bonding between the halogen in the anion and the N atom in the cation. In contrast to these structures, the methylammonium halogenometallates have a one dimensional chain structure which is formed from the sharing of two of the six vertices of an octahedron and this leads to the so called pleated ribbon structure.

In the formation of an entire class of crystals, hydrogen bonds play an important role as can be seen from Fig.(C-1.3). Thus the molecular crystals can be combined by hydrogen bonds to form either 1-D chain structures or 2-D layered structures. There can be other interlinkages possible to form infinite 2-D and 3-D structures as can be seen from the chart.

#### $A_3M_2X_9$ COMPOUNDS AND TRIS(ALKYLAMMONIUM) ENNEAHALOGENO METALLATES:

There are a number of compounds with the chemical formula  $A_3M_2X_9$  where X stands for the halogen atom and M stands for a suitable metal atom. The cation A can be a univalent element like K, Cs or Rb, or it can be a more complex organic group like the alkylammonium group, pyridinium

group, etc. Where the cation is not a complex group, the compounds are close packed structures belonging to the general formula  $A M X_b$ . These are formed by stacking  $AX$  layers, one over the other, and the interstitial spaces created by such a stacking are occupied by  $M$  atoms. If all the interstitial holes are occupied by  $M$  atoms, it results in  $AMX_b$  structure. If only two out of three holes are occupied, the  $A_2M_2X_9$  structure ensues, and the formation of  $A_2MX_{\frac{9}{2}}$  is possible if one half of all the holes are occupied by  $M$  atoms [Wells, 1975]. All the earlier known  $A_2MX_b$  compounds belong to such close packed structures. In such an arrangement, the  $M$  atom is surrounded by six  $X$  atoms leading to the  $MX_b$  octahedra, and among all the known forms of  $A_2MX_b$  compounds either the vertices or faces of these octahedra are shared, but seldom, the edges. Several examples can be cited in this respect. The compounds with the univalent group-I elements like  $K$ ,  $Cs$  and  $Rb$ , and other elements like  $Tl$  in place of  $A$ , and trivalent atoms like  $Cr$ ,  $Mo$ ,  $W$ ,  $V$  and  $Ti$  in place of the metal atom  $M$ , have been synthesized quite early [Powells et al., 1935]. Among these compounds, some of them have face sharing  $MX_b$  octahedra and some of them have vertex sharing  $MX_b$  octahedra. Examples of the former type are:  $Cs_3Tl_2Cl_9$ ,  $Cs_3Cr_2Cl_9$ ,  $Cs_3Bi_2I_9$ ,  $Cs_3Sb_2I_9$ ,  $Cs_3V_2Cl_9$ ,  $Cs_3Ti_2Cl_9$ ,  $K_3W_2Cl_9$  [Hoard et al., 1935; Powells et al., 1935; Brosset, 1935; Wessel et al., 1957; Watson et al., 1958; Lindqvist, 1968]. The confacial bi-octahedral arrangement of  $M-X$  anion in the case of face sharing compounds is illustrated in Fig.(C-1.6). Examples of the other type (vertex sharing) are:  $Cs_3Fe_2Cl_9$ ,  $Cs_3Sb_2Cl_9$ ,  $Cs_3As_2Cl_9$ ,  $Cs_3Bi_2Br_9$  [Lazarini, 1977]. In this latter type the vertex sharing among the  $MX_b$  octahedra leads to hexagonal holes in the solids as can be seen from Fig.(C-1.7a).

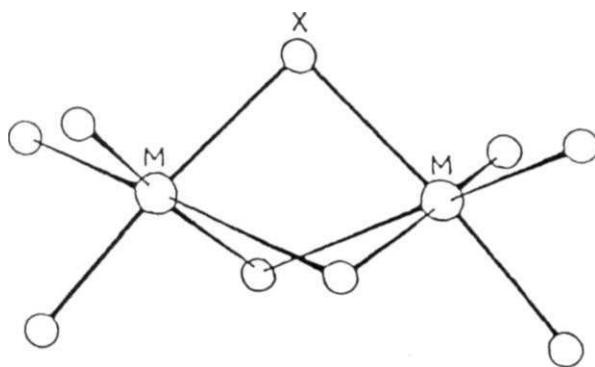
These compounds with their close packed structure provides a contrast to **tris(alkylammonium) nonahalogeno diantimonates** and **dibismuthates**. In these compounds also, the  $MX_6$  octahedra are vertex or face

sharing leading to chain or layers formed by the anions, but there is a large amount of free space available in between these chains or layers and the cations are situated in such free spaces, having considerable amount of freedom for reorientations [Jakubas et.al., 1990a].

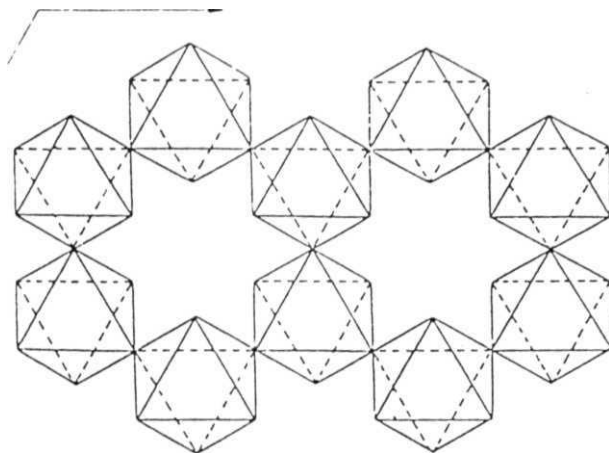
The resemblance in formulae of compounds of this family with the earlier ones is purely due to the geometrical requirements of the structure, rather than to the chemical similarities of the elements. The presence of different cations in this family of compounds affects the entire structure of the compound drastically. Thus, the **tetramethylammonium** compounds of this family stabilize confacial biocuboctahedral structures of the anions, as shown in Fig.(C-1.6) [Ishihara et.al., 1992; Jakubas et.al., 1993b]. For the dimethyl and **trimethylammonium** compounds, we get the two dimensional corrugated layered structures [Jakubas, 1990a]. But, in these cases, the ring structure formed by the  $MX_6$  octahedra shows

6

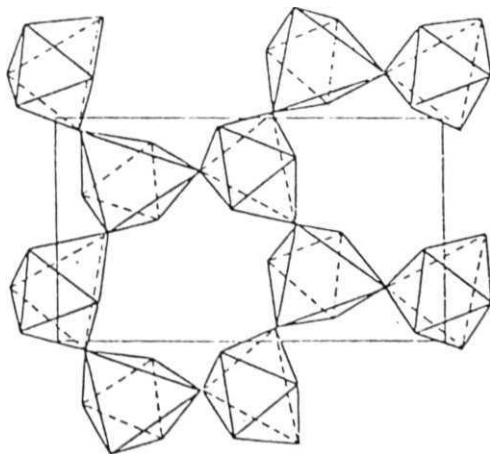
considerable amount of distortion and the void created within the ring does not have perfect hexagonal symmetry (Fig.C-1.7b). The formation of the hydrogen bond linking the anions and cations is one of the major causes of this distortion observed in the anionic structure, leading to ferroelectricity in these solids [Gdaniec et.al., 1988; Jakubas et.al., 1986, 1987, 1988, 1989b; Idziak et.al., 1988; Kallel et.al., 1985; Miniewicz et.al., 1989, 1990; Kosturek et.al., 1990]. In the case of methylammonium cations, we get a pleated ribbon structure of the  $M_2X_9^{3-}$  ions, in principle extending to infinite distances in one dimension (Fig.C-1.8).



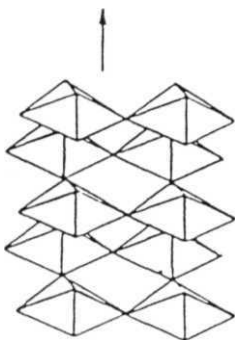
(C - 1.6) Face sharing  $MX_6$  octahedra in  $M_2X_9^{3-}$  anions.



(C - 1.7a) Corrugated layer formation in  $M_2X_9^{3-}$  anions with undistorted voids.



(C - 1.76) Corrugated layer formation in  $M_2X_9^{3-}$  anions with distorted voids.



(C – 1.8) Pleated ribbon structure of  $M_2X_9^{3-}$  anions which extends as one dimensional chain.

An important additional feature observed in the case of me thylammonium compounds is the sensitive dependence of the anionic structure on the type of halogen atoms also. Thus, when X corresponds to Cl a pleted ribbon structure or the zig-zag chain of the BiX<sub>6</sub> octahedra is found in these compounds, and when X is changed to Br the anion assumes the corrugated structure shown in Fig.(C-1.7a). Here, every BiX octahedron shares three of its vertices with three more neighbours, and within the ring structure a hexagonal free space forms. It is to be noted that these voids have perfect hexagonal symmetry in contrast to that of the dimethylammonium and trimethylammonium substituted compounds. When the halogen atom is changed to I, the anions form discrete confacial bioctahedra, as shown in Fig. (C-1.6) [Zaleski et.al., 1990, Jakubas et.al., 1986, 1990a, 1992, 1993; Ishihara et.al., 1992; Miniewicz et.al., 1990]. In addition to these compounds, the tetraethylammonium analogue of Sb Br and Bi Br are also grown, and in these compounds too the M<sub>2</sub>X anions have the confacial bioctahedra structures [Zaleski et.al., 1989a]. The considerable amount of freedom available to the cations is corroborated by the larger unit cell volume of these compounds, in comparison with some other A<sub>3</sub>M<sub>2</sub> compounds, and Table (C-1.1) provides these details for the two sets of compounds.

In stabilizing large metal complexes, the large anions in a compound are always stabilized by the presence of large cations of equal and opposite charge [Basolo, 1968; Martinsen et.al., 1977] and this rule seems to be well adhered to in many complexes involving the elements Bi and Sb. Quite a few compounds are synthesized with large anionic structures stabilized by bulky cations, most of them being organic complexes:

$$(N_2H_5)_4Sb_2Br_{17}, (N_2H_5)_{10}Sb_3Br_{19}, (N_2H_5)_6HBi_3Br_{16} \cdot 10H_2O,$$

TABLE C - 1.1

COMPOUND	SPACE GROUP	a	b	c	$\beta$	UNIT CELL VOLUME ( $\text{\AA}^3$ )
$\text{Cs}_3\text{Bi}_2\text{I}_9$	$\text{P6}_3/\text{mmc}$	8.41		21.18		1297
$\text{K}_3\text{W}_2\text{Cl}_9$	$\text{C}_{6h}^2$	7.16		16.16		717
$\text{Cs}_3\text{Tl}_2\text{Cl}_9$		9.58	9.58	9.58	$83.0^\circ$	863
<hr/>						
$[(\text{CH}_3)_4\text{N}]_3\text{Sb}_2\text{Cl}_9$	$\text{P6}_3/\text{mmc}$	9.25		21.73		1610
$[(\text{CH}_3)_4\text{N}]_3\text{Bi}_2\text{Cl}_9$	$\text{P6}_3/\text{mmc}$	9.265		21.93		1630
$[(\text{CH}_3)_4\text{N}]_3\text{Sb}_2\text{Br}_9$	$\text{P6}_3/\text{mmc}$	9.499		22.23		1736
$[(\text{CH}_3)_4\text{N}]_3\text{Bi}_2\text{Br}_9$	$\text{P6}_3/\text{mmc}$	9.521		22.46		1763
$[(\text{C}_2\text{H}_5)_2\text{NH}]_3\text{Bi}_2\text{Br}_9$	$\text{P2}_1/\text{C}$	12.36	13.91	18.94	$102.0^\circ$	3185
$[(\text{C}_2\text{H}_5)_2\text{NH}]_3\text{Bi}_2\text{I}_9$	$\text{P2}_1/\text{C}$	12.86	14.57	19.37	$102.0^\circ$	3550

TABLE SHOWING THE CRYSTAL STRUCTURE DATA ON SOME  $\text{A}_3\text{M}_2\text{X}_9$  COMPOUNDS AND ALKYLAMMONIUM HALOGENO METALLATES



$(\text{N}_2\text{H}_5)_5\text{Bi}_3\text{I}_{14} \cdot 6\text{H}_2\text{O}$ ,  $(\text{N}_2\text{H}_5)_6\text{HBi}_{14}\text{I}_{19} \cdot 10\text{H}_2\text{O}$  [Pugh, 1954],  $(\text{C}_5\text{H}_5\text{NH})_6\text{Bi}_4\text{Cl}_{18}$  [Aurivillius et.al., 1978]. Other stoichiometries for the anion with Bi are also reported, namely,  $\text{Bi}_2\text{Cl}_6$  ",  $\text{Bi}_2\text{Cl}_6$  and  $\text{Bi}_2\text{Cl}_6$  [Remy et.al., 1928; Plyushehev et.al., 1968, Landers et.al., 1980]. In this line of solids the compound  $[(\text{C}_4\text{H}_9)_4\text{N}]_3\text{Bi}_6\text{Cl}_{30}$  (TEACB) is unique in that it has one of the largest anions, i.e.  $\text{Bi}_6\text{Cl}_{30}$  " [Zaleski et.al., 1989]. This compound is very different from those belonging to the family  $[(\text{CH}_3)_4\text{N}]_3\text{Bi}_3\text{X}_9$ , and is one of the systems investigated using proton NMR measurements as a part of this work.

#### RELATED STUDIES ON TRIS(ALKYLAMMONIUM) ENNEAHALOGENO DIMETALLATES :

Most of the compounds from the tris(alkylammonium) nonahalogeno dimetallates exhibit order-disorder type structural phase transitions. A number of physical techniques have been employed to study these transitions and their relationships with other structural properties [Jakubas et al., 1990a]. The number of reports available on the Bismuth substituted compounds is meager relative to the Antimony substituted compounds. For example no previous reports have been made on two of Bismuth substituted compounds, tris(trimethylammonium) nonachloro dibismuthate (TMACB) and tris(dimethylammonium) nonachloro dibismuthate (DMACB), to the best of the author's knowledge. Most of the physical techniques reveal that the the anionic structures exist in chains, or layers, or cage like structures, with free space in between, and the cations are situated in this space undergoing reorientations in all these compounds.

Both powder and single crystal X-ray diffraction techniques have

been used to reveal the structure of these compounds [Hall et al., 1986; Ishihara et al., 1992; Jakubas et al., 1987; Kallel et al., 1985] and the single crystal structure X-ray work on some of these compounds show the presence of inequivalent cations [Hall et al., 1986; Jakubas et al., 1986a]. Differential thermal analysis (DTA) on these compounds shows the signature of the above mentioned structural phase transitions, [Ishihara et al., 1992; Jakubas et al., 1990b, 1993b] and these are also used to estimate the entropy change following a phase transition [Jakubas et al., 1990a]. The range of values one observes using this method provided additional information about the compound; for instance, the change in entropy following the transition at 168K in the Antimony compound MABA is 11 kJ/mol and this compares well with observed values for the phase transition of plastic crystals, thus indicating a large degree of freedom of reorientation for the cations [Jakubas et al., 1985]. NQR spectroscopy also reveals the presence of structural phase transitions in such systems [Ishihara et al., 1992]. The variation of halogen NQR frequency as a function of temperature shows that at the phase transition temperature, either there is a splitting of a single NQR line into a multiplet or the NQR line completely disappears.

The phase transitions have been studied using other physical techniques also, including dielectric dispersion, pyroelectric measurements, Raman and infrared scattering experiments etc. In dielectric measurements, the real and imaginary part of the dielectric permittivity  $\epsilon$ , ( $\epsilon'$  and  $\epsilon''$ ) recorded as a function of temperature at electric fields of different frequencies show a steep rise at the temperature at which a structural phase transition takes place. The temperature dependence of  $\tan\delta$  (i.e.  $\epsilon''/\epsilon'$ ) also shows a steep rise in

the vicinity of the phase transition temperature and reaches a maximum around the transition temperature. An increase in the  $\tan\delta$  value is indicative of the increased dissipation in the medium and it shows that there is a lag between the applied oscillatory electric field and the dipoles which try to follow this applied field. This means that the dipoles are less free to reorient as one approaches the transition point. Quite a few compounds belonging to the **alkylammonium nonahalogeno metallates** group have been investigated using dielectric relaxation studies [Jakubas et al., 1990a]. All the **methylammonium** salts of this family have been the subjects of study for dielectric measurements and they reveal the presence of at least one structural phase transition as indicated by the temperature dependence of the permittivity  $\epsilon$  [Jakubas et al., 1990a; 1990b]. In  $(\text{CH}_3\text{NH}) \text{Sb}_2\text{Cl}_9$  (MACA), one structural phase transition was observed at 208K as evidenced by an anomaly in permittivity at this temperature [Jakubas et al., 1986a]. In the Bromine analogue of this compound  $(\text{CH}_3\text{NH}) \text{Sb}_2\text{Br}_9$  (MABA), two anomalies were observed in both  $\epsilon_a'$  and  $\epsilon_c'$  (dielectric constants along a and c axes) recorded as a function of temperature at 168K and 131K [Jakubas et al., 1985, 1986b]. In  $(\text{CH}_3\text{NH}) \text{SbI}_9$  (MAIA), dielectric measurements showed the occurrence of a phase transition at 148K [Zaleski et al., 1990]. The three Bismuth analogues of these compounds were also investigated, and dielectric measurements on  $(\text{CH}_3\text{NH}) \text{Bi}_2\text{Cl}_9$  (MACB) show a gradual increase in  $\epsilon_a'$ ,  $\epsilon_b'$  and  $\epsilon_c'$  from 300K onwards reaching a maximum at 385K, which is indicative of a structural phase transition. Above this temperature this compound is found to enter a plastic phase where there is considerable amount of freedom for the cations to reorient [Jakubas et al., 1989a]. Similarly permittivity measurements on the Bromine and Iodine analogues of the Bismuth substituted compounds, namely  $(\text{CH}_3\text{NH})$

$\text{Bi}_2\text{Br}_9$  (MABB) and  $(\text{CH}_3\text{NH}_3)_3\text{Bi}_2\text{I}_9$  (MAIB), also **show** signatures of phase transitions [Jakubas et al., 1990b], revealing that there is a notable disorder in these systems and the cations have considerable freedom to undergo reorientations. Most of the dielectric studies are reported along with pyroelectric measurements and such studies are useful to identify polar phases in these compounds like the ferroelectric phase or ferrielectric phase. The ferroelectric nature of these compounds is associated with the ordering of the cations. Due to the hydrogen bonding between the cations and the halogen atoms of the anion groups, such ordering brings about a spontaneous polarization in these compounds [Miniewicz et al., 1990; Jakubas et al., 1986b; Zaleski et al., 1990].

Compounds where the cations are dimethylammonium and trimethylammonium groups and the metal atom is Antimony,  $[(\text{CH}_3)_2\text{NH}] \text{SbCl}_6$  (DMACA) and  $[(\text{CH}_3)_3\text{NH}] \text{Sb}_2\text{Cl}_9$  (TMACA), have been investigated using dielectric and pyroelectric measurements, leading to the observation of structural phase transitions and other polar properties [Gdaniec et al., 1988; Jakubas et al., 1987; 1988], but it seems that, no study has been made using these techniques on the Bismuth substituted compounds of this family, till date. In DMACA and TMACA, the  $\text{SbCl}_6$  octahedra form 12 membered rings within a unit cell creating hexagonal voids in between and these ring structures extend in the crystallographic ab plane to form layers. Such layers are stacked one over the other, along the c-axis. The cations are either situated within the layers in the hexagonal gaps or they are found in between the layers [Gdaniec et al., 1988]. This arrangement leads to dynamic inequivalence among the cations because of the different molecular potentials experienced by the cations within the layers and in between the layers. Hydrogen bonds are

formed between the N atoms in the cation and the Cl atoms, so that this leads to a slight distortion in the arrangement of the anions. Actually, the shape of the void between the SbCl rings is then a distorted hexagon. The cations in these compounds are also found to undergo fast reorientations.

Among the tetramethylammonium substituted compounds,  $[(CH_3)_4N]SbCl_9$  (TEMACA) and  $[(CH_3)_4N]Sb_2Br_9$  (TEMABA) were subjected to dielectric measurements and the temperature dependence of  $c'$  shows anomalies at 223K and 189K respectively, confirming the presence of a structural phase transition in these compounds also. Dilatometric studies on the Bismuth substituted compounds  $[(CH_3)_4N]Bi_2Cl_9$  (TEMACB) and  $[(CH_3)_4N]_3Bi_2Br_9$  (TEMABB) show that at 151K and 183K respectively, there is a sudden increase in the quantity  $\Delta L/L$ , plotted as a function of temperature, along a and c axes while heating the samples from low temperature. This further shows that, there is an increased freedom for the cation reorientation in this compound in the high temperature phases [Jakubas et al., 1993b]. In all these compounds it has been found that the reorientations of the cations slow down near the vicinity of these transitions. This is an important observation in the light of the information one gets from proton NMR measurements in these systems.

Raman scattering studies and infrared (IR) spectroscopy were employed to investigate some of these compounds [Jakubas et al., 1988, 1993a; Iwata et al., 1993; Belkhal et al., 1993]. They show the existence of different vibrational and rotational modes in the compounds. The presence of these modes and their intensity are sensitively affected by the structural properties of the compound, and therefore these studies

also show the signature of structural phase transitions. A molecule can undergo different kinds of vibrational motions and these include the stretching and the bending motions of the bonds within the molecule. A given molecule is infra-red active only if there is change in its electric dipole moment when it undergoes one of these vibrational motions. On the other hand, the presence of a Raman band is decided by the change in the electric polarizability of the molecule in question, when it undergoes such a motion [Straughan *et.al.*,1976]. The amplitude of the stretching or bending motion of the molecular group will be affected by the surrounding molecular potential and this will in turn be reflected in the intensity of a particular band in an IR or Raman spectrum. Of all the possible modes of vibration, quite a few of them are energetically degenerate and they will give a Raman or IR band at the same wavenumber. When there is a considerable rearrangement of the atomic positions following a structural phase transition, some of these degeneracies may be lifted which may lead to the formation of new bands, or such a rearrangement may lead to a suppression of some bands also. Thus, the Raman and IR spectra recorded as a function of temperature will give us the indication of a structural phase transition and the extent to which it affects the molecular surroundings. For instance, the IR spectrum recorded in DMACA at 300K shows that there is no splitting in the bands corresponding to the vibrations of the DMA cation, indicating that at this temperature the structural inequivalence among these cations revealed by X-ray studies are not reflected on to the IR spectrum at this temperature [Jakubas *et al.*, 1988]. IR studies have been made on the methylammonium compounds MABA and MABB [Jakubas *et al.*, 1993a] showing the presence of structural phase transitions in this solid. MABA has two structural phase transitions at 168K and 131K and MABB shows structural

phase transitions at three temperatures, namely **188K**, **140K** and **104K**. The highest temperature phase is a paraelectric phase and the cations exhibit isotropic reorientation. The spectra around **300K** of these compounds show only one band which is a result of the dynamic averaging caused by the isotropic reorientation of the cations. Raman spectroscopic study on a related compound MACB also shows the insensitivity of the spectra to the inequivalent **methylammonium** cations being present in this compound [Belkyl et al., 1993; Jakubas et al., 1989a]. It is observed that a careful scrutiny of the Raman and **IR** spectra will provide very useful information about the dynamics in the system. In MACB, temperature dependent high frequency Raman spectra shows that there is a rocking motion of the **CH** groups about their 3-fold symmetry axis and this dynamics is considerably faster compared to the **CN** axis reorientation of the cation. The temperature variation of the low frequency Raman spectra in this compound does not show any sudden change in the positions or intensities of the bands at the phase transition temperatures **349K** and **247K**, but there is a continuous broadening of the lines as one goes from **300K** to **393K**. Such a change is attributed to the order-disorder processes being present in the system [Belkyl et al., 1993]. A few other techniques, like Brillouin scattering, were also employed to study these systems [Iwata et al., 1993].

All the techniques highlighted above provide **complementing** information regarding the structural phase transitions in these compounds, depending on the type of coupling the technique provides to the microscopic details of the system. In this respect, NMR measurements become a valuable tool to investigate the microscopic dynamic processes taking place in these systems. Proton relaxation time measurements are

particularly suited to study these systems with the time window accessed by this technique being convenient to study the type of dynamics associated with these systems thereby providing complementary information to the above said techniques. The reorientational motion of the cations in these compounds are coupled to the order parameter of some of these phase transitions, and in this context proton T and M measurements provide an ideal probe to look at the dynamics of the cation and the internal motions present thereof, since changes in the rates of reorientation leave a discernible signature on the T or M data depending on the time scale of such reorientational processes. In the following sections, we provide details on the proton T and M measurements performed on tris[alkylammonium] nonahalogeno dibismuthates as a function of temperature and Larmor frequencies, and discuss the analysis of these results in the light of phase transitions they exhibit.

The systems studied are given below along with their acronyms in parenthesis.

1.  $[(\text{CH}_3)_4\text{N}]_3\text{Bi}_2\text{Cl}_9$  (TEMACB)
2.  $[(\text{CH}_3)_4\text{N}]_3\text{Bi}_2\text{Br}_9$  (TEMABB)
3.  $[(\text{CH}_3)_3\text{NH}]_3\text{Bi}_2\text{Cl}_9$  (TMACB)
4.  $[(\text{CH}_3)_2\text{NH}]_3\text{Bi}_2\text{Cl}_9$  (DMACB)
5.  $[\text{CH}_3\text{NH}_2]_3\text{Bi}_2\text{Cl}_9$  (MACB)
6.  $(\text{NH})_3\text{Bi}_2\text{Cl}_9$  (AMCB)
7.  $(\text{NH}_4)_3\text{Bi}_2\text{Br}_9$  (AMBB)
8.  $[(\text{C}_2\text{H}_5)_4\text{N}]_6\text{Bi}_8\text{Cl}_{30}$  (TEACB)

Some details pertaining to T and  $M_2$  measurements common to all the



systems investigated, are given below.

### Experimental Details - General

#### **T** measurements

Spectrometer	Home made pulsed NMR spectrometer
Pulse sequences used	Inversion recovery, Saturation burst
Temperature variation	Gas flow type cryostat - liquid nitrogen vapours for low temperatures; hot air for high temperatures
Temperature sensing and control	Calibrated Chromel-Alumel thermocouple for sensing; home made PID controller for temperature control; stability better than 0.5 K

#### **M** measurements

Spectrometer	JEOL make cross-coil type CW spectrometer
Temperature variation	Gas <b>flow type</b> cryostat - liquid nitrogen vapours <b>for low</b> temperatures; hot <b>air for high</b> temperatures
Temperature sensing and control	Calibrated Copper - Constantan

thermocouple for sensing; commercial  
temperature controller; stability  
better than 1.0 **K**

# REFERENCES

- (C-1.1) AURIVILLIUS B. , C. STÅLHANDSKE, *Acta Chem. Sc and. , A32*, (1978) 715
- (C-1.2) BASOLO F., *Cord.Chem.Rev. , 3*, (1968) 213
- (C-1.3) BELKYAL I., R. MOKHLISSE, B. TANOUTI, N.B. CHANH AND M. COUZI, *Phys.Stat. Sol.(a)*, **136**, (1993) 45
- (C-1.4) BROSSET C., *Nature*, **135**, (1935) 874
- (C-1.5) GDANIEC M., Z. KOSTURKIEWICZ, R. JAKUBAS AND L. SOBCZYK, *Ferroelectrics*, **77**, (1988) 31
- (C-1.6) HALL M. . M. NUNN, M.J. BAGLEY AND D.B. SOWERBY, *J.Chem.Soc. Dalton Trans.*, **(1986)**, 1231
- (C-1.7) HOARD J.L. AND L. GOLDSTEIN, *J.Chem. Phys.* , **3**, (1935) 199
- (C-1.8) IDZIAK S. AND R. JAKUBAS, *Ferroelectrics*, **80**, (1988) 75
- (C-1.9) ISHIHARA H. , K. WATANABE, A. IWATA, K. YAMADA, Y. KINOSHITA, T. OKUDA, V.G. KRISHNAN, SHI-QI DOU AND A. WEISS, *Z.Naturforsch. , A1a.*, (1992) 65
- (C-1.10) IWATA M. , M. EGUCHI, Y. ISHIBASHI. S. SASAKI, H. SHIMIZU, T. KAWAI AND S. SHIMANUKI, *J.Phys.Soc. Japan*, **62**, (1993) 3315
- (C-1.11) JAKUBAS R., Z. GALEWSKI, L. SOBCZYK AND J. MATUSZEWSKI, *J.Phys.C.* , **18**, (1985) L857
- (C-1.12) JAKUBAS R. , Z. CZAPLA. Z. GALEWSKI, L. SOBCZYK, O.J. ZOGAL AND T. LIS, *Phys.Stat.Sol.(a)*, **93**, (1986a) 449
- (C-1.13) JAKUBAS R. AND A. MINIEWICZ, *Ferroelectrics*, **70**, (1986b) 145
- (C-1.14) JAKUBAS R. , L. SOBCZYK AND J. MATUSZEWSKI, *Ferroelectrics*, **74**, (1987) 339
- (C-1.15) JAKUBAS R. , Z. MALARSKI AND L. SOBCZYK, *Ferroelectrics*, **80**, (1988) 193

- (C-1.16) JAKUBAS R. , P.E. TOMASZEWSKI AND L.SOBCZYK, *Phys.Stat.Sol.(a)*, **111**, (1989a) K27
- (C-1.17) JAKUBAS R. , A. MINIEWICZ, M. BERTAULT, J. SWORAKOWSKI AND A. COLLET, *J.Phys.France*, **50**, (1989b) 1483
- (C-1.18) JAKUBAS R. AND L. SOBCZYK, *Phase Transitions*, **20**, (1990a) 163
- (C-1.19) JAKUBAS R. , J. ZALESKI AND L. SOBCZYK, *Ferroelectrics*, **108**, (1990b) 109
- (C-1.20) JAKUBAS R. , R. DECRESSAIN AND J. LEFEBVRE, *J.Phys.Chem.Solids*, **53**, (1992) 755
- (C-1.21) JAKUBAS R. , G. BATOR, J. BARAN, *J. Phys.Chem. Sol ids*, **54**, (1993a) 1065
- (C-1.22) JAKUBAS R., Z. GALEWSKI, J. MATUSZEWSKI AND J. LEFEBVRE, *Phys.Stat.Solidi(a)*, **136**, (1993b) K19
- (C-1.23) KALLEL A. AND J.W. BATS, *Acta.Cryst.*, **C41**, (1985) 1022
- (C-1.24) KOSTUREK B. , J. PRZESLAWSKI AND R. JAKUBAS, *Sol id. State. Commun.* , **75**, (1990) 673
- (C-1.25) LANDERS A.G. AND T.B. BRILL, *Inorg.Chem.*, **19**, (1980) 744
- (C-1.26) LAZARINI F., *Acta.Cryst.*, **B33**, (1977) 2961
- (C-1.27) LINDQVIST O. , *Acta.Chem. Scand.* , **22**, (1968) 2943
- (C-1.28) MINIEWICZ A., R. JAKUBAS, C. ECOLIVET AND A. GIRARD, *J. Raman. Spect.*, **20**, (1989) 381
- (C-1.29) MINIEWICZ A.. R. JAKUBAS, *Ferroelectrics*, **110**, (1990) 261
- (C-1.30) MINIEWICZ A., J. LEFEBVRE AND R. JAKUBAS, *Ferroelectrics*, **107**, (1990) 183
- (C-1.31) MARTINSEN A., J. SONGSTAD, *Acta.Chem.Scand.*, **A31**, (1977) 645
- (C-1.32) PLYUSHEHEV V., E. STEPINA AND I.V. VLASOVA, *Dokl. Akad.Nauk SSSR*, **180**, (1968) 126
- (C-1.33) POWELLS AND A.F. WELLS, *J.Chem.Soc.*, (1935) 1008

- (C-1.34) PUGH W. , *J.Chem.Soc.* , (1954) 1385
- (C-1.35) REMY H. AND L. PELLENS, *Chem.Ber.*, 61, (1928) 862
- (C-1.36) STRAUGHAN B.P. AND S. WALKER, "Spectroscopy", **vol.2**, Chapman and Hall Ltd., LONDON
- (C-1.37) WATSON W.H.JR. AND J. WASER, *Acta.Cryst.*, 11, (1958) 689
- (C-1.38) WELLS A.F., *Structural Inorganic Chemistry*, Clarendon Press, Oxford, 1975
- (C-1.39) WESSEL AND IJDO, *Act a. Cryst.*, 10, (1957) 466
- (C-1.40) ZALESKI J., T. GLOWIAK, R. JAKUBAS AND L. SOBCZYK, *J.Phys.Chem.Solids*, 50, (1989) 1265
- (C-1.41) ZALESKI J.. R. JAKUBAS, Z. GALEWSKI AND L. SOBCZYK, *Z.Naturforsch.*, **44a**, (1989a) 1102
- (C-1.42) ZALESKI J., R. JAKUBAS, L. SOBCZYK AND J. MROZ, *Ferroelectrics*, 103, (1990) 83

# SECTION C

## PART 2

### RELAXATION AND RESONANCE STUDIES ON

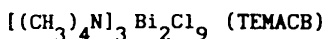


In this section the results of proton T. and  $M_2$  measurements on the two tetramethylammonium compounds of this family, namely,  $[(CH_3)_4N]_3 Bi_2 Cl_9$  (TEMACB) and  $[(CH_3)_4N]_3 Bi_2 Br_9$  (TEMABB) are presented and discussed. Such measurements on the Antimony analogue of these compounds, namely,  $[(CH_3)_4N]_3 Sb_2 Cl_9$  (TEMACA) and  $[(CH_3)_4N]_3 Sb_2 Br_9$  (TEMABA), show that, structural phase transitions are present at 223K and 189K respectively and at the respective transition temperatures, there is a notable change in the dynamics of the cations [Jagadeesh et al., 1992, 1993a]. Substitution of the heavier metal atom like Bi in these configurations, which leads to the compounds TEMACB and TEMABB, increases the unit cell volume observably as evidenced by X-ray studies on these compounds [Jakubas et al., 1988, 1993; Ishihara et al., 1992]. Such an increase in the volume, presumably, will affect the freedom for the tetramethylammonium cation as a whole as well as the internal dynamics of the cation, namely, the methyl group reorientations and the and T and M ought to reflect the dynamic properties of these molecular groups.

TEMACB and TEMABB crystallize in the  $P6/mmc$  space group and they are isostructural with their Antimony counterparts, namely TEMACA and TEMABA [Jakubas et al., 1988; 1993]. The  $BiCl_9^{3-}$  anions exist as

individual confacial biotahedra in these compounds and the TEMA cations which have tetrahedral symmetry are situated in **between** the anionic groups and they can undergo isotropic reorientation under suitable conditions. DTA, NQR and dilatometric measurements on TEMACB and TEMABB reveal the presence of structural phase transitions at 151K and 183K respectively [Ishihara et al., 1992; Jakubas et al., 1993]. Dilatometric measurements show that, both in TEMACB and TEMABB, thermal expansion coefficients (a) along the a and c crystallographic axes above the phase transition temperature are smaller than those below the phase transition temperature, implying an increased amount of disorder in these solids below the phase transition temperatures [Jakubas et al., 1993]. But the relative change in the volume of the unit cell, is more in case of TEMACB than in the case of TEMABB, across the transition temperatures. In what follows, let us look at the results of proton T and M<sub>2</sub> measurements, made as a function of temperature and Larmor frequency, in these two compounds.

#### Specific details



T<sub>1</sub> data :

Larmor frequencies of observation	39.8, 8 and 4 MHz
Temperature range	385K to 77

M<sub>2</sub> data :

Temperature range	425K - 77K
-------------------	------------

Variation of  $T_1$  with  $1/T$  in TEMACB : Fig.(C-2.1)

M

variation as a function of temperature in TEMACB : Fig.(C-2.2)

Optimized motional parameters : Table (C-2.1)

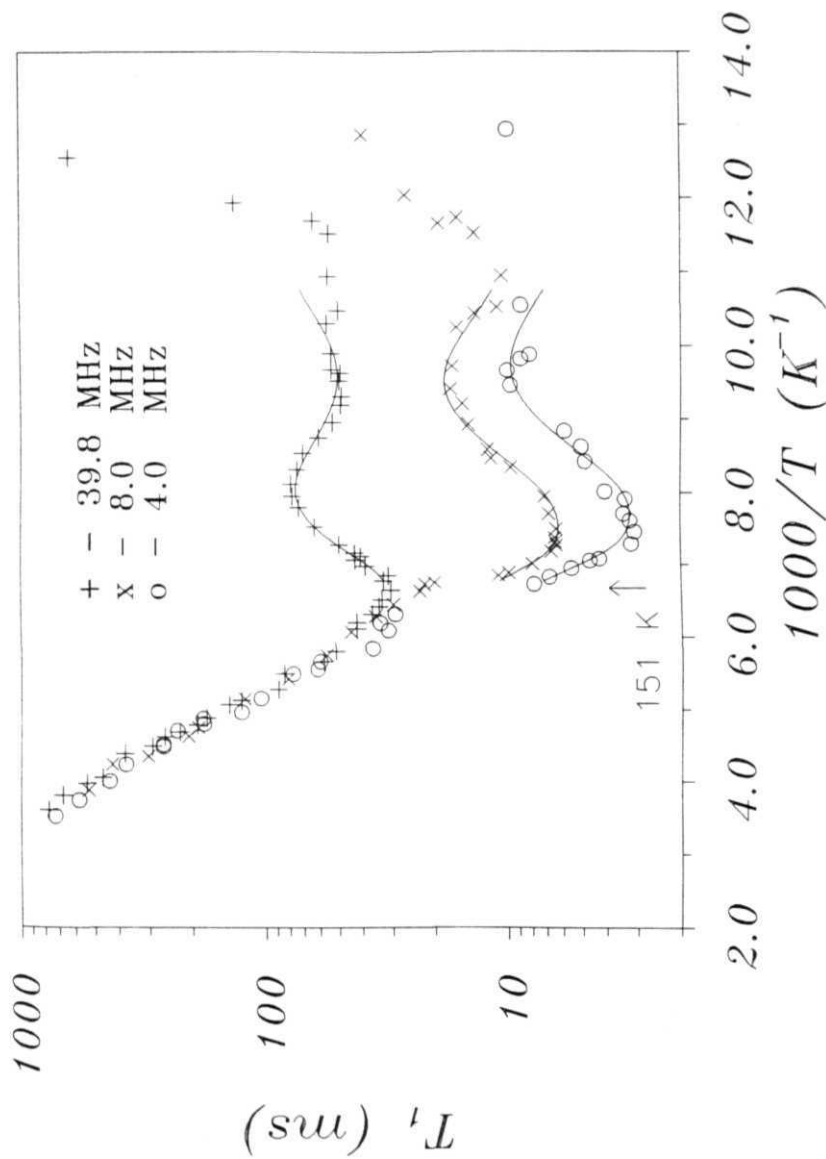
## TEMACB

### RESULTS

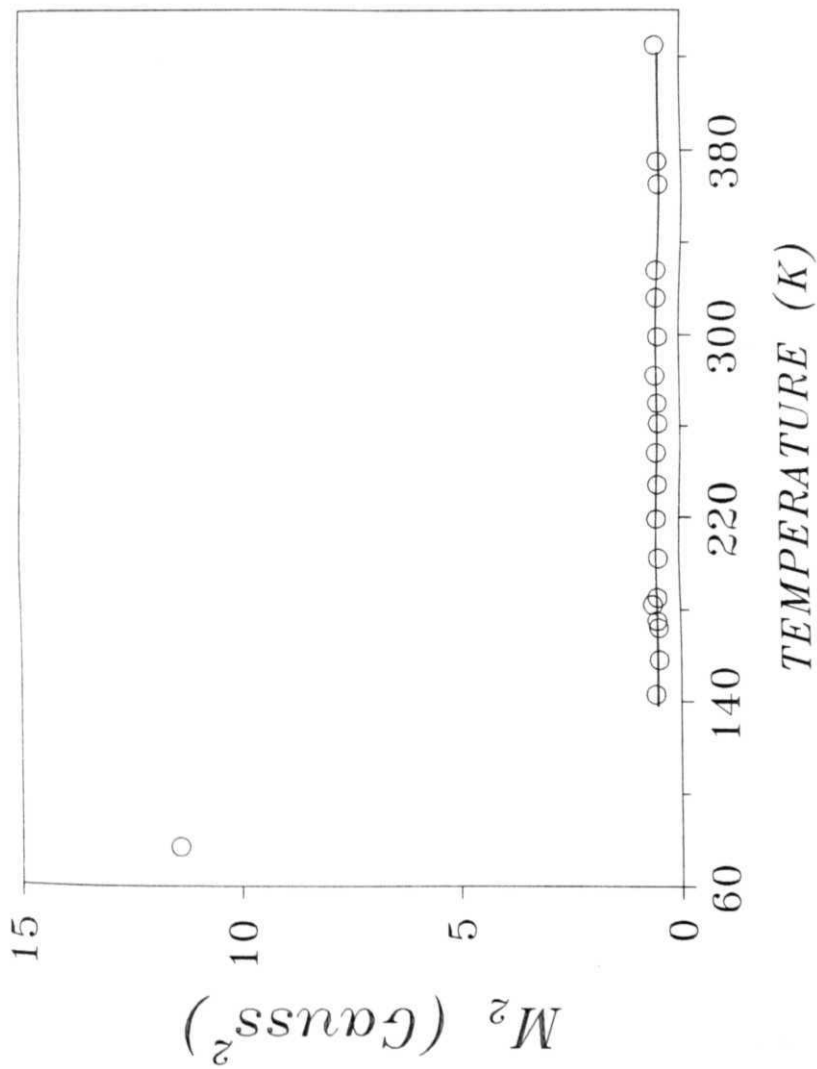
TEMACB was prepared by the slow evaporation technique by mixing stoichiometric ratios of the parent compounds  $[N(CH_3)]Cl$  and  $BiCl_3$  in  $HCl$ . Crystals had the habit of hexagonal plates and were colourless. Elemental analysis on this compound gave the following percentages for the elements C, H and N : C - 15.54% (15.03% expected), H - 3.847. (3.78% expected), N - 4.487. (4.37% expected). Polycrystalline sample of the compound was sealed in 6 mm and 8 mm glass tubes under 10 torr vacuum for  $T_1$  and  $M_2$  measurements.

The  $T_1$  vs.  $1000/T$  ( $T$  = temperature) graph for TEMACB at the Larmor frequencies 39.6, 8 and 4 MHz is shown in Fig. (C-2.1) and the  $M_2$  variation as function of temperature is shown in Fig.(C-2.2). Looking at the  $T_1$  data, we can identify a high temperature portion which ranges from around 370K to 150K and a low temperature region which is below 150K till 77K. The feature which characterizes the high temperature region is that  $T_1$  is independent of frequency in this range. At 151K, we can observe an almost vertical jump in the  $T_1$  values for both 8 and 4 MHz data, and interestingly such a jump is not seen at 39.8 MHz. The low temperature range data is characterized by frequency dispersion of the relaxation data, as well as specific signatures (minima) as a function of





(C-2.1) Variation of  $T_1$  as a function of  $(1000/T)$  in  $[(CH_3)_4N]_3Bi_2Cl_9$ . Solid lines through data points are the fitted curves.



(C - 2.2) Variation of  $M_2$  as a function of  $T$  in  $[(CH_3)_4N]_3 Bi_2Cl_9$ .

temperature at the different **Larmor** frequencies. At 39.8 MHz and below 151 K, formation of a T minimum is seen which is followed by another minimum which is shallower than the minimum immediately below the phase transition temperature. In the case of 8 and 4 MHz, the formation of only two minima are seen but at 39.8 MHz, there is a flat region in the T data below the second minimum which is followed by a rather steep increase in T. around 90K. A discontinuity in T. data is observed in the case of 8 MHz data also, for instance. The slope of the T. data on the higher temperature side of the minimum immediately below the phase transition is more compared to the slope on the lower temperature side. In fact, as we move from the higher frequency 39.8 MHz towards the lower values like 8 and 4 MHz, the slope of T data on the lower temperature side of the first minimum becomes progressively shallower. M data show a constant value at around  $(0.5 \pm 0.1)\text{Gauss}^2$  till the temperature 140 K, and at 77 K it is 11.5 Gauss<sup>2</sup>.

## DISCUSSION

An interesting feature of the T data is **the steep** fall in the T value at 151K at which DTA, NQR and dilatometric studies on this compound has revealed first order structural phase transition [Ishihara, et.al., 1992; Jakubas et.al.. 1993]. Actually, Ishihara et.al., have quoted a value of 155K for the transition from their DTA studies but Jakubas et.al., have quoted a value of 152K in the heating run and 151K in the cooling run of the DSC measurements, for the phase transition. Further, their dilatometric studies reveal the existence of a structural phase transition at 152K only. While this transition leaves a clear signature

on the NMR relaxation data, we did not observe any notable thermal hysteresis of the transition temperature. The  $T$  data have no frequency dispersion above 151K, and the sudden jump of  $T$  at this temperature, accompanied by a frequency dispersion of the relaxation rates indicates that there is a discontinuous jump in the correlation time of certain dynamic processes which could be effectively mediating the relaxation process around this temperature. However, the absence of observable discontinuity around 151K at 39.8 MHz alone is to be noted. Such a behavior is plausible at least in principle, if the location of the minimum happened to coincide with phase transition temperature at this Larmor frequency. Our quantitative analysis of data indicates this fact.

To quantitatively account for the observed behaviour of the  $T$  data and extract relevant dynamic parameters associated with the possible dynamics present in these systems, a suitable theoretical model is needed which takes into account the possible motions of the tetramethylammonium cation and the internal motions present within this group, namely the methyl group dynamics, and which can provide a relationship between the spin-lattice relaxation rate and the relevant dynamic parameters of the above said motions in these compounds. Therefore, to enable the analysis of the data further, we shall look at such a model for the dynamics of the tetramethylammonium group in these type of solids.

#### MODEL FOR SPIN LATTICE RELAXATION RATE ASSOCIATED WITH TEMA GROUP DYNAMICS :

In order to arrive at an expression for the proton spin lattice

relaxation rates of tetramethylammonium cation, the relevant motions associated with this group are to be considered. In this connection, we can identify two cases.

- (a) The reorientation of the methyl group about its three-fold axis, and assuming the time of flight between any two positions to be negligible, the "dwell time" or the average time for which the group is oriented in a given equivalent **configuration** is the correlation time  $T$ .
- (b) The reorientation of the entire tetramethylammonium (TEMA) cation corresponding to a stochastic jump process with an infinite number of equivalent orientations characterized by a correlation time  $T$

Both these processes are thermally activated, leading to Arrhenius dependence on temperature for both the correlation times. For example,  $\tau$  can be written as,

$$(C-2.1) \quad \tau_c = \tau_o \exp(E_a/kT)$$

Here,  $T_o$  is the correlation time at infinite temperature and  $E_a$  is the potential barrier, providing a measure of hindrance for reorientation between any two equivalent positions.

Now, to provide a connection between experiment ( $T$ ) and theoretical model ( $TS$ ), let us consider a pair of nuclei connected by an internuclear vector  $r$ , reorienting about an axis  $Z'$ . Let the angle subtended by this vector on the  $Z'$  axis be given by  $A$  and the azimuthal

angle of rotation of this vector about  $Z'$  be given by  $\phi'$ , where,  $\phi'$  is measured with respect to a reference frame rigidly attached to the internuclear vector. Let the applied static field direction be  $Z$ , and, in principle, the  $Z'$  axis can undergo reorientation about the  $Z$ -axis. Let  $\vartheta$  be the angle subtended by the  $Z'$  axis on the  $Z$  axis and let  $\phi$  define the azimuthal angle of this axis. Both these reorientations can be either looked upon as either the case (a) or the case (b), as we discussed before. Let us denote by  $\tau$ , the correlation time for the reorientation of the internuclear vector about  $Z'$  and let  $\tau$  be the correlation time for the reorientation of the rotation axis  $Z'$  about the  $Z$  axis. We make an important assumption here, namely, the motion about one axis is not related to the motion about the other and essentially, these two processes are uncorrelated. The spin-lattice relaxation rate is given by [BPP, 1948]

$$(C-2.2) \quad 1/T_1 = (3/2) \gamma^4 \hbar^2 r^{-6} I(I+1) [J_1(\omega_0) + J_2(2\omega_0)]$$

The lattice functions  $F(r, \vartheta, \phi)$  and  $F_2(r, \vartheta, \phi)$  defined from the dipolar interaction Hamiltonian can be written in convenient forms as

$$(C-2.3) \quad F_1(t) = (x+iy)z \quad ; \quad F_2(t) = (x+iy)^2$$

and here  $x$ ,  $y$  and  $z$  are the direction cosines of the internuclear vector on the  $(X \ Y \ Z)$  coordinate system, attached to the applied field direction. From the various angles defined above, the direction cosines can be written as [Woessner, 1962]

$$\begin{aligned}
\text{(C-2.4)} \quad x &= \sin\Delta \cos\vartheta \cos\phi' + \cos\Delta \sin\vartheta \cos\phi - \sin\Delta \sin\vartheta \sin\phi' \\
y &= \sin\Delta \cos\phi \sin\phi' + \sin\Delta \cos\vartheta \sin\phi \cos\phi' + \cos\Delta \sin\vartheta \sin\phi \\
z &= \cos\Delta \cos\vartheta - \sin\Delta \sin\vartheta \cos\phi'
\end{aligned}$$

and the lattice functions  $F$  and  $F_{\perp}$ , in terms of these variables is given by

$$\begin{aligned}
\text{(C-2.5)} \quad F_1(t) &= [(1/2)(3\cos^2\Delta - 1)\sin\vartheta\cos\vartheta + \\
&\quad + (1/2)\sin\Delta\cos\Delta(\cos^2\vartheta - \sin^2\vartheta + \cos\vartheta)e^{i\phi'} \\
&\quad + (1/2)\sin\Delta\cos\Delta(\cos^2\vartheta - \sin^2\vartheta - \cos\vartheta)e^{-i\phi'} \\
&\quad - (1/4)\sin^2\Delta(\sin\vartheta\cos\vartheta + \sin\vartheta)e^{i2\phi'} \\
&\quad - (1/4)\sin^2\Delta(\sin\vartheta\cos\vartheta - \sin\vartheta)e^{-i2\phi'}] e^{i\phi}
\end{aligned}$$

and

$$\begin{aligned}
\text{(C-2.6)} \quad F_2(t) &= [(1/2)(3\cos^2\Delta - 1)\sin^2\vartheta + \\
&\quad + \sin\Delta\cos\Delta(\sin\vartheta\cos\vartheta + \sin\vartheta)e^{i\phi'} \\
&\quad + \sin\Delta\cos\Delta(\sin\vartheta\cos\vartheta - \sin\vartheta)e^{-i\phi'} \\
&\quad + (1/4)\sin^2\Delta(1 + \cos^2\vartheta + 2\cos\vartheta)e^{i2\phi'} \\
&\quad + (1/4)\sin^2\Delta(1 + \cos^2\vartheta - 2\cos\vartheta)e^{-i2\phi'}] e^{2i\phi}
\end{aligned}$$

In these expressions the terms in  $\vartheta$  and  $\phi$  describe the reorientation of the  $Z'$  axis and the terms in  $\phi'$  describe reorientation of the internuclear vector about the  $Z'$  axis. These two types of motions are supposed to occur independent of each other. We can group the terms in eqns. (C-2.5) and (C-2.6) in terms of the variables  $(\Delta, \phi')$  and  $(\vartheta, \phi)$  and rewrite the functions  $F$  and  $F_{\perp}$  accordingly. As an example we shall consider the function  $F_{\perp}$ .

$$(C-2.7) \quad F_1(t) = f_a g_a + f_b g_b + f_c g_c + f_d g_d + f_e g_e$$

where,

$$\begin{aligned} f_a &= (1/2)(3\cos^2\Delta-1)\sin\vartheta\cos\vartheta e^{i\phi} \\ f_b &= (1/2)\sin\Delta\cos\Delta(\cos^2\vartheta-\sin^2\vartheta+\cos\vartheta) e^{i\phi} \\ f_c &= (1/2)\sin\Delta\cos\Delta(\cos^2\vartheta-\sin^2\vartheta-\cos\vartheta) e^{i\phi} \\ f_d &= -(1/4)\sin^2\Delta(\sin\vartheta\cos\vartheta+\sin\vartheta) e^{i\phi} \\ f_e &= -(1/4)\sin^2\Delta(\sin\vartheta\cos\vartheta-\sin\vartheta) e^{i\phi} \end{aligned}$$

and

$$g_a = 1 ; g_b = e^{i\phi'} ; g_c = e^{-i\phi'} ; g_d = e^{2i\phi'} ; g_e = e^{-2i\phi'}$$

With these notations, we can write the ensemble average of the lattice function **F** as

$$(C-2.8) \quad \langle F_1^*(t+\tau)F_1(t) \rangle = \sum_{j,k=a}^e \langle f_j^*(t+\tau)f_k(t)g_j^*(t+\tau)g_k(t) \rangle$$

With the assumption that the two reorientational processes are independent of each other, this equation can be recast into

$$(C-2.9) \quad \langle F_1^*(t+\tau)F_1(t) \rangle = \sum_{j,k=a}^e \langle f_j^*(t+\tau)f_k(t) \rangle \langle g_j^*(t+\tau)g_k(t) \rangle$$



Ensemble average of **the term**  $g$  :

We can evaluate the ensemble average of the functions  $g$ , which has the only time dependent variable  $\phi'$ . By considering the motion to be either of type a or of type b. But certain general relations can be established first. Let  $p(\phi'_0 + \phi', ?)$  be the probability of finding the internuclear vector at an angle  $\phi'$  relative to  $\phi'_0$  at time  $T$ , given the condition that at time  $t=0$ , the vector was aligned with an azimuthal angle  $\phi'_0$ . Then  $g(t+\tau)$  can be written as

$$(C-2.10) \quad g(t+\tau) = \sum g(\phi'_0 + \phi') p_0(\phi'_0 + \phi', \tau)$$

where the summation is over all the possible values of  $\phi'$ . With this definition of  $g$ , we can write the ensemble average of  $g$  to be,

$$(C-2.11) \quad \langle g_j^*(t+\tau) g_k(t) \rangle = \langle [\sum g_j(\phi'_0 + \phi') p_0(\phi'_0 + \phi', \tau)]^* g_k(t) \rangle$$

where, the average on the right hand side of eqn.(C-2.11) is over all the possible initial values of  $\phi'_0$ .

Case (a) :

Considering Case (a) to be applicable here, there are three equivalent orientations,  $120^\circ$  apart and we can define the occupational probabilities as  $p(\phi'_0)$ ,  $p(\phi'_0 + 120^\circ)$  and  $p(\phi'_0 - 120^\circ)$ , and assuming the jump process to be random with a correlation time  $\tau$ , and also assuming

that there is an equal *a-priori* probability for the occupation of each orientation, the rate per unit time of jumping from any given orientation is  $2/(3T)$  and we can write an equation for the rate of change of probability with respect to time for the orientation  $\phi'$  as

$$(C-2.12) \quad \frac{dp}{dt}(\phi'_0) = (2/3T) \{ -p(\phi'_0) + (1/2)p(\phi'_0 + 120) + (1/2)p(\phi'_0 - 120) \}$$

Such similar equations can be written for the occupational probabilities corresponding to the other two orientations, namely,  $p(\phi' + 120)$  and  $p(\phi' - 120)$ . By suitably decoupling these equations and solving them with

the boundary conditions,  $p(\phi'_0, 0) = 1$ ,  $p(\phi' + 120, 0) = 0$  and  $p(\phi'_0 - 120, 0) = 0$ , we get the solutions given by

$$(C-2.13.a) \quad p(\phi', \tau) = (1/3) + (2/3) \exp(-\tau/T)$$

$$(C-2.13.b) \quad p(\phi'_0 + 120^\circ, T) = p(\phi'_0 - 120^\circ, \tau) = (1/3) - (1/3) \exp(-\tau/\tau_c)$$

We can substitute the expression for the probabilities into equation (C-2.11) and calculate the ensemble average of the  $g$  functions to be,

$$(C-2.14) \quad \langle \exp[\pm i\phi'(t+\tau)] \exp[\pm i\phi'(t)] \rangle \\ = \langle \exp[\pm 2i\phi'(t+\tau)] \exp[\mp 2i\phi'(t)] \rangle = \exp(-|\tau|/\tau_c)$$

and the average for terms where  $j \neq k$ , is zero.

Case (b) :

Assuming the reorientational process to be given by Case (b), we can write down the occupational probability of finding the internuclear vector at the angle  $(\phi' + \langle p' \rangle)$  at time  $(t+x)$  by the Gaussian distribution as

$$(C-2.15) \quad p(\phi' + \phi', x) = (1/2) (TIT/T)^{1/2} \exp(-\phi'^2 \tau / 4x)$$

By substituting this expression into equation (C-2.11), we can calculate the ensemble average to be

$$(C-2.16.a) \quad \langle \exp[\pm i\phi' (t+\tau)] \exp[\pm i\phi' (t)] \rangle = \exp(-|\tau|/\tau_c)$$

$$(C-2.16.b) \quad \langle \exp[\pm 2i\phi' (t+\tau)] \exp[\mp 2i\phi' (t)] \rangle = \exp(-4|\tau|/T)$$

**Ensemble average of terms f :**

From BPP model, the ensemble average of functions f depending on the coordinates  $\theta$  and  $\phi$ , can be written as

$$(C-2.17) \quad \langle f_j^*(t+\tau) f_j(t) \rangle = \langle f_j^*(t) f_j(t) \rangle \exp(-|\tau|/\tau_{c_j})$$

Substituting expressions from eqns.(C-2.16) and (C-2.17), we can write for the ensemble average of the lattice function F ,

$$\begin{aligned}
 \text{(C-2.18)} \quad \langle F_1^\bullet(t+\tau) F_1(\tau) \rangle = & (1/30)(3\cos^2\Delta-1)^2 \exp[-|\tau|/\tau_{c1}] \\
 & + (1/10)\sin^2 2\Delta \exp[-|\tau|/(1/\tau_{c1}+1/\tau_c)] \\
 & + (1/10)\sin^4 \Delta \exp[-|\tau|/(1/\tau_{c1}+4/\tau_c)]
 \end{aligned}$$

The other  $\langle F(t+x)F(t) \rangle$  are similarly evaluated. By taking the Fourier transform of the respective space functions we get the following expression for the spectral density functions.

$$\text{(C-2.19)} \quad J_i(\omega) = K_i \left[ \frac{A}{1 + \omega^2 \tau_{c1}^2} + \frac{B}{1 + \omega^2 \tau_{c2}^2} + \frac{C}{1 + \omega^2 \tau_{c3}^2} \right]$$

where,

$$\tau_{c2} = [(1/\tau_{c1}) + (1/\tau_c)]^{-1}$$

$$\tau_{c3} = [(1/\tau_{c1}) + (4/\tau_c)]^{-1}$$

$$A = 1/4(3\cos^2\Delta-1)^2$$

$$B = 3/4(\sin^2 2\Delta)$$

$$C = 3/4(\sin^4 \Delta)$$

$$K_0 = 4/5 ; \quad K_1 = 2/15 \quad K_2 = 8/15$$

These expressions can be substituted in eqn. (C-2.2) to arrive at the formula for the spin-lattice relaxation rate and such an expression is in general applicable to any reorientational process like that of the TEMA cation, where, the reorientational rate of the methyl group about its three-fold axis is given by  $x$  and the isotropic reorientation of the entire cation is characterized by the rate  $x$ . With the reasonable assumption that the interaction between two protons on two different TEMA

groups are negligible compared to the intragroup interactions, and taking into account the distribution of angle  $\Delta$  in a **polycrystalline** compound, the expression for spin-lattice relaxation rate for the TEMA group dynamics can be written as [Albert et al., 1972],

$$(C-2.20) \quad (1/T_1) = A g(\omega_o, \tau_{c2}) + B g(\omega_o, \tau_{c1})$$

where,

$$g(\omega_o, \tau_c) \equiv [\tau_c / (1 + \omega_o^2 \tau_c^2)] + [4\tau_c / (1 + 4\omega_o^2 \tau_c^2)]$$

and

$$\tau_{c2}^{-1} \equiv \tau_c^{-1} + \tau_{c1}^{-1}$$

Here, the factors A and B are given by

$$A = (9/20) (\gamma^4 \hbar^2 / r^6)$$

and

$$B = (3/20) (\gamma^4 \hbar^2 / r^6) + (27/10) (\gamma^4 \hbar^2 / r_{\bullet}^6)$$

In the above expressions, r is the interproton distance within a methyl group and  $r_{\bullet}$  is the distance between the center of two adjacent methyl groups. Assuming the standard dimensions for the **tetramethyl** ammonium cation, namely, C-H bond length as 1.09 Å and the C-N bond distance as 1.5 Å, these distances are computed to be  $r = 1.78\text{Å}$  and  $r_{\bullet} = 3.04$  Å. Substitution of these values in the formula for A and B, we get  $A = 8.05 \times 10^9 \text{ s}^{-2}$  and  $B = 4.61 \times 10^9 \text{ s}^{-2}$ . The dipolar interaction

between the protons within a methyl group will be modified by both the motions, namely the reorientation of the  $\text{CH}_3$  group as well as the isotropic tumbling of the TEMA cation. On the other hand, the interaction between the protons belonging to two different methyl groups will be affected predominantly by the isotropic reorientation of the TEMA group only. One of the assumptions which makes this point valid is that, normally the methyl group reorientation is much more rapid compared to that of the isotropic tumbling of the cation, since the methyl group is much smaller in comparison to the bulky cation and this rule will be violated only in conditions where the methyl group itself is highly hindered and reorients at a comparable rate as that of the TEMA cation.

Eqn.(C-2.20) can be written in another convenient form as the sum of two relaxation rates  $(T_1^{-1})'$  and  $(T_1^{-1})''$ , where,  $(T_1^{-1})'$  is the spin-lattice relaxation rate due to the modulation of the dipolar interaction between protons within a given methyl group, and  $(T_1^{-1})''$  is the relaxation rate corresponding to the modulation of the intermethyl group interactions.

$$(C-2.21) \quad T_1^{-1} = (T_1^{-1})' + (T_1^{-1})''$$

The spin-lattice relaxation rate contribution due to the modulation of the intra methyl group interaction is given by,

$$(C-2.22) \quad (1/T_1^{-1})' = (3/20) (\gamma^4 \hbar^2 / r^6) [g(\omega_o, \tau_{c1}) + 3g(\omega_o, \tau_{c2})]$$

Here,  $r$  is the interproton distance within the methyl group.

The contribution to  $T$  due to the **intermethyl** group interaction can be computed by assuming that at the center of each three **spin** set of protons of a methyl group, effectively only one proton is resident but the **strength** of relaxation is multiplied by a factor of 3 to take into consideration the physical presence of three protons in a given methyl group which is assumed to undergo very fast reorientations about their  $C_3$  axes [Albert et al., 1972]. Accordingly the expression for  $(T^{-1})$ , is given by

$$(C-2.23) \quad (1/T_1^{-1})^{-1} = 3 (9/10) (\gamma^4 \hbar^2 / r_{\bullet}^6) g(\omega_o, \tau_{c1})$$

and in this formula, the distance  $r_{\bullet}$ , is the distance between the center of one three spin **set**( $CH_3$  group), to the other. The dipolar interaction between the protons within a methyl group will be modified by both the motions, namely the reorientation of the  $CH_3$  group as well as the isotropic **reorientation** of the TEMA group. One of the assumptions which makes this point valid is that normally the methyl group **reorientation** is much more rapid compared to that of the isotropic tumbling of the cation, since the methyl group is much smaller in comparison to the bulky cation. This could be however violated only **in** conditions where the methyl group itself is highly hindered and reorients at a comparable rate as that of the TEMA cation.

Looking at the functional form of  $g(\omega)$ , we can see that when  $\tau$  is very small such that  $\omega\tau \ll 1$  ( which implies high temperatures as given by the Arrhenius formula, eqn.(C-2.1)),  $T_1$  is independent of  $\omega$  and is

proportional to  $T$ . On the other hand, at very low temperatures where  $T$

-1

-2

becomes large, i.e.,  $\omega\tau \gg 1$ ,  $T$  is proportional to  $\omega$ . Inbetween the two extremes one can expect to get a minimum corresponding to the respective  $T$  and thus for the two reorientational processes we will get two well resolved  $T$  minima in a plot of  $T$  vs  $(1000/T)$ , provided the two correlation times are quite different. The conditions for the occurrence of  $T$  minima for both kinds of reorientation is given by  $\omega\tau \approx 0.616$ , and substitution of this condition into the  $T$  formula gives the following expressions for the minimum values of  $T$  owing to the isotropic tumbling of the cations as well as the  $C_3$  reorientation of the methyl group.

$$(C-2.24) \quad \left( (T_{1min})^{-1} \right)_{TEMA} = \left( \frac{3}{20} \frac{\gamma^4 h^2}{r^6} + \frac{27}{10} \frac{\gamma^4 h^2}{r_*^6} \right) \frac{1.4252}{\omega}$$

and

$$(C-2.25) \quad \left( (T_{1min})^{-1} \right)_{CH_3} = \left( \frac{27}{10} \frac{\gamma^4 h^2}{r_*^6} \right) \frac{1.4252}{\omega}$$

At 8 MHz for example, the minimum value corresponding to the methyl group dynamics is 4.4 ms, and the  $T$  minimum value due to the isotropic reorientation of the TEMA group is 7.6 ms.



## DISCUSSION

Normally, the bulkier TEMA cation undergoes slower tumbling at any given temperature and therefore it is reasonable to expect the TEMA group motion to give a minimum at a higher temperature to the methyl groups. From eqns. (C-2.24) the expected value of the minimum for the isotropic reorientation of the TEMA cation is 38 ms at 39.8 MHz, 7.6 ms at 8 MHz and 3.8 ms at 4 MHz. Similarly the expected minima value due to the 3-fold reorientation of the methyl groups calculated with the help of eqn.(C-2.25) are : 22 ms at 39.8 MHz, 4.4 ms at 8 MHz and 2.2 ms at 4 MHz. But, it can be seen that the minima values immediately below the phase transition are all systematically lower than the values expected for the TEMA dynamics but they are all higher than the values associated with the methyl group dynamics. The possibility that the minimum immediately below the phase transition may correspond to methyl group implies that either the minimum due to TEMA group dynamics must be present at a much higher temperature than the one in region of this observation or the TEMA minimum must occur below this minimum. The latter possibility is ruled out because the methyl group can never be more hindered than the bulky TEMA cation itself. If the first case were to be true, the  $M_a$  value in this temperature should indicate that the TEMA motion has slowed down considerably but the observed value of  $0.5 \text{ Gauss}^2$  corresponds to fast isotropic tumbling of the TEMA cation thus ruling out the first case also as a possibility [Andrew et.al., 1972]. Thus, the first minimum should be corresponding to the TEMA dynamics only.

In order to account for the observed minima values (immediately

below transition) one can infer that some of the methyl groups have their  $T_1$  minimum at or very near this temperature to add to the relaxation rate effectively in this temperature region, thereby making the minimum deeper as is observed. This assignment corresponds to the presence of dynamically inequivalent methyl groups in the compound and many such instances were earlier reported. [Tsang *et.al.*, 1976; O'Reilly *et.al.*, 1967; Sundaram *et.al.*, 1986; Venu *et.al.*, 1987; Watanabe *et.al.*, 1989; Furukawa *et.al.*, 1989, 1990]. Specifically, in other solids belonging to the  $M_2X_9$  group also such instances of dynamic inequivalence among methyl group are reported [Jagadeesh *et.al.*, 1992, 1993a, 1993b]. Further, the values of minima which occur after the first one are shallower than what one expects to get if all the methyl groups are having the same correlation time and give a minimum at the same temperature. This fact, combined with the observation that the slope on the lower temperature side of the first minimum decreases with decreasing frequency, also points out a wide a distribution of correlation times of the methyl groups. Thus, the expression for the spin-lattice relaxation rate given by Albert's formula can be modified in the following fashion to take into account the proposed dynamic inequivalence among the methyl groups, namely,

$$(C-2.26) \quad T_1^{-1} = x A g(\omega, \tau_{C2}^A) + y A g(\omega, \tau_{C2}^B) + z A g(\omega, \tau_{C2}^C) + p A g(\omega, \tau_{C2}^D) + \dots + B g(\omega, \tau_{C1}^A)$$

where,  $x, y, z, p$ , etc., are the inequivalence factors for the respective methyl groups and  $T_1, T_2, \tau_{C2}, x$ , etc. are the corresponding correlation times. A non-linear least square fit program was used to fit

eqn.(C-2.26) to the data in the entire temperature range and such a fitting did not provide a consistent set of parameters for all the Larmor frequencies even after an extensive search using the least square program.

A careful scrutiny of the data shows that independent of the Larmor frequency the  $T_1$  data show a steep increase below 91K. Normally, such an increase is treated as natural with decreasing temperature, in the absence of any other effectively participating dynamic process at lower temperatures. If this were so, the corresponding activation energy estimated from the data is around 25 kJ/mole. The  $T_1$  minimum associated with such a large value of activation energy will shift very little with temperature from one Larmor frequency to another. Thus, the data at 8 MHz should show the presence of such a minimum around this temperature which is not the case as seen from the data. Further, around this temperature at 8 MHz there is a discontinuity in the  $T_1$  data. Thus it seems that, the sharp rise in  $T_1$  at 39.8 MHz and the discontinuity in the data at 8 MHz may correspond to some physical anomaly in the solid, in this temperature region, probably another structural phase transition. Thus, the data were refitted to the equation (C-2.26) avoiding this anomalous behaviour, thus only in the temperature range 151K - 91K. Many possible combinations of methyl group inequivalences were tried in this range and the set fitting the data consistently at both the frequencies corresponds to the inequivalence factors :  $x = 1/12$ ;  $y = 1/12$ ;  $z = 5/12$ ;  $p = 1/12$ . Thus, the expression for  $T_1$ , fitting the data consistently in this temperature range is given by

$$(C-2.27) \quad T_1^{-1} = (1/12) A g(\omega, \tau_{c2}^A) + (1/12) A g(\omega, \tau_{c2}^B) \\ + (5/12) A g(\omega, \tau_{c2}^C) + (1/12) A g(\omega, \tau_{c2}^D) + B g(\omega, \tau_{c1}^A)$$

The solid line passing through all the data points is the curve of best fit and the optimized dynamic parameters,  $(E, \tau)$  are provided in Table (C-2.1). The presence of such a wide distribution of the correlation times within a limited temperature region is observed in other systems as well [Furukawa et.al., 1989, 1990; Venu et.al., 1987]. In the calculation of the dynamic parameters corresponding to widely separated minima in  $T_1$ , the slope of the respective minimum determines  $E_a$  and the position of the minimum on the temperature scale fixes the value of  $\tau$ . But in cases where there are more than one minima present adjacent to one another, the slope corresponding to each minimum will not be clearly discernible and also the position of the minima will not be clearly identifiable. In that situation, it can be argued that, simulation of the experimental data with a given set of inequivalence factors for the minima may not be unique and one may be able to simulate the data with an entirely different set of inequivalence factors and corresponding dynamic parameters as well. Such problems regarding the uniqueness of the model can be removed by collecting  $T_1$  data as a function of, at least, two different Larmor frequencies, and insisting that the given model fits the data at both the frequencies for the same set of dynamic parameters within the estimated errors for them. The uniqueness of the model is ensured by such a procedure as the shift of the position of the minimum from one frequency to the other on the  $1000/T$  scale is sensitively dependent on the dynamic parameters and the overall behaviour of the data as a function of temperature is decided sensitively

TABLE (C-2.1)

SYMMETRIC GROUP				
COMPOUND	TEMA		CH <sub>3</sub>	
	E <sub>a</sub> (kJ/mole)	τ <sub>0</sub> (s)	E <sub>a</sub> (kJ/mole)	(s)
TEMACB				
above P.T.	10.0 ± 0.5	(7.3 ± 0.1)E-13		
below P.T.	13.5 ± 0.5	(5.9 ± 0.05)E-14	35.0 ± 0.5	(8.9 ± 0.3)E-22 (CH -A)
			2.0 ± 0.5	(3.2 ± 0.2)E-09 (CH -B)
			8.0 ± 0.5	(1.6 ± 0.2)E-13 (CH -C)
			21.0 ± 1.0	(6.0 ± 1.0)E-24 (CH <sub>3</sub> -D)
TEMABB				
above P.T.	7.0 ± 0.5	(2.5 ± 0.2)E-12		
below P.T.	14.5 ± 0.5	(8.0 ± 1.00)E-14	16.0 ± 0.5	(3.5 ± 0.5)E-16 (CH <sub>3</sub> -A)
			9.0 ± 0.5	(4.5 ± 0.5)E-13 (CH -B)
			16.5 ± 0.5	(1.0 ± 0.5)E-15 (CH -C)

OPTIMIZED DYNAMIC PARAMETERS FOR THE COMPOUNDS TEMACB  
AND TEMABB

by the proper choice of the inequivalence factors. Thus, only an appropriate model would satisfy the requirement of fitting the data at more than one Larmor frequency with the same set of  $E$ ,  $T$  and  $\tau$  inequivalence factors. In the case of TEMACB  $T$  data were collected at three frequencies and it is found that the above given model fits this data well at all the three frequencies with a given set of dynamic parameters, within error. Even in the case of other compounds investigated as a part of this work  $T$  data were collected at more than one Larmor frequency to ensure the uniqueness of the model used to fit these data.

It is notable that (1/12) of the methyl groups tend to have a minimum at the same temperature where large TEMA cations also have. This indicates that this set of CH groups (CH -A) are highly hindered that their dynamics is as slow as that of the TEMA groups. This seems to be unique to the behaviour of the methyl groups in these compounds. In fact, in the antimony analogue of this compound (TEMACA) also, such highly hindered methyl groups are observed and their inequivalence factor is 1/12 as well.

Mention has to be made about the unusually small value of  $\tau$  in the case of CH -A. The hindering potential for this methyl group has a large value of (35.±2.0) kJ/mole but activation energies of 21±2.0 kJ/mole or more are not uncommon [Albert et.al., 1972; Mahajan et.al., 1972; Tsuneyoshi et.al., 1977; Ratcliffe et.al., 1977]. In comparison, the TEMA group has a smaller activation energy of (13.0 ± 1) kJ/mole. Even though the  $E$  for the CH<sub>3</sub>-A group is large, the fact that it forms a minimum

around as low a temperature as 150 K necessarily implies that the correlation time at infinite temperature for this motion is rather small. In fact, if the  $T$  value is of the order of the normally observed values like 10 s, say, then the expected minimum for the  $\text{CH}_3\text{-A}$  group will be at a much higher temperature and with the TEMA group itself forming a minimum around 150K, this is an improbable situation. This implies that, even though the hindering potential for the  $\text{CH}_3\text{-A}$  group's reorientation is rather high, (which is normally determined by the structural considerations), the coupling of this group to the phonon spectrum in the solid is rather more efficient in that it is able to undergo relatively fast motions despite a large hindering barrier. In fact, such similar situations, where the hindering potential is rather high ( $\approx 125$  kJ/mole), but the  $\tau$  is also very low ( $= 10^{-23}$  s) have been observed in the cationic reorientation of pyridinium complexes [Tai et.al., 1990]. Such a line of understanding is applicable to the values corresponding to the  $\text{CH}_3\text{-B}$  groups also, where, the activation energy is very low but  $T$  is very high, the minimum thus forming around 140K for this group. As far as the values corresponding to group  $\text{CH}_3\text{-D}$  is concerned, the  $\tau$  is very small though the  $E$  value is within a reasonable range. It is however to be noted that with the anomalous behaviour of data around 91 K, the data could be fitted only within a truncated range. In fact, minimum due to  $\text{CH}_3\text{-D}$  does not occur within this range, but we have only a marginal influence of its minimum in the vicinity of this range, adding to the relaxation rate. The corresponding dynamics parameters of this group could be decided obviously with considerable ambiguity only (refer to Table C-2.1).

The model we have assumed thus far is consistent with the values of  $M$ . The low and constant value of  $M$  at  $(0.5 \pm 0.1)$  Gauss indicates fast isotropic reorientation of the TEMA cation as well as fast motion of all the methyl groups [Andrew et.al., 1972].  $\tau_2$  value has increased to a value of  $11 \pm 0.5$  Gauss by 77K. With a residual second moment of 0.5 Gauss, if 1/12 of methyl groups have reached rigid lattice limit along with the TEMA groups and if 11/12 of the methyl groups are still in the motionally narrowed limit, the expected  $M_2$  is 11.6 Gauss [Andrew et al., 1972]. The observed value of 11 Gauss<sup>2</sup> at 77K is close to this value and  $T$  values computed for the different groups at 77K indeed show that only the motion of CH-A group along with TEMA group have reached rigid lattice limit by this temperature ( $\tau_{CH-A} = 4.98e2$  s), while the other methyl groups are still undergoing fast reorientations ( $x_{CH-B} = 1.4e-7$  s;  $x_{CH_3-C} = 5.3e-8$  s;  $x_{CH_3-D} = 2.0e-21$  s), confirming such a scenario. Thus, this confirms our initial assumption that, the 1/12 of methyl groups with an activation energy of  $35 \pm 2$  kJ/mole is as hindered as the TEMA group as far as the reorientational dynamic processes are concerned. The wing-like structure observed at 77K in the CW spectrum may be attributed to one of the following reasons : (i) it may be correspond to the condition where the dynamics of TEMA cation is completely frozen and CH groups are still undergoing fast reorientations [Polak et al., 1973] or (ii) it may be due to the complete freezing of the dynamics of some of the inequivalent methyl groups [Venu, 1985] or (iii) it may also be due to the methyl groups exhibiting tunneling.

The  $T$  data above 151 K is dispersionless, and from the  $M$  data, this region corresponds to the isotropic tumbling of the TEMA cation and



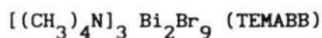
fast reorientation of all the methyl groups. Contribution to the  $T_1$  from TEMA dynamics is expected to be dominant in this region, with a negligible contribution coming from 1/12 of the methyl groups also ( $\text{CH}_3\text{-A}$ ). The activation energy derivable from  $T_1$  vs  $T$  data in this region then essentially corresponds to the isotropic reorientation of the TEMA group. The values of  $E$  and  $T_1$  computed from this linear portion of the  $T_1$  data above the phase transition temperature are given in Table (C-2.1). From the parameters belonging to the TEMA group, both above and below the phase transition temperature, the correlation time at the phase transition temperature as we approach it from a higher temperature is computed to be  $1.98\text{e-}9$  s, whereas from lower temperature, the  $T_1$  value is  $2.5\text{e-}9$  s. Assuming that  $\omega\tau \ll 1$  in the dispersionless region,  $T_1$  value is computed for the above two  $T_1$  values to be 22 ms and 16 ms respectively. As can be seen from the  $T_1$  data, as we approach the transition point from the higher temperature, the  $T_1$  value is 20 ms and this is in very good agreement with the calculated value. The values of  $T_1$  for the two correlation times show that for the given amount of jump in the correlation time, a perceptible change in the value of  $T_1$  at 151 K is expected. In fact, with the minimum being formed near the phase transition temperature in 8 and 4 MHz, the condition  $\omega\tau \ll 1$  may no longer be strictly valid and one should expect to see a frequency dependence on the extent to which the  $T_1$  value jumps from a value of 22 ms and this is indeed the case as can be seen from the Fig. (C-2.1). Returning back to the observation of the absence of a signature of the transition on the  $T_1$  data at 39.8 MHz, first of all we can verify from the values of dynamic parameters of TEMA computed below the transition that the minimum at 39.8 MHz is indeed forming at around 151K and secondly for the above mentioned

values of  $T - S$ , namely,  $1.98\text{e-}9$  s and  $2.5\text{e-}9$  s, the  $T$  values at 39.8 MHz are calculated to be 39 ms and 38 ms, respectively and this is not perceptible within experimental errors.

The observed anomaly in  $T$  values below 91 K perhaps may correspond to another phase transition, but there is no other supportive evidence from other techniques to corroborate this possibility. However, in the family of **alkylammonium** halogeno **antimonates** and **bismuthates**, replacing the antimony atom by bismuth has systematically reduced the transition temperature in all the compounds of the family, and in almost all the compounds of the Bismuth group, a low temperature anomaly is always observed. For example, in DMACB which has a **dimethylammonium** cationic group, there is a very steep rise in the value of  $T$  by an order of magnitude within a temperature region of 1 at around 78 K, which strongly suggest a structural phase transition. Such transitions are seen in these compounds only after the substitution of the bulky Bismuth atom in place of Antimony. In fact, it has been reported in literature in the context of **tetraalkylammonium** metal chlorides that substitution of a heavier metal atom brings down the phase transition temperature in those compounds, which is consistent with our observation also [Kahrizi et.al., 1990]. Apart from the metal atom, the halogen atom also plays an important role in determining the structural phase transitions [Kahrizi et.al., 1991]. Another remarkable feature in connection with this compound is that there is no signature of this on the  $M_2$  data though a clear signature of the phase transition is observed on  $T$  data. The jump in the  $T$  being only from  $1.98\text{e-}9$  s to  $2.56\text{e-}9$  s, which was sufficient to cause a perceptible change in the value of  $T$ , 'this change in  $T$  is not

sufficient to cause a line width transition, a line **width** transition occurring only at time scales corresponding to inverse of linewidth ( $10^{-4}$  s).

It is clear that, substitution of a heavier metal atom like Bi, in the place of Sb, has caused considerable structural inequivalence among the groups in the solid, thereby bringing about a large degree of dynamic inequivalence among the methyl groups. More importantly, the observed phase transition is associated with the freezing of the isotropic motion of the cation. It will be interesting to compare the features of this solid with other **tetramethyl** groups in the family, but we shall postpone that detailed discussion to a latter section.



**T<sub>1</sub> data :**

Larmor frequencies	39.6 and 8 MHz
Temperature range	370K - 77K

**M<sub>2</sub> data :**

Temperature range	: 390K - 77K
-------------------	--------------

Variation of **T** with **1/T** in TEMABB : Fig.(C-2.3)

**M<sub>2</sub>** variation as a function of temperature in TEMABB : Fig.(C-2.4)

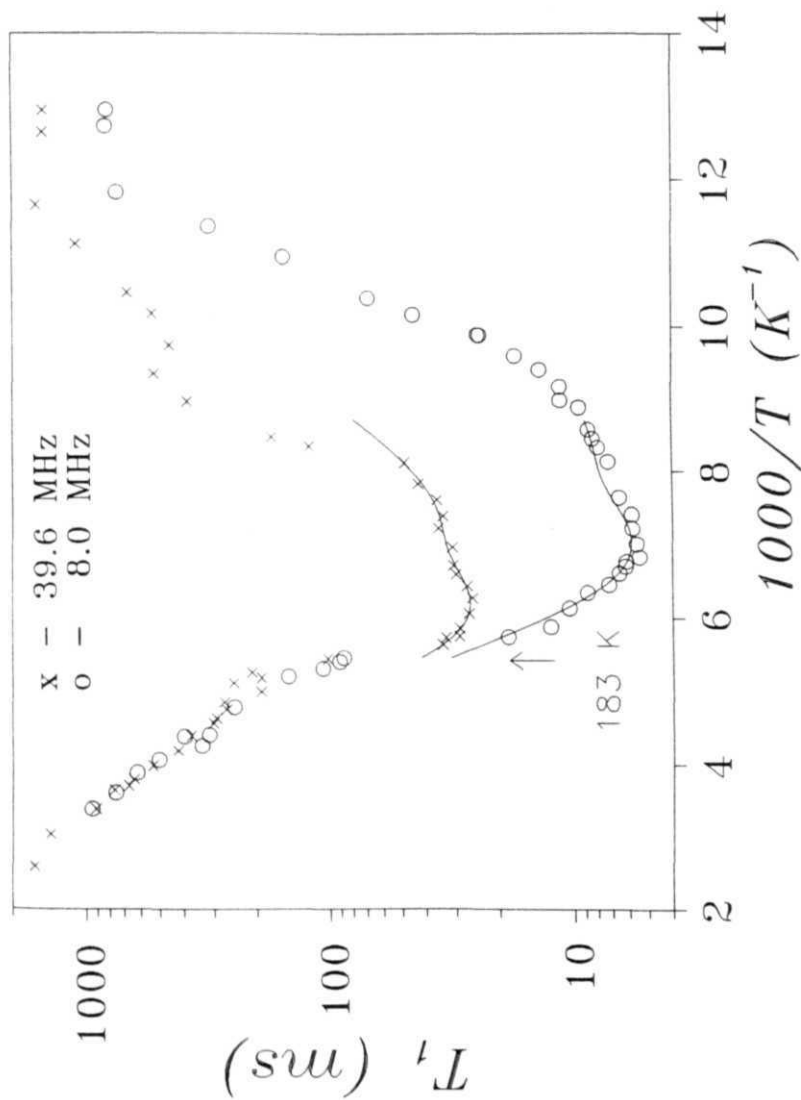
Optimized motional parameters : Table (C-2.1)

# TEMABB

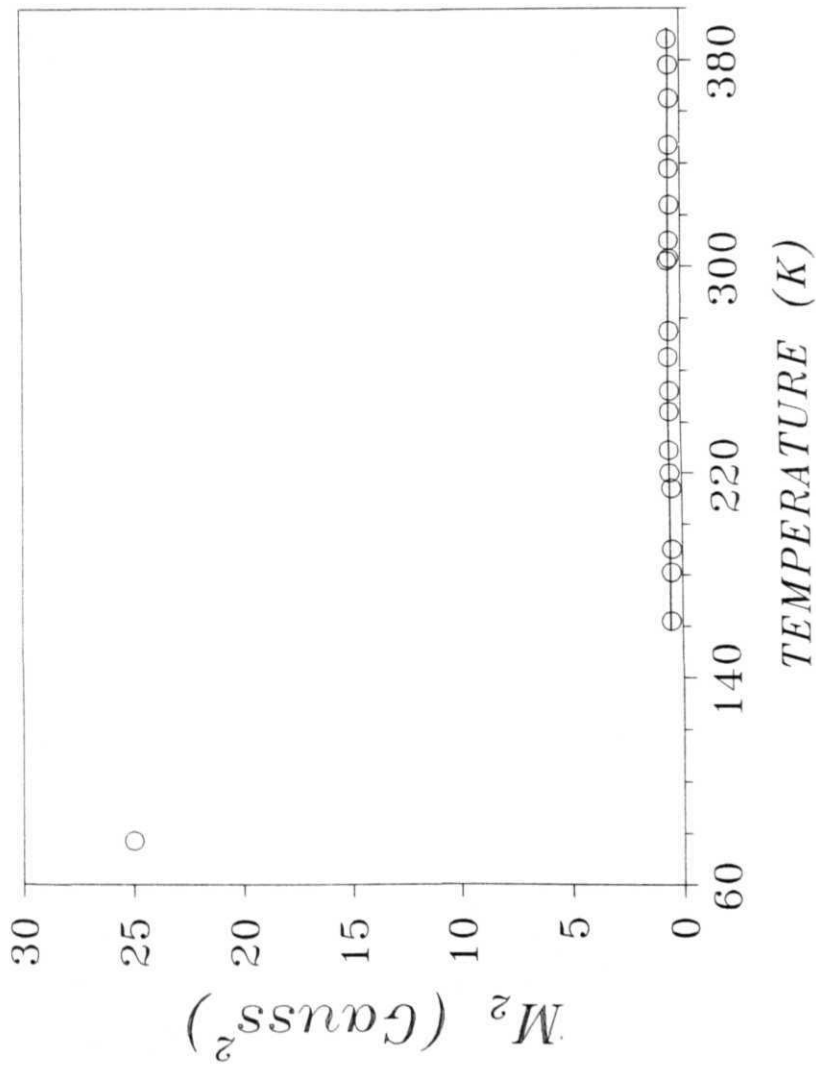
## RESULTS

TEMABB was prepared by mixing the parent compounds  $[N(CH_3)_4] Br$ , and  $BiO$  in a suitable acid medium like  $HBr$  and evaporating the mixture slowly at constant temperature ( $\approx 40^\circ C$ ). Orange coloured crystals separated out from the solution and elemental analysis on the compound showed the following percentages of C, H and N : C - 10.625%. (10.602% expected), H - 2.70% (2.669% expected), N - 2.78% (3.091% expected). The crystals were dried and powdered and sealed under 10 torr vacuum for measurements.

With respect to the T data this compound has qualitatively similar features as that of TEMACB i.e., there is a discontinuous jump in the T. value at 183 K and at a lower temperature like 122 K, there is again a steep rise in the value, which is present only at 39.6 MHz but not at 8 MHz and data at 39.6 MHz shows a shoulder like structure. This compound is found to exhibit a first order structural phase transition, as verified by DTA and dilatometric methods at 183 K, [Jakubas et al., 1993] and thus from the precedence of the previous compound, we can say that this steep fall in this T data is also associated with that structural phase transition occurring at the temperature 183K. Once again T data show a dispersionless region above 183 K and below the transition, we see a minimum followed immediately by a smeared shoulder like structure. At 39.6 MHz the T value increases rather sharply around 122K, and such a signature is not observable in the case of 8 MHz data.  $M_2$  value remains constant around  $(0.6 \pm 0.1)$  Gauss till the observed temperature 160K and at 77K, its value is  $24 \pm 1$  Gauss<sup>2</sup>.



(C-2.3) Variation of  $T_1$  as a function of  $(1000/T)$  in  $[(CH_3)_4N]^3 Bi_2Br_9^-$ . Solid lines through data points are the fitted curves.



(C - 2.4) Variation of  $M_2$  as a function of  $T$  in  $[(CH_3)_4N]_3 Bi_2Br_9$ .

## DISCUSSION

Following the lines of **argument** as in TEMACB, we tried to fit the T data to eqn.(C-2.26), with the various combinations of inequivalence factors and it is found that, no consistent set of the motional parameters are available for which the T data can be fitted at both the frequencies in the entire temperature range. Thus, the data were consequently fitted in a restricted temperature range 183K - 120K, avoiding the anomalous region below 120K as before, to a model given by,

$$(C-2.28) \quad T_1^{-1} = (1/6) A g(\omega, \tau_{c2}^A) + (1/3) A g(\omega, \tau_{c2}^B) \\ + (1/6) A g(\omega, \tau_{c2}^C) + B g(\omega, \tau_{c1}^A)$$

In contrast to the chlorine analogue TEMACB, in this compound 1/6 of the methyl groups are contributing to the minimum at around the same temperature where the TEMA groups also do. Further, it is observed that in TEMABB the minimum has formed much closer to the transition temperature than that of TEMACB. The shoulder like structure following the first minimum is slightly smeared out and from this feature it can be said that **it** occurs because of the presence of more **than** one minima **lying** adjacently. The fitted parameters, (E , T ) are presented in Table a o

(C-2.1). Compared to TEMACB, these values are **all in a** reasonable range. The fitted curve is shown as a solid line through the data points at both the frequencies in the Fig. (C-2.3). The E value for the TEMA reorientation above the phase transition is **7.0±0.5 kJ/mole** and from the above given model, the value below is 15±1.0 kJ/mole. It may be recalled

that in the case of TEMACB, the corresponding values are  $10 \pm 1.0$  kJ/mole and  $13.0 \pm 1.0$  kJ/mole, respectively. In both these cases it is clear that the phase transition to a low temperature phase has increased the hindrance for the reorientation of the cation. From dynamic parameters it is observed that in the chlorine compound, the CH -A group is the most hindered group of all the three methyl groups. But here, in the Bromine compound the other groups are also having a hindrance of a comparable order. In fact, the dynamics of these methyl groups in TEMABB being comparable to one another is reflected in the freezing of the motion of both CH -A and CH -B groups by 77K. This fact is reflected by  $\tau$  which has reached a value of  $24 \text{ Gauss}^2$  by 77K. This value corresponds to the freezing of the isotropic motion of the TEMA cation as well as 1/2 of all the methyl groups in the system [Andrew et.al., 1972]. This can be verified from the values of the motional parameters of the different methyl groups.

The substitution of Bromine in place of Chlorine has marginally reduced the hindrance for the TEMA motion above the phase transition from  $9.6 \pm 1.0$  kJ/mole to  $7.0 \pm 0.5$  kJ/mole. But below the phase transition temperature, the hindrance for the isotropic tumbling of the cation seems to be similar in both the cases. A remarkable observation in connection with the tetramethyl substituted compounds in this family is the fact that, in the compounds TEMABB, TEMACA and TEMABA, with exception of TEMACB, at their respective phase transition temperatures,  $\tau$  corresponding to the isotropic tumbling of the TEMA cation tends to reach a common value, within error. The  $\tau$  values as one approaches the phase transition point from high temperatures are : x -  $2.4 \times 10^{-10}$ s,



$\tau_{\text{TEMABA}} = 2.7 \times 10^{-10} \text{ s}$ ,  $\tau_{\text{TEMABB}} = 3.3 \times 10^{-10} \text{ s}$ . This feature is further discussed later.

# REFERENCES

- (C-2.1) ALBERT S. , J.A. RIMEESTER, H.S. GUTOWSKY, *J.Chem.Phys.* , 56, (1972) 3672
- (C-2.2) ANDREW E.R. , P.C. CANEPA, *J.Magn.Reson.* , 7, (1972) 429
- (C-2.3) BLOEMBERGEN N. , E.M. PURCELL AND R.V. POUND, *Phys.Rev.*, 73, (1948) 679
- (C-2.4) FURUKAWA Y. , C. KOJIMA AND D. NAKAMURA, *Ber. Bunsenges. Phys.Chem.* , 93, (1989) 696
- (C-2.5) FURUKAWA Y. AND D. NAKAMURA, *Bull.Chem.Soc. Japan*, 63, (1990) 2110
- (C-2.6) ISHIHARA H. , K. WATANABE, A. IWATA, K. YAMADA, Y. KINOSHITA, T. OKUDA, V.G. KRISHNAN, SHI-QI DOU AND A. WEISS, *Z.Naturforsch.*, 47a, (1992) 65
- (C-2.7) JAGADEESH B. , P.K. RAJAN, K. VENU AND V.S.S. SASTRY, *Cheat.Phys.*, 163, (1992) 351
- (C-2.8) JAGADEESH B. , P.K. RAJAN, K. VENU AND V.S.S. SASTRY, *J.Phys.Chem. Solids*, 54, (1993a) 527
- (C-2.9) JAGADEESH B., P.K. RAJAN, K. VENU AND V.S.S. SASTRY, *Solid State Commun.*, 86, (1993b), 803
- (C-2.10) JAKUBAS R., Z GALEWSKI, L. SOBCZYK AND J. MATUSZEWSKI, *Ferroelectrics*, 88, (1988) 83
- (C-2.10) JAKUBAS R., Z. GALEWSKI, J. MATUSZEWSKI AND J. LEFEBVRE, *Phys.Stat.Sol.(a)*, 136, (1993) K19
- (C-2.11) KAHRIZI M. AND M.O.STEINTZ, *Solid State Commun.*, 74, (1990) 333
- (C-2.12) KAHRIZI M. , M.O. STEINITZ AND TRUIS-SMITH PALMER, *Solid State Commun.* , 77, (1991) 99
- (C-2.13) MAHAJAN M. AND B.D. NAGESWARA RAO, *J.Phys.Chem. Solids*, 33,

(1972) 2191

(C-2.14) O'REILLY D. AND TUNG TSANG, *J.Chem.Phys.*, 46, (1967) 1291

(C-2.15) POLAK M., L. SHEINBLATT, *J.Mang.Reson.*, 12, (1973) 261

(C-2.17) RATCLIFFE C.I. AND B.A. DUNNEL, *J.Chem. Soc.Faraday.Trans.2*, (2), (1977) 493

(C-2.18) SUNDARAM C.S., J. RAMAKRISHNA, K. CHANDRASEKHAR AND V.S.S. SASTRY, *Ferroelectrics*, 69, (1986) 299

(C-2.19) TAI Y., T. ASAJI, D. NAKAMURA, R. IKEDA, *Z.Naturforsch.*, 45a, (1990) 477

(C-2.20) TSUNEYOSHI T., N. NAKAMURA AND H. CHIHARA, *J.Magn.Reson.*, 27, (1977) 191

(C-2.21) TUNG TSANG AND D.B. UTTON, *J.Chem. Phys.*, 64, (1976) 3780

(C-2.22) VENU K.. *Ph.D Thesis, University of Hyderabad*, (1985)

(C-2.23) VENU K., V.S.S. SASTRY AND J. RAMAKRISHNA, *Phys.Stat.Sol.(b)*, 140, (1987) 251

(C-2.24) WATANABE R., T. ASAJI, Y. FURUKAWA AND D. NAKAMURA, *Z.Naturforsch.*, 44a, (1989) 1111

(C-2.25) WOESSNER D.E., *J.Chem.Phys.*, 36, (1962) 1

## SECTION C

### T A R I 3

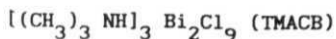
#### RELAXATION AND RESONANCE STUDIES ON $[(CH_3)_3 NH]_3 Bi_2Cl_9$ AND $[(CH_3)_2 NH_2]_3 Bi_2Cl_9$

Trimethylammonium (TMA) and dimethylammonium (DMA) cations are less symmetric in comparison to the **tetramethylammonium** (TEMA) cations which have tetrahedral symmetry. TMA cation has an axis of three-fold symmetry called triad axis and similarly DMA cation has a two-fold symmetric axis which is the diad axis. Unlike in the case of TEMA cations which do not have any unique axis of **reorientation**, for TMA and DMA cations, the triad and diad axes are preferred axes of reorientations, respectively. Because of **the** lower symmetry normally isotropic motion takes place at much higher temperatures in these cations in contrast with the TEMA counterparts of these compounds.  $[(CH_3)_3 NH]_3 Bi_2Cl_9$  (TMACB) and  $[(CH_3)_2 NH]_3 Bi_2Cl_9$  (DMACB) are the Bismuth substituted compounds of the **title** family **which** contain the TMA and DMA cations, respectively. Till date, no other data seems to be available on these compounds to the best of the author's knowledge but the Antimony substituted counterparts of these compounds were investigated with different techniques [Jakubas et al., 1990].  $[(CH_3)_3 NH]_3 Sb_2Cl_9$  (TMACA) is **monoclinic** and crystallizes in the space group Pc and the structure contains  $SbCl_6$  octahedra interlinked to each other by vertex sharing to form a two dimensional network [Kallel et al., 1985]. The cations are situated in between these layers and **inside** the ring like structures formed by the  $MX_6$  octahedra and these are connected to the anions **via** N-H...Cl **hydrogen** bonds.

Crystal structure data reveal the fact that cations are undergoing fast reorientations in this compound [Kallel et al., 1985; Jakubas et al., 1989] and DSC, dielectric and pyroelectric measurements on this compound revealed a structural phase transition in this compound at 367K and it is found that this compound exhibits ferroelectricity [Jakubas et al., 1986].

$[(CH_3)_2NH_2]_3Sb_2Cl_9$  (DMACA) is also monoclinic and crystallizes in the space group P2/a and it has a similar structure as to that of TMACA. Here also, the cations are either situated in between layers of  $M_2X_6$  anions inside the hexagonal voids present within a layer [Gdaniec et al., 1988] and they are linked via hydrogen bonds to the anions. A structural phase transition is observed in DMACA at 242K using dielectric dispersion studies and IR spectroscopy, In both TMACA and DMACA the formation hydrogen bonds tend to distort the anionic structure and this may be related to the observed ferroelectricity in these compounds. Proton NMR measurements on TMACA and DMACA revealed the presence of TMA and DMA cations which are dynamically inequivalent and the reorientations of the cations are associated with the observed phase transitions in these compounds which is manifested as clear discontinuities in the T data [Jagadeesh et al., 1993a, 1994]. Substitution of Bismuth in such a case will necessarily bring about some changes in the dynamic properties of the cations as it was in the case of tetramethylammonium compounds and it will be of further interest to look for possible presence of structural phase transitions in the Bi substituted compounds and their influence on the dynamics of the cations. In this section the results of T. and M. measurements on the compounds  $[(CH_3)_3NH]_3Bi_2Cl_9$  (TMACB) and  $[(CH_3)_2NH_2]_3Bi_2Cl_9$  (DMACB)

are presented discussed.



Specific Details

#### **T measurements**

Larmor frequencies : 8 and 39.6 MHz

Temperature range : 425 K to 77 K

#### **M. measurements**

Temperature range of observation : 370K to 77K

T. data fitted to the appropriate model : Fig.(C-3.3)

M variation as a function of temperature . Fig.(C-3.4)

Optimized dynamic parameters : Table (C-3.1)

TMACB crystals were grown by slow evaporation technique from the parent compounds  $[(\text{CH}_3)_3\text{NH}]\text{Cl}$  and  $\text{BiCl}_3$  in a suitable acid medium (HCl) and the well grown crystals were made into powder and dried before they were sealed under 10 torr vacuum in glass tubes for measurements.

## **TMACB**

### **RESULTS**

T. data, collected at larmor frequencies 8 and 39.6 MHz, can be considered, for convenience, corresponding to two regions. Region I (above 300K) and II (below 300K). In region I, the data show a well formed shoulder which is followed by a rather broad minimum, including a shallow region around 167 K at 39.6 MHz, and around 135 K at 8 MHz. At

about 100K, the T shows a small discontinuity at both the frequencies. The data do not show well resolved minima which can be attributed either only to the TMA dynamics or to the methyl group dynamics. But the wide minimum suggests that, a rather wide distribution of the correlation times may be present for the relevant dynamic process in this compound.  $M_2$  value is constant at  $1.5 \pm 0.1 \text{ Gauss}^2$  at higher temperatures, and which it increases to  $2.5 \pm 0.1 \text{ Gauss}^2$  as the sample is cooled to about 140K. At 77K, the  $M_2$  value has increased to  $6 \pm 0.5 \text{ Gauss}^2$ .

## DISCUSSION

If all the TMA cations are undergoing isotropic tumbling, while the methyl groups are undergoing rapid reorientations the expected  $M_2$  is  $1.2 \pm 0.1 \text{ Gauss}^2$  [Andrew et.al., 1972]. In this context the value of  $1.5 \pm 0.1 \text{ Gauss}^2$  indicates the possibility that the isotropic reorientation of some of the TMA groups may perhaps be frozen by NMR time scales. To analyze T data, a relevant model is needed which can take into account the following dynamics in TMA which are : (i) the reorientation of TMA cation about its triad axis and (ii) the reorientation of the methyl groups about their C axes and an expression for the spin-lattice relaxation rate should be derivable in terms of the correlation times associated with the above said motions from the model. Such a suitable model is discussed in the following before analyzing the T data of TMACB further. Similar considerations apply in the case of the DMA cation and the following section, therefore, also includes the model relevant for the DMA dynamics, which is used to analyze the T data in the case of DMACB.

## THE MODEL :

In working out the model for the spin-lattice relaxation rate in the case of a symmetric cation like **tetramethylammonium** ion, two kinds of molecular motions were assumed to be present. One is the C reorientation of the methyl group and the other is the isotropic reorientation of the TEMA cation as a whole (Section C-1). The TEMA cation has perfect tetrahedral symmetry (assuming that the cation is not distorted due to other crystal field forces), and this tetrahedron has four 3-fold symmetric axes and three 2-fold axes. The isotropic tumbling of the TEMA cation can be looked upon as the random reorientation of these symmetry axes in space and this kind of a motion is also referred to as the reorientation about the pseudo symmetric C and C axes, in literature [ Takeda *et.al.*, 1982; Sato *et.al.*, 1982, 1986a, 1986b, 1987]. While calculating T it was assumed that the isotropic reorientation of this cation has innumerable number of equivalent orientations in space and the probability of finding the ion in any one of the equivalent positions evolves as an exponential function in time which resulted in a simple exponential time dependence of the correlation functions of the space dependent terms in the dipolar Hamiltonian [ Woessner, 1962]. However, owing to the tetrahedral symmetry there is no other lower order motion possible in the case of a tetramethylammonium cation except for the internal motions of the methyl groups. But an interesting situation arises, when we consider a **trimethylammonium** (TMA) or a **dimethylammonium** (DMA) ion. Here, owing to the presence of the lone protons in one or two of the apexes of the tetrahedron, the molecule assumes a lesser order of symmetry. In the case of TMA, this has only one preferred axis of 3-fold symmetry (the triad axis) and DMA has only one preferred axis of 2-fold symmetry (the



diad axis), and at any given energy reorientation of these ions about these symmetric axes are more probable for energetic reasons.

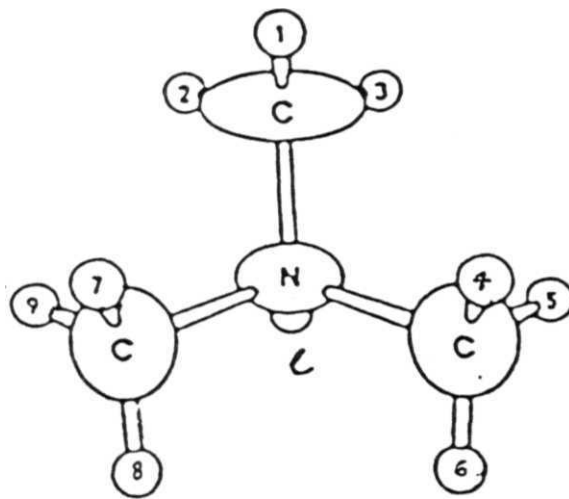
In the light of this, new model taking into account the finite number of equivalent positions of the molecules are needed to calculate the spin-lattice relaxation rates due to the dynamics of the TMA and DMA cations. The models developed by Sjöblom et.al., and Venu et.al. taking care of these factors, are applicable to such systems, as for instance in the case of compounds TMACB and DMACB, respectively. We shall discuss these models briefly below, leading to an expression for the spin lattice relaxation rate.

### Trimethyl Ammonium Dynamics

The basic idea behind this model, and similarly the model for the DMA cation dynamics, can be mentioned as follows. For example in TMA, any given proton in a methyl group can contribute to the relaxation process by the modulation of its interaction with two of **its** immediate neighbours within the methyl group, six other protons in other methyl groups and one more lone proton. This modulation can come about by (i) the reorientation of the methyl group about its **C** axis, (ii) the **reorientation** of the TMA cation about its triad axis and these two motions can **in** principle be uncorrelated. But we can envisage two other possible motions, i.e. (i) the correlated motion of both the TMA cation and one of the methyl groups (ii) the correlated motion of TMA and two of the methyl groups. Each pair of protons which are in the positions *i* and *j* have an occupational probability *p*. and owing to the aforementioned reorientational processes, this probability becomes time

dependent. The site probability of a given position  $ij$  will have an outflowing component due to the fact any one of the above processes can take this pair away from the position " $ij$ " and similarly it will have an inflowing component, since, these can also in principle bring any other pair of protons to this position " $ij$ ". It is clear that the time rate of change of the probability  $p$  is proportional to these outflowing and inflowing components which in turn depend on the reorientational rates of the processes. Let us define " $r$ " to be the average rate of reorientation of the CH group, " $R$ " to be rate of reorientation of the TMA group, and  $R'$  and  $R''$  are the reorientation rates of the correlated motion of TMA and one methyl group, which we shall call the first kind, and the correlated motion of the TMA ion and two of the methyl groups, which we shall call the second kind. It is worthwhile to note here that the inverse of the rate of reorientation gives the dwell time of the molecule in one of the allowed configurations and the reorientation gives us the average rate at which a given configuration of the molecule changes to any other possible configuration.

Referring to Fig(C-3.1), as an example, let us consider the proton pair 12. This pair can reach (i) positions 23 and 31 due to the rotation of the methyl group only at a rate  $r/3$  and reach 12 itself at a rate  $2r/3$ ; (ii) positions 45 and 78 by the reorientation of the TMA cation alone at a rate  $R/3$ , and reach 12 itself at a rate  $2R/3$ ; (iii) positions 23, 31, 56, 64, 89 and 97 at a rate  $RV_{12}$ , positions 45 and 78 at a rate  $R'/6$ , and reach 12 itself at a rate  $5RV_6$  due to the correlated motion of the first kind, and (iv) positions 23, 31, 56, 64, 89 and 97 at a rate  $R''/6$  and 12 itself at a rate  $R''$  due to the correlated motion of the second kind. We can similarly figure out the various



(C - 3.1) Model of the trimethylammonium (TMA) cation.

reorientation rates with which other proton pairs within a methyl group can reach various positions. These reorientations will be able to modulate the **intra-methyl** proton-proton interactions. By symmetry, we can see that

$$p_{23} = p_{31}; \quad p_{45} = p_{78}; \quad \text{and} \quad p_{56} = p_{64} = p_{89} = p_{97}$$

and we can write the rate equations for all these probabilities. As an example, the rate equation for the pair 12 is given by

$$(C-3.1) \quad \dot{p}_{12} = - \left( \frac{2}{3}r + \frac{2}{3}R + \frac{5}{6}R' + R'' \right) p_{12} + \left( \frac{r}{3} + \frac{R'}{12} + \frac{R''}{6} \right) (p_{23} + p_{31}) \\ + \left( \frac{R}{3} + \frac{R'}{6} \right) (p_{45} + p_{78}) + \left( \frac{R'}{12} + \frac{R''}{6} \right) (p_{56} + p_{64} + p_{89} + p_{97})$$

Because of the equality of the probabilities due to symmetry, we have only four unique probabilities  $p_{12}$ ,  $p_{23}$ ,  $p_{45}$  and  $p_{56}$  as far as the **intramethyl** group interactions are concerned, and we have four unique rate equations for these probabilities. Since, each probability is coupled to the other three through the rate equation, these can be elegantly written in the form of a matrix equation as given below.

(C-3.2)

$$d/dt \begin{bmatrix} p_{12} \\ p_{23} \\ p_{45} \\ p_{56} \end{bmatrix} = \begin{bmatrix} d_{11} & \frac{2}{3}r + \frac{R'}{6} + \frac{R''}{3} & \frac{2}{3}R + \frac{R'}{3} & \frac{R'}{3} + \frac{2}{3}R'' \\ \frac{r}{3} + \frac{R'}{12} + \frac{R''}{6} & d_{22} & \frac{R'}{6} + \frac{R''}{3} & \frac{2}{3}R + \frac{R'}{2} + \frac{R''}{3} \\ \frac{R}{3} + \frac{R'}{6} & \frac{R'}{6} + \frac{R''}{3} & d_{33} & \frac{2}{3}r + \frac{R'}{3} + \frac{2}{3}R'' \\ \frac{R'}{12} + \frac{R''}{6} & \frac{R}{3} + \frac{R'}{4} + \frac{R''}{6} & \frac{r}{3} + \frac{R'}{6} + \frac{R''}{3} & d_{44} \end{bmatrix} \begin{bmatrix} p_{12} \\ p_{23} \\ p_{45} \\ p_{56} \end{bmatrix}$$

Here, each diagonal element is given by the sum of all the other terms

in the respective row, with a negation. For example, d is given by  $-(\frac{2}{3}r + \frac{2}{3}R + \frac{7}{6}R' + R'')$ . Finding out the solution to the above set of equation can be simplified by taking linear combination of the probabilities p and p as well as p and p<sub>56</sub> and we can recast the above equation as the following.

### (C-3.3)

d/dt

$$\begin{bmatrix} p_{12} - p_{23} \\ p_{45} - p_{56} \end{bmatrix} = \begin{bmatrix} - \left( r + \frac{2}{3}R + \frac{11}{12}R' + \frac{7}{6}R'' \right) & \frac{2}{3}R + \frac{R'}{6} - \frac{R''}{3} \\ \frac{R}{3} + \frac{R'}{12} - \frac{R''}{6} & \left( r + \frac{R}{3} + \frac{5}{6}R' + \frac{4}{3}R'' \right) \end{bmatrix} \begin{bmatrix} p_{12} - p_{23} \\ p_{45} - p_{56} \end{bmatrix}$$

Similarly, taking the linear combination  $p_{12} + 2p_{23}$  and  $p_{45} + 2p_{56}$ , we can write down an equation similar to (C-3.3). These two equations can be solved for the initial conditions :  $p_{12}(0)=1, p_{23}(0)=p_{45}(0)=p_{56}(0)=0$ . From these solutions we obtain the following expressions for the individual probabilities, which are once again written in the form of a matrix equation.

(C-3.4)

$$\begin{bmatrix} p_{12} \\ p_{23} \\ p_{45} \\ p_{56} \end{bmatrix} = \frac{1}{9} \begin{bmatrix} 2 & 4 & 2 & 1 \\ -1 & -2 & 2 & 1 \\ 2 & -2 & -1 & 1 \\ -1 & 1 & -1 & 1 \end{bmatrix} \begin{bmatrix} e^{-k_1 t} \\ e^{-k_2 t} \\ e^{-k_3 t} \\ 1 \end{bmatrix}$$

where,

$$k_1 = r + \frac{3}{4} R' + \frac{3}{2} R''$$

$$k_2 = r + R + R' + R''$$

and

$$k_3 = R + R' + R''$$

In a similar fashion, we can write down the rate equations for the site probabilities of inter-methyl proton pairs and also the lone proton - methyl proton pairs, and a solution of the same can be worked out. In the case of the intermethyl group interaction the expression for the following unique probabilities can be obtained, namely  $p_{1A}$ ,  $p_{1E}$ ,  $p_{25}$ ,  $p$ ,  $p_{57}$ ,  $p$ , which are also exponentially decaying functions of time with the time constant given by  $k$ ,  $k$ ,  $k_1$ ,  $k$  and  $k$ , where  $k$  to  $k_1$  are as defined in eqn. (C-3.4) and  $k$  and  $k$  are given by the following equations.

$$\begin{aligned} (C-3.5) \quad k_4 &= 2r + \frac{3}{2} R' + \frac{3}{4} R'' \\ k_5 &= 2r + R + R' + R'' \end{aligned}$$

Now these probabilities are connected to the correlation functions of the space dependent parts of the dipolar Hamiltonian, by defining

$$(C-3.6) \quad X_{mn}(\mu) = F_{mn}(\mu) - \overline{F_{mn}(\mu)}$$

where,

$$F_{mn}^{(0)} = \frac{\gamma^2 h^2}{r_{mn}^3} (1 - 3 \cos^2 \theta_{mn})$$

$$F_{mn}^{(1)} = F_{mn}^{(-1)*} = \frac{\gamma^2 h^2}{r_{mn}^3} \sin \theta_{mn} \cos \theta_{mn} e^{-i\phi_{mn}}$$

$$F_{mn}^{(2)} = F_{mn}^{(-2)*} = \frac{\gamma^2 h^2}{r_{mn}^3} \sin^2 \theta_{mn} e^{-i2\phi_{mn}}$$

The correlation function for the **intramethyl** proton pairs can be written as

$$(C-3.7) \quad G(t)_{\text{intra}} = \frac{1}{9} [ \langle X_{12}^*(0) X_{12}(t) \rangle + \langle X_{23}^*(0) X_{23}(t) \rangle + \dots \\ + \langle X_{97}^*(0) X_{97}(t) \rangle ]$$

Each of these averages can be expressed as a sum of terms with the individual probabilities corresponding to each pair. For instance, the term  $\langle X_{12}^*(0) X_{12}(t) \rangle$  can be expressed as

$$(C-3.8) \quad \langle X_{12}^*(0) X_{12}(t) \rangle = X_{12}^*(0) [ p_{12} X_{12}(0) + p_{23} (X_{23}(0) + X_{31}(0)) + \\ p_{45} (X_{45}(0) + X_{78}(0)) + p_{56} (X_{56}(0) + X_{64}(0)) + \\ X_{89}(0) + X_{97}(0) ]$$

Substituting similar expressions for all the pair correlation functions in eqn.(C-3.7), we arrive at the following concise form for the correlation function pertaining to the intra methyl group dipolar interaction. For the sake of clarity, we are dropping the index  $\mu$ , here.

$$(C-3.9) \quad G(t)_{\text{intra}} = p_{12}C_1 + p_{23}C_2 + p_{45}C_3 + p_{56}C_4$$

Here, we have grouped all the terms with respect to the **probabilities**  $p_{12}$ ,  $p_{23}$ ,  $p_{45}$  and  $p_{56}$ . As an example, the coefficient of the probability  $p$  in the above equation can be given by

$$(C-3.10) \quad C_1 = \frac{1}{9} [ :X_{12}^2 + :X_{23}^2 + :X_{31}^2 + :X_{45}^2 + :X_{56}^2 + :X_{64}^2 + :X_{78}^2 + :X_{89}^2 + :X_{97}^2 ]$$

Detailed expressions for all the terms are available [Sjöblom et al., 1975]. The explicit forms of the **probabilities** can be substituted from the equations like (C-3.4) into eqn.(C-3.9) and the terms with respect to the  $k$ -s can be regrouped again to give the following expression for the correlation function.

$$(C-3.11) \quad G^\mu(t)_{\text{intra}} = \frac{1}{9} \sum_{i=1}^3 K_i^\mu e^{-k_i t}$$

Here,

$$(C-3.12) \quad \begin{aligned} K_1^\mu &= 2C_1^\mu - C_2^\mu + 2C_3^\mu - C_4^\mu \\ K_2^\mu &= 4C_1^\mu - 2C_2^\mu - 2C_3^\mu + C_4^\mu \\ K_3^\mu &= 2C_1^\mu + 2C_2^\mu - C_2^\mu + C_4^\mu \end{aligned}$$

An expression similar to (C-3.12) can be derived for the **intermethyl** group interactions and the lone proton - methyl proton interactions. The general expression for the spin-lattice relaxation rate of the proton  $i$  due to the modulation of **its** dipolar interaction with proton  $j$  can be



$$(C-3.13) \quad (T_1^{-1})_{ij} = (3/2) \frac{I(I+1)}{\hbar^2} [J_{ij}^1(\omega_0) + J_{ij}^2(2\omega_0)]$$

and the spectral density functions  $J(\omega)$  are related to the correlation functions of the lattice functions by the relation

$$(C-3.14) \quad J_{mn}^{\mu}(\omega_0) = \int_{-\infty}^{\infty} G_{mn}^{\mu}(\tau) e^{-i\omega\tau} d\tau$$

Substituting the correlation functions for the intra, inter and lone proton interaction terms into the above equations, we arrive at the following general formula for the spin-lattice relaxation rate for the dynamics of the TMA cation.

$$(C-3.15) \quad (1/T_1) = \frac{9}{20\hbar^2} \sum_{\mu=1}^2 \left[ \sum_{i=1}^3 K_i^\mu \frac{k_i}{k_i^2 + (\mu\omega_o)^2} + \sum_{j=1}^5 L_j^\mu \frac{k_j}{k_j^2 + (\mu\omega_o)^2} \right. \\ \left. \sum_{n=1}^3 M_n^\mu \frac{k_n}{k_n^2 + (\mu\omega_o)^2} \right] \\ \text{(intra)} \qquad \qquad \qquad \text{(inter)} \\ \qquad \qquad \qquad \text{(lone-proton)}$$

Absorbing the prefactor outside the brackets in eqn. (C-3.15), the expression for  $T$  can be rewritten as

$$(C-3.16) \quad (1/T_1) = \sum_{\mu=1}^2 \left[ \sum_{i=1}^3 K_i^{\prime\mu} \frac{k_i}{k_i^2 + (\mu\omega_o)^2} + \sum_{j=1}^5 L_j^{\prime\mu} \frac{k_j}{k_j^2 + (\mu\omega_o)^2} \right]$$

(intra) (inter)

$$\sum_{n=1}^3 M_n^{\prime\mu} \frac{k_n}{k_n^2 + (\mu\omega_o)^2} \Bigg]$$

(lone-proton)

The relaxation constants  $K'$ ,  $L'$  and  $M'$  are evaluated numerically for given dimensions of the trimethylammonium cation and for a polycrystalline sample, and these constants are given in Table (C-3.1) [Sjöblom et.al., 1975]. It has been shown that, the values for spin-lattice relaxation rates seem to be fairly independent of the inclusion of the correlated motions of methyl groups and the cation (with rates  $R'$  and  $R''$ ). So, a simpler model would be to neglect the rates of correlated reorientations  $R'$  and  $R''$ , and this simplifies the expressions for the time constants of the probabilities to

(C-3.17)

$$\begin{aligned} k_1 &= r \\ k_2 &= r + R \\ k_3 &= R \\ k_4 &= 2r \\ k_5 &= 2r + R \end{aligned}$$

**TABLE (C-3.1)**

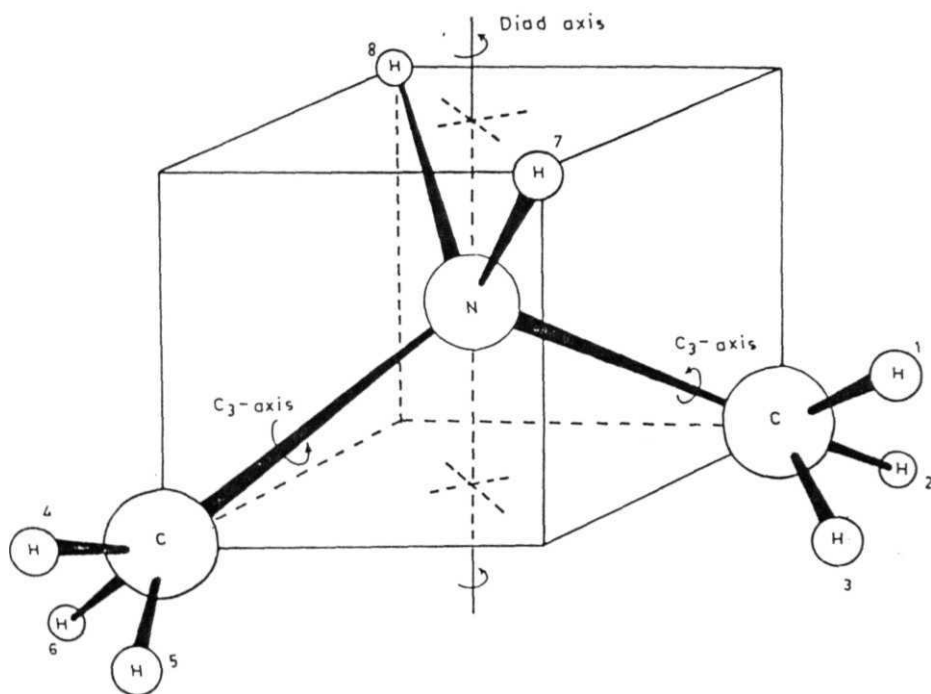
RELAXATION CONSTANTS ( $\times 10^8$ )  $K's$ ,  $L's$  AND  $M's$  FOR THE TMA GROUP

$\mu$	$i$	$K_1^\mu$	$L_1^\mu$	$M_1^\mu$
1	1	24.22	1.74	0.63
	2	48.45	7.28	4.30
	3	19.99	11.68	6.86
	4			1.16
	5			2.39
2	1	94.84	.6.83	2.56
	2	193.08	29.49	17.29
	3	81.22	46.65	28.16
	4			4.58
	5			9.78

The dimethylammonium ions differ from the trimethylammonium cation in that, it has only a diad axis of rotation and it has two equivalent configurations which can be sampled by the pure diad rotation and there are two lone protons. Fig.(C-3.2) illustrates the geometry of a DMA cation with all the proton pairs numbered. The model [Venu et.al., 1993] proceeds in a similar fashion to calculate the rate equations for the individual site probabilities of the various proton pairs, which are then solved to arrive at the probabilities. Using these the correlation functions of the lattice functions are worked out for the intra, inter and lone proton - methyl proton contributions, the details of which are readily available [ Venu et.al., 1993]. We shall provide below the final expression for the spin-lattice relaxation rate for the dimethylammonium dynamics, and the relevant relaxation constants  $K'$ ,  $L'$  and  $M'$  are provided in Table (C-3.2).

$$(C-3.18) \quad (1/T_1) = \sum_{\mu=1}^2 \left[ \sum_{m=1}^3 K'_m{}^{\mu} \frac{k_m}{k_m^2 + (\mu\omega_o)^2} + \sum_{p=4}^5 L'_p{}^{\mu} \frac{k_p}{k_p^2 + (\mu\omega_o)^2} \right. \\ \left. \sum_{n=1}^3 M'_n{}^{\mu} \frac{k_n}{k_n^2 + (\mu\omega_o)^2} \right] \\ \text{(intra) (inter) (lone-proton)}$$

The above formulae are valid in the case where there is no dynamic inequivalence among the cations or the methyl groups. Where there is a possibility of dynamic inequivalence among the molecular groups, these have to be suitably modified to incorporate the inequivalence factors.



(C — 3.2) Model of the dimethylammonium (DMA) cation.

TABLE (C-3.2)

RELAXATION CONSTANTS ( $\times 10^8$ ) K's, L's AND M's FOR THE DMA GROUP

$\mu$	i	$K_i^\mu$	$M_i^\mu$	$L_i^\mu$
1	1	30.59	3.00	
	2	25.43	1.68	
	3	11.88	4.50	
	4			1.23
	5			<b>1.62</b>
2	1	122.34	12.36	
	2	101.74	7.08	
	3	47.5	17.64	
	4			5.07
	5			<b>6.17</b>

To facilitate this, the relaxation rate in the case of, for example, TMA dynamics can be rewritten regrouping terms with respect to the individual reorientation rates  $r$  and  $R$  and thus leading to a sum of spectral density function terms depending on the correlation time for the methyl group reorientation and the cation reorientation as in the case of TEMA dynamics [ Albert **et.al.**, 1972].

$$(C-3.19) \quad (1/T_1) = \sum_{\mu=1}^2 \left[ (K_1' + L_1' + M_1') \frac{r}{r^2 + \mu\omega^2} + (K_2' + L_2' + M_2') \frac{(r+R)}{(r+R)^2 + \mu\omega^2} \right. \\ \left. + (K_3' + L_3' + M_3') \frac{R}{R^2 + \mu\omega^2} + (L_4' + L_5') \frac{2r}{(2r)^2 + \mu\omega^2} \right]$$

Considering the fact that the methyl group dynamics are much faster at a given temperature than the cationic reorientation, we assume that  $r > R$ . and in such a case the above formula can be modified to be

$$(C-3.20) \quad (1/T_1) = \sum_{\mu=1}^2 \left[ A g(\omega, r) + A' g'(\omega, r) + B g(\omega, R) \right]$$

where,

$$A = (K_1' + L_1' + M_1' + K_2' + L_2' + M_2')$$

$$A' = (L_4' + L_5')$$

$$B = (K_3' + L_3' + M_3')$$

$$\text{and} \quad g(\omega, r) = \frac{r}{r^2 + (\mu\omega)^2} \quad ; \quad g'(\omega, r) = \frac{2r}{(2r)^2 + (\mu\omega)^2}$$

Now, the presence of dynamically inequivalent methyl groups or TMA groups can be incorporated with ease in eqn.(C-3.20). For instance, if  $r_1$  and  $r_2$  are the reorientation rates of two dynamically **inequivalent** methyl groups with inequivalence factors  $x$  and  $y$ , and similarly if  $R_1$  and  $R_2$  are the reorientation rates of two dynamically inequivalent TMA groups with inequivalence factors  $p$  and  $q$ , then these factors can be substituted into eqn.(C-3.20) as

$$(C-3.21) \quad (1/T_1) = \sum_{\mu=1}^2 \left[ x \left( A g(\omega, r_1) + A' g'(\omega, r_1) \right) + y \left( A g(\omega, r_2) + A' g'(\omega, r_2) \right) + p B g(\omega, R_1) + q B g(\omega, R_2) \right]$$

The formula for the **dimethylammonium** dynamics can also be regrouped in terms of the individual correlation times of the methyl group and the DMA cation, and the inequivalence, if any, can be incorporated in the formula in a similar fashion.

Data below 300 K : (region II)

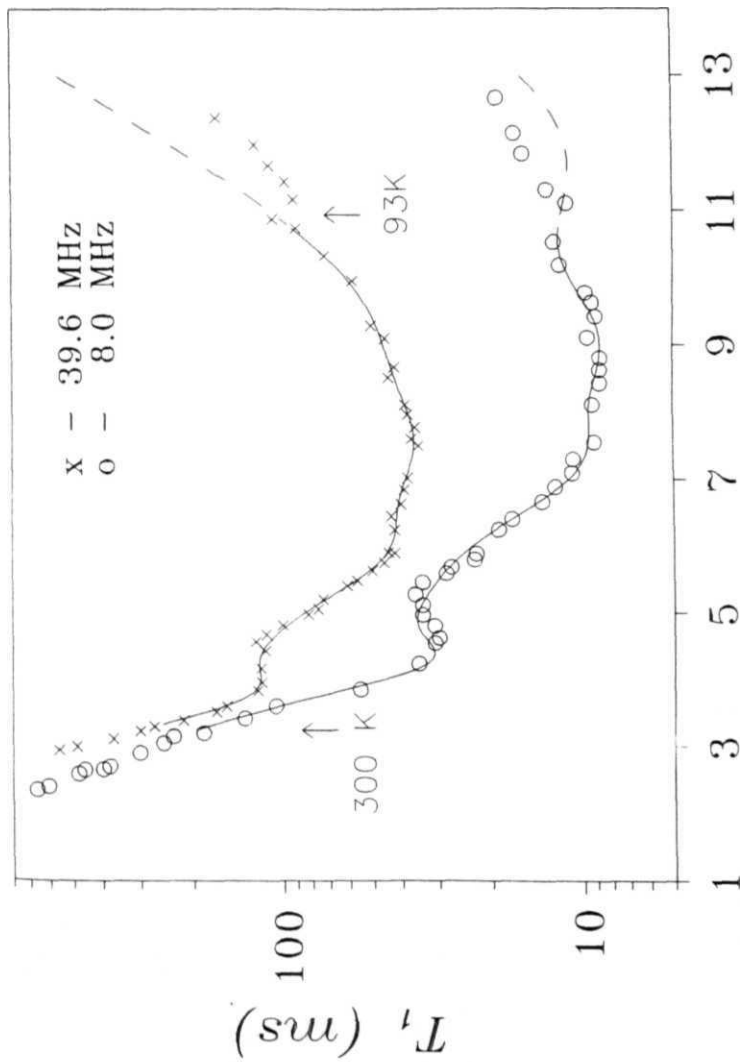
The expected values of minima for **CH<sub>3</sub>** motion at 8 MHz and 39.6 MHz are 4.0 **ms** and 19.8 **ms**, respectively as computed from eqn. (C-3.16). Similarly, the minima values for the TMA dynamics are 9.5 ms and 47 ms at 8 and 39.6 MHz respectively. The broad minimum in **T** data at 8 MHz is around 9 ms and the least value of **T** at 39.6 MHz is approximately 35 ms. These values do not match with the minima values corresponding all the methyl groups giving a minimum at this temperature. But the observed



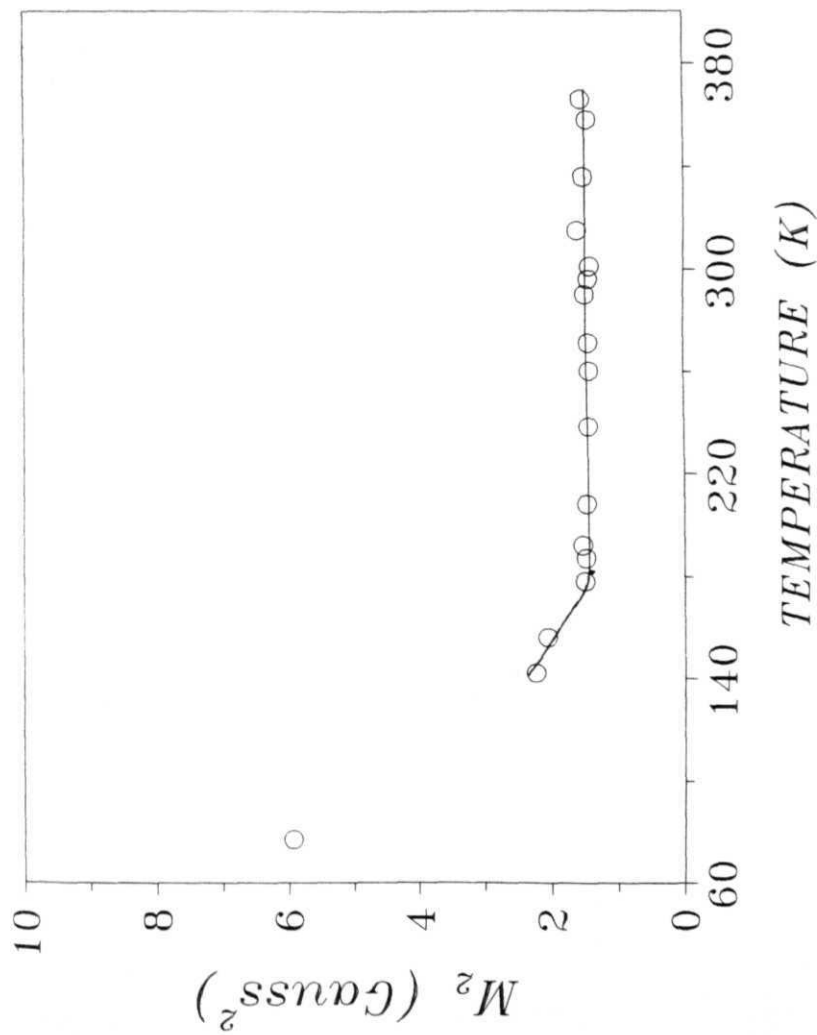
minimum at 8 MHz **near** 9 ms cannot be, obviously, assigned to TMA dynamics either, due to the following reasons. First of all, if we were to assign this to the reorientation about the triad axis of all the cations, then the shoulder like structure has to be necessarily due to the internal dynamics of the methyl groups. This in turn **would** imply that the methyl group dynamics is slower than the TMA group dynamics which is not physically acceptable. Secondly, if this minimum at 8 MHz has to be treated as a well resolved minimum attributable to the TMA dynamics solely, then at 39.6 MHz this minimum should have moved towards higher temperatures, and more importantly, the value of the minimum at 39.6 MHz must scale as the **Larmor** frequency, which is not the case (the minimum at 39.6 MHz, being at least 7 to 8 ms deeper than the expected value). The shallow nature of the minimum of the **T** data further indicates that it is not due to a single correlation time of the assigned motion. So, suitable model necessarily incorporating certain dynamic inequivalence among the methyl groups and/or the TMA groups is necessary, and from the above discussion the shoulder like structure should primarily correspond to the dynamics of at least some of the TMA groups. The small **discontinuity** observed in the data around **100K** at both the frequencies seems to correspond to a possible structural phase transition, and hence the data is restricted upto **100K** only while fitting to the molecular models. Similar restriction on the high temperature side (region I) also apply ( see the subsequent discussion).

Models with several combinations of inequivalence factors among the methyl groups and TMA groups were tried, with data at two Larmor frequencies providing additional and unique check on the self consistency of the model parameters. Substituting various inequivalence

factors in eqn.(C-3.20), a non linear least square fit program was employed to fit the above model to the data at both the frequencies in the temperature range 300K - 100K. After extensive computation, it was concluded that the combination of inequivalence factors, which is able to simulate the experimental data very satisfactorily are :  $x = (1/6)$ ;  $y = (1/6)$ ;  $z = (4/6)$  and  $p = (1/6)$ ;  $q = (1/6)$ ;  $r = (2/6)$ , where  $x$ ,  $y$  and  $z$  correspond to the inequivalence factors associated with three inequivalent TMA groups (TMA-A, TMA-B and TMA-C), and similarly  $p$ ,  $q$  and  $r$  correspond to the inequivalence factors for the methyl groups ( $\text{CH}_3$ -A,  $\text{CH}_3$ -B and  $\text{CH}_3$ -C). The optimized dynamic parameters ( $E$  and  $x$ ) are provided in Table (C-3.1). Fig.(C-3.3) gives the data at both the frequencies and the solid line which runs through the points are the fitted curves with the minimum possible summed squared deviation. The theoretical curves are extrapolated beyond 100K and are shown in Fig.(C-3.3). There is a systematic deviation of the experimental data from the theoretical curve at both frequencies near 100K, and the small discontinuity thus seem to correspond to a possible structural phase transition at this temperature. It may be noted that in both the Bismuth based compounds which we discussed in the previous section (TEMACB and TEMABB) we find some anomalies in the  $T$  data at lower temperatures typically around 100K. Thus, the anomaly observed in the present compound at about 100K seem to correspond to the presence of a structural phase transition. From the motional parameters tabulated in Table (C-3.1), we can compute the correlation times for all the groups at 77 K and it is seen that, the TMA-A is well into rigid lattice limit, whereas the correlation times of TMA-B and TMA-C are of the order of  $10^{-4}$  s by this temperature. From the correlation times of the methyl groups, it is seen that all the methyl groups are still undergoing fast



(C - 3.3) Variation of  $T_1$  as a function of  $(1000/T)$  in  $[(CH_3)_3NH]_3Bi_2Cl_9$ . Solid lines through data points are the fitted curves.



(C - 3.4) Variation of  $M_2$  as a function of  $T$  in  $[(CH_3)_3NH]_3Bi_2Cl_9$ .

**TABLE (C-3.3)**

MOLECULAR GROUP	INEQ.	$E_a$ (kJ/mole)	$T_o$ seconds
TMA - A	1/6	27.0±1.0	(7.0±1.0)E-15
TMA - B	1/6	11.0±1.0	(1.2±0.2)E-11
TMA - C	4/6	13.0±1.0	(2.0±1.0)E-13
CH - A	1/6	11.5±0.5	(6.0±1.0)E-14
CH - B	1/6	10.5±0.5	(1.5±0.5)E-13
CH - C	2/6	7.0±0.5	(9.0±0.5)E-13

OPTIMIZED DYNAMIC PARAMETERS FOR THE COMPOUND  
 $[(CH_3)_3NH]_3 Bi_2 Cl_9$

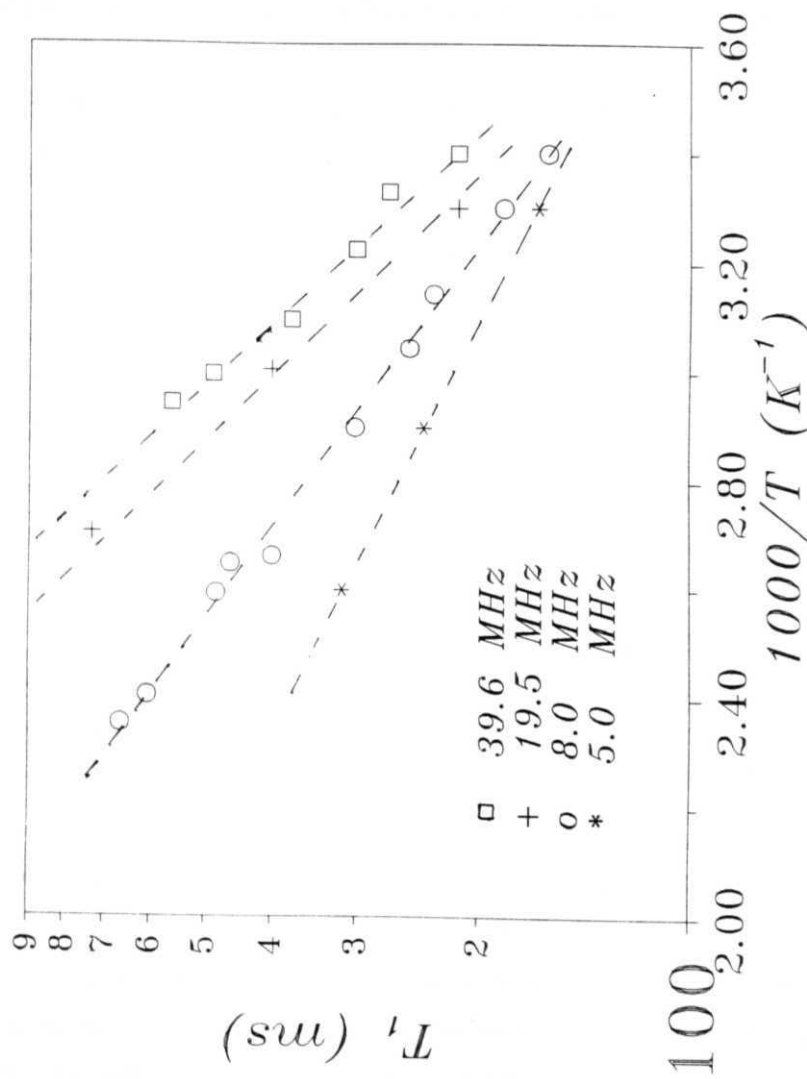
reorientations near 77 K. If triad rotation of all the TMA cations are frozen by NMR time scales by 77 K, then one would expect to get a  $M_2$  value of 9.9 Gauss, but in the present case the  $M_2$  at 77K is only 6.2

Gauss. This indicates that not all the TMA groups are frozen completely by 77K, as can be seen from the individual correlation times of these groups at this temperature. The increase of  $M_2$  with variation of temperature from 140K downwards, as we cool the sample to 77K may be expected to be smooth. Such a smooth increase is observed in the case of TMACA, the antimony analogue of the present compound [Idziak et.al., 1987]. The discontinuity found in the T data around 100K is small indicating that the jump in the correlation time of the associated motional process may not be very large. If the jump in the correlation time is not very large, such that the associated dynamics has not reached the vicinity of the rigid lattice limit, it may not show up as an increase in the  $M_2$  data also. Such instances are also noticed in the previous two compounds in the Bismuth group (TEMACB and TEMABB) [refer Section C-2]. In the antimony analogue of this compound TMACA, a discontinuity in the T data around 125K was reported at 90 MHz, but a systematic study of the same compound in lower range of larmor frequencies ranging from 4 MHz to 39.8 MHz did not show any such feature [Idziak et.al., 1987; Jagadeesh et.al., 1993a].

Data above 300K : (region I)

Based on our assignment of different motional processes as above, one normally expects the high temperature T. data to show a dispersionless region, while such is not the case (Fig. C-3.3). Such slope changes are seen in cases where there is a structural phase

transition in the solid as for instance in the case of the **tetramethyl-antimony** compounds of this family (TEMACA and TEMABA) [ Jagadeesh, **et.al.**, 1992, 1993b]. But the dispersion in the  $T_1$  data observed in this case is different in that after the  $T_c$  values for the two different frequencies merge at a point around 300 K, the data almost immediately peel off above this temperature without having any portion of dispersionless region further. Different possibilities **were** considered to explain this peculiar behaviour of the data at high temperatures. One possibility could be that there may be cross-relaxation of the protons at 8 MHz through the Chlorine **NQR** levels as the **NQR** frequencies are supposed to lie around 8 MHz in these compounds. But, normally, this kind of cross-relaxation through the energy levels of some other nucleus will be discernibly effective in cases where the relaxation processes of the host nuclear species (proton) are inherently inefficient, and the  $T_1$ -s through **this** relaxation are rather large (say, a few seconds), and in the present case this is not so. Thus, for TMACB this cross relaxation process does not seem a priori to be responsible for the observed variation of  $T_1$ . To confirm this, data were collected at two other frequencies (5 MHz and 19.5 MHz), and the magnified portion of the high temperature data is shown in Fig.(C-3.5). If cross-relaxation were responsible for the observed deviation in the data **at** 8 MHz, **then the**  $T_1$  values at 5 MHz must be higher than the values at 8 MHz at the corresponding temperatures. But, such is not the case (Fig.(C-3.5)) ruling out cross-relaxation process. Another process could be the self-diffusion of the molecules concerned. There are many instances where **self-diffusion** mediates the relaxation process in other solid systems [Ishida et.al., 1985, 1989 ; **Iwai**, 1993; Hattori et.al., 1990; Tanabe et.al., 1991].



(C - 3.5) Enlarged plot of  $T_1$  data above 300K in  $[(CH_3)_3NH]_3Bi_2Cl_9$ .



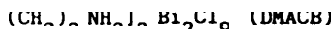
In such cases, the  $T$  values depend on the **larmor** frequency. But, considering the rather high value of the second moment (1.5 Gauss ) in this temperature region, compared to expected low values ( $\approx 0.05$  Gauss ) with effective diffusion, even this possibility cannot be considered.

We had noted earlier that the  $M_2$  value at these temperatures shows the possibility of the **isotropic** motion of only some of the cations to be frozen. For an asymmetric molecular group like TMA, the isotropic motion is a highly hindered process and one would expect this to take place at fairly high temperatures, but if there is considerable amount of freedom available for the cation for some reason, this motion can take place even at these moderate temperatures. In the present case, therefore, there seems to be some TMA cations whose motions are less hindered, and their  $T$  minimum due to isotropic reorientations is above 300 K, higher than the maximum temperature in the present study. As we move towards the lower temperature side of this minimum, the  $T$  values scale like  $\omega$  at any given temperature, and they increase with decreasing temperature, their relaxation rates becomes progressively negligible. This allows for some other lower order dynamic process, like the triad **reorientation**, becoming more dominant, and as a result the  $T$  vs  $1/T$  curve could take a downward turn, and as we go further down in temperature, the dispersion of the data, which is essentially due to the process governing a higher temperature minimum, and whose importance to  $T$  is rapidly decreasing, disappears smoothly and all the data points join together to form a dispersionless region. Normally In a normal case, this dispersionless region persists for a finite temperature range below which the minimum due to this low-order dynamics is expected to form. But **in** the present case no sooner the data from different

frequencies converged towards a common point (as 300 ms at 300K), the  $T_2$  shows dispersion below this temperature, and this kind of a behaviour is not common. This "sudden discontinuity" in the  $T_2$  data suggest the occurrence of another structural phase transition, as a result of which the correlation time changes in a discontinuous fashion, leading to the abrupt change in the qualitative description of  $T_2$  variation with temperature. Thus, one way of accounting for the high temperature behaviour of this data is to assume that the dispersion in data seen above 300 K is indicative of the isotropic motion of some of the cations, and to explain the sudden onset of dispersion below 300 K as due to a phase transition in this temperature region. To corroborate the above proposition, we note that in all the Bi compounds there is a phase transition corresponding to the high temperature transition in the Sb analogue but the temperature of this transition is lowered in all the cases. Therefore, in a way, following the general pattern, we can expect a phase transition in TMACB around 300 K corresponding to the phase transition observed at 367K in TMACB. The highest temperature reached in these measurements is around 425 K and from the general trend of the  $T_2$  data at this temperature, it looks like the  $T_2$  minimum due to the isotropic motion of the cation may form only at a higher temperature.

To summarize, there is a signature of isotropic motion of the trimethylammonium cation in the compound TMACB in high temperatures and a possibility of a structural phase transition at 300K exists. The  $T_2$  data which show a shoulder like structure followed by a broad minimum is fitted to Sjöblom et.al.'s model, in the temperature range 300 K to 100 K. The trimethylammonium cations are dynamically inequivalent in the ratio 1:1:4 and the methyl groups are dynamically inequivalent in the

ratio 1:1:2:2. It is clear that when Bi is placed in place of Sb, this causes a large degree of structural inequivalence in the system as evidenced by more number of inequivalent sites available in these compounds compared to the Sb compounds, as, for instance in the Antimony analogue of this compound (TMACA) there are only two inequivalent set of TMA cations and methyl groups in the ratio 1:2 [Jagadeesh et al., 1993a]. In general in the  $A M_2 X$  family of solids there is a considerable amount of structural inequivalence which is more pronounced in the case of Bismuth substituted compounds which is reflected in the form of dynamic inequivalence among the molecular groups. Structure data can in principle reveal the presence of such an inequivalence but there seems to be no structure data available in the case of the TMACB, to the best of the author's knowledge. A signature of low temperature phase transition, possibly associated with the methyl group dynamics, is seen at 98 K. The activation energy of TMA-A is high at  $27 \pm 1.0$  kJ/mole compared to the other trimethylammonium groups. The hindrance for this group is rather high and this is also supported by the fact that, at 77K, this group is well into the rigid lattice limit, whereas the other two TMA groups are just reaching this condition by this temperature. The model we have assumed with the specified inequivalences is commensurate with the behaviour of the M data as a function of temperature.



### Specific Details

#### T measurements

Larmor frequencies	:	8 and 39.6 MHz
Temperature range	:	435 K to 77 K

### M<sub>0</sub> measurements

Temperature range of observation

370K to 77K

$T_1$  data at 8 and 39.6 MHz, with the

fitted curve

: Fig. (C-3.6)

$M_2$  variation as a function of

temperature

: Fig. (C-3.7)

### Optimized dynamic parameters

: Table (C-3.2)

DMACB crystals were grown by evaporating a mixture of the parent compounds  $[(CH_3)_4NH]Cl$  and  $BiCl_3$  in  $HCl$  medium at a constant temperature. The clear crystals were powdered and dried and sealed in glass tubes at 10 torr vacuum.

## DMACB

## RESULTS

T data at high temperatures ( $\approx$  above 250K) at 8 MHz show the formation of a minimum with a rather steep slope. This minimum is not seen in 39.6 MHz data within the high temperature limit investigated, and it is expected to shift to higher temperatures with increasing frequency. The M data is at a low value of around  $1.0 \pm 0.2$  Gauss above 390 K, and at 390 K, the M value increases sharply to  $4 \pm 0.5$  Gauss<sup>2</sup>.

As we go down in the temperature scale, the  $T_c$  data at 8 and 39.6

MHz merge together and below 250K they do not show any frequency dispersion. At 152 K, there is a perceptible downward jump in the T value and below this temperature, a fairly broad minimum is seen at both 39.6 as well as 8 MHz. Further, the data at 39.6 MHz show a shoulder like structure below 91 K and the lowest point on this shoulder is at 140 ms. In the low temperature region the  $M_2$  value increases from approximately 4 Gauss to  $10 \pm 1$  Gauss around 240 K. At 77 K, the value of  $M_2$  has increased to  $12 \pm 1$  Gauss.

## DISCUSSION

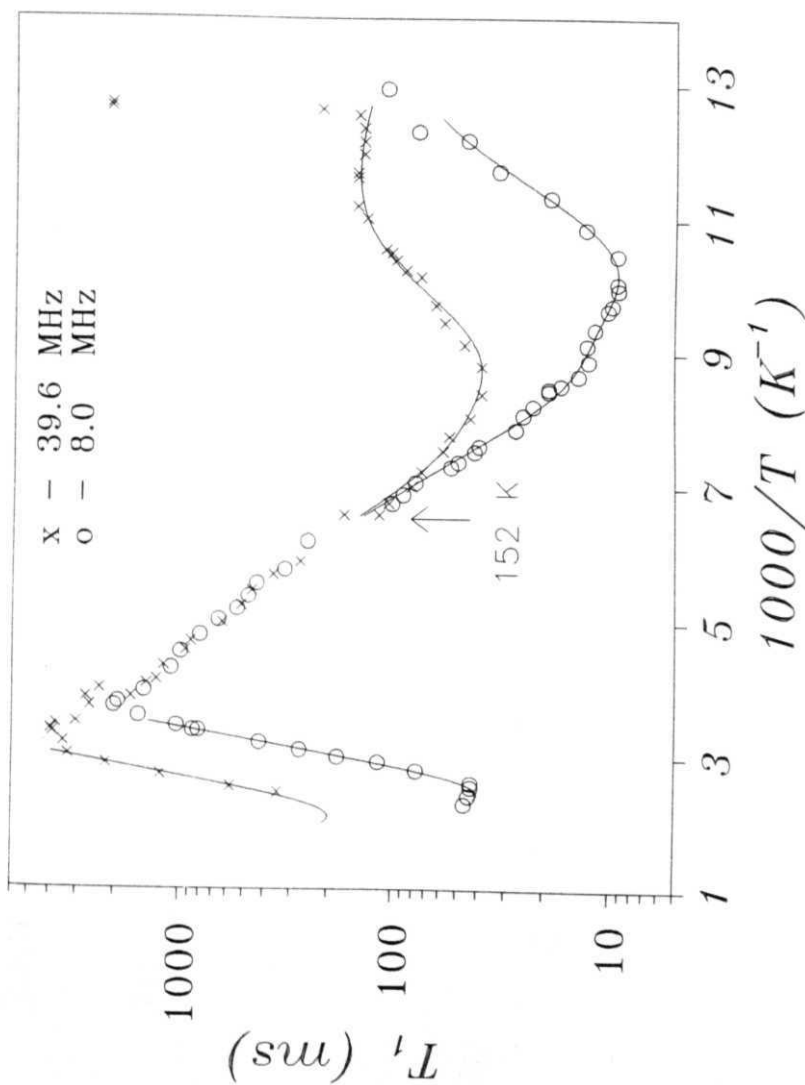
From the value of  $M_2$  expected for the isotropic motion of the DMA cation, this motion of the DMA cation seems to be present above 390K. The increase in this value to  $4.0 \pm 1.0$  Gauss corresponds to the freezing of isotropic motion of only 50% of the DMA cation. The other 50% of the DMA cations, which have more freedom for reorientation give a minimum in the T at a relatively low temperature ( $\approx 400K$  at 8 MHz) compared to the fairly high temperatures at which isotropic motion of these kind of cations are expected to give a minimum. Thus, we assign the high temperature minimum to the isotropic reorientation of the 50% of the cations (similar to the case of TMACB). The high temperature data, between 435 K to 295 K is fitted at both the frequencies to a simple model with

$$(C-3.22) \quad T_1^{-1} = \frac{C}{a} g(\omega, \tau_c)$$

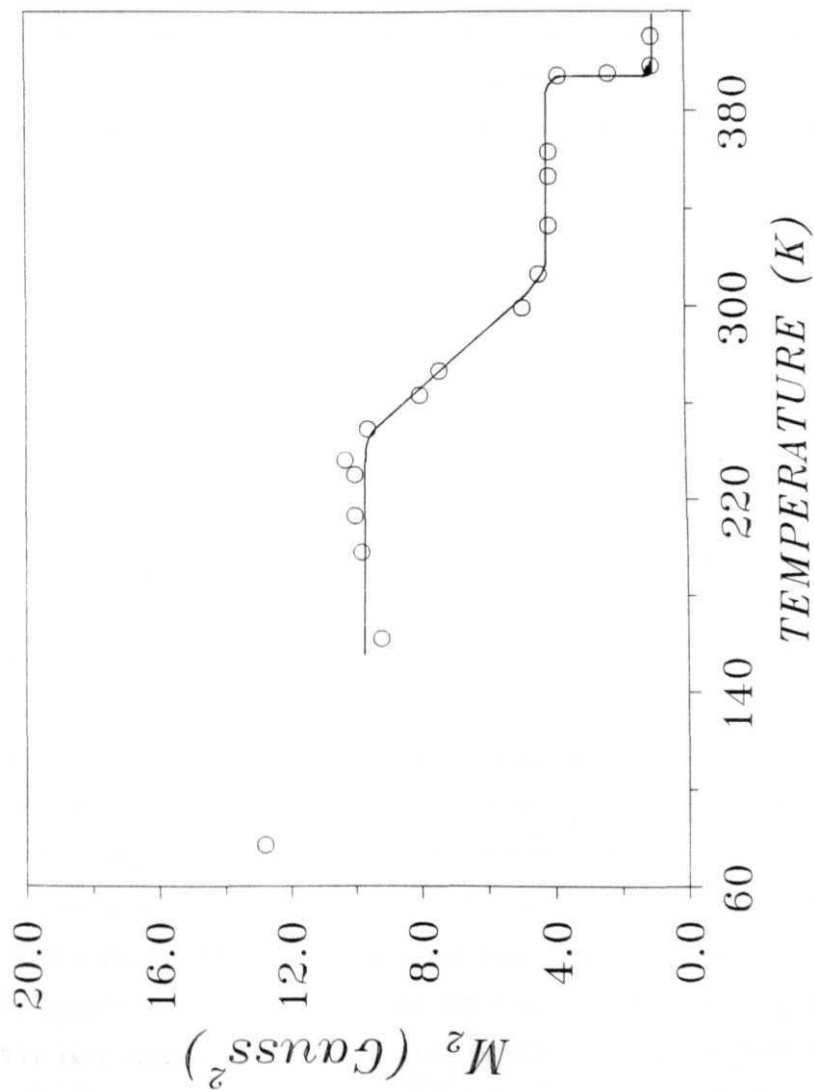
where  $a$  is the inequivalence factor (2 in the present case) and  $C$  is the equality factor and this is also optimized as a part of finding out the

most probable values for  $E$  and  $\tau$ . A non linear least squares program was employed to fit the data at both the frequencies. The optimized value of  $C$  was found to be  $1.6e9$  s. The fitted dynamic parameters  $E$  and  $\tau$ , for the isotropic reorientation is tabulated in Table (C-3.2) and computed curves are shown in Fig.(C-3.6). Formation of  $T$  minimum due to isotropic reorientation of the DMA cation around such relatively low temperatures is observed in the compound  $[(CH_3)_2NH_2]_2 ZnCl_4$  also [Manjula, 1993].

The dispersionless region of the data below **290K** with the observed temperature dependence corresponds to the reorientation of the DMA cation about its diad axis. This is because the comparatively slower motion of the bulky DMA cation is expected to have a considerable contribution to the spin-lattice relaxation rate in this intermediate temperature region than the fast reorienting methyl groups. As one can perhaps anticipate from the figure (C-3.6), if the vertical downward jump at **152 K** were not there, this dispersionless region would have continued to end up eventually in a minimum corresponding to the dynamic process. The discontinuity at **152 K** causes the  $T$  value drop from **170 ms** to approximately **120 ms**. This can be compared with the similar abrupt jumps we observe in the **tetramethylammonium** compounds TEMACB and TEMABB. This jump, thus, seems to correspond to a structural phase transition in this system. In the antimony analogue of the same compound, DMACA, it is found that there is structural phase transition at **242 K**, which manifests as a sharp jump in the  $T$  data and immediately below the phase transition, the isotropic motion of the DMA cation completely freezes and only the reorientation of the DMA cation about its **diad** axis is seen in the  $T$  data ( Jagadeesh et.al., 1994]. If we



(C-3.6) Variation of  $T_1$  as a function of  $(1000/T)$  in  $[(CH_3)_2NH_2]_3Bi_2Cl_9$ . Solid lines through data points are the fitted curves.



(C-3.7) Variation of  $M_2$  as a function of  $T$  in  $[(CH_3)_2NH_2]_3Bi_2Cl_9$ .



follow the pattern we have observed so far for all the compounds, perhaps the transition which was observed in the case of DMACA at 242 K has shifted to a corresponding temperature of 152 K in the case of DMACB.

It is also to be noted that whereas no  $T$  minimum due to the isotropic tumbling of the cation was observed in DMACA in the typical temperature range covered, in case of DMACB we have seen the minimum due to the isotropic motion of the cation. The minima value expected from the theoretical model for the diad axis motion of the DMA cation at 8 and 39.6 MHz are 21.5 ms and 106.5 ms, respectively. Similarly, the expected minima values for the methyl group motions at 8 and 39.6 MHz are 4.6 ms and 28 ms, respectively. It is clear from Fig (C-3.6) that, neither of the minima corresponds to any one of these values, and in fact the minimum value at 8 MHz is around 9 ms which is higher than the value expected for the methyl group and lower than the value expected for the DMA motion. This feature is similar to the case of the data at 39.6 MHz also. These observations as well as the shoulder like structure found at the lower temperature side of the data at 39.6 MHz imply that there is dynamic inequivalence among the different molecular groups in DMACB. We have tried several models incorporating different combinations of dynamic inequivalences which will fit the current data, and the inequivalence combination which fitted the data consistently at both the frequencies is given by  $x = 1/2$  and  $y = 1/2$  ( $x$  and  $y$  are the inequivalence factors for the methyl groups). There does not seem to be any dynamic inequivalence among the DMA cations as given by this model. This is a remarkable deviation from the data observed for TMACB where the TMA groups are also found to be dynamically inequivalent. From these

inferences we may suggest that the phase transition at 152 K has changed the structure of the solid considerably such that the DMA ions are all dynamically equivalent below the transition temperature. We note, however, that we have fitted the data with a limit on the points on the lower temperature given by 79 K. The fitted curve is quite good at both the frequencies, as can be seen from Fig.(C-3.6). The optimized parameters are provided in Table (C-3.4). Such a situation was also observed in the compound  $[(CH_3)_2 NH]^+ ZnCl_4^-$ , where the DMA cations do not show any dynamic inequivalence [Manjula, 1993].

As in the case of TMACB there are no structural or any other information available for DMACB also, but the proton spin relaxation data point to the possibility of an increased amount of structural inequivalence in the system with the introduction of the Bismuth atom in place of Antimony. At 78 K, there is a rather steep jump of the  $T$  value from around 200 ms to 2100 ms at 39.6 MHz and this should be corresponding to a low temperature phase transition in this system. A similar **discontinuity** is observed around this temperature in the case of the 8 MHz data also. As has been noted in the case of the last three Bismuth compounds, TEMACB, TEMABB and TMACB, in DMACB also there seems to be, thus, a low temperature phase transition, thereby establishing the general trend of an additional low temperature transition in Bismuth compounds unlike the case of Antimony compounds. Noting the fact that the  $M_2$  value is around 12 Gauss at 77 K, some of the dynamics of the systems seems to have been positively frozen by this temperature. If 2-fold reorientation of all the **dimethylammonium** cations are frozen, then the second moment for such a condition is calculated to be 14

2  
Gauss [Andrew et al., 1972]. On the other hand, if we extrapolate the

TABLE (C-3.4)

MOLECULAR GROUP	INEQ.	$E_a$ (kJ/mole)	$\tau_o$ seconds
<i>high temperatures</i>			
DMA	--	35±1.0	(4.5±0.5)E-13
<i>low temperatures</i>			
DMA	--	11.5±0.5	(6.0±1.0)E-14
CH <sub>3</sub> - A	1/2	11.5±0.5	(7.0±1.0)E-15
CH <sub>3</sub> - B	1/2	2.0±0.5	(2.0±0.2)E-11

OPTIMIZED DYNAMIC PARAMETERS FOR THE COMPOUND  
 $[(CH_3)_2NH_2]_3Bi_2Cl_9$

correlation times for the different dynamics to **77K**, calculated with the help of the dynamic parameters given in Table (C-3.2), it is seen that none of the motions have reached the rigid lattice limit. Now, the observed second moment value points to the fact that at least some of the motions are frozen at **77 K**. Thus, these considerations strongly imply that the well-defined phase transition observed at **78K** must have caused a drastic change in the correlation time of the different dynamic processes, and that it must have slowed down the dynamics to a large extent due to the transition.

To summarize, in the case of the **dimethylammonium** compound DMACB, a minimum due to the isotropic motion is seen at high temperatures. Two well defined phase transitions are observed at **152K** and **78K**, and the second transition seemed to have caused a large change in the correlation time associated with the respective dynamics. Dynamic inequivalence among the methyl groups are observed in the ratio 1:1 but surprisingly, the DMA cation does not seem to exhibit any dynamic inequivalence.  $M_2$  data show that the isotropic motion of **50%** of the cations are **frozen** by **395K** and the remaining groups are also frozen by **230 K**. A general trend of the orientational disorder is being increased in the case of the Bismuth based compounds in contrast to the Antimony based compounds is also observed. It is well recorded that the compounds TMACA and DMACA show ferroelectricity in their low temperature phases, and the ability of these compounds to form hydrogen bonds between the cation and anions seems to play an important role in this regard. These two compounds are layered compounds unlike TEMACB and TEMABB. Thus, both TMACB and DMACB also might exhibit ferroelectricity, though there are no specific information available as yet from other techniques, on these two compounds.

# REFERENCES

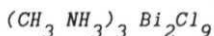
- (C-3.1) ALBERT S. , H.S. GUTOWSKY, J.A. RIPMEESTER, *J.Chem.Phys*, 56, (1972) 3672
- (C-3.2) ANDREW E.R. , P.C. CANEPA, *J.Magn. Reson*, 7, (1972) 429
- (C-3.3) BLOEMBERGEN N. , E.M. PURCELL AND R.V. POUND, *Phys.Rev.*, 73, (1948) 679
- (C-3.4) GDANIEC M. , Z. KOSTURKIEWICZ, R. JAKUBAS, L. SOBCZYK, *Ferroelectrics*, 77, (1988) 31
- (C-3.5) HATTORI M. , S. FUKADA, D. NAKAMURA AND R. IKEDA, *J.Chem.Soc.Faraday Trans.*, 86, (1990) 3777
- (C-3.6) IDZIAK S., R. JAKUBAS. *Solid State Commun.*, 62, (1987) 173
- (C-3.7) ISHIDA H., R. IKEDA AND D. NAKAMURA, *J.Chem.Soc.Faraday Trans.*, 2, (1985) 963
- (C-3.8) ISHIDA H. , N. MATSUHASHI, R. IKEDA AND D. NAKAMURA, *J.Chem.Soc.Faraday Trnas.*, 85, (1989) 111
- (C-3.9) IWAI S., M. HATTORI AND D. NAKAMURA, *J.Chem.Soc.Faraday Trans.*, 89, (1993) 827
- (C-3.10) JAGADEESH B. , P.K. RAJAN, K. VENU AND V.S.S. SASTRY, *Chem.Phys.*, 163, (1992) 351
- (C-3.11) JAGADEESH B. , P.K. RAJAN, K. VENU AND V.S.S. SASTRY, *Solid State Commun.*, 86, (1993a) 803
- (C-3.12) JAGADEESH B. , P.K. RAJAN, K. VENU AND V.S.S. SASTRY, *J. Phys.Chem. Sol ids*, 54, (1993b) 527
- (C-3.13) JAGADEESH B. , P.K. RAJAN, K. VENU AND V.S.S. SASTRY, *Solid State Commun.*, 1994, (communicated)
- (C-2.14) JAKUBAS R. , Z. CZAPLA, Z. GALEWSKI AND L. SOBCZYK, *Ferroelectrics Lett.*, 5, (1986) 143

- (C-2.15) JAKUBAS R., A. MINIEWICZ, M. BERTAULT, J. SWORAKOWSKI AND A. COLLET, *J.Phys.France*, 50, (1989) 1483
- (C-3.16) JAKUBAS R., L. SOBCZYK, *Phase Transitions*, 20, (1990) 163
- (C-3.17) KALLEL A. AND J.W. BATS, *ActaCryst.*, **C41**, (1985) 1022
- (C-3.18) MANJULA R., *M.Phil Dissertation*, University of Hyderabad, 1993
- (C-3.19) SATO S. , R. IKEDA AND D. NAKAMURA, *Ber.Bunsengess.Phys.Chem.* , 86, (1982) 936
- (C-3.20) SATO S., R. IKEDA AND D. NAKAMURA, *Ber. Bunsengess. Phys.Chem.* , 59, (1986a) 1981
- (C-3.21) SATO S. , R. IKEDA AND D. NAKAMURA, *J.Chem.Soc. Faraday Trans.-II*, 82, (1986b) 2053
- (C-3.22) SATO S., AND D. NAKAMURA, *Bul.Chem.Soc. Japan*, 60, (1987) 509
- (C-3.23) SJÖBLOM R. AND M. PUNKKINEN, *J.Magn.Reson.*, 20, (1975) 491
- (C-3.24) TAKEDA S. , G. SODA AND H. CHIHARA, *Mol.Phys.*, 47, (1982) 501
- (C-3.25) TANABE T. , D. NAKAMURA AND R. IKEDA, *J.Chem.Soc.Faraday Trans.*, 87, (1991) 987
- (C-3.26) VENU K. AND V.S.S. SASTRY, *Z.Naturforsch.*, **48a**, (1993) 713
- (C-3.27) WOESSNER D.E., *J.Chem.Phys*, 36, (1962) 1

## SECTION C

### PART 4

#### RELAXATION AND RESONANCE STUDIES ON



Methylammonium substituted compounds are one of the widely studied systems using various techniques. The methylammonium cations are found to exist in different compounds with varied type of anionic structures, like  $AMX$  [Krishnan et al., 1991; Xu et al., 1991; Yamamuro et al., 1992; Korfer et al., 1988; Ishibashi et al., 1989; Fuess et al., 1985],  $A_2MX_4$  [Nakayama et al., 1992; Srinivasan, et al., 1992] and  $A_3MX_6$  [Macintosh et al., 1992; Ikeda et al., 1976]. Most of these compounds exhibit structural phase transitions and the dynamics of the methylammonium cation is seen to be related to these phase transitions in many of these compounds. This cation is found to exhibit different types of motions, which include the isotropic reorientation of the entire cation [Xu et al., 1991; Macintosh et al., 1992],  $180^\circ$  flip motion of the cation perpendicular to its axis [Chapuis et al., 1975] and the reorientation of the cation about its C-N bond [Krishnan et al., 1991; Xu et al., 1991; Nakayama et al., Korfer et al., 1988; Ishida et al., 1989; Ikeda et al., 1976]. The substitution of different halogen atoms in these compounds is seen to affect the structural characteristics and thus the dynamic properties of the cations and anions in these compounds, considerably [Krishnan et al., 1991; Nakayama et al., 1992].

In fact, in the case of  $A_3M_2X$  systems and specifically in case of the methylammonium compounds, substituting different halogens in the

order of Cl, Br and I affects in a drastic way, the basic structure of these compounds [Jakubas et al., 1990a]. Thus, in  $(\text{CH}_3\text{NH}_2)_3\text{Sb}_2\text{Cl}_9$  (MACA), the anions form one dimensional chain-like structures but in  $(\text{CH}_3\text{NH}_2)_3\text{SbBr}_3$  (MABA), anions form two-dimensional corrugated layers, as one would find in the case of tri- and di-methyl ammonium compounds of this family [Jakubas et al., 1985, 1986, 1990a; Mackowiak et al., 1990], though the hexagonal voids created in between the six membered anion rings are highly symmetric in the case of MABA whereas these voids are considerably distorted in the case of tri- and di-methyl ammonium compounds. For the iodine substituted compounds, the anionic structure is entirely different and in this case  $\text{MX}_6$  octahedra exist in isolated face sharing configuration, similar to the tetramethylammonium compounds of this family [Miniewicz et al., 1990; Jakubas et al., 1990b]. In all these compounds, depending on the anionic structure, the cations have varying extents of freedom to undergo motion but the cation dynamics plays an important role in the structural phase transition observed, in all of them. The Antimony substituted compound  $(\text{CH}_3\text{NH}_3)^3\text{Sb}_2\text{Cl}_9$  (MACA) has been investigated through proton T and  $M_z$  measurements [Jagadeesh et al., 1994] and the results of these measurements show the presence of one phase transition at 208K and the presence of isotropic motion of the cation as well as reorientations about the C-N axis were seen in this compound. Thus, it is an interesting extension to see the effect of substitution of the bigger Bi atom in place of Sb and observe the changes it may bring about in the structural and the dynamic properties of cations which may get influenced by such structural changes. There are reports on some methylammonium compounds wherein the structural phase transition is not influenced by the cationic dynamics but is related to only the reorientational motion of the anions [Ikeda et al., 1976].

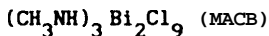


Therefore, it will also be interesting to see the extent to which the cation dynamics get coupled to structural phase transitions in these compounds.

Bismuth substituted methylammonium compounds have been studied through different techniques like infrared spectroscopy [Jakubas et.al., 1993], dielectric and pyroelectric measurements [Jakubas et al., 1989, 1990b, Miniewicz et al., 1990; Iwata et al., 1993], X-ray diffraction and Raman scattering [Belkyl et al., 1993; Iwata et al., 1993] as well as NMR and NQR investigations [Jakubas et al., 1992; Ishihara et al., 1992].

$(\text{CH}_3\text{NH}_3)_3\text{Bi}_2\text{Cl}_9$  (MACB) is the chlorine analogue of the Bismuth substituted compounds in this group, which is reported to exhibit more than one structural phase transition [Jakubas et al., 1989; Ishihara et al., 1992; Belkyl et al., 1993]. Proton second moment ( $M$ ) measurements as well as spin-lattice relaxation time ( $T_1$ ) measurements have been carried out as a function of temperature and the results of these measurements are presented here.

### Specific details



$T_1$  data :

Larmor frequency of : 8 MHz  
observation

Temperature range : 370K to 77

$M_2$  data :

Temperature range : 390K - 77K

$M_2$  variation as a function of temperature in MACB : Fig.(C-4.1)

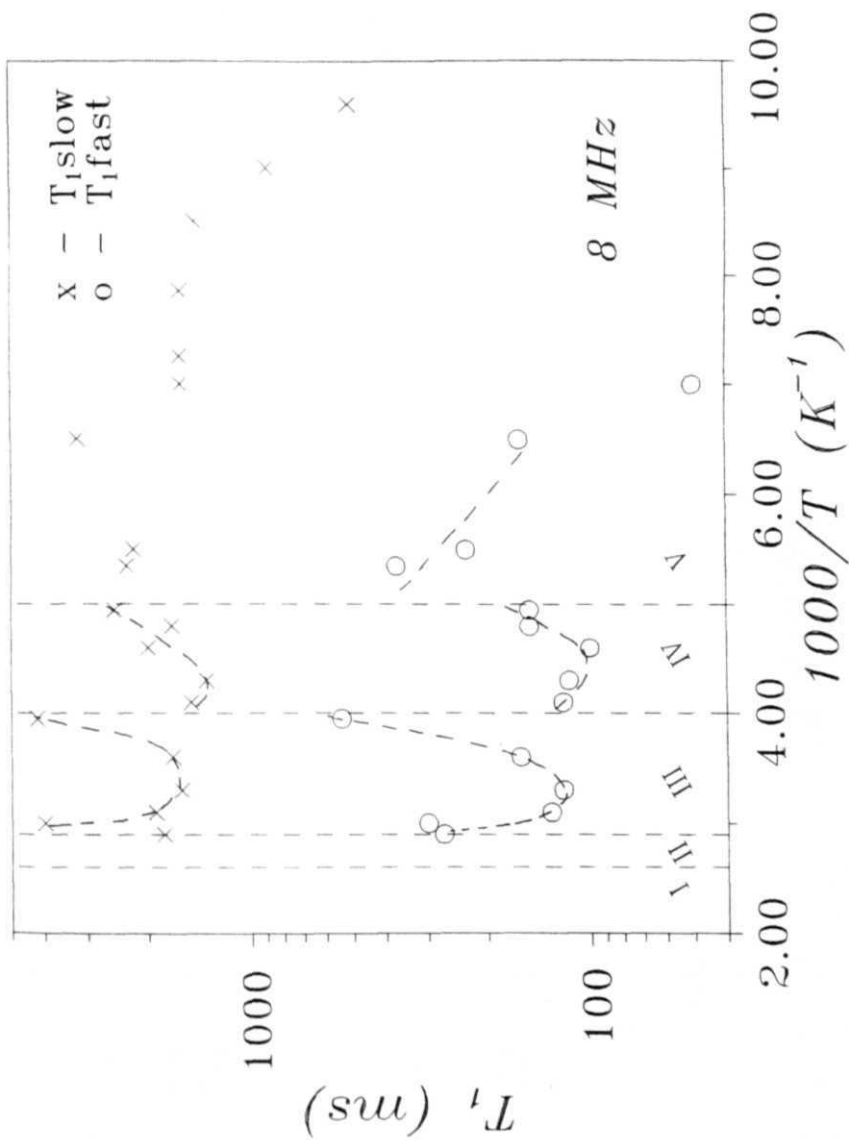
Variation of  $T_1$  with  $1/T$  in MACB : Fig.(C-4.2)

The MACB crystals were grown by the slow evaporation technique from a stoichiometric mixture of  $(CH_3NH_3)Cl$  and  $BiCl_3$  in  $HCl$ . Powdered and dried sample was sealed in 6 mm and 8 mm glass tubes under 10 torr vacuum for  $T$  and  $M$  measurements.  $\tau_2$  values were calculated from the absorption spectra obtained by numerically integrating the derivative spectra. The typical error in  $T$  and  $M$  data were 10%.

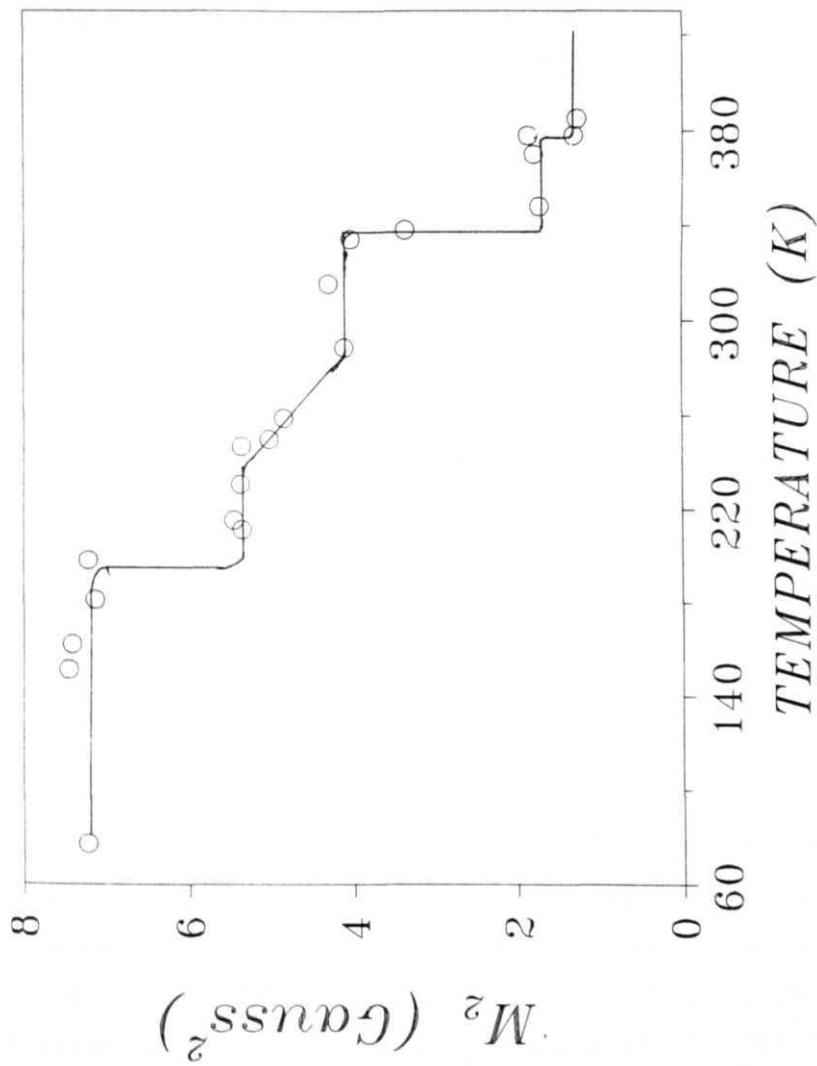
## RESULTS

$M_2$  variation as a function of temperature is shown in Fig.(C-4.1) and  $T$  data as a function of  $1/T$  at 8 MHz is shown in Fig.(C-4.2).  $M$  remains at a value of 7.510.5 Gauss in the temperature range 77K - 200K. At around 200K,  $\tau_2$  value decreases to a plateau of 5.510.5 Gauss. At around 250K, this value further decreases to yet another plateau of  $4.0 \pm 0.3$  Gauss<sup>2</sup> and by 340K,  $\tau_2$  goes down to 1.710.2 Gauss<sup>2</sup>. At 380K, we see that, there is an additional step in the  $M_2$  data, which reduces the value from 1.7 Gauss<sup>2</sup> to 1.210.2 Gauss<sup>2</sup>.

The magnetization recovery in this compound shows marked non-exponentiality, from the highest temperature studied here (370K) till around 140K (Fig. C-4.3). In methylammonium cations, this non-exponentiality may be attributed to the cross-correlation in the intra group interaction of the proton within a  $CH_3$  group or a  $NH_3$  group



(C - 4.2)  $T_1$  variation as a function of  $1/T$  in  $(CH_3NH_3)_3Bi_2Cl_9$ .



(C - 4.1)  $M_2$  variation as a function of temperature in  $(CH_3NH_3)_3Bi_2Cl_9$ .

[Xu et al., 1991; Nakayama et al., 1992; Ikeda, 1976; Hilt et al., 1964; Baud et al., 1968]. A two exponential model was used to fit this magnetization recovery, and where ever possible the two relaxation times denoted by  $T_{1fast}$  and  $T_{1slow}$  were computed from the magnetization recovery. The variation of the two kinds of relaxation times as a function of temperature is shown, in Fig.(C-4.2).

## RESULTS

The MACB crystals are orthorhombic belonging to space group Pmcn [Jakubas et al., 1989; I. Belkhal et al., 1993]. Jakubas and co-workers reported only a high temperature structural phase transition in this compound at 385K ( $T_1$ ) while Belkhal et al. found two more from DSC and dielectric studies at 349K ( $T_2$ ) and 247K ( $T_3$ ) [Belkhal et al., 1993; Jakubas et al., 1992]. However, the latter group did not observe the signature of the high temperature phase transition reported by Jakubas et al. DSC and NQR investigation on MACB carried out by Ishihara et al. further revealed the presence of one more low temperature phase transition at 200K ( $T_4$ ) [Ishihara et al., 1992].

The lattice parameters for MACB found by Jakubas et al. are given by :  $a = 20.422 \text{ \AA}$ ;  $b = 7.697 \text{ \AA}$ ;  $c = 13.248 \text{ \AA}$ , and  $Z = 4$ . (In their original communication, Jakubas et.al., have used a different notation for the lattice parameters, which was also pointed out by Belkhal et al. For the sake of consistency, we are using here the same notation as used by Belkhal et al.). MACB is isomorphous with its antimony analogue MACA [Jakubas et al., 1989] and also  $\beta$ -Cs Sb Cl [Kihara et al., 1974]. It is made up of infinite  $MX_6$  polyanions which form one-dimensional zig-zag

double-chain-stack structure directed along the b-axis and it contains three crystallographically inequivalent  $\text{CH}_3\text{NH}_3^+$  ions. The isomorphism of MACA and MACB should imply a similar ordering of methylammonium cations in the polyanion sub-lattice in MACB, and one can expect certain similarities in the properties related to the cations. From dielectric measurements, it is found that the phase above 385K does not have an analogue in MACA and this phase may be a plastic phase where there is considerable freedom for the methylammonium cations to undergo isotropic reorientation [Jakubas et al., 1989; Timmermans, 1961]. The change in the symmetry through this high temperature transition was also observed by powder X-ray diffraction.

The transition observed at 349K did not show any change in the symmetry of the compound and above and below 349K, the MACB crystal was found to be in the orthorhombic phase only and this is a peculiar situation [Belkhal et al., 1993]. It is speculated that such an existence of "equisymmetric" phases above and below the phase transition may be due to the presence of a parent space group of higher symmetry above the transition temperature. Nevertheless, when the sample temperature is increased through T<sub>c</sub>, there is contraction of the lattice along the a direction and expansion of the lattice along the b and c axes. Detailed Raman spectra recorded on this compound as a function of temperature in the high frequency region reveal certain important points in relation to the dynamics of the cation. The three crystallographically inequivalent cations did not leave any mark regarding this inequivalence on the Raman spectra, but it is worthwhile to note that the time window accessed by the Raman spectra is around 10<sup>-13</sup> s. From the different modes observed in the high frequency region from room temperature to 93K, it is found that

the CH groups and NH groups execute fast reorientations about the C-N axis. This is a clear indication of the presence of the uncorrelated motion of the methylammonium cations in this phase [Nakayama et al., 1992; Ikeda et al., 1976; Xu et al., 1991; Jakubas et al., 1992]. NQR and DTA studies on MACB revealed the presence of two structural phase transitions. NQR frequency versus temperature plot shows that there are four Cl lines above 300K and as the sample is cooled this plot shows a discontinuity at 249K. As the temperature of the compound is reduced further, two of the NQR lines merge with each other at 200K and below this temperature there are only three lines observable. DTA measurements also show endothermic peaks at 249K and 200K, thereby confirming the presence of phase transitions at these two temperatures [Ishihara et al., 1992]. The anomalous temperature dependence of NQR lines above 250K is attributed to the high temperature phase transition at 385 K reported by Jakubas et al.

We can analyze the proton NMR data in the light of these observations made through various other techniques in MACB. It is remarkable that the M data (Fig. C-4.1) show a line width transition near all the four temperatures, where structural phase transitions have earlier been observed by different methods (385K, 349K, 247K and 200K). The  $M_2$  value observed above 385K is  $1.2 \text{ Gauss}^2$  and this small value indicates the presence of isotropic reorientation of the methyl ammonium cations in this compound, in accordance with the observation by Jakubas et al. [Jakubas et al., 1989]. When isotropic reorientation is present, the intra group contribution to the second moment gets averaged out and only the interionic interaction contributes to this value. It has been observed in the Sb analogue (MACA) that the interionic contribution to

the second moment is 1.5 Gauss . Since MACB is **isomorphous** with MACA and the lattice parameters of MACA (  $a=19.66$  Å;  $b=7.920$  Å and  $c=13.33$  Å) are comparable with that of MACB, we can assume that **this** value is a reasonable estimate of the interionic contribution to  $M_2$  in the case of MACB also [Jakubas et al., 1986]. As we decrease the temperature, there is a slight increase in the value of  $M_2$  to  $1.7 \pm 0.2$  Gauss<sup>2</sup> around **380K**. It is possible that, following the structural phase transition at **385K**, there is a slight decrease in the reorientational freedom of the cations. However, the **smallness** of the  $M_2$  value of (1.7 Gauss ) still indicates the presence of isotropic motion of the cations only. As we have pointed out already, there are three steps in the **M** data all corresponding to the three remaining transition temperatures. The **M** values increase to 4.0 G<sup>2</sup>, 5.5 G<sup>2</sup> and finally to 7.5 G<sup>2</sup>, at around **340K**, **250K** and **200K** respectively. The low temperature plateau value of  $7.5 \pm 0.5$  Gauss agrees reasonably well with the value corresponding to the motion of the MA ion, either uncorrelated or correlated, about the C-N axis [Ikeda et al., 1976; Ishida et al., 1989; Ishihara et al., 1992]. We can account for the observed increase of **M** in three stages in the following manner. Among the three MA ions executing isotropic reorientation, let us assume that one of them gets frozen into a lower order reorientation, namely the rotation about the C-N axis, coincidental with the transition temperature **349K**. In such a case, the calculated value of  $f_y$  for  $1/3^{\Gamma}$  of MA executing C-N reorientation and  $2/3$  of them **undergoing** isotropic reorientation, with a residual moment of 1.5 Gauss **will** be, 3.6 Gauss , which is reasonably close to the observed value of 4.0 Gauss . Further, if one more MA group changes its reorientational mode from isotropic motion to C-N axis rotation following the phase transition at **247K**, then <sup>2</sup> the calculated value of  $M_2$  in such a case will be 5.7 Gauss , which is



also in good agreement with the observed value (5.5 Gauss ) of the plateau from 250K till 210K. Finally, following the lowest temperature transition at 200K if we assume the third MA cation also to slow down to execute only C-N axis reorientations, then the expected second moment value of 7.5 Gauss can account for the observed value of 7.5+0.5 Gauss also. The three individual methyl ammonium cations freezing into a more hindered rotational state at different temperatures may be an indication of the presence of the three crystallographically inequivalent cations in this compound [Jakubas et al., 1989; Belkhal et al., 1993], and perhaps, the non-exponentiality in the magnetization recovery is related to the presence of such inequivalent groups. A similar occurrence is seen in the case of MACA (Jagadeesh et al., 1994]. The slowing down of the isotropic motion of each of the cations, perhaps, is triggering each of the observed phase transitions, leading to the freezing of the isotropic motion of that ion below the corresponding phase transition temperature.

The temperature dependence of  $T$  values at 8 MHz is shown in this compound in Fig.(C-4.2). The non-exponential magnetization recovery was fitted to a two exponential model using a non-linear least square fitting program and the two components of relaxation times ( $T_{fast}$  and  $T_{slow}$ ) were recovered. Fig.(C-4.3) shows one such magnetization recovery and the solid line passing through the points is the best fitted curve. In Fig.(C-4.2) the values of both  $T_{fast}$  and  $T_{slow}$  are plotted up to the temperature 140K, and below this value the non-exponentiality of the magnetization recovery is seen to disappear. The  $T_{slow}$  values are of the order of few seconds whereas  $T_{fast}$  values in the range of 100's of ms. Let us denote the phase above 385 K by the phase-I. Similarly, let the phases in the range 385K - 350K, 350K - 250K, 250K - 200K and below 200K

be denoted by II, III, IV and V respectively. We do not have any data in phase I and the region of phase II is very narrow. There are only two points available in this phase which show an increasing tendency with decreasing temperature, but obviously we cannot comment further on this. But, at the  $T_c$  corresponding to the II-III transition, both  $T_{1fast}$  and  $T_{1slow}$  values show a steep decrease in their values. These values tend to increase with decreasing temperature in phase III, until at the  $T$  related to III-IV transition they show a steep fall. Below this temperature, i.e. 250K, the  $T$  values tend to increase again, but there seems to be another discontinuity at the  $T$  corresponding to the IV-V transition. This is more clearly seen in the case of the  $T_{1slow}$  component than for the fast component, which disappears around this temperature region. Below 170K, the  $T_{1slow}$  value tends to decrease monotonically with decreasing temperature and this seems to continue till 77K. It is of course difficult to make any precise quantitative estimates from this data, which has an increased amount of scatter also. However, a rough estimate of the slope from the monotonically decreasing region is given by  $3.5 \pm 0.5$  kJ/mole, which is much smaller than typical potential barrier for the internal rotation in these cations. (of the order of 8.0 kJ/mole [Ikeda et al., 1976]). This indicates the possibility that there is a correlated motion of the methyl ammonium cation in phase V. Normally,  $T_{1slow}$  minima corresponding to the correlated motion of the MA cation are seen to occur at temperatures below 77K [Xu et al., 1991; Ikeda et al., 1976; Nakayama et al., 1992] and in MACB also, perhaps, the minimum corresponding to the correlated motion of the cations may be expected below 77K.

In the Sb analogue of this compound, MACA, the activation energy

corresponding to the correlated motion of the cations is 8.7 kJ/mole which is much higher than the corresponding value for MACB [Jagadeesh et al., 1994]. This difference may perhaps, be attributed to the strength of the N-H...Cl hydrogen bonds, which is considerable in the case of MACA [Jakubas, et al., 1986]. The crystal structure data do not explicitly show the formation of hydrogen bonds in the case of MACB, but if we assume them to be present their strength seems to be much smaller as shown by the E value for correlated motion of MA cation in phase V in MACB [Jakubas, 1989; Belkhal, 1993]. In fact, the potential barrier for the reorientation about the C-N axis in the case of Iodine counterpart of this compound,  $(\text{CH}_3\text{NH}_3)_3\text{Bi}_2\text{I}_9$  (MAIB), is smaller at 2.2 kJ/mole and this indicates that the strength of the hydrogen bond N-H...I is much smaller than that of MACB [Jakubas et al., 1992]. This observation is commensurate with the fact that, with the halogen atoms being changed from Cl to Br to I, the hydrogen bond strengths decrease progressively [Nakayama et al., 1992; Xu et al., 1991]. Two structural phase transitions are recorded in MAIB at 142K and 223K [Jakubas et al., 1990b, 1992; Miniewicz et al., 1990;] and in this compound also, in the highest temperature phase, isotropic reorientation of the cations are seen. The Bromine analogue of MACB,  $(\text{CH}_3\text{NH}_3)_3\text{BiBr}$  (MABB), is found to exhibit three structural phase transitions at 104K, 140K and 188K [Jakubas et al., 1990b, 1993; Ishihara et al., 1992] and two types of inequivalent MA cations are present in this system. In the highest temperature phase of MABB, above 188K, the cations are found to undergo isotropic motion [Ishihara et al., 1992; Jakubas et al., 1993].

In summary, T and M measurements made on MACB record the presence of the four structural phase transitions in this compound, which were

detected only in a partial manner from other techniques. The coincidence of the NMR time window with the respective dynamic process associated with different phase transitions may be the reason for the observation of the signatures of all the transitions. In the high temperature phase, above 385K, MACB cations are found to undergo isotropic reorientation. The three types of crystallographically inequivalent cations seem to experience distinct dynamic environments, as seen from the second moment data. The progressive freezing of the isotropic motion of each of these cations seems to be closely associated with the three observed phase transitions, as seen from  $M_2$  data, and  $T_1$  data also show the presence of these transitions. Further, nonexponentiality in magnetization recovery is seen in all the phases in this compound, as is observed in many other methylammonium substituted compounds, which may be attributed to the cross correlation in the intra group interaction of the protons within the methyl or NH groups. In the lowest temperature phase, the cations are found to undergo correlated motions about the C-N axis, as hinted by the rough estimate of activation energy made from the  $T_1$  data. The presence of more than one phase transition which are nearby renders the region of different phases rather narrow in this compound and the not so straight forward way of estimating the  $T_1$ -s from the non-exponential recovery of magnetization using a non-linear least-squares fitting procedure makes the  $T_1$ -s less reliable and these factors make any serious attempt on a quantitative estimate of the relevant dynamic parameters from the  $T_1$  data rather difficult though they qualitatively explain the presence of the various transitions in this compounds. Therefore, no further attempt was made to record the  $T_1$  data at a different Larmor frequency in this compound alone.

# REFERENCES

- (C-4.1) BAUD M.F., P.S. HUBBARD, *Phys.Rev.*, **170**, (1968) 384
- (C-4.2) BELKYAL I., R. MOKHLISSE, B. TANOUTI, N.B. CHANH AND M. COUZI, *Phys.Stat.Solidi (a)*, 136, (1993) 45
- (C-4.3) CHAPUIS G. , H. AREND AND R. KIND, *Phys.Stat.Solidi.* **31**, (1975), 449
- (C-4.4) FUESS H., M. KORFER, H. AREND AND R. KIND, *Solid State Commun.*, 56, (1985) 137
- (C-4.5) HILT R.L. AND P.S. HUBBARD, *Phys.Rev.A*, **134**, (1964) 392
- (C-4.6) IKEDA R. , Y. KUME, D. NAKAMURA, Y. FURUKAWA AND H. KIRIYAMA, *J.Magn. Reson.* , 24, (1976) 9
- (C-4.7) ISHIBASHI Y. AND V. DVORAK, *J.Phys.Soc.Japan*, 12, (1989) 4493
- (C-4.8) ISHIDA H. , N. MATSUHASHI, R. IKEDA AND D. NAKAMURA, *J.Chem.Soc. Faraday Trans.*, 85, (1989) 111
- (C-4.9) ISHIHARA H. , K. WATANABE, A. IWATA, K. YAMADA, Y. KINOSHITA, T. OKUDA, V.G. KRISHNAN. SHI-QI DOU AND A. WEISS, *Z.Naturforsch.*, 47a, (1991) 65
- (C-4.10) IWATA M. , M. EGUCHI, Y. ISHIBASHI, S. SASAKI, H. SHIMIZU, T. KAWAI AND S. SHIMANUKI, *J.Phys.Soc.Japan*, 62, (1993) 3315
- (C-4.11) JAGADEESH B. , P.K. RAJAN, K. VENU AND V.S.S. SASTRY, *Proceedings of 36 Solid State Physics Symposium*, **1993**, 505
- (C-4.12) JAKUBAS R., Z. GALEWSKI. L. SOBCZYK AND J. MATUSZEWSKI, *J.Phys.C*, 18, (1985) L857
- (C-4.13) JAKUBAS R. , Z.CZAPLA, Z.GALEWSKI, L.SOBCZYK, O.J. ZOGAL AND T. LIS, *Phys.Stat.Solidi (a)*, 93, (1986) 449
- (C-4.14) JAKUBAS R. , P.E. TOMASZEWSKI AND L. SOBCZYK, *Phys.Stat.Solidi*

- (a), **111**, (1989) K27
- (C-4.15) JAKUBAS R. AND L. SOBCZYK, *Phase Transitions*, 20, (1990a) 163
- (C-4.16) JAKUBAS R. , J. ZALESKI AND L. SOBCZYK. *Ferroelectrics*, 108, (1990b) 109
- (C-4.17) JAKUBAS R. , R. DECRESSAIN AND J. LEFEBVRE, *J.Phys.Chem.Sol ids*, 53, (1992) 755
- (C-4.18) JAKUBAS R. , G. BATOR AND J. BARAN, *J.Phys.Chem.Sol ids*, 54, (1993) 1065
- (C-4.19) KIHARA K. AND T. SUDO, *Acta Cryst.*, **B30**, (1974) 1088
- (C-4.20) KORFER M. , H. JUSS, M. PRAGER AND E.J. ZEHNDER, *Ber.Bunsengess. Phys.Chem.*, 92, (1988) 68
- (C-4.21) KRISHNAN V.G., SHI-QI DOU AND A. WEISS, *Z.Naturforsch.*, 46a, (1991) 1063
- (C-4.22) MACKOWIAK M. , N. WEIDEN, A. WEISS, *Phys.Stat.Solidi (a)*, **119**, (1990) 77
- (C-4.23) MacINTOSH M.R., M.L.H. GRUWEL, K.N. ROBERTSON AND R.E. WASYLISHEN, *Can.J.Chem.*, 70, (1992) 849
- (C-4.24) MINIEWICZ A. AND R. JAKUBAS, *Ferroelectrics*, **110**, (1990) 261
- (C-4.25) NAKAYAMA H. , T. EGUCHI AND N. NAKAMURA, *J.Chem.Soc. Faraday Trans.*, 88, (1992) 3067
- (C-4.26) SRINIVASAN T.K.K., M. MYLRAJAN AND J.B. SRINIVASA RAO, *J.Raman Spectroscopy*, 33, (1992) 21
- (C-4.27) TIMMERMANS J., *J.Phys.Chem. Solids*, 18, (1961) 1
- (C-4.28) XU Q. , T. EGUCHI, H. NAKAYAMA AND N. NAKAMURA, *Z.Naturforsch.*, **46a**, (1991) 240
- (C-4.29) YAMAMURO N.O., T. MATSUO AND H. SUGA, *J.Phys.Chem.Sol ids*, **53**, (1992) 935

## SECTION C

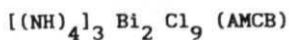
### PART 5

#### RESONANCE AND RELAXATION STUDIES ON



The ammonium compounds of  $\text{A}_2\text{MX}$  family present a contrasting situation compared to their other counterparts. The cations in these compounds have tetrahedral symmetry, but with no internal dynamics within the cation. The majority of investigations on the ammonium substituted compounds show the presence of isotropic reorientation of the cation [Cooke et al., 1952; Gutowsky et al., 1954; Ishida et al., 1985; Chihara et al., 1990] or the cation undergoes reorientation about the three-fold and 2-fold axes of the tetrahedron characterized by two different correlation times [O'Reilly et al., 1967]. To investigate the dynamics of the ammonium cation in the structurally different compounds of the family tris(alkylammonium) nonahalogeno dimetallates, proton T. and  $\text{M}_\text{L}$  measurements are made on the Bismuth analogues of these compounds, namely,  $(\text{NH}_4)_3\text{Bi}_2\text{Cl}_9$  (AMCB) and  $(\text{NH}_4)_3\text{Bi}_2\text{Br}_9$  (AMBB). It appears that there are no other reports on these compounds in literature, as of now. The results on the Antimony substituted compounds are reported elsewhere [Jagadeesh, 1994].

## Specific Details



### T Measurements

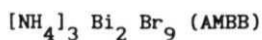
Temperature range : 415K - 77K

Larmor frequencies : 8 and 5 MHz

Fig. (C-5.1) Variation of  $T_1$  as a function of  $1/T$  in AMCB.

### M Measurements

Temperature range : 400K - 77K



### T MEASUREMENTS

Temperature range : 385K - 77K

Larmor frequencies : 8 and 39.6 MHz

### M MEASUREMENTS

Temperature range : 420K - 77K

Fig. (C-5.2) Variation of  $T_1$  as a function of  $1/T$  in AMBB.

Fig. (C-5.3) Variation of  $M_2$  as a function of  $T$  in AMBB.

AMCB was grown by slow evaporation technique from a stoichiometric mixture of  $(\text{NH}_4)\text{Cl}$  and  $\text{BiCl}_3$  in  $\text{HCl}$ . The crystals were colourless. AMBB was grown by mixing  $(\text{NH}_4)\text{Br}$  and  $\text{BiOBr}$  in  $\text{HBr}$  and AMBB crystals were orange in colour. The crystals were, powdered, dried and sealed under



10 torr vacuum for measurements.

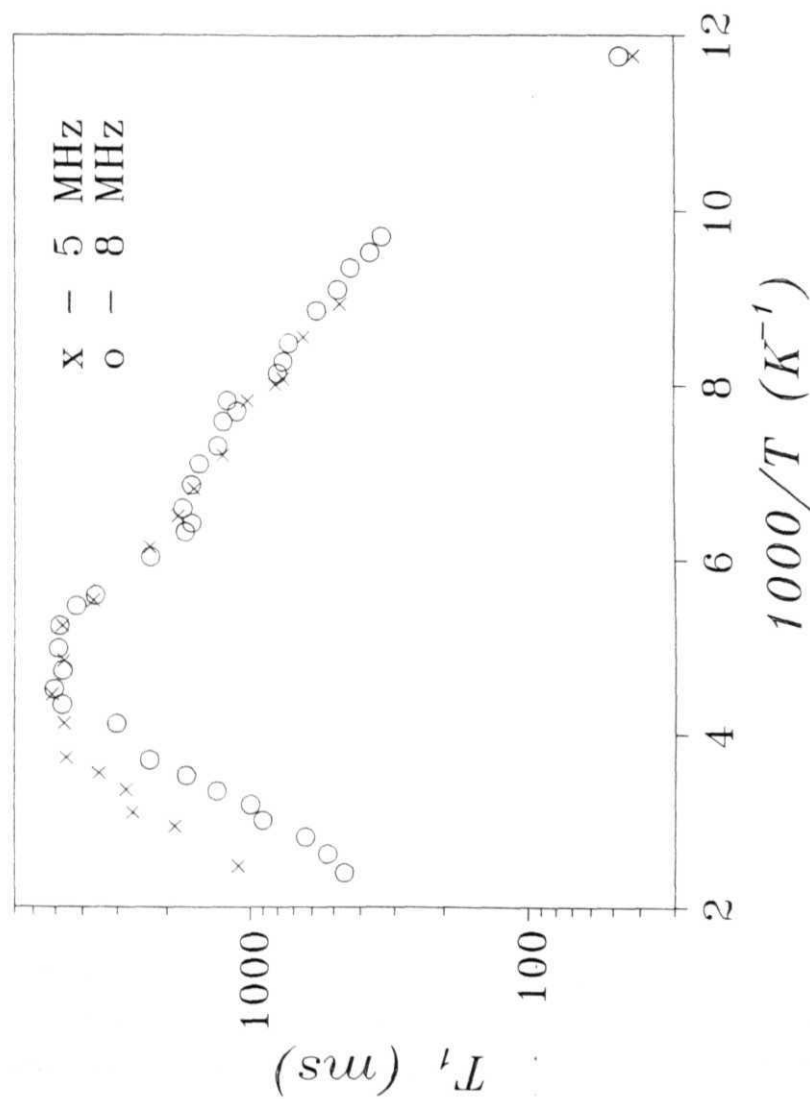
## AMCB

### RESULTS

Results of  $T$  measurements on AMCB is provided as a  $T$  vs  $1/T$  graph in Fig.(C-5.1). The  $T$  values of AMCB are relatively high at few seconds in comparison with the relaxation times in other ammonium compounds.  $T$  value reaches a maximum of 5 seconds around 200K and above this temperature, it decreases with increasing  $T$ . Below 200K also, there is a decrease in  $T$  with decreasing  $T$ . We observe this feature at around 200K both at 8 and 5 MHz. The data above 200K show frequency dispersion and the notable behaviour above this temperature is the fact that,  $T$  values corresponding to 5 MHz are higher than the values at 8 MHz. The data show a change in slope from a higher to lower value around 160K and a further small change is observed around 125K. Below this temperature, the data seem to be linear as a function of  $1/T$  without any dispersion but the value of  $T$  at 77K is lower than the extrapolated value from the data below 125K.  $M$  values calculated for this compound from CW measurements remains at a low and constant  $1.0 \pm 0.1$  Gauss from approximately 400K till 77K.

### DISCUSSION

The observed  $M$  value of 1 Gauss in this compound is rather low compared with what is normally found in other ammonium compounds, typically undergoing isotropic reorientation. The expected value of  $M_2$



(C - 5.1)  $T_1$  variation as a function of  $1/T$  in  $(NH_4)_3 Bi_2 Cl_9$ .

if the ammonium cations are fast reorienting is 3 Gauss and thus a lower value of 1 Gauss<sup>2</sup> in the present case shows that the ammonium cations are moving rather freely and fast. Conductivity measurement in this compound may provide some information about the dynamics of the ammonium cations in this compound like it is observed in other situations [Furukawa et al., 1990; Sasaki et al., 1989; Kobayashi et al., 1988]. The maximum like structure with frequency dependence has been observed in other compounds also and in such cases more than one possibility exist to explain this behaviour. For instance, such a typical behaviour is observed in **n-alkylammonium** chlorides, other compounds which tend to exhibit plastic crystalline phase like  $\text{CH}_3\text{NH}_3\text{NO}_3$ ,  $[(\text{CH}_3)_4\text{N}]\text{SCN}$ ,  $(\text{CH}_3\text{NH}_3)_2\text{SO}_4$ , and some ammonium compounds like  $(\text{NH}_4)_2\text{InF}_6$  and  $(\text{NH}_4)_2\text{GaF}_6$  also [Iwai et al., 1993; Fukuda et al., 1987; Tanabe et al., 1991; Hattori et al., 1990; Ishida et al., 1985, 1989, 1990; Sasaki et al., 1989]. In these compounds, the decrease in T with increasing temperature and the frequency dependence of T data above the maximum are explained to be due to self-diffusion of the cations concerned apart from the reorientational motions present. But, contrastingly, in the case of AMCB such an explanation cannot be given for the reasons that : (i) there is anomalous dependence of T on  $\omega$ , namely, for higher  $\omega$  (8 MHz) the T. values are lower than the corresponding values at 5 MHz; and (ii) the observed second moment is 1.0 Gauss<sup>2</sup> throughout the temperature range. Where there is self-diffusion of the cations, the  $M_2$  values reduce to a very small value of the order of 0.005 Gauss<sup>2</sup> [Riggin et al., 1972; Tanabe et al., 1991; Ishida et al., 1985, 1989; Furukawa et al., 1990; Sasaki et al., 1989]. But, in the present case the  $M_2$  value remains at 1 Gauss<sup>2</sup> and

this does not support the possibility of self-diffusion. The other possibility seems to be that there is a cross relaxation of the proton nuclear levels via the Chlorine NQR levels, **in this** compound. The NQR frequencies of the Cl nuclei in  $A_3M_2X_9$  compounds are expected to be in the range of 8 MHz [Ishihara et al., 1992]. In fact, such a similar situation is observed in the case of tetramethylammonium compounds, where the proton nuclear levels are observed to undergo cross-relaxation via the Bromine and Iodine NQR levels, showing a similar anomalous frequency dependence of T on the Larmor frequency [Sato et al., 1986].

The presence of very fast motion suggested by the second moment values implies that the conventional relaxation mechanism through the modulation of the dipole-dipole interaction between protons is very **inefficient** and perhaps this is **reflected** in the higher values of T, which are of the order of seconds in this temperature region, compared to much smaller values of T observed for other ammonium compounds [Sasaki et al., 1989; Chihara et al., 1990; Koksai, 1984]. This fast motion of the cation may also be responsible for causing a maximum in the relaxation time due to the spin-rotation interaction [Venu et al., 1985, 1987; Koksai et al., 1978; Ikeda et al., 1973]. The activation energy computed for the possible isotropic motion of the NH<sub>4</sub><sup>+</sup> cation from the T values below 125K is 5.5±0.5 kJ/mole. The small value of M i.e. 1.0±0.1 Gauss, **indicates** an increase in the inter ammonium distance to 3.9 Å, which is consistent with the activation energy quoted above [Gutowsky et al., 1954, Venu et al., 1986].

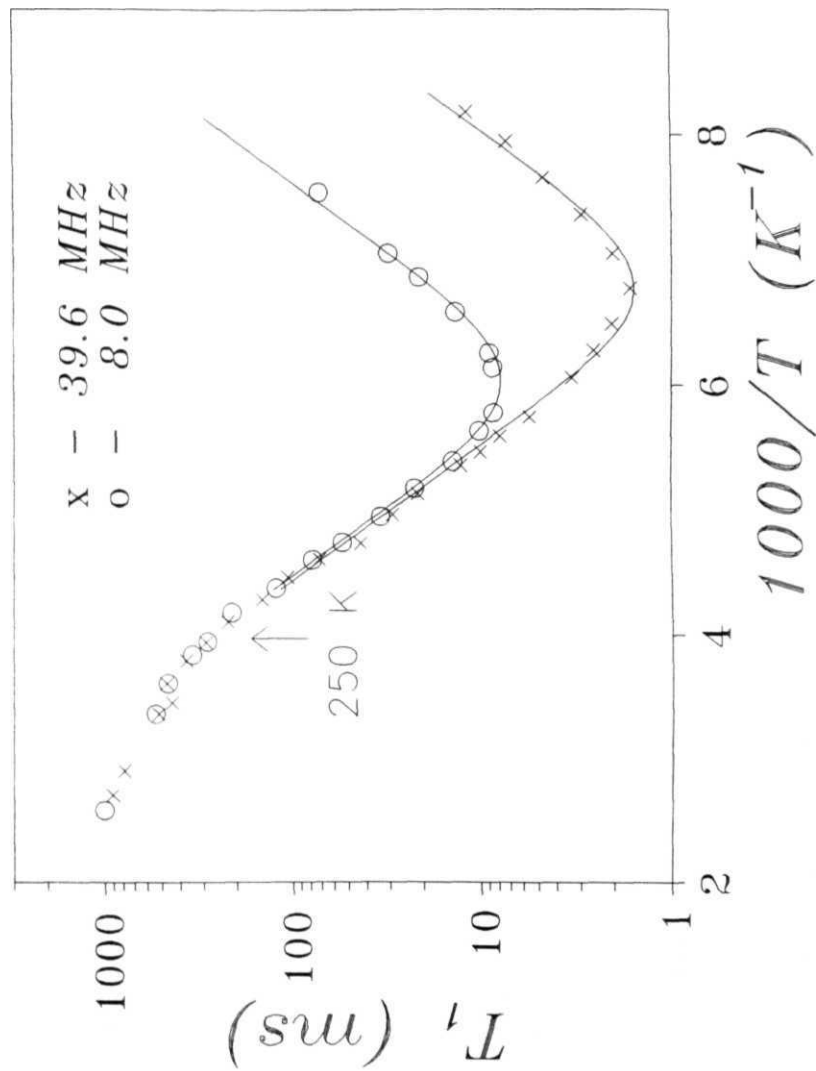
## AMBB

### RESULTS

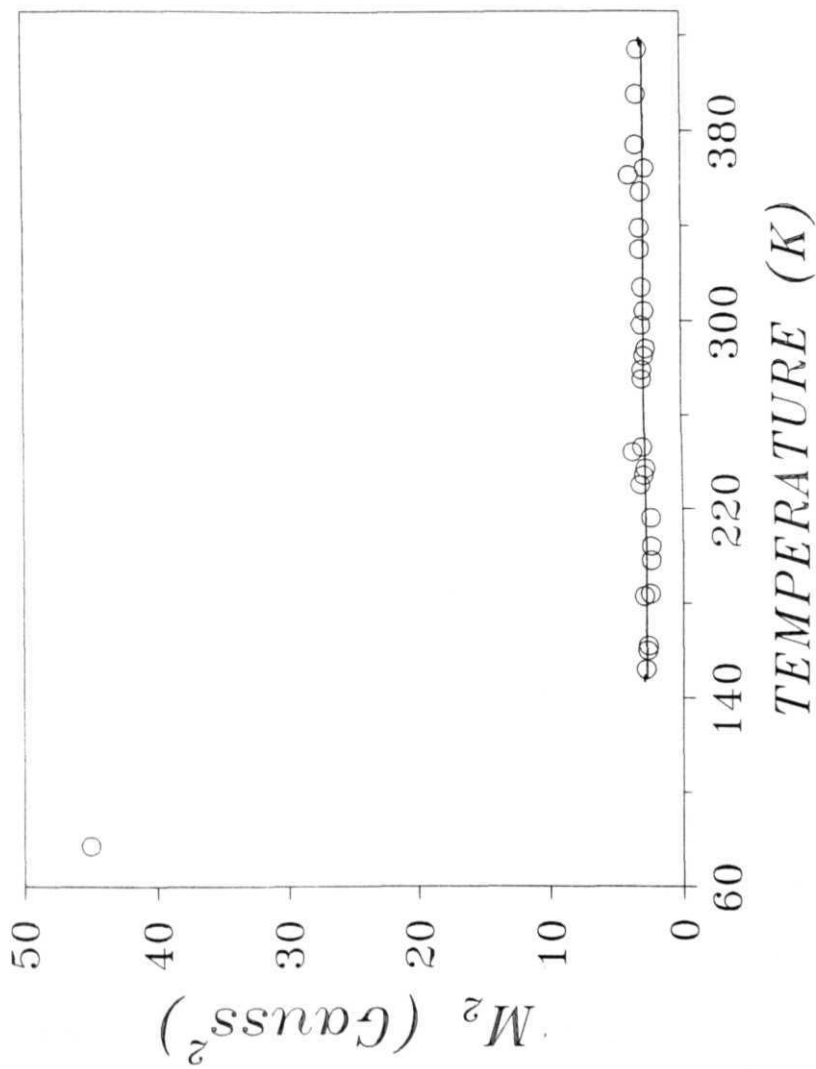
In comparison to AMCB, AMBB shows an entirely different behaviour as far as the  $T$  data are concerned.  $T$  data below 250 K show a single minimum at both the Larmor frequencies, i.e., 8 and 39.6 MHz as it is observed in many other ammonium compounds [Koksal, 1984; Chihara et al., 1990; Venu et al., 1986] and there is clear change in the slope of  $T$  vs  $1/T$  curve above 250K (Fig.C-5.2). The value of the activation energy calculated from data above 250K is  $7.0 \pm 0.5$  kJ/mole. The temperature dependence of  $M$  is shown in Flg.(C-5.3) and it is seen that the  $M_2$  value remains at a constant value of  $2.5 \pm 0.3$  Gauss<sup>2</sup> from about 420K to 140K. At 77K,  $M_2$  has reached a value of 45 Gauss<sup>2</sup>.

### DISCUSSION

The perceptible change observed in the slope of  $T$  vs  $1/T$  curve may indicate the presence of a structural phase transition in this compound around 250K. Such a discontinuity in the  $T$  data has been observed to be associated with structural phase transitions in other ammonium compounds also [Venu et al., 1986; Woessner et al., 1967, O'Reilly et al., 1967; Sasaki et.al., 1989]. However there was no change observed in the value of  $M_2$  around the transition temperature, unlike some other ammonium compounds, [Gutowsky et al., 1954; Venu et al., 1986].



(C - 5.2)  $T_1$  variation as a function of  $1000/T$  in  $(NH_4)_3Bi_2Br_9$



(C - 5.3) Variation of  $M_2$  as a function of temperature in  $(NH_4)_3Bi_2Br_9$ .

The Model :

The  $T$  data in ammonium compounds is analyzed using O'Reilly's model for the isotropic reorientation of ammonium ions, where the spin-lattice relaxation rate is given by [O'Reilly et al., 1967],

$$(C-5.1) \quad T_1^{-1} = C \left( \frac{\tau_c}{1 + \omega^2 \tau_c^2} + \frac{4\tau_c}{1 + 4\omega^2 \tau_c^2} \right)$$

where,  $C$  is the appropriate relaxation constant given by  $(9/10)(r_h/r)$ , where  $r$  is the **interproton** distance within the ammonium group. From BPP formula, the general expression for  $T_1$  is given by

$$(C-5.2) \quad T_1^{-1} = \frac{3}{2} \gamma^4 \hbar^2 I(I+1) \left[ \sum_{l \neq j} J_{lj}^{(1)}(\omega) + J_{lj}^{(2)}(2\omega) \right]$$

where,  $J(\omega)$  is given by the expression

$$(C-5.3) \quad J(\omega) = \int_{-\infty}^{\infty} G(\tau) \exp(-i\omega\tau) d\tau$$

and  $G(\tau)$  is given by

$$(C-5.4) \quad G(T) = \langle F(t) F(t+\tau) \rangle$$

The lattice functions of the dipolar interaction in this case is given by

$$(C-5.5a) \quad F_{lk}^{(1)} = r^{-3} \sin\theta_{lk} \cos\theta_{lk} \exp(-i\phi_{lk})$$



$$(C-5.5b) \quad F_{ik}^{(2)} = r^{-3} \sin^2 \theta_{ik} \exp(-2i\phi_{ik})$$

where  $r$  is the distance between any two protons in the **NH** tetrahedron. In **NH** there are six proton pairs and the reorientational process can be thought of as a given pair of protons moving from one configuration to the other. It can be seen that, any given proton pair has a probability  $[(1/6)+(5/6) \exp(-\tau/\tau_c)]$  to remain in its initial configuration and a probability  $[(1/6)-(1/6) \exp(-\tau/\tau_c)]$  of being in one of the remaining five orientations at time  $\tau$ . If at time  $t$ , a given proton pair  $ij$  is in the initial configuration, then at time  $(t+\tau)$ , one can write the following expressions for the lattice functions [O'Reilly et al., 1967]

$$(C-5.6) \quad F_{ij}(t+\tau) = \left[\frac{1}{6} + \frac{5}{6} \exp(-\tau/\tau_c)\right] F_{ij} + \sum_{ik \neq ij} F_{ik} \left[\frac{1}{6} - \frac{1}{6} \exp(-\tau/\tau_c)\right]$$

and the average given in eqn.(C-5.4) can be expressed as

$$(C-5.7) \quad \langle F_{ij}(t) F_{ij}(t+\tau) \rangle = \left[\frac{1}{6} + \frac{5}{6} \exp(-\tau/\tau_c)\right] |F_{ij}|^2 + \sum_{ik \neq ij} F_{ij} F_{ik} \left[\frac{1}{6} - \frac{1}{6} \exp(-\tau/\tau_c)\right]$$

After averaging over the initial positions, this expression can be suitably modified to

$$(C-5.8) \quad \langle F_{ij}(t) F_{ij}(t+\tau) \rangle = \frac{1}{36} [\exp(-\tau/\tau_c)] (5 \sum_{ij} |F_{ij}|^2 - \sum_{ij} \sum_{ik \neq ij} F_{ij} F_{ik})$$

This expression is to be substituted into eqn. (C-5.4) from which eqn.(C-5.1) for a polycrystalline sample can be derived. The expected minimum value for the the isotropic motion at 8 MHz varies from 1.85 ms to 1.07 ms for a variation of the interproton distance from 1.73 Å to 1.58 Å. The minimum value at 8 MHz for AMBB is 1.65 ms and it scales as the ratio of the Larmor frequency (at 39.6 MHz it is 8.2 ms). These minima are well within the extreme values quoted above and thus the above given model adequately explains the T data. This also indicates that there are no inequivalences among the ammonium ions and all are reorienting with a single correlation time T [O'Reilly et al., 1967]. From the values of the minima given above for AMBB, the interproton distance can be calculated to be  $(1.68 \pm 0.001)$  Å units and by substituting this value, the corresponding relaxation constant is calculated to be  $2.25 \times 10^{-10}$  s. This value is used in eqn.(C-5.1) and the model is fitted to the data by the least squares method, and the most probable values of  $E_a$  and  $\tau_0$  are computed to be,  $17.5 \pm 0.5$  kJ/mole and  $(7.5 \pm 0.5) \times 10^{-15}$  s.

The  $M_2$  value of  $2.5 \text{ Gauss}^2$  indicates fast isotropic reorientation of the ammonium ion [Gutowsky et al., 1954]. From the value of the interproton distance given above, the rigid lattice limit value of  $M_2$  from the intra-ammonium interaction can be computed from Van Vleck's formula to be around  $55 \text{ Gauss}^2$  [Venu et al.; 1986, Gutowsky et al., 1954]. The value of  $45 \text{ Gauss}^2$  observed at 77K shows that, this motion is reaching rigid lattice limit by this temperature though not completely in that limit. In fact, the correlation time computed from the above given motional parameters indicated the same scenario.

(NH<sub>4</sub>) Bi Cl<sub>9</sub> (AMCB) and (NH<sub>4</sub>) Bi Br<sub>9</sub> (AMBB) along with their Antimony counterparts make interesting comparison. In the case of the Chlorine analogue of AMCB ((NH<sub>4</sub>) Sb<sub>2</sub>Cl<sub>9</sub> (AMCA)) and the Bromine analogue of AMBB ((NH<sub>4</sub>) Sb<sub>2</sub>Br<sub>9</sub> (AMBA)), the T<sub>1</sub> data show a similar behaviour as observed in AMCB. There are no minima observed in these compounds and T<sub>1</sub> values are higher in these compounds also, i.e., of the order of few seconds. It is interesting to note that while the T<sub>1</sub> values in AMCA are smaller at 8 MHz compared to those at other Larmor frequencies indicating the possibility of cross-relaxation as in the case of AMCB, in AMBA the T<sub>1</sub> values are smaller at 40 MHz compared to the corresponding values at other frequencies which are even lower than 40 MHz [Jagadeesh, 1994]. This also points to the possibility that there is perhaps a cross-relaxation of the proton levels, with the NQR levels of the Bromine nuclei. There is a maximum like structure with temperature in these two compounds too, but in the case of AMCA the frequency dispersion continues even to temperatures much below this value in contrast to AMCB, where the T<sub>1</sub> data at 8 and 5 MHz merge around 230K in a more or less discontinuous way. If a structural phase transition were to be present around this temperature, it may cause a change in the dynamic environment of the ammonium ion, thereby causing a jump in its correlation time, bringing it into the region where the conventional relaxation mechanism may also become effective, resulting in a region of T<sub>1</sub> without any frequency dispersion provided  $\omega\tau \ll 1$  in this region. So far, we could observe a trend among the other AMX compounds, namely substitution of the bulkier Bismuth ion seems to have increased the amount of disorder in the system and has brought down the

phase transition temperatures. There has been indications that, Bi replacing Sb, as far as other compounds are concerned, has observably increased the freedom of reorientation of the cation also as can be seen from the formation of even isotropic minima in the case of TMA and DMA cations, within a lower temperature region. But the situation seems to be somewhat different in the case of ammonium compounds, where as we move from **AMCA** toward **AMBB** the dynamics of the cations have become perceptibly slow. In the case of **AMCA** we do not see any minimum and the **T** data have not gone into the dispersionless region within the observed temperature range. In the case of **AMBA**, the hindrance seems to have increased a bit where we see a normal variation of **T** as in the case of the limit  $\omega\tau \ll 1$  within the observed range of temperature, and in the case of **AMCB** though there is no formation of minima yet, the data start showing a dispersionless region at a higher temperature compared to the other two Sb compounds. Finally, the dynamics seems to have slowed down considerably in the case of **AMBB** as we are able to see a normal minimum in **T** within the observed range of temperature and the **M** data also lends support to this possibility. This is an interesting and contrasting behaviour in comparison with the other compounds of the  $A_3M_2X_9$  family.

# REFERENCES

- (C-5.1) CHIHARA H. AND N. NAKAMURA, *Z.Naturforsch.*, **45a**, (1990) **541**
- (C-5.2) COOKE A.H. AND L.E. DRAIN, *Proc.Phys.Soc. (LONDON)*, **A65**, (1952) 894
- (C-5.3) FUKUDA S. , H. YAMAMOTO, R. IKEDA AND D. NAKAMURA, *J.Chem.Soc. Faraday Trans.-I*, **83**, (1987) 3207
- (C-5.4) FURUKAWA Y. , A. SASAKI AND D. NAKAMURA, *Solid State Ionics*, **42**, (1990) 223
- (C-5.5) GUTOWSKY H.S., G.E. PAKE AND R. BERSOHN, *J. Chem.Phys.*, **22**, (1954) 643
- (C-5.6) HATTORI M. , S. FUKUDA, D. NAKAMURA AND R. IKEDA, *J.Chem.Soc. Faraday Trans.*, **86**, (1990) 3777
- (C-5.7) IKEDA R. AND C.A. McDOWELL, *Mol.Phys.*, **25**, (1973) 1217
- (C-5.8) ISHIDA H., R. IKEDA AND D. NAKAMURA, *J.Chem.Soc. Faraday Trans.*, **81**, (1985) 963
- (C-5.9) ISHIDA H., N. MATSUHASHI, R. IKEDA AND D. NAKAMURA, *J.Chem.Soc. Faraday Trans.-I*, **85**, (1989) 111
- (C-5.10) ISHIDA H. , K. TAKAGI, T. IWACHIDO, M. TERASHIMA, D. NAKAMURA AND R. IKEDA, *Z.Naturforsch.*, **54a**, (1990) 923
- (C-5.11) ISHIHARA H. , K. WATANABE. A. IWATA, K. YAMADA. Y. KINOSHITO, T. OKUDA, V.G. KRISHNAN, SHI-QI DOU AND A. WEISS, *Z.Naturforsch.*, **47a**, (1992) 65
- (C-5.12) Iwai S., M. HATTORI AND D. NAKAMURA, *J.Chem.Soc.Faraday Trans.*, **89**, (1993) 827

- (C-5.13) JAGADEESH B., Ph.D THESIS, *University of Hyderabad*, **1994**.
- (C-5.14) KOBAYASHI A., Y. YOSHIOKA, N. NAKAMURA AND H. CHIHARA,  
*Z.Naturforsch.*, **43a**, (1988) 233
- (C-5.15) KOKSAL F. AND S. BACHELI, *J.Chem.Soc. Faraday Trans.-II*, **74**,  
(1978) 1844
- (C-5.16) KOKSAL F., *J.Phys.Chem.Solids*, **45**, (1984) 1201
- (C-5.17) O'REILLY D.E. AND T. TSANG, *J.Chem.Phys.*, **46**, (1967) 1291
- (C-5.18) RIGGIN M.T., R.R. KNISPEN AND M.M. PINTAR, *J.Chem.Phys.* , **56**,  
(1972) 2911
- (C-5.19) SASAKI A., Y. FURUKAWA AND DAIYU NAKAMURA, *Ber.Bunsenges.*  
*Phys.Chem.*, **93**, (1989) 1142
- (C-5.20) SATO S. , R. IKEDA AND D. NAKAMURA, *Bull.Chem.Soc. Japan*, **59**,  
(1986) 1981
- (C-5.21) TANABE T. , D. NAKAMURA AND R. IKEDA, *J.Chem.Soc. Faraday*  
*Trans.*, **87**, (1991) 987
- (C-5.22) VENU K. , V.S.S. SASTRY AND J. RAMAKRISHNA, *Chem.Phys.Lett.*,  
**122**, (1985) 280
- (C-5.23) VENU K., V.S.S. SASTRY, J. RAMAKRISHNA, *Chem.Phys.*, **107**, (1986)  
**123**
- (C-5.24) VENU K., V.S.S. SASTRY AND J. RAMAKRISHNA, *Phys.Stat.Sol.(b)*,  
**140**, (1987) 251
- (C-5.25) WOESSNER D.E. AND B.S. SNOWDEN Jr., *J. Phys.Chem.*, **71**, (1967)  
**952**

# SECTION C

PART 6

RESONANCE AND RELAXATION STUDIES ON  
 $^{13}\text{C}$ ,  $^1\text{H}$ ,  $^{15}\text{N}$ ,  $^{31}\text{P}$ ,  $^{109}\text{Ag}$ ,  $^{209}\text{Bi}$ ,  $^{207}\text{Pb}$ ,  $^{208}\text{Pb}$ ,  $^{209}\text{Po}$

So far, we have seen the results of proton spin lattice relaxation time (T<sub>1</sub>) as well as the second moment (M<sub>2</sub>) investigations on a family of A M<sub>n</sub>X compounds. In the vicinity of the structural phase transitions observed in these compounds, the dynamics of the cations are considerably affected. It is also seen that, the type of cation seems to have a strong influence on the structure of anion and as a consequence the overall structure of the compound. Whereas in the case of tetrahedrally symmetric cations like tetramethylammonium, the anions tend to exist in isolated and discrete molecular structures like the confacial biocubical structures, in the case of the less symmetric cations like trimethylammonium and dimethylammonium, the compound tend to form layered structures, the layers arising due to the the vertex sharing octahedra formed by the MX<sub>6</sub> anions, which form corrugated rings of hexagonal symmetry. From its structure, methylammonium cation does not seem to be as asymmetric as trimethyl and dimethylammonium ions are and it can form one dimensional linear chain by the sharing of vertices. These observations indicate that the cationic structure plays an important role in determining the overall structure of the compound pointing out to the possibility that such an influence may lead to some very new type of anionic structures. Compounds with complex anionic structures are not uncommon and had been synthesized especially with Sb and Bi. Compounds of hydrazine with complex anionic structures as Sb<sub>2</sub>Br<sub>9</sub><sup>3-</sup>, SbBr<sub>6</sub><sup>3-</sup> and

$\text{Bi}_3\text{Br}_{16} \cdot 10\text{H}_2\text{O}$ ,  $\text{Bi}_3\text{I}_{14} \cdot 6\text{H}_2\text{O}$  and  $\text{Bi}_4 \cdot \text{I}_{17} \cdot 10\text{H}_2\text{O}$  have been observed quite early [Pugh, 1954] and more recently, some other unusual anionic structures like,  $\text{Sb}_2\text{I}_{28}^{-4}$ ,  $\text{Sb}_6\text{I}_{22}^{-}$  and  $\text{Bi}_4\text{Cl}_{18}$  were also recorded [Pohl et al., 1988a, 1988b; Aurivillius et al., 1978; Jakubas et al., 1990].

This tendency of the Bismuth salts to group into large clusters leads to complex anionic structures, and, of course, the type of cation also is equally important in determining the particular kind of stoichiometry we get for the anion [Landers et al., 1980]. It has been observed that despite the the variety of anionic structures observed so far and their complexity, most of these compounds differ little in their skeletal structure and the difference is mainly in terms of the number of halogen bridges and the number of terminal halogens present, as well as the different bond lengths. Unlike in the case of A M<sub>n</sub>X group of compounds where there is only vertex sharing or face sharing of MX<sub>6</sub> octahedra, in these complex structures edge sharing is also present [Aurivillius et al., 1978]. Structural analysis in these kind of compounds reveal that the presence of 6s lone pair of electron plays a role in determining the kind of bonding among the Bismuth and the halogen atoms, and in these compounds, generally, Bismuth seems to have a tendency to attain six coordination. Though the reason behind the nature of Sb and Bi to form such complex anionic structures with halogen atoms is not apparent, it is noted that metal complexes with larger structures are normally stabilized by large counter ions, preferably ions of the same but opposite charge [Martinsen et al., 1977; Basolo, 1968].

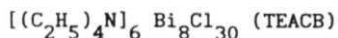
$[(\text{C}_2\text{H}_5)_4\text{N}]_4 \text{Bi}_8\text{Cl}_{30}$  (TEACB) is one such unique compound with a hitherto unobserved anionic group, namely  $\text{Bi}_8\text{Cl}_{30}$  with the huge structure



stabilized by six of the tetraethylammonium counter ions. Interestingly, the ethylammonium groups are found to form much simpler salts also, like  $(C_2H_5)_4MX$  ( $X = Cl, Br$  and  $I$ )  $[(C_2H_5)_4N]_2 NiCl_4$ ,  $[(C_2H_5)_4N]_2 CoCl_4$ , [Koksal, 1979; Stucky et al., 1967], and especially many compounds formed with Bi are observed, namely,  $(C_2H_5NH_3) BiCl_4$ ,  $[(C_2H_5)_2NH_2] BiCl_4$ ,  $(C_2H_5NH_3)_3 BiCl_6$  and  $[(C_2H_5)_2NH_2]_3 BiCl_6$ ,  $[(C_2H_5)_2NH_2]_3 BiBr_6$ , [Landers et al., 1980; Lazarini, 1985, 1987; Blazic et al., 1985]. A few of the compounds belonging to the  $M_nX$  group are also synthesized, namely,  $[(C_2H_5)_2NH_2]_3 Bi_2Br_9$ ,  $[(C_2H_5)_2NH_2]_3 Bi_2I_9$ ,  $[(C_2H_5)_4N]_3 Bi_2Br_9$ ,  $[(C_2H_5)_4N]_3 Sb_2Br_9$  [Lazarini, 1985; Zaleski et al., 1989]. As can be seen from these examples, it is not necessary that in all the compounds where n-ethylammonium cations are present they stabilize only large or complex anionic structures. In fact, the variety of compounds which are formed by varying the size of the cation with the ethylammonium group in different sizes like the mono, di or tetraethylammonium, shows how the formation of different anionic structures sensitively depend on the type of cation, a point which we have mentioned already [Lazarini, 1985]. Apart from the size and shape of the cation, it is observed that the concentration of the parent species in solution as well as the normality or concentration of the solvent medium, which is used to grow these crystals, also play important roles in determining the kind of structures we will ultimately end up with [Pugh, 1954; Landers et al., 1980; Lazarini, 1985]. Perhaps, this explains in part, the formation of seemingly very different compounds like TEACB and  $K(C_2H_5)_4N]_2 Bi Br$ , from more or less same parent compounds. But the structural and other investigations of these kind of complexes have revealed the underlying commonalty of the skeletal structure of these compounds, though these compounds appear to be very different as observed from their chemical formulae. These complexes are

constructed with octahedral complexes, by sharing the vertex, edge or the face, and the difference from one compound to the other seems to originate mainly from the total number of octahedra which coordinate to form the final anion structure. Thus, this may also be pointed as a possible reason for the formation of different kinds of compounds from the same parent compounds, depending only on the variation of the ratio of the abundance of parent compounds and the normality of the solvent medium. Thus, it was thought worthwhile to study as a contrasting case the possible dynamics in the new compound  $[(C_2H_5)_4N]_6 Bi_8Cl_{30}$  (TEACB) using proton magnetic relaxation studies.

### Specific details



#### $T_1$ data :

Larmor frequencies of : 39.8, 20 and 10 MHz  
 observation  
 Temperature range : 430K to 77

#### $M_2$ data :

Temperature range : 380K - 77K

Variation of  $T$  with  $1/T$  in TEACB : Fig.(C-6.1)

$M_2$  variation as a function of temperature in TEACB : Fig.(C-6.2)

Optimized motional parameters : Table (C-6.1)

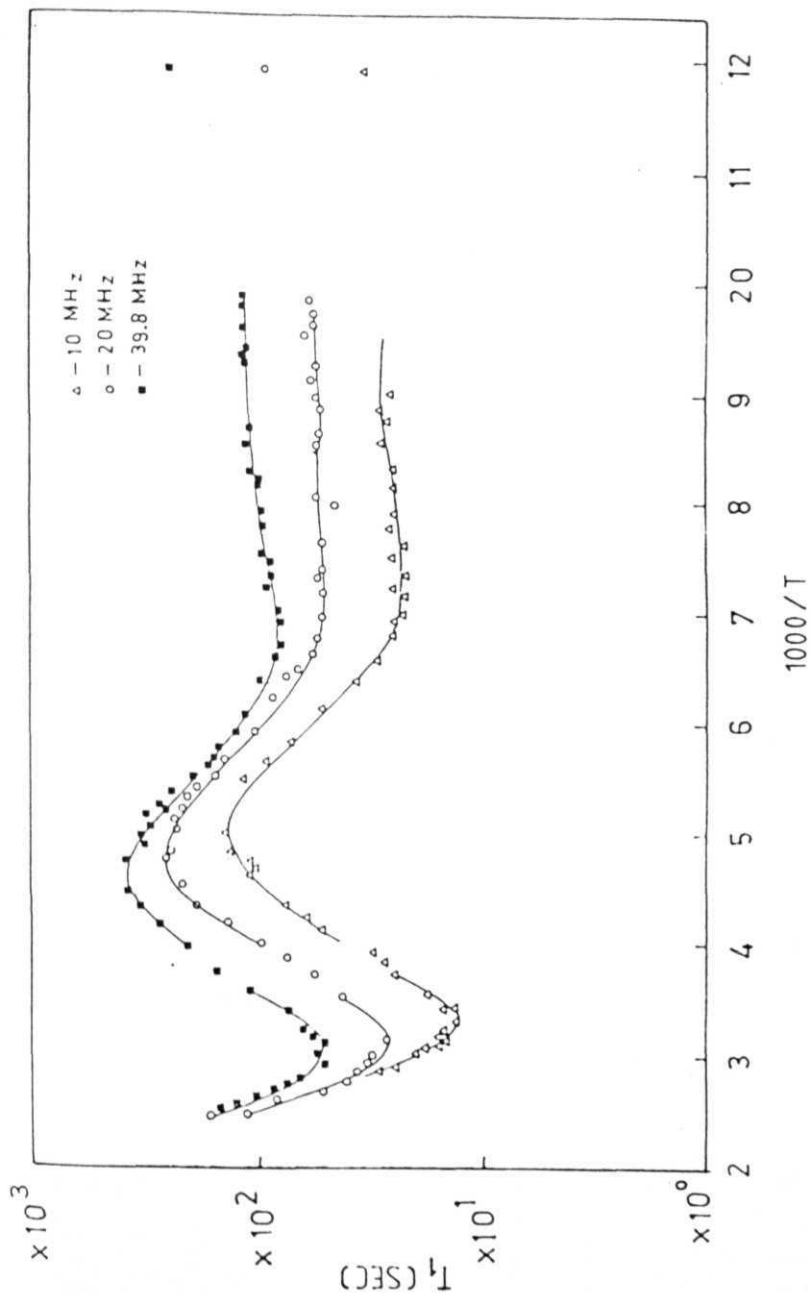
## RESULTS

TEACB was grown by the slow evaporation technique from a stoichiometric mixture of the parent compounds tetraethylammonium chloride (TEA)Cl and BiCl in the suitable acid medium, HCl. The dried polycrystalline sample was sealed under 10 torr vacuum in 6 mm and 8 mm glass ampoules for T and  $M_2$  measurements respectively. The error in T and  $M_2$  data are 5% and 10% respectively. The variation of T as a function of temperature at 10, 20 and 39.8 MHz is provided in Fig.(C-6.1) and the M variation as a function of temperature is shown in Fig.(C-6.2).

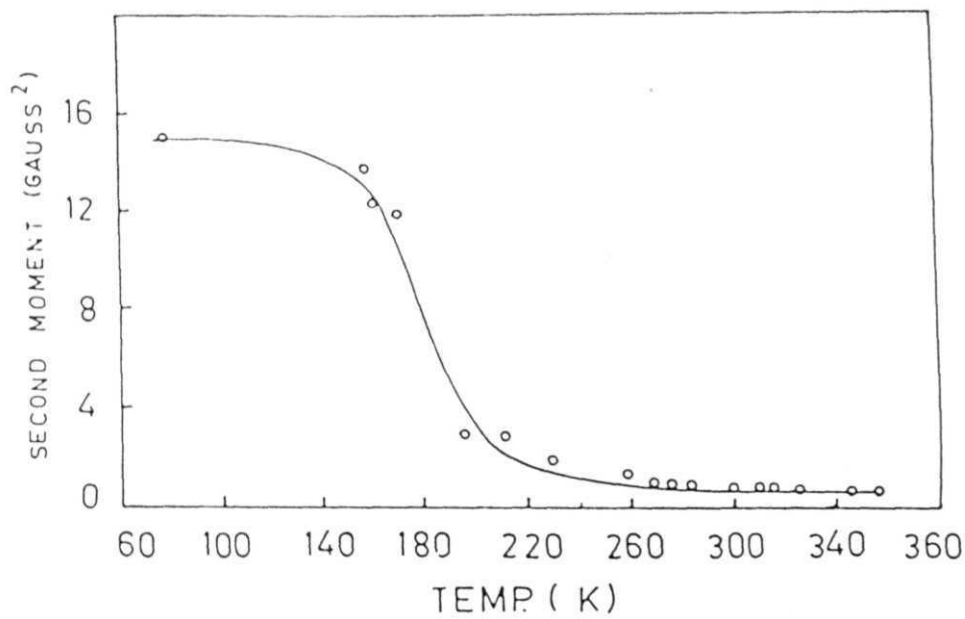
T. data show clear formation of minima at all the three frequencies. The data below 250 K start decreasing with decreasing temperature, and below 140K the data show a wide plateau like region with minimal variation of T with temperature.  $M_2$  value is constant around 0.6±0.1 Gauss from 350 K till 250K and it tends to increase around 240K and reaching a value of 2.5 Gauss approximately. It further increases smoothly to a value of 15 Gauss around 180 K, and remains at that value till 77 K.

## DISCUSSION

X-ray studies on TEACB have shown these crystals to be monoclinic, belonging to the space group C2/m with Z=2 [Zaleski et al., 1989] at room temperature. There are three independent TEA cations in the structure which lie in the symmetry plane. The anions consist of eight edge-sharing BiCl<sub>6</sub> octahedra. The overall structure of the Bi<sub>8</sub>Cl<sub>30</sub> anion is shown in

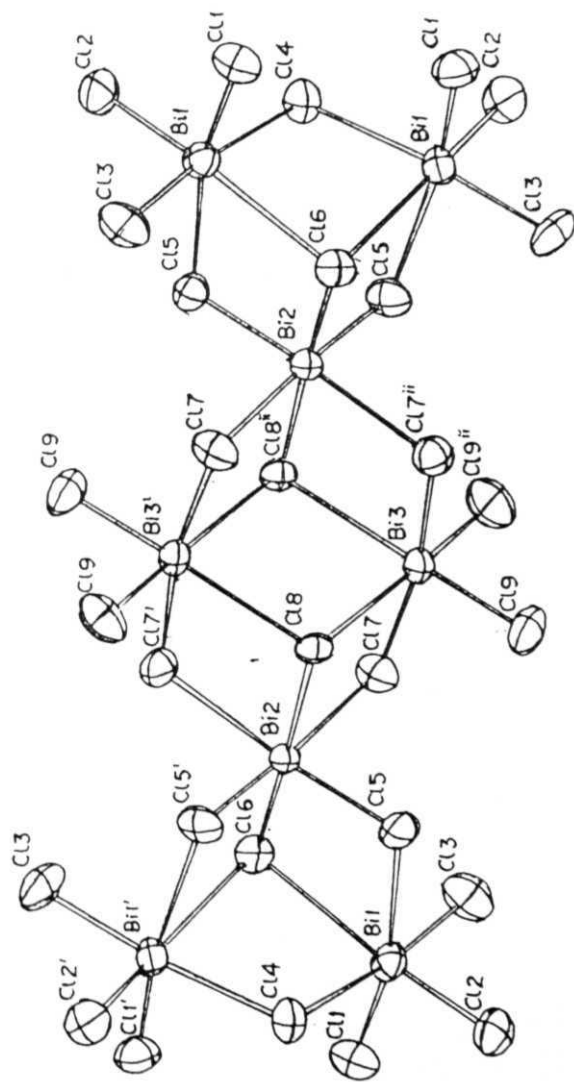


(C - 6.1)  $T_1$  variation as a function of  $1/T$  in  $[(C_2H_5)_4N]_6 Bi_8Cl_{30}$ .

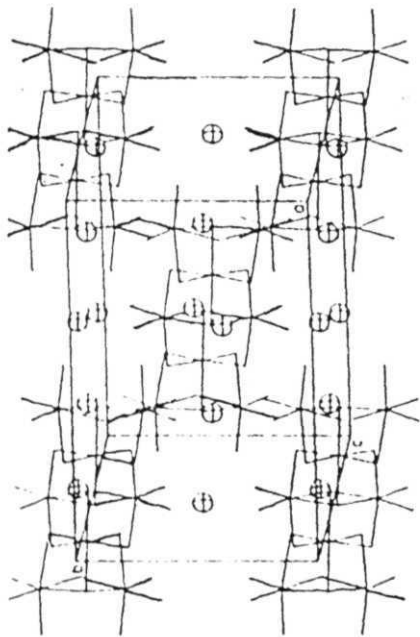


(C - 6.2)  $M_2$  variation as a function of temperature in  $[(C_2H_5)_4N]_6Bi_8Cl_{30}$ .

Fig.(C-6.3). There are three kinds of Bismuth atoms in the anion, given by : Bi(1) which has three bridging and three terminal halogen atoms; Bi(2) which consists of six bridging halogen atoms; and Bi(3) which has four bridging and two terminal halogen atoms. This situation is to be contrasted with the case of  $A M_n X$  compounds, where only vertex or face sharing is present, or even simpler structures like  $MX_n$  or  $MX_n$ , and in these cases only one kind of metal atom is present in the overall anion structure, each one being surrounded by a given number of terminal and bridging atoms. For instance, in the case of the one dimensional pleated ribbon chain of tris(methylammonium) nonachloro diantimonate (MACA), each metal atom is surrounded by three terminal chlorines and three bridging chlorines [Jakubas et al., 1986, 1990], and in the case of 2-Picolinium tetrahalobismuthate salts, each bismuth atom is surrounded by two terminal halogen atoms and four bridging halogen atoms [Robertson et al., 1967]. Same can be said about  $MX_5$  groups also. In a given unit cell of TEACB, one  $BiCl_6$  anion is situated at the center and four more anions are partially pointing into the unit cell, to give a total occupancy of  $Z=2$ . Fig.(C-6.4) shows a view of the unit cell with the ellipsoids representing the cations placed in the cavities formed by the anions. There is sufficient freedom available in the voids for the cations to exhibit reorientation. Nevertheless, the TEA cations are placed in the cavities close to each other that one can expect their motion to be correlated also [Zaleski et al., 1989]. Electric permittivity measurements on TEACB has revealed two close lying anomalies at 240.7K and 241.2K on the cooling run, and on the heating run only one anomaly at 243.8K is observed, which is indicative of hysteresis present in the compound. DSC studies on the compound revealed one reversible anomaly at 242K on cooling, confirming a first order phase transition in this



(C - 6.3) Structure of  $\text{Bi}_8\text{Cl}_{30}^{6-}$  anion.



(C - 6.4) View of the unit cell in  $[(C_2H_5)_4N]_6 Bi_8Cl_{30}$ .



compound [Zaleski et al., 1989].

The proton  $T$  and  $M$  data of TEA cations in solids are normally analyzed in terms of two types of dynamic processes of the TEA group, namely, the three fold reorientations of the methyl groups and isotropic tumbling of the TEA cation as a whole [Koksal, 1979; Reynhardt et al., 1981]. It has been found that if both the methyl group dynamics and TEA dynamics are in the rigid lattice limit, the second moment is expected to be around 33 Gauss. If the TEA group dynamics alone has frozen but the methyl group dynamics is active for NMR purposes, then we should expect a value of about 15 Gauss<sup>2</sup> as the second moment value [Reynhardt et al., 1981]. Along with the C reorientation of the methyl group, if TEA cations are exhibiting isotropic tumbling then we expect to get a low second moment of 0.6 Gauss. If we compare these values with the  $M$  variation of TEACB as a function of temperature (Fig.C-6.2), it is observed that TEA cations are undergoing isotropic tumbling from 350K to 260K. But around the phase transition temperature (241K),  $M$  first discontinuously jumps to 2.5 Gauss<sup>2</sup> and from there on smoothly increases to 15±1 Gauss<sup>2</sup> by 77K indicating that the TEA group dynamics is affected around the phase transition temperature.

From the analysis of  $M$  data given above, it appears that the bulky TEA cation undergoes isotropic tumbling above 240K and the minimum in  $T$ , above 240K therefore, is to be attributed to the isotropic tumbling of the cation. In fact, in compounds having the TEA groups the isotropic tumbling of the cation forms a  $T$  minimum following which minimum due to the methyl group reorientations is observed [Koksal, 1979]. It is to be noted that TEA cation also has the tetrahedral symmetry as the

tetramethyl cations, and therefore to analyze the current T data quantitatively the spin-lattice relaxation rate derived for the case of the TEMA [Albert et al., 1972] can be suitably modified for the tetrahedrally symmetric TEA cation [Rajan et al., 1993] as

$$(C-6.1) \quad T_1^{-1} = A g(\omega, \tau_{c2}) + B g(\omega, \tau_{c1})$$

where,

$$\tau_{c2}^{-1} = \tau_c^{-1} + \tau_{c1}^{-1}$$

Here, T is the correlation time for the reorientations of the methyl groups, and  $\tau$  is the correlation time for the isotropic tumbling of the TEA cation.  $g(\omega, \tau)$  is given by the equation

$$(C-6.2) \quad g(\omega, \tau_c) = \frac{\tau_c}{1 + \omega^2 \tau_c^2} + \frac{4\tau_c}{1 + 4\omega^2 \tau_c^2}$$

The relaxation constants A and B are given by

$$(C-6.3a) \quad A = \frac{9\gamma^4 \hbar^2}{20 r^6}$$

$$(C-6.3b) \quad B = \frac{A}{3} + 5 \left( \frac{9}{10} \right) \frac{\gamma^4 \hbar^2}{r_*^6}$$

Here, r is of course the inter proton distance within a methyl group, and  $r_*$  is the distance between the centers of the ethyl groups. The factor 5 is included to take into account the presence of 5 protons within an ethyl group. The values of r and  $r_*$  were determined using the dimensions of TEA group provided by Reynhardt et.al., [1981], i.e. N-C-C angle =

125° and N-C distance = 2.4 Å. These values are :  $r = 1.78$  Å and  $r_{\perp} = 4.42$  Å. The relaxation constants are then computed to be  $8.05 \times 10^{-9}$  s and  $3.13 \times 10^{-9}$  s for A and B, respectively. Though this is a somewhat simplified model for the complex TEA ion, this is found to account for the data adequately (as is discussed later). A more detailed model is not available for further analysis.

Normally, the bulky TEA cation exhibits motions which are much slower compared to those of the methyl group at any given temperature. Thus the value of  $T$  minima expected for the isotropic motion of TEA cation can be computed by assuming that : (i) the methyl group dynamics is much faster than the TEA dynamics in the temperature range where TEA group dynamics is expected to lead to a  $T$  minimum (and thus  $T$  is negligible compared to  $T$  ); and (ii) substituting the condition  $\omega\tau = 0.616$  in eqn.(C-6.1). This leads to an expression for the TEA  $T$  minimum, as

$$(C-6.4) \quad (T_{\min}^{-1})_{\text{TEA}} = B \frac{1.4252}{\omega}$$

Similarly, the expected minimum value due to the C reorientation of the methyl groups can be computed by assuming that the correlation time corresponding to TEA dynamics is far different from that of methyl group around the temperature where methyl group dynamics leads to a  $T$  minimum. Thus,  $T_{\min}$  due to the methyl group dynamics is given by

$$(C-6.5) \quad (T_{\min}^{-1})_{\text{CH}_3} = A \frac{1.4252}{\omega}$$

Substituting the values of the relaxation constants in eqns.(C-6.4) and (C-6.5), we can compute the expected T<sub>1</sub> minima values due to methyl group reorientation and isotropic motion of TEA cation to be 5.5. ms and 13 ms, respectively, at 10 MHz. Comparing these values with the minima observed experimentally, it is observed that the first minimum agrees quite well with the expected minima values for isotropic reorientation of the TEA cation at all the frequencies. But if we observe the plateau region, the lowest value of T<sub>1</sub> in this range is much higher than that of what is expected for a T<sub>1</sub> minimum due to the methyl group dynamics. Such shallow regions of T<sub>1</sub> whose values are much higher than those expected for well resolved minima due to methyl groups are encountered in the case of other compounds also. Such plateau regions are due to adjacently lying minima due to dynamically inequivalent methyl groups [Ishida et al., 1984, 1989; Venu et al., 1987; Furukawa et al., 1989; Ishida et al., 1984]. It has been shown from crystal structure studies in TEACB at room temperature that the cation is disordered, and the structural inequivalence present may be causing the methyl groups to be dynamically inequivalent in this compound. Looking at the T<sub>1</sub> data, it is clear that there is a wide distribution of correlation times of the methyl groups and there may be more than two methyl groups forming the T<sub>1</sub> minima in this temperature range to give such a flat region in T<sub>1</sub> [Ishida et al., 1989; Venu et al., 1987]. Incorporating the dynamic inequivalence among the methyl group, the formula for T<sub>1</sub> can be written as

$$(C-6.6) \quad T_1^{-1} = x \cdot A g(\omega, \tau_{c2}^A) + y \cdot A g(\omega, \tau_{c2}^B) + \dots \\ + n \cdot A g(\omega, \tau_{c2}^Z) + B g(\omega, \tau_{c1})$$

Here, the T-S with the superscript A, B, C and so on refer to the correlation times for the C reorientation of the different dynamically inequivalent methyl groups present in the compound and x, y, ... are the corresponding inequivalence factors. Attempt was made to fit eqn.(C-6.6) to the observed data, and it is found that the presence of at least four inequivalent methyl groups is called for to simulate the experimental data, within the observed range of temperature. From the trend of the temperature dependence of T, it is possible that there are more inequivalent methyl groups forming minima down at lower temperatures. The inequivalence factors of the four methyl groups are : 0.2, 0.05, 0.1 and 0.1. With these values, eqn.(C-6.6) was fitted to the data and the model was fitting to the data in the entire region well except that, around 240K, there was a systematic deviation of the fitted curve from the observed T values at all the three frequencies. This seems to be due to the presence of the structural phase transition around 241K. There is perhaps a discontinuous change in the correlation time of the isotropic motion of the TEA cation at this temperature causing the observed deviation of T from the expected trend. Thus, the data in the high temperature region, i.e. 400K to 250K was fitted to a simple model given by

$$(C-6.7) \quad T_1^{-1} = B g(\omega, \tau_{c1})$$

which takes into account only the isotropic tumbling of the TEA cation. The data below 240K were fitted to the model which includes the presence of four inequivalent methyl groups in this region. It was difficult to fix the motional parameters corresponding to the isotropic motion of the TEA cation with considerable reliability from the low temperature region,

as the contribution to the spin lattice relaxation **rate in this** region is expected to be predominantly from the methyl groups **only**. Thus the TEA parameters determined in the low temperature are expected to **have** relatively large error. The most probable values of the dynamic parameters for the TEA group motion above and below the phase transition as well as the motional parameters for the four  $\text{CH}_3$  groups are presented in Table (C-6.1). The activation energies of the methyl groups are in around  $6.0 \pm 0.5$  kJ/mole indicating the relative freedom they have in this compound, which can be contrasted with the large values found for CH group motion in compounds like TEMACB. The trend of T data further shows that, the minima corresponding to the remaining methyl groups may form below 77K.

Proton relaxation data provides the following information about the dynamics of TEA in TEACB. The signature of the phase transition at 241K is observed on both T and M data. Analysis of T data shows that, TEA cations undergo isotropic tumbling in the high temperature phase. There is stepwise freezing of M and by 77K, the dynamics of the TEA group have reached rigid lattice limit but the methyl groups have not. In the **low** temperature phase, there is a wide distribution of T s of the methyl groups and minima corresponding to some of the methyl groups are occurring possibly below 77K. The dynamic features observed are consistent with the expected disorder from structural considerations.

TABLE (C-6.1)

Symmetric group	$\tau$ (s)	$\Delta G^\ddagger$ (kJ/mole)
TEA group		
(a) high temp.phase	$(1.3 \pm 0.5)E-13$	$14.0 \pm 2.0$
(b) low temp. phase	$(1.0 \pm 1.0)E-11$	$8.0 \pm 2.0$
$(CH_3)_A$	$(4.0 \pm 1.0)E-13$	$6.0 \pm 1.0$
$(CH_3)_B$	$(7.0 \pm 1.0)E-14$	$7.0 \pm 2.0$
$(CH_3)_C$	$(3.0 \pm 1.0)E-12$	$4.0 \pm 2.0$
$(CH_3)_D$	$(5.0 \pm 1.0)e-13$	$5.0 \pm 2.0$

OPTIMIZED DYNAMIC PARAMETERS FOR THE COMPOUND

# REFERENCES

- (C-6.1) ALBERT S., H.S. GUTOWSKY AND J.A. RIPMEESTER, *J.Chem.Phys.* , 56, (1972) 3672
- (C-6.2) AURIVILLIUS B. AND C. STALHANDSKE, *Ada Chem.Scand.* , **A32**, (1978) 715
- (C-6.3) BASOLO F., *Coord. Chem.Rev.* , **3**, (1968) 213
- (C-6.4) BLAZIC B. and F. LAZARINI, *Act a Cryst.*, **C41**, (1985) 1619
- (C-6.5) FURUKAWA Y., C. KOJIMA AND D. NAKAMURA, *Ber. Bunsenges. Phys.Chem.* , 93, (1989) 696
- (C-6.6) ISHIDA H., R. IKEDA AND D. NAKAMURA, *Ber.Bunsenges. Phys.Chem.* , 88, (1984) 546
- (C-6.7) ISHIDA H., N. MATSUHASHI, R. IKEDA AND D. NAKAMURA, *J.Chem.Soc. Faraday Trans.* , 85, (1989) 111
- (C-6.8) JAKUBAS R., 2. CZAPLA, Z. GALEWSKI, L. SOBCZYK, O.J. ZOGAL AND T. LIS, *Phys.Stat.Solidi (a)*, 93, (1986) 449
- (C-6.9) JAKUBAS R. AND L. SOBCZYK, *Phase Transitions.* 20, (1990) 163
- (C-6.10) KOKSAL F. , *Z.Naturforsch.* , **34a**, (1979) 1296
- (C-6.11) LANDERS A.G. AND T.B. BRILL. *Inorg.Chem.*, **19**, (1980) 744
- (C-6.12) LAZARINI F. , *ActaCryst.*, **C41**, (1985) 1617
- (C-6.13) LAZARINI F. , *ActaCryst.*, **C43**, (1987) 637
- (C-6.14) MARTINSEN A. AND J. SONGSTAD, *Ada Chem.Scand.* , **A31**, (1977) 645
- (C-6.15) POHL S. , D. HAASE, R. LOTZ AND W. SAAK, *Z.Naturforsch.* , **43b**, (1988a) 1033
- (C-6.16) POHL S. , R. LOTZ, D. HAASE AND W. SAAK, *Z.Naturforsch.*, **43b**, (1988b) 1144
- (C-6.17) PUGH W., *J.Chem.Soc.*, (1954) 1385



- (C-6.18) REYNHARDT E.C. AND J.P.S. RASH, *J.Magn.Reson.*, 42, (1981) 88
- (C-6.19) ROBERTSON B.K., W.G. McPHERSON AND E.A. MEYERS, *J. Phys.Chem.*, 71, (1967) 3531
- (C-6.20) RAJAN P.K., B. JAGADEESH, K. VENU AND V.S.S. SASTRY, *Phase Transitions*, 44, (1993) 227
- (C-6.21) STUCKY G.D., J.B. FOLKERS AND T.J. KISTENMACHER, *ActaCryst.*, 23, (1967) 1064
- (C-6.22) VENU K., V.S.S. SASTRY AND J. RAMAKRISHNA, *Phys.Stat.Sol. (b)*, 140, (1987) 251
- (C-6.23) ZALESKI J., R. JAKUBAS, Z. GALEWSKI AND L. SOBCZYK, *Z.Naturforsch.*, 44a, (1989) 1106

# SECTION C

## PART 7

### CONCLUSIONS

In the previous sections the results of proton T and M measurements on tris(alkylammonium) nonahalogeno dibismuthates, made as a function of temperature and Larmor frequency, were presented and the data were analyzed with the relevant molecular model for each compound. In this section we attempt to correlate the outcome of such analyses, by comparing the details of cation dynamics in compounds within this family as well as in their Antimony substituted counterparts.

The detailed study of Bismuth compounds shows that isotropic reorientations of the cations take place readily in the case of  $[(CH_3)_4N]_3Bi_2Cl_9$  and  $t(CH_3)_4N]_3BiBr_9$  where the tetramethylammonium group has tetrahedral symmetry and there is no preferred axis of rotation for these groups. But in  $[(CH_3)_3NH]_3Bi_2Cl_9$  and  $[(CH_3)_3NH]_3Bi_2Cl_9$  which have less symmetric cations, there are preferred axes of reorientation and the isotropic reorientations thus take place only at higher temperatures. In fact, the signature of isotropic reorientations for such asymmetric groups are expected to be seen at temperatures higher than the typical range of present work ( $\approx 400K$  to  $77K$ ) In the present systems, however, the effect of such isotropic reorientations are observed well within this temperature range. In  $[(CH_3)_3NH]_3Bi_2Cl_9$  the signature of the isotropic reorientation on T data is observed (T minima) but the analysis of data shows that the potential barrier to be overcome for such a motion is of the order of 30 kJ/mole, which is much higher than the corresponding values for the tetramethylammonium compounds  $[(CH_3)_4N]_3Bi_2Cl_9$  and

$[(CH_3)_4N]_3Bi_2Br_9$  ( 10 and 8 kJ/mole respectively). On the other hand, in  $(NH_4)_3Bi_2Cl_9$  and  $(NH_4)_3Bi_2Br_9$  which contain tetrahedrally symmetric  $NH_4^+$  cations similar to the tetramethylammonium cations, isotropic motion is observed with an activation energy for this dynamics being only about 7 kJ/mole as shown by their T and M data, though there is no possibility of any internal dynamics for these cations. Even in  $(CH_3NH_2)_2BiCl_2$  in which the methylammonium cation has two symmetric axes of rotation in principle (one along the C-N axis and another perpendicular to the C-N axis), the cations undergo isotropic reorientations. But the hindrance to the isotropic reorientation seems to increase as the cation becomes less and less symmetric in these compounds. For instance, the activation energy for isotropic reorientations in these compounds are given by :  $[(CH_3)_4N]_3Bi_2Cl_9$  - 13.5 kJ/mole,  $[(CH_3)_4N]_3Bi_2Br_9$  - 14.5 - kJ/mole,  $[(CH_3)_2NH_2]_3Bi_2Cl_9$  " 34 kJ/mole,  $(NH_4)_3Bi_2Cl_9$  and  $(NH_4)_3Bi_2Br_9$  - s 7 kJ/mole and these values are calculated in the phase above the high temperature transition observed in these compounds. The nature of T data in the high temperature phase of  $[(CH_3)_4N]_3Bi_2Cl_9$  and  $(CH_3NH_2)_2Bi_2Cl_2$  does not allow one to calculate the corresponding E in these compounds, nevertheless the values quoted above show the trend of progressive increase in the hindrance to the isotropic reorientation of the cations as we move towards asymmetric groups. Further, as we approach the ammonium substituted compounds the cations feel lesser hindrance as they preserve the tetrahedral symmetry as the TEMA cations. At lower temperatures the asymmetric groups undergo lower order dynamics also like threefold reorientations as observed in the case of  $(CH_3NH_2)_2Bi_2Cl_2$  and  $[(CH_3)_4N]_3Bi_2Cl_9$  and twofold reorientations in the case of  $[(CH_3)_4N]_3Bi_2Cl_9$  as these groups have a preferred axis of reorientation. There is a large degree of structural disorder in the

Bismuth substituted compounds which is reflected in the considerable amount of dynamic inequivalence among the methyl groups and the cations themselves.

It is worthwhile to look at the features of cation dynamics in the Antimony substituted compounds of this family in the light of the above observations. T minima corresponding to the isotropic reorientation of the cations are observed only in the case of TEMA compounds of this family and in the case of TMA and DMA substituted compounds the corresponding minima are seen to occur only at much higher temperatures. But, as in the case of the Bismuth analogues, the hindrance to the isotropic reorientation of the cations increases progressively as we move towards less symmetric cations. The calculated activation energies for the isotropic reorientation in the case of the Antimony substituted compounds in the high temperature phase are given by :  $[(CH_3)_4N] Sb Cl_9$  - 7.5 kJ/mole,  $[(CH_3)_4N]_3 Sb_2Br_9$  - 7 kJ/mole,  $[(CH_3)_3NH]_3 Sb_2Cl_9$  - 9.0 kJ/mole and  $[(CH_3)_2NH] Sb_2Cl_9$  - 27.5 kJ/mole. The increased amount of structural inequivalence caused by the substitution of the Bismuth atom is seen in the case of  $[(CH_3)_2NH] Bi_2Cl_9$  compared to  $[(CH_3)_3NH]_3 Sb_2Cl_9$ . In the case of  $[(CH_3)_2NH] Sb_2Cl_9$  both the trimethylammonium cation as well as the methyl groups have dynamic inequivalence in the ratio 1:2, while in  $[(CH_3)_2NH] Bi_2Cl_9$  trimethylammonium cations are inequivalent in the ratio 1:1:4 and methyl groups are inequivalent in the ratio 1:1:2:2. Further, substitution of Bismuth has also increased the freedom of reorientation for at least some of the cations, as a consequence of the increased amount structural disorder in Bismuth compounds. This can be seen from the fact that the signature of the minimum, and corresponding frequency dispersion, due to isotropic reorientation in  $[(CH_3)_3NH]_3$

Bi Cl is observed between 300K and 400K as seen from T data. On the other hand, in  $[(CH_3)_4NH] SbCl_9$  the T data suggest the presence of such a minimum due to isotropic reorientation to be at much higher temperatures. A similar observation can be made in the case of  $[(CH_3)_4NH] BiCl_9$  where we see the formation of a minimum due to isotropic reorientation of the cation at about 400K, while in  $[(CH_3)_2NH_2]_3 Sb_2Cl_9$  this minimum seems to form at much higher temperatures only.

All the Bismuth substituted compounds exhibit at least one structural phase transition and, barring  $(CH_3)_4NH BiCl_9$ , these transitions are at or below room temperature ( $\approx 300K$ ). T and  $M_n$  data show the signature of these transitions and in some cases like  $[(CH_3)_4N] Bi_2Cl_9$  and  $[(CH_3)_4N]_3 Bi_2Br_9$ , perceptible discontinuities are found in  $T_1$  data. Analysis of T data in these compounds shows that across such transitions the corresponding dynamics of the cations **have become more** hindered. The T data further show the possibility of additional structural phase transitions at much lower temperatures (in the vicinity of 100K) in most of these compounds, unlike the case with Antimony substituted compounds of this family. In fact, in a comparable temperature range of observation all the Antimony compounds show the presence of only one structural phase transition. Table (C-7.2) gives a list of observed structural phase transitions in both Bismuth and Antimony substituted compounds of this family.

Table (C-7.1) contains the list of the dynamic parameters ( $E_a$ ,  $T_o$ ) for the four tetramethylammonium compounds i.e.  $[(CH_3)_4N]_3 Bi_2Cl_9$ ,  $[(CH_3)_4N]_3 Bi_2Br_9$ ,  $[(CH_3)_4N]_3 Sb_2Cl_9$  and  $[(CH_3)_4N]_3 Sb_2Br_9$ . In the

TABLE C - 7.1

COMPOUND		DYNAMIC PARAMETERS			
	SYM. GROUP	PHASE-I		PHASE-II	
		$E_a$ (kJ/m)	$\tau_0$	$E_a$ (kJ/m)	$\tau_0$
TEMACA	TEMA	7.5	4.4E-12	12.6	2.5E-13
	CH <sub>3</sub> - A			<b>15.9</b>	1.7E - 14
	CH <sub>3</sub> - B			9.2	1.5E -13
	CH <sub>3</sub> - C			6.9	1.2E - 14
TEMABA	TEMA	6.7	4.3E - 12	<b>18.0</b>	5.4E - 15
	CH - A			20.0	3.4E - 16
	CH <sub>3</sub> - B			10.0	1.7E - 13
	CH <sub>3</sub> - C			<b>7.1</b>	<b>9.1E - 14</b>
TEMACB	TEMA	10.0	7.3E -13	13.5	5.9E - 14
	CH - A			35.0	8.9E - 22
	CH - B			2.0	3.2E - 9
	CH - C			8.0	1.6E - 13
	CH - D			21.0	6.0E - 24
TEMABB	TEMA	7.0	2.5E - 12	<b>14.5</b>	8.0E - 14
	CH <sub>3</sub> - A			16.0	3.5E - 16
	CH <sub>3</sub> - B			9.0	4.5E - 13
	CH - C			16.5	<b>1.0E - 15</b>

DYNAMIC PARAMETERS FOR THE FOUR TETRAMETHYLAMMONIUM COMPOUNDS

Antimony compounds,  $[(CH_3)_4N]_3Sb_2Cl_9$  and  $[(CH_3)_4N]_3Sb_2Br_9$  transitions at 223K and 189K were detected with proton magnetic resonance. In the related Bismuth compounds  $[(CH_3)_4N]_3Bi_2Cl_9$  and  $[(CH_3)_4N]_3Bi_2Br_9$  transitions are seen from the present studies at 151K and 183K respectively. Further, possibilities of additional low temperature transitions were also detected at about 90K and 120K in these systems, respectively. From table (C-7.1), it is seen that substitution of Br in place of Cl has increased the freedom of reorientation for the **TEMA** cation for both Sb and Bi substituted compounds, and this is observed to be true both above and below the transition temperature. In contrast, when we compare  $[(CH_3)_4N]_3SbCl_9$  and  $[(CH_3)_4N]_3BiCl_9$  where the metal atom is changed from Sb to Bi and the halogen is Cl, the reorientational freedom has decreased above the phase transition, as indicated by the increase of E from 7.5 kJ/mole to 10.2 kJ/mole. Similarly, if we compare these values between  $[(CH_3)_4N]_3SbBr_9$  and  $[(CH_3)_4N]_3BiBr_9$  there is an increase in the activation energy from 6.7 kJ/mole to 8.0 kJ/mole, which also points to the increase in the hindrance of the cation when we substitute the heavier Bi atom in place of Sb.

Table (C-7.2) gives the relevant crystal structure data and percentage increase in the volume, molecular weight and density within a unit cell when the halogen atom is replaced from Cl to Br **and** when the metal atom is changed from Sb to Bi, for all the four **tetramethyl** compounds. When the halogen atom is changed from Cl to Br, the unit **cell** volume of Sb compounds increases by **7.25%** **and the** corresponding increase in case of Bi compounds is **7.54%**. On the other hand, **when we substitute Bi in place** of Sb with Cl as the halogen atom, the percentage increase in this volume is a small 1.2%. Similarly, for the compounds with Br as the

TABLE C - 7.2

COMPOUND	X - TAL STR DATA		Cl → Br		Sb → Bi (Cl)		Sb → Bi (Br)	
	P6 <sub>3</sub> /mmc sp.gr; Z = 2		%ρ	%V	%ρ	%V	%ρ	%V
TEMACA	a=0.925nm c=2.173nm	ρ=1.6 V=1.61nm <sup>3</sup>						
			29.2	7.25	19.2	1.2		
TEMABA	a=0.9499 b=2.223nm	ρ=2.261 V=1.736nm						
TEMACB	a=0.9265nm c=2.193	ρ=1.98 V=1.6303						
			21.7	7.54			10.7	1.5
TEMABB	a=0.9521 c=2.246nm	ρ=2.53 V=1.7632						

CRYSTAL STRUCTURE DATA ON THE TETRAMETHYLAMMONIUM COMPOUNDS SHOWING THE PERCENTAGE CHANGE IN VOLUME AND DENSITY OF UNIT CELL



halogen atom, the percentage increase in the volume is **1.554**. Whereas there is a perceptible increase in the unit cell volume with the change in the halogen atom, indicating increased freedom for the cation reorientation when the metal atom is changed, the change in unit cell volume is very small, indicating in turn an increased hindrance for the cation reorientation.

In the case of all these four tetramethyl ammonium compounds, both above and below the phase transition temperatures, the cations undergo isotropic reorientation. Across the phase transition, there is a discontinuous change in the correlation time of this reorientation, which is seen as a perceptible change in the value of  $T_1$ .  $M_2$  data do not show any step wise freezing of the corresponding dynamic processes at the  $T$  of all the four tetramethyl ammonium compounds, as the corresponding correlation times immediately below the transition temperature **have not** reached values comparable to the inverse of the linewidths.

$M_1$  data show a step wise increase at 363K in  $[(CH_3)_4NH] SbCl_9$  **where** a phase transition is observed, and this was attributed to the freezing of the isotropic motion of, at least, some of the TMA cations.  $[(CH_3)_3NH] Bi_2Cl_9$  seems to be different in the sense that  $M_2$  data do not show any signature of this transition at 300K, even though  $T_1$  data show the possibility of this transition. In  $[(CH_3)_4NH] SbCl_9$  also there is a **step wise** increase in  $M_2$  at the phase transition temperature (247K) and  $T_1$  data at this temperature show a sudden discontinuity. In the case of the Antimony substituted compounds  $[(CH_3)_4N]_3 Sb_2Cl_9$  and  $[(CH_3)_4N]_3 SbBr$  we see only a slope change in  $T_1$  data, whereas in both  $[(CH_3)_3NH]_3 SbCl_9$  and  $[(CH_3)_2NH_2]_3 Sb_2Cl_9$  the occurrence of the phase transition

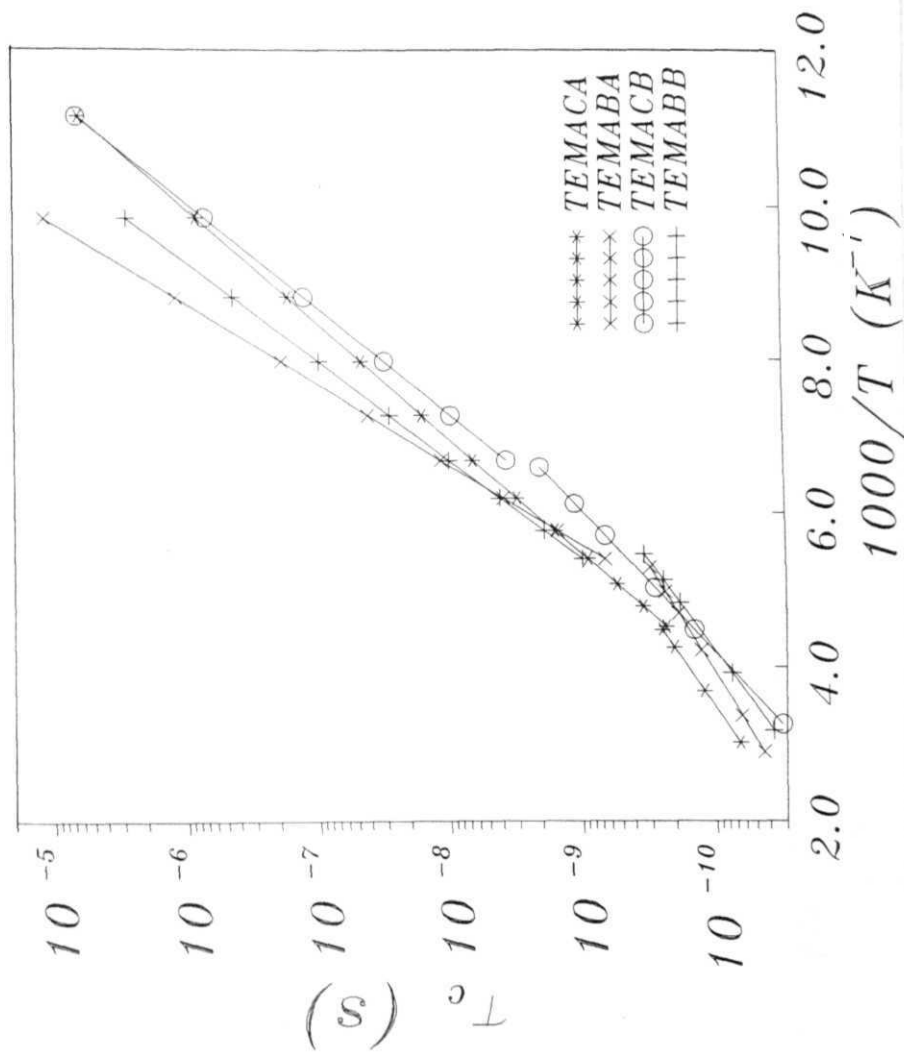
TABLE C - 7.3

	$\tau_c$ COMP. WITH $E_a$ , $\tau_0$ ABOVE $T_C$	$\tau_c$ COMP. WITH $E_a$ , $\tau_0$ BELOW $T_C$
TEMACA	2.6E - 10s	2.2E - 10s
TEMABA	3.0E - 10s	5.1E - 10s
TEMACB	2.1E - 9s	3.1E - 9s
TEMABB	3.3E - 10s	1.02E - 9s

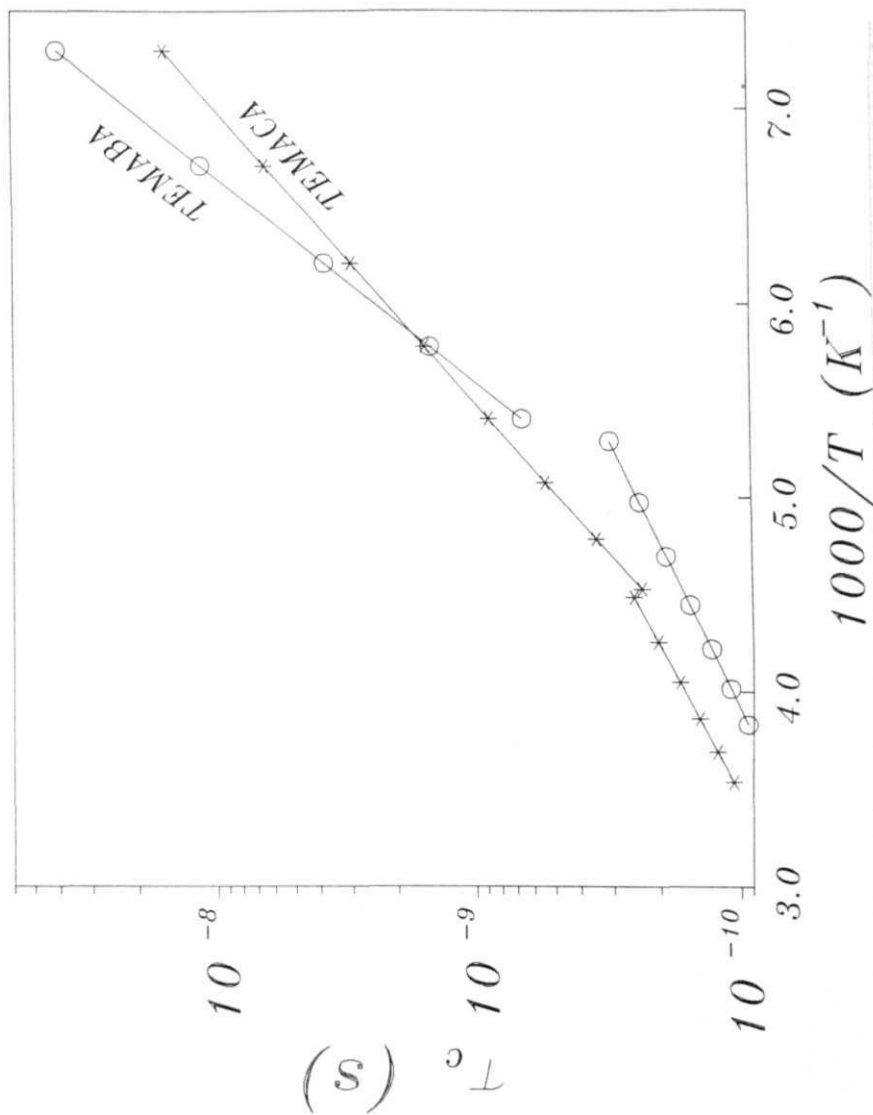
CORRELATION TIMES COMPUTED FOR THE TETRAMETHYLAMMONIUM COMPOUNDS BOTH ABOVE AND BELOW THE PHASE TRANSITION TEMPERATURES.

leaves the signature on T data as a sudden **discontinuity**. Such a sudden change in T values is thus seen to occur in these compounds **only when** the cations are of lesser symmetry (TMA and DMA) compared to **the more** symmetric TEMA groups. Also, when the cations are of lesser symmetry considerable amount of disorder is created in the structure, **partly due** to the formation of hydrogen bonds between the **cations** and the halogen atoms. Qualitative differences in the signatures of these transitions on the T data in these two types of systems (Sb and Bi substituted compounds) indicate the progressive increase in the structural disorder in Bi substituted compounds.

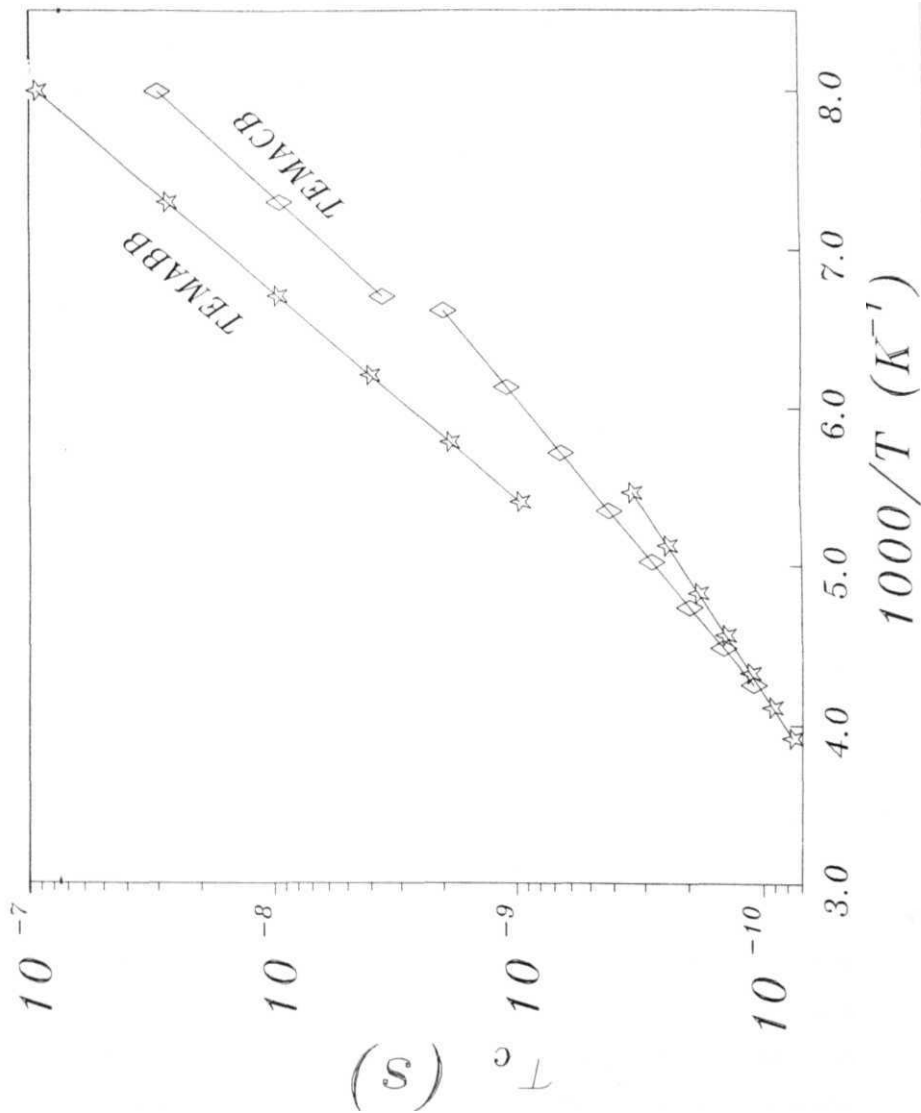
The number of possible structural phase transitions observed in Bi compounds is more relative to the Sb systems, within the observed **range** of temperature. While the high temperature transitions in each of the Bi compound seem to have a counterpart in comparable temperature range in the respective Sb systems, there is the signature of at least one phase transition at much lower temperatures (around 100K) in all the Bismuth substituted systems. Thus in  $[(CH_3)_4N] BiCl$  there seems to be a structural phase transition near 91 K, in  $[(CH_3)_4N] BiBr$  there is a signature on the T data of a phase transition at 120K, in  $[(CH_3)_4NH]_3 BiCl$  such an occurrence is seen at around 125K, and in  $[(CH_3)_2NH_2]_4 BiCl$  a discontinuity in T is seen at 154K as also a **steep** increase in T data at 78K. The methylammonium substituted compound  $(CH_3NH_2)_4 BiCl$  shows the presence of four structural phase transitions while the Antimony counterpart  $(CH_3NH_2)_4 Sb_2Cl_9$  shows **only** one. If we compare the transition temperatures among Sb and Bi substituted compounds, the temperatures of transitions are lowered in case of Bi compounds. Even in some of **AMX**. compounds where A is the tetramethylammonium cation, the



(C-7.1) Graph showing the variation of  $\tau_c$  as a function of  $1000/T$  in the four tetramethylammonium compounds (TEMACA, TEMABA, TEMACB and TEMABB)



(C-7.2) Graph showing the variation of  $\tau_c$  as a function of  $1000/T$  in the Sb substituted compounds TEMACA and TEMABA



(C-7.3) Graph showing the variation of  $\tau_c$  as a function of  $1000/T$  in the Bi substituted compounds TEMACB and TEMABB

transition temperatures are observed to have shifted towards lower values as the metal atom changed from a lighter one like Co, through bulkier ones like Mn, Cu, Zn and Cd.

The dynamics of the four tetramethylammonium compounds exhibit interesting behaviour at their respective phase transition temperatures. Fig.(C-7.1) shows the correlation time of all the four compounds as a function of inverse temperature. For clarity,  $T$  variation as function of  $1/T$  is shown for the Sb and Bi substituted compounds in a limited temperature range, separately (Fig. C-7.2 and C-7.3) is seen that in three of the four tetramethyl compounds,  $[(CH_3)_3N]_3Sb_2Cl_9$ ,  $[(CH_3)_4N]_3SbBr$  and  $[(CH_3)_4N]_3BiBr$ ,  $T$  has reached a value of about  $3e-10$  s at the respective phase transition temperatures as we move towards  $T$  from higher temperatures (Table C-7.3). Only in the case of  $[(CH_3)_4N]_3BiCl$  the correlation time at  $T$  is nearly  $2.0e-9$  s. It seems that the correlation time of the associated dynamics of the cation reaches a value of the order of  $1e-10$  s at the respective phase transition temperature in these compounds.

The conclusion of the above discussion based on detailed NMR studies of tris(alkylammonium) nonahalogeno dibismuthates may be summarized as :

- The amount of structural inequivalence in these compounds is increased with the substitution of the heavier metal atom Bi in place of Sb, which is clearly reflected in the motional properties of the cations as well as their internal dynamics.
- The number of phase transitions observed from these studies is

more in case of compounds of the title family than the ones which have Sb as the metal atom.

- There is a tendency for the phase transition temperatures to be lowered in case of Bi substituted compounds compared to their Sb counterparts.
- The freedom for the reorientation of the cations gets restricted in the high temperature phase as we move towards compounds with more asymmetric cationic groups.
- \* As one changes the halogen atom from Cl to Br, there is an increased amount of freedom for the cations in the high temperature phase in the tetramethylammonium compounds of this family. But the reverse seems to be true in the case of ammonium compounds.
- At the high temperature phase transition the correlation time corresponding to the isotropic reorientation of three of the four tetramethylammonium compounds reaches a value of  $3.0 \times 10^{-10}$  s.

The phases below 367K and 247K in  $[(CH_3)_3NH] Sb_2Cl_9$  and  $[(CH_3)_2NH_2] Sb_2Cl_9$  are found to be ferroelectric as evidenced by other studies, and such investigations on  $[(CH_3)_3NH]_3 Bi_2Cl_9$  and  $[(CH_3)_2NH_2]_3 BiCl$  will be essential to confirm if such polar properties are exhibited by these crystals also. Though the signature of the possible phase transitions in these compounds are recorded perhaps, for the first time, using the present proton NMR measurements, further studies are



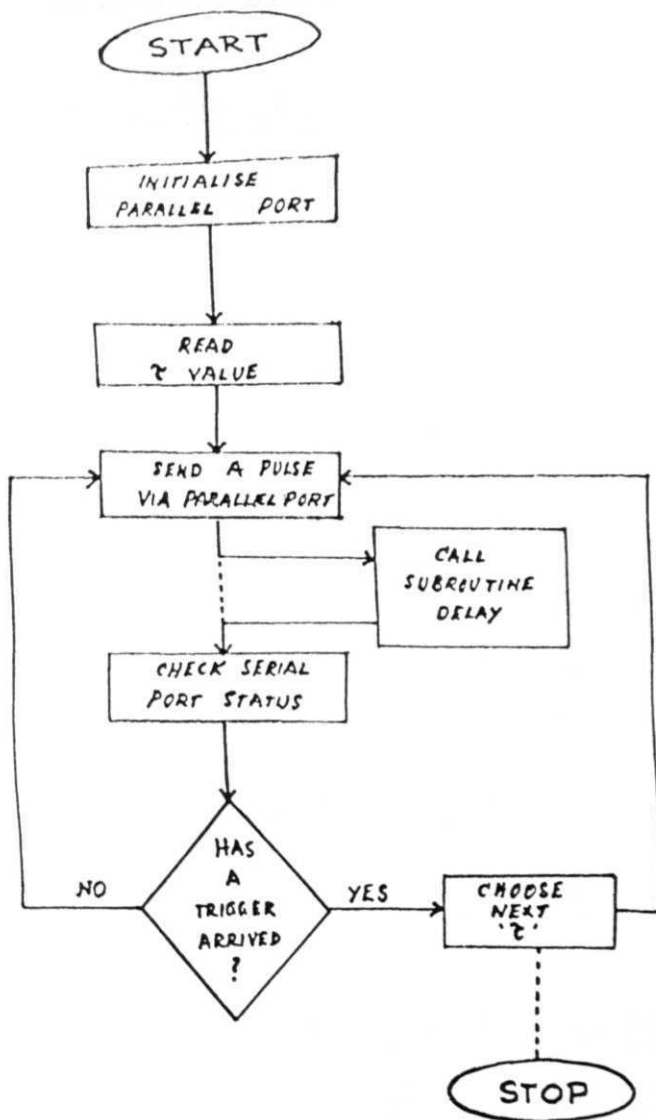
obviously required to corroborate and further characterize the occurrence of these transitions.  $(\text{CH}_3\text{NH})_2\text{Bi}_2\text{Cl}_9$  shows a behaviour similar to plastic crystals in its highest temperature phase and promises to be an interesting system for further scrutiny. Synthesis of other crystals **of this family with** halogens like **Br and I and their** systematic studies open up promising future possibility for further understanding of this interesting family of solids. The present studies **have** indicated the possibility of some interesting features in some of these compounds at temperatures below 77K which could not be recorded because the facilities to reach this very low temperatures are not readily available in the laboratory. Such studies on these systems therefore will prove to be very useful in confirming the possibility of occurrence of some of the features below 77K as predicted from the current studies and they will also enable one to observe some other interesting phenomena like tunneling in these solids.

## A P P E N D I X I

This appendix contains the following assembly level programs to be used with the  $\mu$ P-based pulse programmer developed as a part of this work. The flow diagram showing the logic of the program is provided for each case.

1. Program to generate a one pulse sequence
2. Program to generate the inversion recovery pulse sequence
3. Program to generate the saturation burst pulse sequence
4. Program to generate the Carr-Purcell pulse sequence

Hardware and other details of the pulse programmer are available in sub-section (B-3). What is shown here is only a sample listing of some of the programs. Programs were also developed to generate all the other pulse sequences mentioned in text, though they are not listed here.



FLOW DIAGRAM FOR ONE PULSE SEQUENCE

PROGRAM : 1 ONE PULSE SEQUENCE WITH RS-232-C COMMUNICATION

PART : 1 - RS-232-C COMMUNICATION

VERSION : 5

DATE : 4.2.89

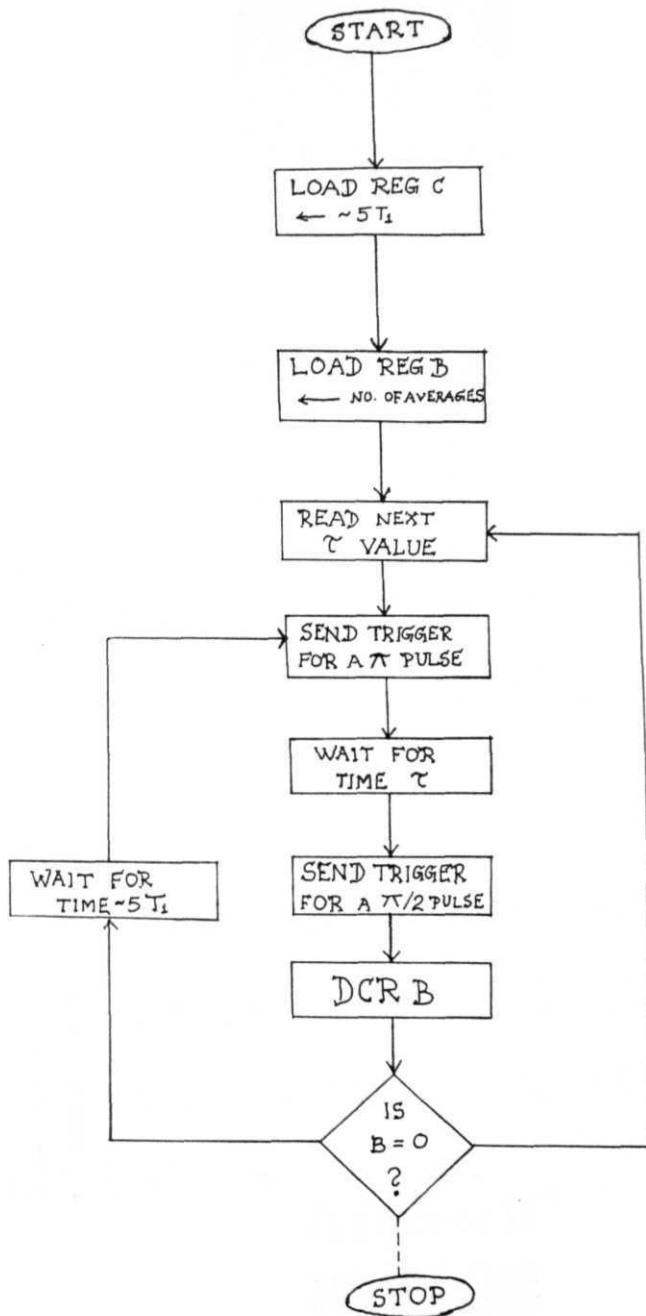
CODE 1-1.5

ADD.	MNEM.	OPCOD.	ADD.	MNEM.	OPCOD.	ADD.	MNEM.	OPCOD.	ADD.	MNEM.	OPCOD.	ADD.	MNEM.	OPCOD.
5300	MVI A	3E	531D	08	08	533C	08	08	5359	INX H	23	5378	09	09
5301	40	40	531E	MOV C A	4F	533D	MOV M A	77	535A	XTHL	E3	5379	RAR	1F
5302	OUT	D3	531F	MOV E C	59	533E	INX H	23	535B	DCR C	OD	537A	RAR	1F
5303	09	09	5320	LXI H	21	533F	DCR D	15	535C	JNZ	C2	537B	JNC	D2
5304	MVI A	3E	5321	00	00	5340	JNZ	C2	535D	52	52	537C	77	77
5305	4B	4B	5322	52	52	5341	25	25	535E	53	53	537D	53	53
5306	OUT	D3	5323	MVI D	16	5342	53	53	535F	LXI H	21	537E	IN	DB
5307	09	09	5324	06	06	5343	DCR C	OD	5360	00	00	537F	08	08
5308	MVI A	3E	5325	MVI B	06	5344	JNZ	C2	5361	54	54	5380	DCR B	05
5309	14	14	5326	03	03	5345	23	23	5362	MOV M E	73	5381	JNZ	C2
530A	OUT	D3	5327	IN	DB	5346	53	53	5363	JMP	C3	5382	77	77
530B	09	09	5328	09	09	5347	MOV C E	4B	5365	53	53	5383	53	53
530C	IN	DB	5329	RAR	1F	5348	CALL	CD	5366	MVI A	3E	5384	JMP	C3
530D	09	09	532A	RAR	1F	5349	66	66	5367	D3	D3	5385	00	00
530E	RAR	1F	532B	JNC	D2	534A	53	53	5368	DCR C	OD	5386	50	50
530F	RAR	1F	532C	27	27	534B	LXI H	21	5369	JZ	CA			
5310	JNC	D2	532D	53	53	534C	00	00	536A	73	73			
5311	OC	OC	532E	IN	DB	534D	51	51	536B	53	53			
5312	53	53	532F	08	08	534E	PUSH H	E5	536C	MVI D	16			
5313	IN	DB	5330	DCR B	05	534F	LXI H	21	536D	03	03			
5314	08	08	5331	JNZ	C2	5350	00	00	536E	ADD D	82			
5315	IN	DB	5332	27	27	5351	52	52	536F	DCR C	OD			
5316	09	09	5333	53	53	5352	MOV A M	7E	5370	JNZ	C2			
5317	RAR	1F	5334	IN	DB	5353	INX H	23	5371	6E	6E			
5318	RAR	1F	5335	09	09	5354	MOV D M	56	5372	53	53			
5319	JNC	15	5336	RAR	1F	5355	INX H	23	5373	MOV C A	4F			
531A	15	15	5337	RAR	1F	5356	ADD D	82	5374	RET	09			
531B	53	53	5339	34	34	5357	XTHL	E3	5375	MVI B	06			
531C	IN	DB	533A	53	53	5358	MOV M A	77	5376	04	04			
									5377	IN	DB			

PROGRAM : 1 ONE PULSE SEQUENCE WITH RS-232-C COMMUNICATION

PART : 2 - PULSE GENERATION      VERSION : 3      DATE : 4.2.89      CODE : 1-2.3

ADD.	MNEM.	OPCOD.	ADD.	MNEM.	OPCOD.	ADD.	MNEM.	OPCOD.
5000	MVI A	3E	501D	08	08	503B	50	50
5001	80	80	501E	IN	DB	503C	MVI A	3E
5002	OUT	D3	501F	09	09	503D	FF	FF
5003	07	07	5020	RAR	1F	503E	ANA E	A3
5004	LXI H	21	5021	RAR	1F	503F	JZ	CA
5005	00	00	5022	JNC	D2	5040	46	46
5006	51	51	5023	1E	1E	5041	50	50
5007	SHLD	22	5024	50	50	5042	DCR E	1D
5008	90	90	5025	IN	DB	5043	JNZ	C2
5009	50	50	5026	08	08	5044	42	42
500A	MVI A	3E	5027	LHLD	2A	5045	50	50
500B	01	01	5028	95	95	5046	MVI A	3E
500C	OUT	D3	5029	50	50	5047	FF	FF
500D	04	04	502A	SHLD	22	5048	ANA D	A2
500E	MVI A	3E	502B	90	90	5049	JZ	CA
500F	00	00	502C	50	50	504A	52	52
5010	OUT	D3	502D	JMP	C3	504B	50	50
5011	04	04	502E	OA	OA	504C	DCR D	15
5012	CALL	CD	502F	50	50	504D	MVI E	1E
5013	30	30	5030	MOV C M	4E	504E	FF	FF
5014	50	50	5031	INX H	23	504F	JMP	C3
5015	IN	DB	5032	MOV D M	56	5050	42	42
5016	09	09	5033	INX H	23	5051	50	50
5017	RAR	1F	5034	MOV E M	5E	5052	MVI A	3E
5018	RAR	1F	5035	INX H	23	5053	FF	FF
5019	JNC	D2	5036	SHLD	22	5054	ANA C	A1
501A	OA	OA	5037	95	95	5055	JZ	CA
501B	50	50	5038	50	50	5056	5E	5E
501C	IN	DB	5039	LHLD	2 A	5057	50	50
			503A	90	90	5058	DCR C	OD



FLOW DIAGRAM FOR INVERSION  
RECOVERY SEQUENCE

PROGRAM : 2 INVERSION RECOVERY SEQUENCE WITH 232-C COMMUNICATION

PART 1 : RS-232-C COMMUNICATION

VERSION : 1

CODE : 2-1. 1

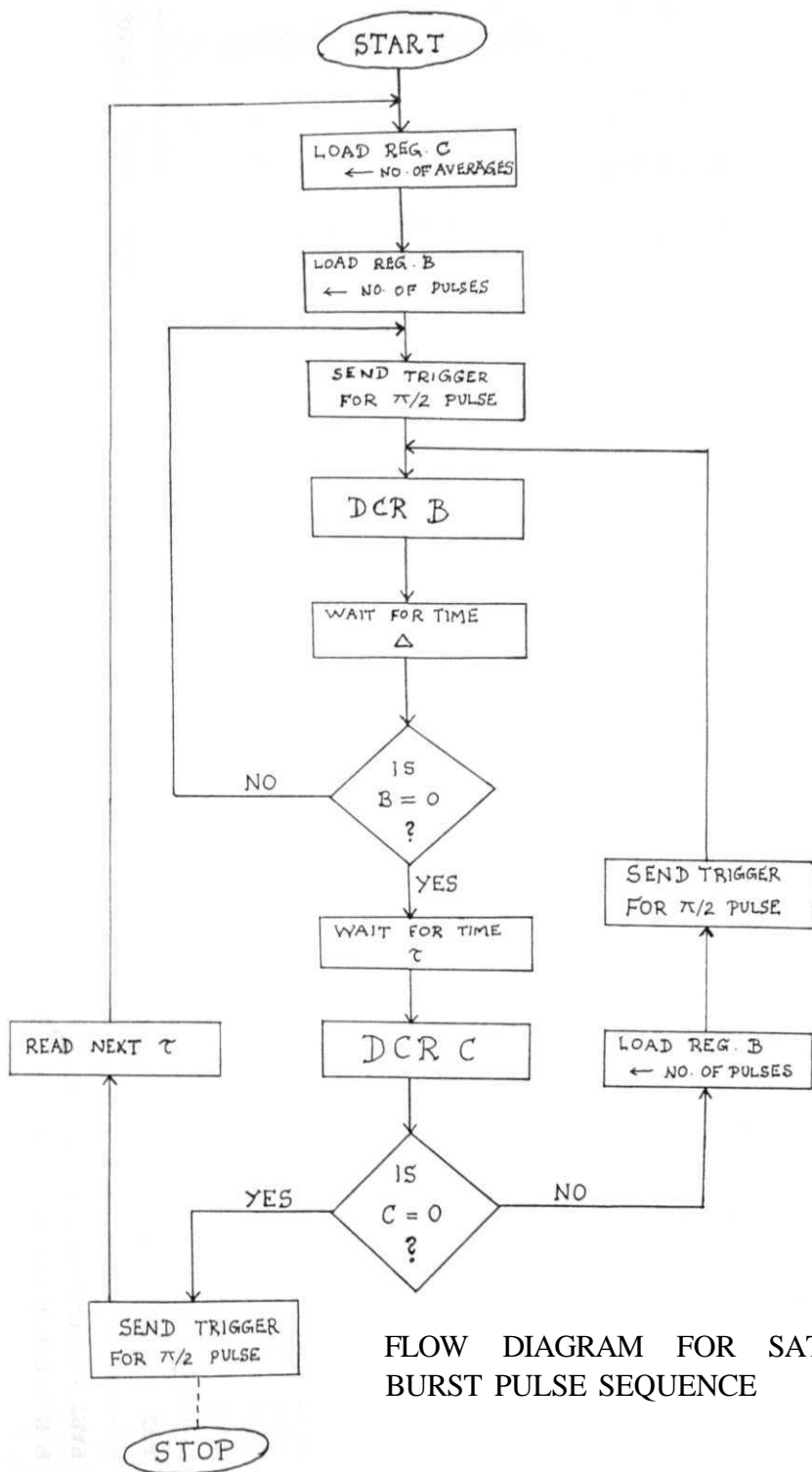
ADD.	MNEM.	OPCOD.	ADD.	MNEM.	OPCOD.	ADD.	MNEM.	OPCOD.	ADD.	MNEM.	OPCOD.
5300	MVI A	3E	531D	09	09	533C	INX A	23	5359	08	08
5301	40	40	531E	RAR	IF	533D	ADD D	82	535A	JMP	C3
5302	OUT	D3	531F	RAR	IF	533E	XTHL	E3	535B	00	00
5303	09	09	5320	JNC	D2	533F	MOV M A	77	535C	50	50
5304	MVI A	3E	5321	IC	IC	5340	INX H	23	535D		
5305	4B	4B	5322	53	53	5341	XTHL	E3	535E		
5306	OUT	D3	5323	IN	DB	5342	DCR B	05	535F		
5307	09	09	5324	08	08	5343	JNZ	C2	5360		
5308	MVI A	3E	5325	MOV M A	77	5344	39	39	5361		
5309	15	15	5326	INX H	23	5345	53	53	5362		
530A	OUT	D3	5327	DCR D	15	5346	DCR C	OD	5363		
530B	09	09	5328	JNZ	C2	5347	JNZ	C2	5365		
530C	IN	DB	5329	IC	IC	5348	37	37	5366		
530D	09	09	532A	53	53	5349	53	53	5367		
530E	RAR	1F	532B	DCR C	OD	534A	DCR E	1D	5368		
530F	RAR	1F	532C	JNZ	C2	534B	LXI H	21	5369		
5310	JNC	D2	532D	1A	1A	534C	00	00	536A		
5311	OC	OC	532E	53	53	534D	52	52	536B		
5312	53	53	532F	LXI H	21	534E	MOV M E	73	536C		
5313	IN	DB	5330	00	00	534F	INX H	23	536D		
5314	08	08	5331	51	51	5350	MOV M E	73	536E		
5315	MOV C A	4F	5332	PUSH H	E5	5351	IN	DB	536F		
5316	MOV E C	59	5333	LXI H	21	5352	09	09	5370		
5317	LXI H	21	5334	00	00	5353	RAR	1F	5371		
5318	00	00	5335	52	52	5354	RAR	1F	5372		
5319	52	52	5336	MOV C E	4B	5355	JNC	D2	5373		
531A	MVI D	16	5337	MVI B	06	5356	51	51	5374		
531B	06	06	5339	MOV A M	7E	5357	53	53	5375		
531C	IN	DB	533A	INX H	23	5358	IN	DB	5376		

PROGRAM : 2 INVERSION RECOVERY SEQUENCE

PART 2 : PULSE SEQUENCE GENERATION VERSION : 4 CODE : 2 - 2.4

ADD.	MNEM.	OPCOD.	ADD.	MNEM.	OPCOD.	ADD.	MNEM.	OPCOD.	ADD.	MNEM.	OPCOD.	ADD.	MNEM.	OPCOD.
5000	MVI A	3E	501E	54	54	503C	FF	FF	505A	JMP	C3	5078	50	50
5001	80	80	501F	MV1A	3E	503D	ANA E	A3	505B	4B	4B	5079	LHLD	2A
5002	OUT	D3	5020	02	02	503E	JZ	CA	505C	50	50	507A	05	05
5003	07	07	5021	OUT	D3	503F	45	45	505D	RET	C9	507B	54	54
5004	LX1 H	21	5022	04	04	5040	50	50	505E	MVI A	3E	507C	SHLD	22
5005	00	00	5023	MV1A	3E	5041	DCR E	1D	505F	01	01	507D	00	00
5006	51	51	5024	00	00	5042	JNZ	C2	5060	OUT	D3	507E	54	54
5007	PUSH H	E5	5025	OUT	D3	5043	41	41	5061	08	08	507F	JMP	C3
5008	LXI H	21	5026	04	04	5044	50	50	5062	MV1 B	06	5080	6F	6F
5009	03	03	5027	CALL	CD	5045	MVI A	3E	5063	05	05	5081	50	50
500A	51	51	5028	5E	5E	5046	FF	FF	5064	IN	DB	5082	MVI B	06
500B	SHLD	22	5029	50	50	5047	ANA D	A2	5065	09	09	5083	01	01
500C	00	00	502A	XTHL	E3	5048	JZ	CA	5066	RAR	IF	5084	CMP B	B8
500D	54	54	502B	CALL	CD	5049	51	51	5067	RAR	IF	5085	JNZ	C2
500E	MVI A	3E	502C	35	35	504A	50	50	5068	JC	DA	5086	00	00
500F	08	08	502D	50	50	504B	DCR D	15	5069	70	70	5087	53	53
5010	OUT	D3	502E	LX1 H	21	504C	MVI E	1E	506A	50	50	5088	INX H	23
5011	04	04	502F	00	00	504D	FF	FF	506B	DCR B	05	5089	MOV A M	7E
5012	MVI A	3E	5030	51	51	504E	JMP	C3	506C	JNZ	C2	508A	DCX H	2B
5013	00	00	5031	XTHL	E3	504F	41	41	506D	64	64	508B	MOV M A	77
5014	OUT	D3	5032	JMP	C3	5050	50	50	506E	50	50	508C	JMP	C3
5015	04	04	5033	0E	0E	5051	MVI A	3E	506F	RET	C9	508D	51	51
5016	CALL	CD	5034	50	50	5052	FF	FF	5070	IN	DB	508E	53	53
5017	35	35	5035	MOV C M	4E	5053	ANA C	A1	5071	08	08			
5018	50	50	5036	INX H	23	5054	JZ	CA	5072	LX1 H	21			
5019	SHLD	22	5037	MOV D M	56	5055	5D	5D	5073	00	00			
501A	05	05	5038	INX H	23	5056	50	50	5074	52	52			
501B	54	54	5039	MOV E M	5E	5057	DCR C	0D	5075	DCR	35			
501C	LHLD	2A	503A	INX H	23	5058	MVI D	16	5076	JZ	CA			
501D	00	00	503B	MVI A	3E	5059	FF	FF	5077	82	82			





FLOW DIAGRAM FOR SATURATION BURST PULSE SEQUENCE

ADD.	MNEM.	OPCOD.	ADD.	MNEM.	OPCOD.	ADD.	MNEM.	OPCOD.	ADD.	MNEM.	OPCOD.	ADD.	MNEM.	OPCOD.
5000	MVI A	3E	501F	MVI A	3E	503E	07	07	505D	75	75	507C	MVI A	3E
5001	C3	C3	5020	30	30	503F	LXI H	21	505E	52	52	507D	FF	FF
5002	STA	32	5021	DCR A	3D	5040	00	00	505F	LHLD	2A	507R	ANA E	A3
5003	CE	CE	5022	JNZ	C2	5041	51	51	5060	70	70	507F	JZ	CA
5004	40	40	5023	21	21	5042	SHLD	22	5061	52	52	5080	86	86
5005	MVI A	3E	5024	50	50	5043	70	70	5062	MVI B	06	5081	50	50
5006	28	28	5025	JMP	C3	5044	52	52	5063	0A	0A	5082	DCR E	1D
5007	STA	32	5026	17	17	5045	MVI B	06	5064	MVI A	3E	5083	JMP	C3
5008	CF	CF	5027	50	50	5046	0A	0A	5065	03	03	5084	7C	7C
5009	40	40	5028	MVI A	3E	5047	MVI A	3E	5066	OUT	D3	5085	50	50
500A	MVI A	3E	5029	C3	C3	5048	01	01	5067	04	04	5086	MVI A	3E
500B	50	50	502A	STA	32	5049	OUT	D3	5068	MVI A	3E	5087	FF	FF
500C	STA	32	502B	CE	CE	504A	04	04	5069	00	00	5088	ANA D	A2
500D	DO	DO	502C	40	40	504B	MVI A	3E	506A	D3	D3	5089	JZ	CA
500E	40	40	502D	MVI A	3E	504C	00	00	506B	04	04	508A	92	92
500F	MVI A	3E	502E	50	50	504D	OUT	D3	506C	C3	C3	508B	50	50
5010	0B	0B	502F	STA	32	504E	04	04	506D	4F	4F	508C	DCR D	15
5011	SIM	30	5030	CF	CF	504F	DCR B	05	506E	50	50	508D	MVI E	1E
5012	EI	FB	5031	40	40	5050	JZ	CA	506F	MVI A	3E	508E	FF	FF
5013	MVI A	3E	5032	MVI A	3E	5051	59	59	5070	01	01	508F	JMP	C3
5014	80	80	5033	51	51	5052	50	50	5071	DCR A	3D	5090	82	82
5015	OUT	D3	5034	STA	32	5053	CALL A	CD	5072	JNZ	C2	5091	50	50
5016	07	07	5035	DO	DO	5054	6F	6F	5073	71	71	5092	MVI A	3E
5017	MVI A	3E	5036	40	40	5055	50	50	5074	50	50	5093	FF	FF
5018	FF	FF	5037	MVI A	3E	5056	JMP	C3	5075	RET	C9	5094	ANA C	A1
5019	OUT	D3	5038	0B	0B	5057	47	47	5076	MOV C M	4E	5095	JZ	CA
501A	04	04	5039	SIM	30	5058	50	50	5077	INX H	23	5096	9E	9E
501B	MVI A	3E	503A	EI	FB	5059	CALL r	CD	5078	MOV D M	56	5097	50	50
501C	00	00	503B	MVI A	3E	505A	76	76	5079	INX H	23	5098	DCR C	0D
501D	OUT	D3	503C	80	80	505B	50	50	507A	MOV E M	5E	5099	MVI D	16
501E	04	04	503D	OUT	D3	505C	SHLD	22	507B	INX H	23	509A	FF	FF

P R O G R A M :   **3**      A S S E M B L Y   L I S T I N G   O F   S A T U R A T I O N   B U R S T   P R O G R A M  
P A R T   :   1   V E R S I O N   :   2      C O D E   :   3 - 1 . 2      P A G E   :   2

---

A D D .      **M N E M .**      **O P C O D .**

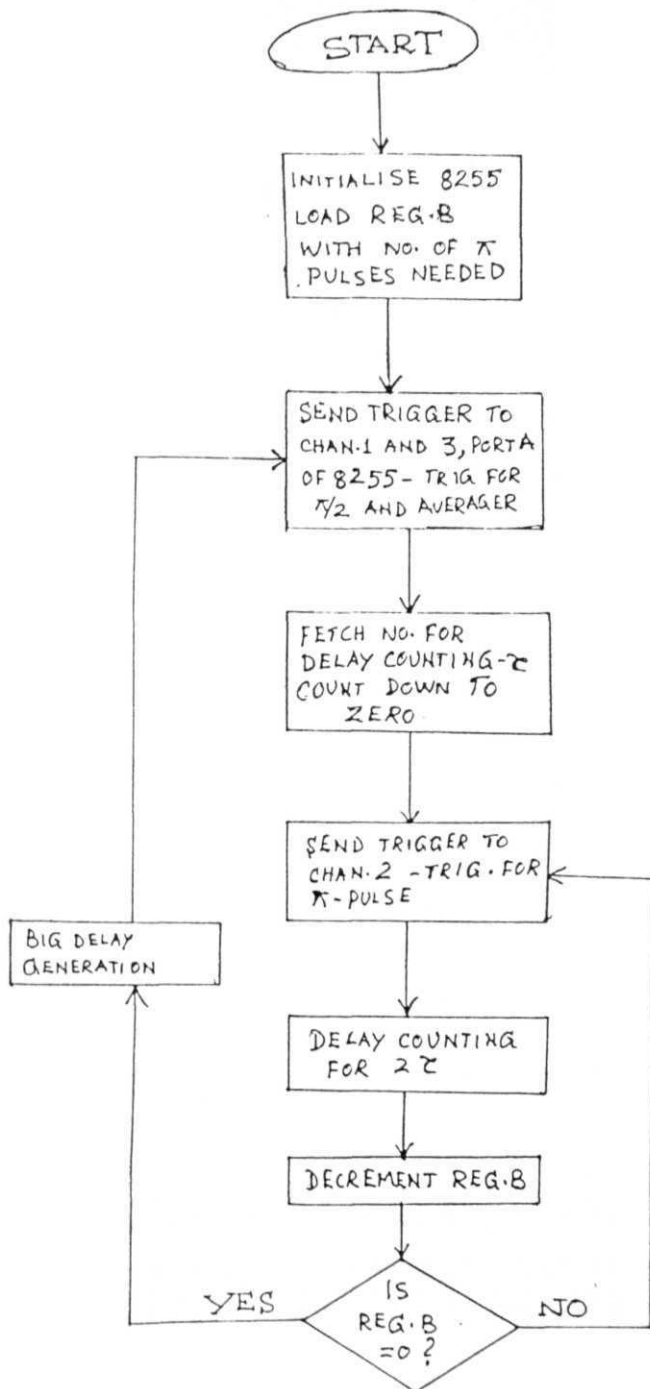
---

509B	<b>JMP</b>	C3
<b>509C</b>	80	80
509D	50	50
<b>509</b>	E    RET	C9

---

I. S. S		
5150	LHLD <b>2</b>	A
5151	75	75
5152	52	52
5153	SHLD <b>FB</b>	
5154	70	70
5155	52	52
5156	<b>MVI</b> A	3E
5157	08	08
5158	SIM	30
5159	<b>EI</b>	FB
<b>515A</b>	JMP	C3
515B	45	45
<b>515C</b>	50	50

---



INITIALISE 8255  
LOAD REG. B  
WITH NO. OF  $\pi$   
PULSES NEEDED

SEND TRIGGER TO  
CHAN.1 AND 3, PORT A  
OF 8255 - TRIG FOR  
T/2 AND AVERAGER

FETCH NO. FOR  
DELAY COUNTING- $\pi$   
COUNT DOWN TO  
ZERO

SEND TRIGGER TO  
CHAN. 2 - TRIG. FOR  
 $\pi$ -PULSE

## BIG DELAY GENERATION

DELAY COUNTING  
FOR  $2\tau$

DECREMENT REG.8

YES

REG. B  
= 0 ?

NO

### FLOW DIAGRAM FOR CARR-PURCELL SEQUENCE

# P R O G R A M : 4 ASSEMBLY LISTING OF CARR-PURCELL SEQUENCE

PART 1 : VERSION : 1 CODE : 4 - 1.1

ADD.	MNEM.	OPCOD.	ADD.	MNEM.	OPCOD.	ADD.	MNEM.	OPCOD.	ADD.	MNEM.	OPCOD.
5000	MVI A	3E	501D	50		503B	DCR B	05	I.S.S		
5001	OB	0B	501E	LHLD	2A	503C	JNZ	C2	5150	LHLD	2A
5002	SIM	30	501F	70		503D	21	21	5151	75	75
5003	E1	FB	5020	50		503E	50	50	5152	50	50
5004	MVI A	3E	5021	MVI A	3E	503F	CALL $\tau$ 2	CD	5153	SHLD	22
5005	80	80	5022	06	06	5040	00	00	5154	70	70
5006	OUT	D3	5023	OUT	D3	5041	51	51	5155	50	50
5007	07	07	5024	04	04	5042	SHLD	22	5156	MVI A	3E
5008	LXI H	21	5025	MVIA	3E	5043	75	75	5157	08	08
5009	00	00	5026	00	00	5044	50	50	5158	SIM	30
500A	52	52	5027	OUT	D3	5045	LHLD	2A	5159	E1	FB
500B	SHLD	22	5028	04	04	5046	70	70	515A	JMP	C3
500C	70	70	5029	CALL $\tau$ 2	CD	5047	50	50	515B	OE	OE
500D	50	50	502A	00	00	5048	CALL $\tau$ 2	CD	515C	50	50
500E	MVIB	06	502B	51	51	5049	00	00			
500F	0A	0A	502C	SHLD	22	504A	51	51			
5010	MVIA	3E	502D	75	75	504B	SHLD	22			
5011	01	01	502E	50	50	504C	75	75			
5012	OUT	D3	502F	LHLD	2A	504D	50	50			
5013	04	04	5030	70	70	504E	LHLD	2A			
5014	MVIA	3E	5031	50	50	504F	70	70			
5015	00	00	5032	CALL $\tau$ 2	CD	5050	50	50			
5016	OUT	D3	5033	00	00	5051	JMP	C3			
5017	04	04	5034	51	51	5052	OE	OE			
5018	CALL $\tau$ 2	CD	5035	SHLD	22	5053	50	50			
5019	00	00	5036	75	75						
501A	51	51	5037	50	50						
501B	SHLD	22	5038	LHLD	2A						
501C	75	75	5039	70	70						
			503A	50	50						

## A P P E N D I X II

This appendix contains the listing of the following programs developed as a part of the automation of the spectrometer. The programs use both GPIB and RS-232-C standard interfaces to communicate between different devices.

1. Program establishing contact between PC,  $\mu$ P based pulse programmer and the digitizer for transfer of relevant parameters of experiment and collection of data.
2. Program to run the automated experiment for T measurement using the inversion recovery sequence.
3. Program to run the automated experiment for T measurement using saturation burst sequence.
4. Program to run the automated experiment for T measurement using Hahn echo sequence. Program automatically searches for the peak values of the echoes as a function of delay time, **and** uses this data to calculate T .

These programs are sample listings from a group developed as a part of automation of the pulsed NMR facility. Several other programs were also developed with different specific tasks to perform, including automatic search for NQR resonances in a user defined range of frequency, programs for ZSEEM (Zeeman Spin Echo Envelope Modulation) experiments in NQR, automation of a Field Cycling - NMR spectrometer, etc.

P R O G R A M   N O : 1

```

1      CLEAR ,59745!      ' BASIC DECLARATIONS
2      IBINIT1 = 59745!
3      IBINIT2 = IBINIT1 + 3      'Lines 1 through 6 MUST be included in your
program.
4      BLOAD "bib.m",IBINIT1
5      CALL IBINIT1(IBFIND,IBTRG,IBCLR,IBPCT,IBSIC,IBLOC,IBPPC,IBBNA,IBONL,
IBRSC,BSRE,IBRSV,IBPAD,IBSAD,IBIST,IBDMA,IBEOS,IBTMO,IBEOT,IBRDF,IBWRTF)
6      CALL IBINIT2(IBGTS,IBCAC,IBWAIT,IBPOKE,IBWRT,IBWRTA,IBCMD,IBCMDA,IBRD,IBRDA,
IBSTOP,IBRPP,IBRSP,IBDIAG,IBXTRC,IBRDI,IBWRTI,IBRDIA,IBWRTIA,IBSTA%,IBERR%,IBCNT%)
10     BOARD$ = "GP1B0" : CALL IBFIND (BOARD$,BRD%)
11     DEVICE$ = "SCOPE" : CALL IBFIND(DEVICE$,DEV%)
50     CLS
60     REM
70     REM
80     REM      *****
90     REM      * THE PROGRAM ESTABLISHES RS-232-C COMMUNICATION AND TRANSFERS *
100    REM      * THE SUITABLE NUMBERS TO THE PULSE PROGRAMMER TO GENERATE DELAY *
110    REM      * BETWEEN PULSES, THE VALUES OF DELAYS AND THE ORDER BEING *
120    REM      * CHOSEN BY THE USER.
130    REM      + + + + +
140    REM      + REFER PROGRAM 1-1.5 OF MF-III IN PKR-1
150    REM      + + + + +
160    REM      + PROGRAM FOR TWO PULSE SEQUENCE
170    REM      + + + + +
180    REM      - - - - -
190    REM      | BLOCK 1
200    REM      | - - - - -
210    REM      |
220    REM      | THIS BLOCK FINDS OUT THE REPETITION RATE OF THE PULSE SEQUENCE.
230    REM      | IN AN EXPERIMENT LIKE T1 MEASUREMENT A TYPICAL SEQUENCE USED IS
240    REM      | THE (PI - TAU - PI/2) - 5T1 - (PI - TAU... SEQUENCE. HERE FOR
250    REM      | INSTANCE THE REPETITION RATE IS 5 x T1. THIS VALUE MUST BE GIVEN
260    REM      | BY THE USER.
270    REM      | - - - - -
280    REM
290    REM
300    INPUT "THE REPETITION RATE IN MILLI SECONDS ",RATE
310    PRINT
320    INPUT "HOW MANY NO. OF AVERAGES";AV$
330    PRINT
340    INPUT "GIVE THE NAME OF THE FILE WHERE THE WAVEFORM IS TO BE
STORED ",N$
350    PRINT
360    REM
370    REM      - - - - -
380    REM      | END OF BLOCK - 1
390    REM      | - - - - -
400    REM
410    REM
420    REM      - - - - -
430    REM      | BLOCK - 2
440    REM      | - - - - -
450    REM      | THIS BLOCK CONTAINS THREE SUBROUTINES FOR THE CALCULATION OF
460    REM      | SUITABLE NUMBERS FOR EACH DELAY VALUE THE USER CHOOSES, WHICH

```

```

470 REM : ARE NAMED AS NC, ND AND NE. THESE ARE THE NUMBERS TO BE PASSED :
480 REM : ON TO THE PULSE PROGRAMMER FOR DELAY COUNTING. :
490 REM : :
500 REM : REFERENCE TO ALGORITHMS OF THE SUBROUTINES :
510 REM : Algorithm for calculating NC, ND AND NE. :
520 REM : in PKR - 1 :
530 REM : :
540 REM : -----
550 REM :
560 REM :
570 REM * PROGRAM FOR CALCULATION OF NC, ND, NE FOR VARIOUS VALUES OF TAU *
580 DIM T(50),C(50),D(50),E(50)
590 T(1) = RATE
600 INPUT "ENTER THE NO. OF TAU VALUES YOU WANT ", A
610 B = A
620 FOR K = 2 TO (A+1)
630 S$ = STR$(K-1)
640 PRINT "PLEASE GIVE THE TAU VALUE NO: " + S$ + " IN MILLI SECONDS"
650 INPUT T(K)
660 NEXT K
670 PRINT "THE FOLLOWING ARE THE TAU VALUES YOU ENTERED"
680 PRINT "IF YOU WANT TO GIVE A NEW SET ENTER Y"
690 PRINT "IF NOT PRESS ENTER TO CONTINUE"
700 TAU$ = "TAU"
710 FOR J = 1 TO A
720 L$ = TAU$ + STR$(J) : M$ = "MILLI SECONDS"
730 PRINT L$ TAB(20) T(J+1);M$
740 NEXT J
750 INPUT CON$
760 IF CON$ = "Y" THEN GOTO 600
770 PERIOD = 3.27E-07
780 RANGE1 = 1.22428 : RANGE2 = 303.5783 : RANGE3 = 76980.43
790 FOR I = 1 TO (A+1)
800 IF T(I) <= RANGE1 THEN GOTO 860
810 IF T(I) <= RANGE2 THEN GOTO 950
820 IF T(I) <= RANGE3 THEN GOTO 1090
830 NEXT I
840 GOTO 1250
850 REM *** SUBROUTINE RANGE1 ***
860 FIRST = 174 * PERIOD
870 T = T(I) * .001
880 LEFT = T - FIRST
890 NE1 = LEFT/(14*PERIOD)
900 NE = INT(NE1)
910 E(I) = NE
920 GOTO 830
930 REM ***** SUBROUTINE RANGE1 ENDS *****
940 REM *** SUBROUTINE RANGE2 ***
950 T = T(I) * .001
960 TERM1 = 174 * PERIOD
970 LEFT1 = T - TERM1
980 ND1 = LEFT1/ (3606*PERIOD)
990 ND = INT(ND1)
1000 NEWT = TERM1 + (3606 * PERIOD * ND)
1010 DELSTAR1 = T - NEWT
1020 REM
1030 NE1 = DELSTAR1/(14*PERIOD)
1040 NE = INT(NE1)
1050 D(I) = ND : E(I) = NE

```



```

1060      GOTO 830
1070      REM ***** SUBROUTINE RANGE2 ENDS *****
1080      REM *** SUBROUTINE RANGE3 ***
1090      T = T(1) * .001
1100      TERM1 = 174 * PERIOD
1110      T11 = T - TERM1
1120      NC1# = T11/(919572!* PERIOD)
1130      NC = INT(NC1#)
1140      NEWT1# = TERM1 + (919572! * PERIOD * NC)
1150      DELSTAR1# = T - NEWT1#
1160      ND1# = DELSTAR1#/(3606 * PERIOD)
1170      ND = INT(ND1#)
1180      NEWT2# = (3606 * PERIOD * ND)
1190      DELSTAR2# = DELSTAR1# - NEWT2#
1200      NE1# = DELSTAR2#/(14*PERIOD)
1210      NE = INT(NE1#)
1220      C(I)=NC :D(I)=ND :E(I)=NE
1230      GOTO 830
1240      REM **** SUBROUTINE RANGE3 ENDS ****
1250      DIM CH(A+1),CL(A+1),DH(A+1),DL(A+1),EH(A+1),EL(A+1)
1260      G1# = CHR$(A+1)
1270      AM# = CHR$(1)
1280      FOR M = 1 TO (A+1)
1290      CH(M) = 0 :DH(M) = 0 :EH(M) = 0
1300      IF C(M) < 127 GOTO 1320
1310      CL(M) = C(M) - 127 : CH(M) = 127 :GOTO 1330
1320      CL(M) = C(M)
1330      IF D(M) < 127 GOTO 1350
1340      DL(M) = D(M) - 127 : DH(M) = 127 :GOTO 1360
1350      DL(M) = D(M)
1360      IF E(M) < 127 GOTO 1380
1370      EL(M) = E(M) - 127 : EH(M) = 127 :GOTO 1390
1380      EL(M) = E(M)
1390      NEXT M
1400 REM -----
1410 REM                               END OF BLOCK - 2
1420 REM
1430 REM
1440 REM -----
1450 REM                               BLOCK - 3
1460 REM
1470 REM : THE RS-232-C COMMUNICATION IS ESTABLISHED AND THE SUITABLE
1480 REM : NUMBERS ARE TRANSFERED TO THE PULSE PROGRAMMER.
1490 REM :
1500 REM
1510      OPEN "COM1:300,N,7,1,CS,DS" AS #1
1520      PRINT #1,G1#;:CLOSE #1
1530      FOR J = 1 TO (A+1)
1540      OPEN "COM1:300,N,7,1,CS,DS" AS #1
1550      CH# = CHR$(CH(J)):PRINT #1,CH#;
1560      CL# = CHR$(CL(J)):PRINT #1,CL#;
1570      DH# = CHR$(DH(J)):PRINT #1,DH#;
1580      DL# = CHR$(DL(J)):PRINT #1,DL#;
1590      EH# = CHR$(EH(J)):PRINT #1,EH#;
1600      EL# = CHR$(EL(J)):PRINT #1,EL#;
1610      CLOSE #1
1620      NEXT J
1630 REM

```

```

1640 REM -----
1650 REM                      END OF BLOCK - 3
1660 REM -----
1670 REM
1690 REM -----
1700 REM :                      BLOCK - 4                      :
1710 REM -----
1720 REM :   IN THIS BLOCK THE PROGRAM TRIGGERS THE GENERATION OF THE PULSE :
1730 REM :   BY THE PULSE PROGRAMMER WITH THE CONSENT OF THE USER. AFTER THE :
1740 REM :   PULSE SEQUENCE STARTS WITH ONE DELAY VALUE, THE PROGRAM WAITS :
1750 REM :   FOR USER'S INTERRUPTION TO CHANGE THE DELAY VALUE TO THE NEXT :
1760 REM :   VALUE FROM THE LIST OF VALUES CHOSEN BY THE USER,ALREADY. :
1770 REM :   AFTER,ALL THE DELAY VALUES ARE EXHAUSTED THE PROGRAM TRIES TO :
1780 REM :   KNOW IF THE USER WOULD LIKE TO REPEAT THE EXPERIMENT WITH THE :
1790 REM :   SAME PARAMETERS AS BEFORE OR THE USER WANTS TO GIVE A NEW SET OF :
1800 REM :   PARAMETERS. BASED ON THE ANSWER TO THE QUERY THE PROGRAM BRANCHES :
1810 REM :   TO THE APPROPRIATE PART. :
1820 REM : :
1830 REM -----
1840                      OPEN "COM1:300,N,7,1,CS,DS" AS #1
1850                      PRINT #1,AM$;:CLOSE #1
1860 COUNT = 1
1870 GOSUB 2110
1880 IF COUNT = A GOTO 1960
1890                      OPEN "COM1:300,N,7,1,CS,DS" AS #1
1900                      ON COM(1) GOSUB 1930
1910                      COM(1) ON
1920                      GOTO 1920
1930                      PRINT #1,AM$;:CLOSE #1:BEEP
1940                      COUNT = COUNT +1
1950                      GOTO 1870
1960                      PRINT "DO YOU WANT TO REPEAT THE EXPERIMENT "
1970                      INPUT "WITH THE SAME SETTINGS (YES/NO)";RES$
1980                      IF RES$ = "NO" GOTO 1990 : A = B : GOTO 2000
1990                      AM$ = CHR$(0)
2000                      OPEN "COM1:300,N,7,1,CS,DS" AS #2
2010                      PRINT #2,AM$; : CLOSE #2
2020                      IF RES$ = "NO" GOTO 50
2030                      GOTO 1840
2040 REM
2050 REM
2060 REM + + + + +
2070 REM                      END OF BLOCK - 4
2080 REM                      AND
2090 REM                      END OF PROGRAM
2100 REM + + + + +
2110 FOR I = 1 TO 3000 : NEXT I
2120 QUERY$ = "ACQ? SWP" : ANS$ = SPACE$(24)
2130 CALL IBWRT(DEV%,QUERY$) : CALL IBRD(DEV%,ANS$)
2140 CMD$ = "ACQ HSR:AVE,NUM: "+AV$
2150 PRINT CMD$
2160 CALL IBWRT(DEV%,CMD$)
2170 BIT1 = VAL(AV$) : PRINT BIT1
2180 FOR JK = 1 TO 5000: NEXT JK
2190 CALL IBWRT(DEV%,QUERY$) : CALL IBRD(DEV%,ANS$)
2200 ANS1 = VAL(RIGHT$(ANS$,3)):PRINT ANS1
2210 IF ANS1 = BIT1 GOTO 2240
2220 FOR PK = 1 TO 5000 : NEXT PK
2230 GOTO 2190

```

```
2240 FILE$ = N$ + STR$(COUNT)
2250 SOUR$ = "DATA SOU:ACQ" : CALL IBWRT(DEV%,SOUR$)
2260 CHAN$ = "DATA CHA:CH2" : CALL IBWRT(DEV%,CHAN$)
2270 ENCD$ = "DATA ENC:HEX" : CALL IBWRT(DEV%,ENCD$)
2280 WAVE$ = "WAVFRM?" : CALL IBWRT(DEV%,WAVE$)
2290 CALL IBRDF(DEV%,FILE$)
2300 RETURN
```

PROGRAM NO: 2

```

1      CLEAR ,35000!          ' BASIC Declarations
2      IBINIT1 = 35000!
3      IBINIT2 = IBINIT1 + 3   ' Lines 1 through 6 MUST be included in your
program.
4      BLOAD "bib.m",IBINIT1
5      CALL IBINIT1(IBFIND,IBTRG,IBCLR,IBPCT,IBSIC,IBLOC,IBPPC,IBBNA,IBONL,IBRSC,
IBRSRE,IBRSV,IBPAD,IBSAD,IBIST,IBDMA,IBEOS,IBTMO,IBEOT,IBDRD,IBWRT)
6      CALL IBINIT2(IGTS,IBCAC,IBWAIT,IBPOKE,IBWRT,IBWRTA,IBCMD,IBCMDB,IBRD,
IBRDA,IBSTOP,IBRPPE,IBRSP,IBDIAG,IBXTRC,IBREDI,IBWRTI,IBRDIA,IBWRTIA,IBSTA%,IBERR%,
IBCNT%)
10     BRD$ = "GPIBO" : CALL IBFIND(BRD$,BRD%)
15     SCOPE$ = "DEV3" : CALL IBFIND(SCOPE$,SCOPE%)
20     DEV$ = "DEV2" : CALL IBFIND(DEV$,DELAY%)
25     CLS
100    REM X X X X X X X X X X X X PROGRAM TEE ONE X X X X X X X X X X X
110    REM INVERSION RECOVERY SEQUENCE
115    REM X X X X X X X X X X X X X X X X X X X X X X X X X X X X X
120    REM * * * * PART ONE * * * *
130    REM THIS PART OF THE PROGRAM DOES THE FOLLOWING
140    REM 1. ASKS THE USER FOR TAU VALUES IN MILLI SECONDS.
170    REM 2. ASKS FOR THE REPETITION RATE i.e. 5T1
180    REM 3. ASKS FOR THE NO. OF AVERAGES TO BE DONE.
210    REM 4. ASKS FOR THE FILE NAME IN WHICH THE WAVEFORM IS TO BE STORED.
240    REM * * * - - - - - * * * *
250    REM + + + + + PART ONE BEGINS + + + + +
260    REM <=====> DECLARATIONS <=====>
270    REM DIM TAU(100),A(30),B(30),ITAU(100)
290    DIM Y(100),YL(100),E(100)
300    DIM CX(100),CY(100),FX(100),FY(100),T$(30)
310    DIM JTAU(100)
320    AFLAG = 0
330    REM
340    REM
350    REM <=====>-----<=====>
360    REM
370    REM ???????????????? QUERIES ??????????????????
380    REM INPUT "INPUT VALUES FROM KEYBOARD OR FILE ? ENTER CHOICE (K/F)" ",KF$"
400    IF (KF$ = "K") OR (KF$ = "k") THEN GOTO 520
410    OPEN "INVDATA" FOR INPUT AS #3
420    INPUT #3, TAUI : TAUI = TAUI
430    FOR I = 1 TO TAUI
440        INPUT #3,TAU(I) : ITAU(I) = TAU(I)
450    NEXT I
460    INPUT #3, RATE
470    INPUT #3, AVERAGE
480    INPUT #3. WEIGHT
```

```

490 INPUT #3, FILENAME$
500 CLOSE #3
510 GOTO 870
520 OPEN "INVDATA" FOR OUTPUT AS #3
530 INPUT "HOW MANY TAU VALUES DO YOU HAVE "; TAU0 : TAU01 = TAU0
540 PRINT #3, SPC(5) TAU0
550 PRINT "GIVE THE TAU VALUES IN MILLI SECONDS "
560 FOR J = 1 TO TAU0
570 PRINT "TAU"+STR$(J)+" = ": INPUT TAU(J): PRINT
580 PRINT #3, SPC(10),TAU(J)
590 NEXT J
600 PRINT "THESE ARE THE TAU VALUES YOU GAVE " : PRINT
610 FOR K = 1 TO TAU0
620 PRINT "TAU"+STR$(K),TAB(20),TAU(K)
630 NEXT K
640 PRINT "ENTER TO PROCEED"
650 INPUT;QUE$
660 FOR LK = 1 TO TAU0 : ITAU(LK) = TAU(LK)
670 NEXT LK
680 INPUT "WHAT IS THE REPETITION RATE (GIVE IN SECONDS PLEASE)"; RATE :PRINT
690 PRINT #3, SPC(5),RATE
700 INPUT "HOW MANY NO. OF AVERAGES DO YOU NEED ";AVERAGE
710 PRINT #3, SPC(5),AVERAGE
720 PRINT
730 INPUT "GIVE THE WEIGHT FOR AVERAGING ";WEIGHT
740 PRINT #3, SPC(5),WEIGHT
750 PRINT
760 PRINT " GIVE THE FILE NAME IN WHICH THE WAVEFORM IS TO BE STORED"
770 PRINT
780 PRINT " YOU CAN GIVE THE COMPLETE PATH , IF YOU WANT TO SAVE THE "
790 PRINT
800 PRINT " FILE IN A DIRECTORY OTHER THAN THE CURRENT DIRECTORY "
810 PRINT
820 INPUT;FILENAME$
830 PRINT #3, SPC(5),FILENAME$
840 CLOSE #3
850 REM
860 REM ?????????????????? QUERIES END ??????????????????????????????
870 GOSUB 2320
880 WORD1$ = "P@132000000" : CALL IBWRT(DELAY%,WORD1$)
890 WORD2$ = "Q@131000000" : CALL IBWRT(DELAY%,WORD2$)
900 WORD3$ = "R@123000000" : CALL IBWRT(DELAY%,WORD3$)
910 WORD4$ = "S@113000000" : CALL IBWRT(DELAY%,WORD4$)
920 WORD5$ = "T@133000000" : CALL IBWRT(DELAY%,WORD5$)
930 REM
940 REM
950 REM MASTER ----- LOOP
960 LPRINT SPC(15) "TAU (m.sec)"SPC(15)"DELTA V (volts)"
970 OPEN "VOLTS" FOR OUTPUT AS #3
980 PRINT #3,SPC(15)"TAU (m.sec)" SPC(15)"DELTA V (volts) "
990 FOR JK = 1 TO TAU0
1000 REM
1010 IF TAU(JK) <= 9.998999 GOTO 1060
1020 IF TAU(JK) <= 99.999 GOTO 1070
1030 IF TAU(JK) <= 999.99 GOTO 1080
1040 IF TAU(JK) <= 9999.901 GOTO 1090
1050 IF TAU(JK) <= 99999! GOTO 1100
1060 GOSUB 1140 : GOTO 1110
1070 GOSUB 1290 : GOTO 1110

```

```

1080 GOSUB 1440 : GOTO 1110
1090 GOSUB 1590 : GOTO 1110
1100 GOSUB 1740 : GOTO 1110
1110 NEXT JK
1120 CLOSE #3 :IF AFLAG = 1 THEN GOTO 2890 ELSE GOTO 2620
1130 REM * * * * *
1140 REM SUBROUTINE RANGE 1
1150 REM
1160 D1 = TAU(JK) * 10000 : D11$ = STR$(D1)
1170 PART1$ = "P"
1180 PART2$ = CHR$(74-LEN(D11$))
1190 PART3$ = MID$(D11$,2) : PART4$ = "!"
1200 WORDP1$ = PART1$+PART2$+PART3$+PART4$
1210 CALL IBWRT(DELAY%,WORDP1$)
1220 CALL IBWRT(DELAY%,WORD1$)
1230 GOSUB 1920
1240 RETURN
1250 REM * * * * *
1260 REM SUBROUTINE WORKING PROPERLY.
1270 REM WWW SAVED IN THE NAME C:\GP1B-PC\T1R1.BAS AS AN ASCII FILE IN PC 1
1280 REM
1290 REM SUBROUTINE RANGE 2
1300 REM
1310 D2 = TAU(JK) * 1000 : D21$ = STR$(D2)
1320 PART1$ = "Q"
1330 PART2$ = "D"
1340 PART3$ = MID$(D21$,2) : PART4$ = "!"
1350 WORDQ1$ = PART1$+PART2$+PART3$+PART4$
1360 CALL IBWRT(DELAY%,WORDQ1$)
1370 CALL IBWRT(DELAY%,WORD2$)
1380 GOSUB 1920
1390 RETURN
1 4 0 0 R E M * * * * *
1410 REM WWW SUBROUTINE IS WORKING PROPERLY
1420 REM WWW SAVED IN THE NAME C:\GP1B-PC\T1R2.BAS IN PC1 AS AN ASCII FILE
1430 REM
1440 REM SUBROUTINE RANGE 3
1450 REM
1460 D3 = TAU(JK) * 100 : D31$ = STR$(D3)
1470 PART1$ = "R"
1480 PART2$ = "D"
1490 PART3$ = MID$(D31$,2) : PART4$ = "!"
1500 WORDR1$ = PART1$+PART2$+PART3$+PART4$
1510 CALL IBWRT(DELAY%,WORDR1$)
1520 CALL IBWRT(DELAY%,WORD3$)
1530 GOSUB 1920
1540 RETURN
1550 REM * * * * *
1560 REM WWW SUBROUTINE IS WORKING PROPERLY
1570 REM WWW SAVED IN THE NAME C:\GP1B-PC\T1R3.BAS IN PC1 AS AN ASCII FILE
1580 REM
1590 REM SUBROUTINE RANGE 4
1600 REM
1610 D4 = TAU(JK) * 10 : D41$ = STR$(D4)
1620 PART1$ = "S"
1630 PART2$ = "D"
1640 PART3$ = MID$(D41$,2) : PART4$ = "!"
1650 WORDS1$ = PART1$ + PART2$ + PART3$+PART4$
1660 CALL IBWRT(DELAY%,WORDSU)

```

```

1670 CALL IBWRT(DELAY%,WORD4%)
1680 GOSUB 1920
1690 RETURN
1700 REM + + + + +
1710 REN \\\ SUBROUTINE IS WORKING PROPERLY
1720 REM \\\ SAVED IN THE NAME C:\GP1B-PC\T1R4.BAS IN PC1 AS AN ASCII FILE
1730 REM
1740 REM SUBROUTINE RANGE 5
1750 REM
1760 D5 = TAU(JK) : D51$ = STR<(D5)
1770 PART1$ = "T"
1780 PART2$ = "D"
1790 PART3$ * MID$(D51$,2) : PART4$ = "!"
1800 WORDT1$ < PART1$+PART2$+PART3$+PART4$
1810 CALL IBWRT(DELAYX,WORDT1$)
1820 CALL IBWRT(DELAY%,WORD5%)
1830 GOSUB 1920
1840 RETURN
1850 REM + + + + +
1860 REM \\\ SUBROUTINE IS WORKING PROPERLY
1870 REM \\\ SAVED IN THE NAME C:\GP1B-PC\T1R5.BAS IN PC1 AS AN ASCII FILE
1880 REM
1890 REM
1900 REM SUBROUTINE WAVETRANS
1910 REM - - - - -
1920 MASKX = &H4000 : WAIT1% = 11 : TRIG$ = "O"
1930 CALL IBTHO(BRD%,WAIT1%) : CALL IBWAIT(BRD%,MASK%)
1940 CMD$ = "ACQ REP:AVE,HSR:AVE,LSR:AVE,SCA:AVE,SMO:ON,VEC:ON,NUM:"
1950 VER$ = STR<(AVERAGE):CMD1$ = CMD$ + MID*(VER$,2)
1960 WEIT$ = ",WEI:"+MID$(STR$(WEIGHT),2)
1970 CMD2$ = CMD1$ * WEIT$
1980 CALL IBWRT(SCOPEX,CMD2t)
1990 QUERY$ = "ACQ? SWP" : CALL IBWRT(SCOPEX,QUERY%)
2000 ANS$ = SPACE*(30) : CALL IBRD(SCOPEX,ANS%)
2010 FOR R = 1 TO AVERAGE
2020 ON COM(1) GOSUB 2060 : COM(1) ON
2030 OPEN"COM1:300,N,7,1,CS,DS" AS #1
2040 PRINT #1,TRIG$;
2050 GOTO 2050
2060 CLOSE #1 : COM(1) OFF : RETURN 2070
2070 GOSUB 2390
2080 NEXT R
2090 QUERY$ = "ACQ? SWP" : CALL IBWRT(SCOPEX,QUERY%)
2100 ANS$ = SPACE*(30) : CALL IBRD(SCOPEX,ANS%) : SWEEPX = VAL(MID$(ANS$,22))
2110 IF SWEEPX = AVERAGE THEN GOTO 2140
2120 OPEN"COM1:300,N,7,1,CS,DS" AS #2 : PRINT #2,TRIG$; : CLOSE #2
2130 GOSUB 2390 : GOTO 2090
2140 REM ~~~~~ WAVEFORM TRANSFER DETAILS ~~~~~
2150 REM ~~~~~
2160 IF (JK <> 1) OR (AFLAG = 1) THEN GOTO 2190
2170 CLS:INPUT "PLEASE SET THE CURSORS AND ENTER TO PROCEED",ABC$
2180 CLS:PRINT SPC(15)"TAU (m.sec)"SPC(15)"DELTA V (volts)"
2190 CMD$ = "DELTA V? VAL" : CALL IBWRT(SCOPEX,CMD%)
2200 VOLT$ = SPACE$(35) : CALL IBRD(SCOPEX,VOLT!)
2210 PRINT SPC(20)TAU(JK)TAB(45)VAL(MID$(VOLT$,14))
2220 PRINT #3,SPC(20)TAU(JK)TAB(45)VAL(MID$(VOLT$,14))
2230 IF AFLAG = 0 THEN A(JK) = VAL(MID$(VOLT$,14))
2240 IF AFLAG < 1 THEN B(JK) = VAL(MID$(VOLT$,14))
2250 IF AFLAG = 1 THEN GOTO 2270

```

[illegible]



```

2790 PRINT "          THE NEW TAU YOU HAVE GIVEN.  • : PRINT
2800 PRINT » GIVE THE NO. OF TAU VALUES YOU WANT TO GIVE ": INPUT TAUO
2810 PRINT
2820 PRINT "GIVE THE TAU VALUES IN MILLI SECONDS PLEASE ":PRINT
2830 FOR KK = 1 TO TAUO
2840 PRINT "TAU"+STR$(KK) : INPUT TAU(KK)
2850 NEXT KK
2860 FOR LN = 1 TO TAUO : JTAU(LN) = TAU(LN) : NEXT LN
2870 AFLAG = 1
2880 GOTO 970
2890 KOUNT = TAU01
2900 FOR M = 1 TO TAUO
2910 F = 0
2920     FOR L = 1 TO TAU01
2930         IF ITAU(L) <> JTAU(M) THEN GOTO 2950
2940         A(L) = B(M): F = 1
2950     NEXT L
2960     IF F = 1 GOTO 3000
2970     KOUNT = KOUNT + 1
2980     ITAU(KOUNT) = JTAU(M)
2990     A(KOUNT) = B(M)
3000     NEXT M
3010     TAU01 = KOUNT : AFLAG = 0
3020     LPRINT SPC(15) "TAU(m.sec)" SPC(15) "M(tau) (volts)"
3030     FOR N = 1 TO TAU01
3040         LPRINT SPC(20) ITAU(N) TAB(45) A(N)
3050     NEXT N
3060     GOTO 2620
3070     FOR J = 1 TO TAU01
3080         AM IN = ITAU(J) : K = J
3090         AAMIN = A(J)
3100         FOR I = J TO TAU01
3110             IF ITAU(I) >= AMIN THEN GOTO 3140
3120             AM IN = ITAU(I) : K = I
3130             AAMIN = A(I)
3140         NEXT I
3150         ATEMP = ITAU(J)
3160         ITAU(J) = AMIN
3170         ITAU(K) = ATEMP
3180         AATEMP = A(J)
3190         A(J) = AAMIN
3200         A(K) = AATEMP
3210     NEXT J
3220     CLS
3230     PRINT SPC(15) "TAU(m.sec)" SPC(15) "A(TAU) (volts)"
3240     FOR S = 1 TO TAU01
3250         PRINT SPC(20) ITAU(S) TAB(45) A(S)
3260     NEXT S : PRINT
3270     NN = 0
3280     PRINT "THE FIRST N A(TAU)'s WILL BE NEGATIVED. PLEASE ENTER N "
3290     INPUT NN
3300     FOR T = 1 TO NN
3310         IF A(T) < 0 THEN GOTO 3330
3320         A(T) = -A(T)
3330     NEXT T
3340     N » TAU01
3350     REM program for t1 cal
3360     PRINT:PRINT:PRINT:PRINT
3370     CLS:INPUT "NO. OF POINTS PLEASE ";N0

```

```

3380     INPUT "yo please";Y0
3390     S1=0:S2=0:S3=0:S4=0:S5=0
3400 INPUT ZX
3410     FOR I = 1 TO NO
3420     YL(I)=LOG(Y0-A(I))
3430     S1=S1+ITAU(I);S2=S2+YL(I);S3=S3+ITAU(I)^2
3440     S4=S4+ITAU(I)*YL(I);S5=S5+YL(I)^2
3450 NEXT I
3460     D=S3-(S1^2)/NO
3470     M=(S4-S1*S2/NO)/D
3480     B=(S2*S3-S1*S4)/(D*NO)
3490     D1=SQR((S3-(S1^2)/NO)*(S5-(S2^2)/NO));R=(S4-(S1*S2)/NO)/D1
3500     S6=0:S7=0
3510     FOR I=1 TO NO
3520     Y(I)=M*ITAU(I)+B
3530     E(I)=Y(I)-YL(I)
3540     S6=S6+E(I)^2
3550     S7=S7+(E(I)/Y(I))^2
3560 NEXT I
3570 PRINT "x(i)";TAB(10);"ym(i)";TAB(20);"yl(i)";TAB(40);"y(i)";TAB(60);"e(i)"
3580 FOR I=1 TO NO
3590     YL(I) = (INT(YL(I)*1000))/1000
3600     Y(I) = (INT(Y(I)*1000))/1000
3610     PRINT ITAU(I);TAB(10);A(I);TAB(20);YL(I);TAB(40);Y(I);TAB(60);E(I)
3620 NEXT I
3630     SD=SQR(S6/NO)
3640     DY=SQR(S7/NO)
3650     T1=1/M
3660     DT=DY*T1:PRINT:PRINT
3670     PRINT "t1=";T1;TAB(50);"error=";DT:PRINT:PRINT
3680 PRINT"rmsd = ";SD;TAB(50);"corr.=";R
3690 GOSUB 5220
3700 FOR I=1 TO NO
3710     CX(I)=ITAU(I);CY(I)=YL(I):NEXT I
3720 GOTO 3880
3730 SCREEN 0
3740 INPUT "how many bad data points do you have";MM
3750 PRINT:PRINT:PRINT "type the x(i)'s of the bad points"
3760 FOR I=1 TO MM
3770     INPUT"";X1(I)
3780 FOR J=1 TO NO
3790     IF ITAU(J)<>X1(I) THEN 3850
3800     IF J=NO THEN 3840
3810     FOR K=J TO NO-1
3820     ITAU(K) = ITAU(K+1):A(K)=A(K+1)
3830 NEXT K
3840 NO=NO-1
3850 NEXT J
3860 NEXT I
3870 GOTO 3390
3880 REM variables (exptl) are cx and cy
3890 REM variables (calc.) are fx and fy
3900 REM necessary changes are to be made in the main programme
3910 PRINT:PRINT
3920 PRINT "DO YOU NEED COMPUTED CURVE (yes/no)"
3930 PRINT:PRINT
3940 INPUT" ";Q$
3950 IF Q$="yes" THEN TQ=1
3960 IF Q$="no" THEN TQ=0

```

```

3970 PRINT:PRINT:PRINT
3980 PRINT"do you want to specify limits (yes/no)?"
3990 INPUT " ";K$
4000 IF K$="yes" GOTO 4020
4010 GOTO 4070
4020 INPUT " xmin:";X0
4030 INPUT"xmax:";X9
4040 INPUT"ymin:";Y0
4050 INPUT"ymax:";Y9
4060 GOTO 4170
4070 X9=CX(1):X0=CX(1):Y9=CX(1):Y0=CX(1)
4080 FOR I= 1 TO NO
4090 IF CX(1)>X9 THEN X9=CX(1)
4100 IF CX(1)<X0 THEN X0=CX(1)
4110 IF CY(1)>Y9 THEN Y9=CX(1)
4120 IF CY(1)<Y0 THEN Y0=CX(1)
4130 NEXT
4140 DX=(X9-X0)/10:DY=(Y9-Y0)/10
4150 X9=X9+DX:Y9=Y9+DY
4160 X0=X0-DX:Y0=Y0-DY
4170 IX=570/(X9-X0):IY=160/(Y9-Y0)
4180 FOR I=1 TO N
4190 CX(1)=50+(CX(1)-X0)*IX
4200 CY(1)=170-(CY(1)-Y0)*IY
4210 NEXT
4220 PRINT:PRINT:PRINT
4230 INPUT "title of the plot ";T$
4240 PRINT:PRINT:PRINT
4250 PRINT "after examining the plot"
4260 PRINT:PRINT
4270 PRINT "PRESS Y IF A HARDCOPY IS NEEDED"
4280 PRINT:PRINT
4290 PRINT "r if data is to be processed"
4300 PRINT:PRINT
4310 PRINT"otherwise any key"
4320 PRINT:PRINT
4330 CLS
4340 SCREEN 2
4350 LINE (10,5) - (630,190),,B
4360 LINE (35,170)-(620,170)
4370 LINE (50,10)-(50,185)
4380 XL=107
4390 FOR I= 1 TO 10
4400 LINE (XL,168) - (XL,172)
4410 XL=XL+57
4420 NEXT
4430 YL=10
4440 FOR I=1 TO 10
4450 LINE(48,YL)-(52,YL)
4460 YL=YL+16
4470 NEXT
4480 XL=107:YK=20
4490 FOR I= 1 TO 4
4500 XC(1)=X0+(XL-50)/IX
4510 XL=XL+65
4520 NEXT
4530 YK=10
4540 FOR I= 4 TO 1 STEP -1
4550 YC(1)=Y0+(170-YK)/IY

```

```

4560      YK=YK+40
4570      NEXT
4580      FOR I= 1 TO 4
4590      X1(I)=XC(I)
4600      NEXT
4610      I=1
4620      XQ(I)=INT(ABS(XC(I)))
4630      X1(I)=XC(I)
4640      L=0:K=0
4650      IF XQ(I)=0 THEN XC(I)=XC(I)*10:L=L+1:XQ(I)=INT(ABS(XC(I))):GOTO 4650
4660 IF XQ(I) > 10 THEN XC(I)=XC(I)/10:K=K+1:XQ(I)=INT(ABS(XC(I))):GOTO 4660
4670 IF L=0 THEN PP = K
4680 IF K=0 THEN PP = -L
4690 IF L=0 AND K=0 THEN PP=0
4700      PP$=STR$(PP)
4710      FOR I= 1 TO 4
4720      X1(I)=X1(I)*(10^(-PP))
4730      X1(I)=(INT(X1(I)*100))/100
4740      NEXT
4750      FOR I= 1 TO 4
4760      Y1(I)=YC(I)
4770      NEXT
4780      I=1
4790      YQ(I)=INT(ABS(YC(I)))
4800      Y1(I)=YC(I)
4810      L=0:K=0
4820      IF YQ(I)=0 THEN YC(I)=YC(I)*10:L=L+1:YQ(I)=INT(ABS(YC(I))):GOTO 4820
4830      IF YQ(I)>10 THEN YC(I)=YC(I)/10:K=K+1:YQ(I)=INT(ABS(YC(I))):GOTO 4830
4840      IF L=0 THEN PP=K
4850      IF K=0 THEN PP=-L
4860      IF L=0 AND K=0 THEN PP=0
4870      PP$=STR$(PP)
4880      FOR I=1 TO 4
4890      Y1(I)=Y1(I)*(10^(-PP))
4900      Y1(I)=(INT(Y1(I)*10))/10
4910      NEXT
4920      QX=87
4930      FOR I= 1 TO 4
4940      X1$(I)=STR$(X1(I))
4950      QX=QX+65
4960      NEXT
4970      QY=126
4980      FOR I= 1 TO 4
4990      Y1$(I)=STR$(Y1(I))
5000      QY=QY-40
5010      NEXT
5020      FOR I= 1 TO NO
5030      LINE (CX(I)-1,CY(I)-1) - (CX(I)+1,CY(I)+1),,B
5040      NEXT
5050      IF TQ=1 THEN GOTO 5070
5060      GOTO 5190
5070      FOR I= 1 TO NO
5080      FX(I)=50+(ITAU(I)-X0)*IX
5090      FY(I)=170-(Y(I)-Y0)*IY
5100      NEXT
5110      M=NO-1
5120      FOR I= 1 TO M
5130      LINE (FX(I),FY(I))-(FX(I+1),FY(I+1))
5140      NEXT

```

```

5150     YY=2«(ABS(SD))«(ABS(IY))
5160     LINE (600,100)-(600,100-YY)
5170     LINE (599,100-YY) - (601,100-YY)
5180     LINE (599,100) - (601,100)
5190     INPUT ZX
5200     SCREEN 0
5210     GOTO 5410
5220 REM -10700
5230     AX=0:AY=0
5240     FOR I= 1 TO NO
5250     AX=AX+ITAU(I):AY=AY+YL(I)
5260     NEXT 1
5270     AX=AX/NO:AY=AY/NO
5280     A1=0:A2=0:A3=0
5290     FOR I= 1 TO NO
5300     A1=A1+(YL(I)-AY)^2
5310     A2=A2+(ITAU(I)-AX)*(YL(I)-AY)
5320     A3=A3+(ITAU(I)-AX)^2
5330     NEXT
5340     S=(A1-(A2^2)/A3)/(NO-2)
5350     SB=S/(SQR(A3))
5360     PRINT "s=";S;"sb=";SB
5370     RR=ABS(SB*T1*T1)
5380     PRINT:PRINT "error in t1 =" ;RR
5390     SL = A2/A3 : SS = 1/SL : PRINT "t1 is " ;SS
5400     RETURN
5410     CLS
5420     PRINT "YOU HAVE THE FOLLOWING OPTIONS TO CHOOSE FROM: • : PRINT
5430     PRINT "      1. A HARD COPY OUTPUT OF THE T1 DATA " : PRINT
5440     PRINT "      2. MANIPULATION OF EXISTING DATA " : PRINT
5450     PRINT "      3. MODIFICATION OF THE EXPTL. PARAMETERS" : PRINT
5460     PRINT "      4.T1 FIT OF ENTIRE DATA SET " : PRINT
5470     PRINT "      PLEASE ENTER THE APPROPRIATE NUMBER FOR " : PRINT
5480     PRINT "      FOR THE OPTION YOU CHOOSE (1/2/3/4) " : PRINT
5490     INPUT OPT
5500     IF OPT = 1 THEN GOTO 5560
5510     IF OPT = 2 THEN GOTO 3730
5520     IF OPT = 3 THEN GOTO 2620
5530     IF OPT = 4 THEN GOTO 3370
5540     CLS : PRINT " GIVE THE APPROPRIATE NUMBER PLEASE (1/2/3) "
5550     PRINT : GOTO 5490
5560     INPUT "GIVE THE SAMPLE NAME AND TEMPERATURE ", SAMP$,TEMR
5570     LPRINT SPC(5) "SAMPLE IS " + SAMP$,TAB(50),"TEMP. ",TEMR," C" : LPRINT
5580     D* « DATE* : T* = TIME$
5590     LPRINT SPC(5), D$, TAB(50), T*
5600     LPRINT "x(i)";TAB(10);"ym(i)";TAB(20);"yl(i)";TAB(40);"y(i)";TAB(60);"e(i)"
5610     LPRINT:FOR I = 1 TO NO
5620     LPRINT ITAU(I);TAB(10);A(I);TAB(20);YL(I);TAB(40);Y(I);TAB(60);E(I)
5630     NEXT 1 : LPRINT
5640     PRINT "t1=";T1;TAB(50);"error=";DT:PRINT:PRINT
5650     LPRINT"rmsd=";SD;TAB(50);"corr.=";R
5660     LPRINT "s=";S;"sb=";SB
5670 LPRINT:LPRINT "error in t1 = ";RR
5680     LPRINT "t1 if " ;SS
5690     LPRINT: LPRINT " [tau,A(tau)] VALUES ARE STORED IN FILE VOLTS"
5700     LPRINT: LPRINT " WAVEFORMS ARE STORED IN • • FILENAME$. "X, WHERE"
5710     LPRINT: LPRINT " X = A,B,C,... etc. " :
5720     LPRINT: LPRINT "EXPTL. PARAMETERS ARE STORED IN FILE INVDATA"
5730     CLS : PRINT "IF YOU WANT TO DO THE EXPERIMENT AGAIN WITH THE "

```

```
5740 PRINT:PRINT "SAME PARAMETERS, ENTER C. "  
5750 PRINT:PRINT "IF YOU WANT TO QUIT, ENTER Q"  
5760 INPUT QUR$  
5770 IF (QUR$ = "Q") OR (QUR$ = "q") THEN STOP  
5780 GOTO 410
```

## PROGRAM NO

```

1 CLEAR .60000! : IBINIT1=60000! : IBINIT2=IBINIT1+3 : BLOAD "c:\gpib\bbib.m",
IBINIT1
2 CALL IBINIT1(IBFIND,IBTRG,IBCLR,IBPCT,IBSIC,IBLOC,IBPPC,IBBNA,IBONL,IBRSC,
IBRSRE,IBRSV,IBPAD,IBSAD,IBIST,IBDMA,IBEOS,IBTMO,IBEOT,IBRDF,IBWRTF,IBTRAP)
3 CALL IBINIT2(IGTS,IBCAC,IBWAIT,IBPOKE,IBWRT,IBWRTA,IBCMD,IBCMDA,
IBRD,IBRDA,IBSTOP,IBRPP,IBRSP,IBDIAG,IBXTRC,IBRDI,IBWRTI,IBRDIA,IBWRTIA,
IBSTA%,IBERR%,IBCNT%)
10 BRD$ = "GP1B0" : CALL IBFIND(BRD$,BRD%)
15 SCOPE$ = "TEKSCOP" : CALL IBFIND(SCOPE$,SCOPE%)
20 DEVI = "DELAY" : CALL IBFIND(DEV$,DELAY%)
25 CLS
100 REM X X X X X X X X X X X X X X PROGRAM TEE ONE X X X X X X X X X X X X
110 REM SATURATION BURST SEQUENCE
115 REM X X X X X X X X X X X X X X X X X X X X X X X X X X X X X X X X X X
170 REM * « » » PART ONE * * « *
180 REM
190 REM THIS PART OF THE PROGRAMME DOES THE FOLLOWING
200 REM
210 REM 1. ASKS THE USER FOR TAU VALUES IN MILLI SECONDS.
220 REM
230 REM 2. ASKS FOR THE REPETITION RATE i.e. 5T1
240 REM
250 REM 3. ASKS FOR THE NO. OF AVERAGES TO BE DONE.
260 REM
270 REM 4. ASKS FOR THE FILE NAME IN WHICH THE WAVEFORM IS TO BE
280 REM STORED.
290 REM * * * * - - - - - * * * *
300 REM • + • + • + PART ONE BEGINS +• + + + •
310 REM <=====> DECLARATIONS <=====>
320 REM
330 DIM TAU(100),A(30),B(30),ITAU(100),IATAU(30)
340 DIM Y(100),YL(100),E(100)
350 DIM CX(100),CY(100),FX(100),FY(100),T$(30)
360 DIM JTAU(100),KTAU(100),OFFTEMP(20),SLOPE(20)
370 AFLAG « 0
380 REM
390 REM
400 REM <=====>-----<==== ***** =====>
410 REM
420 REM ?????????????????????? QUERIES ??????????????????????
430 REM
440 INPUT "INPUT VALUES FROM KEYBOARD OR FILE ? ENTER CHOICE (K/F)" ",KF$
450 IF (KFI - "K") OR (KFI = "k") THEN GOTO 540
460 OPEN "BURSDATA" FOR INPUT AS #3
470 INPUT #3, TAUTO : TAU01 = TAUTO
480 FOR T = 1 TO TAUTO
490 INPUT #3,TAU(T) : ITAU(T) = TAU(T)
500 NEXT T
510 INPUT #3, AVERAGE
520 INPUT #3, WEIGHT
530 GOTO 770
540 KILL "BURSDATA"
550 OPEN "BURSDATA" FOR APPEND AS #3
560 CLS:INPUT "HOW MANY TAU VALUES DO YOU HAVE "; TAUTO : TAU01 = TAUTO

```

```

570     PRINT #3,SPC(5) TAU0
580     CLS:PRINT "GIVE THE TAU VALUES IN MILLI SECONDS ."
590 FOR J = 1 TO TAU0
600         PRINT "TAU"+STR$(J)+" = ": INPUT TAU(J): PRINT
610     PRINT #3, SPC(10),TAU(J)
620 NEXT J
630     CLS:PRINT "THESE ARE THE TAU VALUES YOU GAVE " : PRINT
640 FOR K = 1 TO TAU0
650         PRINT "TAU"+STR$(K),TAB(20),TAU(K)
660 NEXT K
670     PRINT "ENTER TO PROCEED"
680     INPUT:QUE$
690     FOR LK = 1 TO TAU0 : ITAU(LK) = TAU(LK)
700     NEXT LK
710     CLS:INPUT "HOW MANY NO. OF AVERAGES DO YOU NEED ":AVERAGE
720     PRINT #3, SPC(5),AVERAGE
730     PRINT
740     CLS:INPUT "GIVE THE WEIGHT FOR AVERAGING ":WEIGHT
750     PRINT #3, SPC(5),WEIGHT
760     PRINT
770     CLS: PRINT "DO YOU NEED WAVEFORMS TO BE STORED? (Y/N)":PRINT
780     INPUT WF$
790     IF (WF$ = "N") OR (WF$ = "n") THEN GOTO 910
800     CLS:PRINT " GIVE THE FILE NAME IN WHICH THE WAVEFORM IS TO BE STORED"
810     PRINT
820     PRINT " YOU CAN GIVE THE COMPLETE PATH , IF YOU WANT TO SAVE THE "
830     PRINT
840     PRINT " FILE IN A DIRECTORY OTHER THAN THE CURRENT DIRECTORY "
850     PRINT
860     PRINT " CURRENT DIRECTORY : C:\RAJAN\GPIB "
870     PRINT
880     PRINT " PLEASE INDICATE WHETHER YOU NEED THE FIRST WAVEFORM OR " : PRINT
890     INPUT " THE LAST WAVEFORM TO BE STORED (F/L) ",ORD$
900     INPUT:"FILENAME" = ",FILENAME$
910     CLOSE #3
920     CLS:PRINT " GIVE THE FILE NAME TO SAVE DATA PTS. [tau,A(tau)] "
930     PRINT:INPUT EXP1$
940     CLS: INPUT " GIVE THE SET PT. AND VARIAC SETTING", SETPT$,VARIAC$
950     CLS: INPUT " TH.EMF(START) = ", EMF1
960 REM ?????????????????? QUERIES END ?????????????????????????????
970     WORD1$ = "P0232000000" : CALL IBWRT(DELAY$,WORD1$)
980     WORD2$ = "Q0231000000" : CALL IBWRT(DELAY$,WORD2$)
990     WORD3$ = "R0223000000" : CALL IBWRT(DELAY$,WORD3$)
1000     WORD4$ = "S0213000000" : CALL IBWRT(DELAY$,WORD4$)
1010     WORD5$ = "T0233000000" : CALL IBWRT(DELAY$,WORD5$)
1020 REM
1030 REM
1040 REM MASTER . . . . . LOOP
1050     REM LPRINT SPC(15)> "TAU (m.sec)"SPC(15)"DELTA V (m.volts)" : CLS
1060     PRINT SPC(15) "TAU (m.sec)"SPC(15)"DELTA V (m.volts)"
1070     PRINT SPC(20);TAU(1);
1080     REM LPRINT SPC(10);1;TAB(20);TAU(1);
1090     OPEN EXP1$ FOR OUTPUT AS #2
1100     PRINT #2,SPC(15)"TAU (m.sec) "SPC(15)"DELTA V (m.volts) "
1110     CLOSE #2
1120     WAVKOUNT < 0 : OFFSETT = 0
1130     FOR JK = 1 TO TAU0
1140 REM
1150         IF TAU(JK) <= 9.998999 GOTO 1200

```



[illegible]

```

1750 CALL IBWRT(DELAY%,WORDR1$)
1760 CALL IBWRT(DELAY%,WORD3$)
1770 GOSUB 2160
1780 RETURN
1790 REM . . . . .
1800 REM \\\\\\ SUBROUTINE IS WORKING PROPERLY
1810 REM \\\\\\ SAVED IN THE NAME C:\GPIB-PC\TIR3.BAS IN PC1 AS AN ASCII FILE
1820 REM - - - - -
1830 REM SUBROUTINE RANGE 4
1840 REM
1850 D4 = (TAU(JK)+OFSETT) * 10 : D41* = STR$(D4)
1860 PART1* = "S"
1870 PART2* = "D"
1880 PART3* = MID$(D41*,2) : PART4* = "!"
1890 WORDS1$ = PART1$+PART2$+PART3$+PART4$
1900 CALL IBWRT(DELAY%,WORDS1$)
1910 CALL IBWRT(DELAY%,WORD4$)
1920 GOSUB 2160
1930 RETURN
1940 REM + + + + +
1950 REM \\\\\\ SUBROUTINE IS UORKING PROPERLY
1960 REM \\\\\\ SAVED IN THE NAME C:\GPIB-PC\TIR4.BAS IN PC1 AS AN ASCII FILE
1970 REM - - - - -
1980 REM SUBROUTINE RANGE 5
1990 REM
2000 D5 = (TAU(JK)+OFSETT) : D51* = STR$(D5)
2010 PART1$ = "T"
2020 PART2$ = "D"
2030 PART3$ = MID$(D51*,2) : PART4$ = "!"
2040 WORDT1$ = PART1$+PART2$+PART3$+PART4$
2050 CALL IBWRT(DELAY%,WORDT1$)
2060 CALL IBWRT(DELAY%,WORD5$)
2070 GOSUB 2160
2080 RETURN
2090 REM + + + + +
2100 REM \\\\\\ SUBROUTINE IS WORKING PROPERLY
2110 REM \\\\\\ SAVED IN THE NAME C:\GPIB-PC\TIR5.BAS IN PC1 AS AN ASCII FILE
2120 REM - - - - -
2130 REM
2140 REM SUBROUTINE WAVETRANS
2150 REM
2160 CMD$ = "ACQ REP:SAM,HSR:SAM,LSR:SAM,SCA:SAM" : CALL IBWRT(SCOPE%,CMD$)
2170 SWEEP* = AVERAGE - 1
2180 MASK* = &H4000 : WAIT1* = 11
2190 CALL IBTMO(BRD%,WAIT1$) : CALL IBWAIT(BRD%,MASK%)
2200 QUERY$ = "ACQ? SWP" : CALL IBWRT(SCOPE%,QUERY$)
2210 ANS$ = SPACE$(30) : CALL IBRD(SCOPE%,ANS$)
2220 IF VAL(MID$(ANS$,22)) < 1 THEN GOSUB 2690 ELSE 2240
2230 GOTO 2200
2240 CMD$ = "ACQ REP:AVE,HSR:AVE,LSR:AVE,SCA:AVE.SMO:ON,VEC:ON,NUM:"
2250 VER$ = STR$(AVERAGE):CMD1$ = CMD$ + MID$(VER$,2)
2260 WEIT$ = ",WEI:" + MID$(STR$(WEIGHT),2)
2270 CMD2$ = CMD1$ + WEIT$
2280 CALL IBWRT(SCOPE%,CMD2$)
2290 SWEEP% = 0
2300 GOSUB 2690
2310 QUERY$ = "ACQ? SWP" : CALL IBWRT(SCOPE%,QUERY$)
2320 ANS$ = SPACE*(30) : CALL IBRD(SCOPE%,ANS$) t SWEEPX = VAL(MID$(ANS$,22))
2330 IF SWEEP% = AVERAGE THEN GOTO 2360

```

```

2340 GOSUB 2690
2350 GOTO 2310
2360 REM ~~~~~ WAVEFORM TRANSFER DETAILS ~~~~~
2370 REM ~~~~~

2380 IF (JK <> 1) OR (AFLAG = 1) THEN GOTO 2420
2390 CLS:INPUT "PLEASE SET THE CURSORS AND ENTER TO PROCEED",ABC$
2400 CLS:PRINT SPC(15) "TAU (m.sec)" SPC(15) "DELTA V (m.volts)"
2410 PRINT SPC(20) "TAU(JK)";
2420 CMD$ = "DELTAV? VAL" : CALL IBWRT(SCOPE%,CMD$)
2430 VOLT$ = SPACE$(35) : CALL IBRD(SCOPE%,VOLT$)
2440 PRINT TAB(45)VAL(MID$(VOLT$,14))*1000!
2450 OPEN EXP1* FOR APPEND AS #2
2460 PRINT #2,TAB(45)VAL(MID$(VOLT$,14))*1000!
2470 CLOSE #2
2480 IF AFLAG = 0 THEN A(JK) = VAL(MID$(VOLT$,14))*1000!
2490 IF AFLAG = 1 THEN B(JK) = VAL(MID$(VOLT$,14))*1000!
2500 IF AFLAG = 1 THEN GOTO 2550
2510 REM LPRINT TAB(45) VAL(MID$(VOLT$,14))*1000!
2520 REM -+--+--+--+--+--+--+--+--+--+--+--+--+--+--+--+--+--+--+--+--+--+
1530 REM W A V E F O R M T R A N S F E R F R O M H E R E
2540 REM -+--+--+--+--+--+--+--+--+--+--+--+--+--+--+--+--+--+--+--+--+--+
2550 IF (WF$ = "N") OR (WF$ = "n" ) THEN GOTO 2660
2560 IF ORD* = "F" OR ORD* = "f" THEN GOTO 2600
2570 WAVKOUNT = WAVKOUNT + 1
2580 IF WAVKOUNT <> TAUO THEN GOTO 2660
2590 WAVE1t < "DATA SOU:ACQ,CHA:CH2,ENC:HEX" : CALL IBWRT(SCOPE%,WAVE1$)
2600 WAVE2$ = "WAV?" : CALL IBWRT(SCOPE%,WAVE2$)
2610 CALL IBRDF(SCOPE%,FILENAME$)
2620 WF$ = "N"
2630 REM-----*+*+*+*+*+*+*+*+*+*+*+*+*+*+*+*+*+*+*+*+*+*+*+*+*+*+*+*+
1640 REM W A V E F O R M T R A N S F E R E N D S H E R E
2650 REM-----*+*+*+*+*+*+*+*+*+*+*+*+*+*+*+*+*+*+*+*+*+*+*+*+*+*+*+*+
2660 PRINT SPC(20)TAU(JK+1);
2670 REM LPRINT SPC(10);(JK+1);TAB(20);TAU(JK+1);
2680 RETURN
2690 REM DDDDDDDDDDDD SUBROUTINE DELAY DDDDDDDDDDDD
2700 REM -----
2710 SWEEP1X = AVERAGE - SWEEPX
2720 TME = SWEEP1X * TAU(JK) * .001
2730 AA = .001 : BB = .003
2740 FOR N = 5 TO 17
2750 IF (TME > AA) AND (TME < BB) THEN GOTO 2820
2760 AA < AA * 10
2770 CC = AA
2780 AA = BB
2790 BB = CC
2800 NEXT N
2810 GOTO 2860
2820 VX = N :CALL IBTMO(BRD%,V%)
2830 MASKX = &H4000
2840 CALL IBWAIT(BRD%,MASKX)
2850 RETURN
2860 VX = 13
2870 CALL IBTMO(BRD%,V%)
2880 GOTO 2850
2890 REM
2900 REM THIS SUBROUTINE IS STORED AS "T1DELAY.BAS" IN THE
2910 REM FOLLOWING PLACES
2920 REM C:\GP1B IN PC2

```

[illegible]

```

3450      KTAU(KAN) = ITAU(KAN)
3460      IATAU(KAN) = A(KAN)
3470      NEXT KAN
3480      REM LPRINT SPC(15) "TAU(m.sec)" SPC(15) "M(tau) (m.volts)"
3490      FOR N = 1 TO TAU01
3500      REM LPRINT SPC(10) I;TAB(20);ITAU(N) TAB(45) A(N)
3510      NEXT N
3520      GOTO 3040
3530      FOR KAN = 1 TO TAU01
3540      KTAU(KAN) = ITAU(KAN)
3550      IATAU(KAN) = A(KAN)
3560      NEXT KAN
3570      FOR J = 1 TO TAU01
3580      AMIN = ITAU(J) : K = J
3590      AAMIN = A(J)
3600      FOR I = J TO TAU01
3610      IF ITAU(I) >= AMIN THEN GOTO 3640
3620      AMIN = ITAU(I) : K = I
3630      AAMIN = A(I)
3640      NEXT I
3650      ATEMP = ITAU(J)
3660      ITAU(J) = AMIN
3670      ITAU(K) = ATEMP
3680      AATEMP = A(J)
3690      A(J) = AAMIN
3700      A(K) = AATEMP
3710      NEXT J
3720      CLS
3730      PRINT SPC(15) "TAU(m.sec)" SPC(15) "A(TAU) (m.volts)"
3740      FOR S = 1 TO TAU01
3750      PRINT SPC(5) S SPC(10) ITAU(S) TAB(45) A(S)
3760      NEXT S : PRINT
3770      INPUT "ENTER TO PROCEED ", ENT
3780      REM N = TAU01
3790      REM program for t1 cal
3800      PRINT:PRINT:PRINT
3810      CLS:INPUT "NO. OF POINTS PLEASE ";NO
3820      INPUT "yo please";Y0
3830      S1=0:S2=0:S3=0:S4=0:S5=0
3840      FOR I = 1 TO NO
3850      YL(I)=LOG(Y0-A(I))
3860      S1=S1+ITAU(I):S2=S2+YL(I):S3=S3+ITAU(I)^2
3870      S4=S4+ITAU(I)*YL(I):S5=S5+YL(I)^2
3880      NEXT I
3890      D=S3-(S1^2)/NO
3900      M=(S4-S1*S2/NO)/D
3910      B=(S2*S3-S1*S4)/(D*NO)
3920      D1=SQR((S3-(S1^2)/NO)*(S5-(S2^2)/NO)):R=(S4-(S1*S2)/NO)/D1
3930      S6=0:S7=0
3940      FOR I=1 TO NO
3950      Y(I)=M*ITAU(I)+B
3960      E(I)=Y(I)-YL(I)
3970      S6=S6+E(I)^2
3980      S7=S7+(E(I)/Y(I))^2
3990      NEXT I
4000      PRINT "x(i)";TAB(10);"ym(i)";TAB(20);"yl(i)";TAB(40);"y(i)";TAB(60);"e(i)"
4010      FOR I=1 TO NO
4020      YL(I)=(INT(YL(I)*1000))/1000
4030      Y(I)=(INT(Y(I)*1000))/1000

```

```

4040 PRINT ITAU(I);TAB(10);A(I);TAB(20);YL(I);TAB(40);Y(I);TAB(60);E(I)
4050 NEXT I
4060 SD=SQR(S6/N0)
4070 DY=SQR(S7/N0)
4080 T1=1/M
4090 DT=DY*T1:PRINT:PRINT
4100 PRINT "t1=";T1;TAB(50);"error=";DT:PRINT:PRINT
4110 PRINT"rmsd=";SD;TAB(50);"corr.=";R
4120 GOSUB 5410
4130 FOR I=1 TO NO
4140 CX(I)=ITAU(I):CY(I)=YL(I):NEXT I
4150 GOTO 4310
4160 SCREEN 0
4170 INPUT "how many bad data points do you have";MM
4180 PRINT:PRINT:PRINT "type the x(i)'s of the bad points"
4190 FOR I=1 TO MM
4200 INPUT";X1(I)
4210 FOR J=1 TO NO
4220 IF ITAU(J)<>X1(I) THEN 4280
4230 IF J=NO THEN 4270
4240 FOR K=J TO NO-1
4250 ITAU(K) = ITAU(K+1):A(K)=A(K+1)
4260 NEXT K
4270 NO=NO-1
4280 NEXT J
4290 NEXT I
4300 GOTO 3830
4310 REM variables (exptl) are cx and cy
4320 REM variables (calc.) are fx and fy
4330 REM necessary changes are to be made in the main programme
4340 PRINT:PRINT
4350 PK$ = INKEY$
4360 IF PK$ = "" THEN GOTO 4350
4370 X9=CX(I):X0=CX(I):Y9=CY(I):Y0=CY(I)
4380 FOR I= 1 TO NO
4390 IF CX(I)>X9 THEN X9=CX(I)
4400 IF CX(I)<X0 THEN X0=CX(I)
4410 IF CY(I)>Y9 THEN Y9=CY(I)
4420 IF CY(I)<Y0 THEN Y0=CY(I)
4430 NEXT
4440 DX=(X9-X0)/10:DY=(Y9-Y0)/10
4450 X9=X9+DX:Y9=Y9+DY
4460 X0=X0-DX:Y0=Y0-DY
4470 IX=570/(X9-X0):IY=160/(Y9-Y0)
4480 FOR I=1 TO NO
4490 CX(I)=50+(CX(I)-X0)*IX
4500 CY(I)=170-(CY(I)-Y0)*IY
4510 NEXT
4520 PRINT:PRINT:PRINT
4530 CLS
4540 SCREEN 2
4550 LINE (10.5) - (630,190),,B
4560 LINE (35,170)-(620,170)
4570 LINE (50,10) -(50.185)
4580 XL=107
4590 FOR I= 1 TO 10
4600 LINE (XL,168) - (XL,172)
4610 XL=XL+57
4620 NEXT

```

```

4630     YL=10
4640     FOR I=1 TO 10
4650         LINE(48,YL)-(52,YL)
4660         YL=YL+16
4670     NEXT
4680     XL=107:YK=20
4690     FOR I= 1 TO 4
4700         XC(I)=X0+(XL-50)/IX
4710         XL=XL+65
4720     NEXT
4730     YK=10
4740     FOR I= 4 TO 1 STEP -1
4750         YC(I)=Y0+(170-YK)/IY
4760         YK=YK+40
4770     NEXT
4780     FOR I= 1 TO 4
4790         X1(I)=XC(I)
4800     NEXT
4810         I*1
4820     XQ(I)=INT(ABS(XC(I)))
4830     X1(I)=XC(I)
4840     L=0:K=0
4850     IF XQ(I)=0 THEN XC(I)=XC(I)*10:L=L+1:XQ(I)=INT(ABS(XC(I))):GOTO 4850
4860     IF XQ(I) > 10 THEN XC(I)=XC(I)/10:K=K+1:XQ(I)=INT(ABS(XC(I))):GOTO 4860
4870     IF L=0 THEN PP = K
4880     IF K=0 THEN PP=-L
4890     IF L = 0 AND K = 0 THEN PP=0
4900     PP$=STR$(PP)
4910     FOR I= 1 TO 4
4920         X1(I)=X1(I)*(10^(-PP))
4930         X1(I)=(INT(X1(I)*100))/100
4940     NEXT
4950     FOR I= 1 TO 4
4960         Y1(I)=YC(I)
4970     NEXT
4980     I=1
4990     YQ(I)=INT(ABS(YC(I)))
5000     Y1(I)=YC(I)
5010     L=0:K=0
5020     IF YQ(I)=0 THEN YC(I)=YC(I)*10:L=L+1:YQ(I)=INT(ABS(YC(I))):GOTO 5020
5030     IF YQ(I)>10 THEN YC(I)=YC(I)/10:K=K+1:YQ(I)=INT(ABS(YC(I))):GOTO 5030
5040     IF L=0 THEN PP=K
5050     IF K=0 THEN PP=-L
5060     IF L=0 AND K=0 THEN PP=0
5070     PP$=STR$(PP)
5080     FOR I=1 TO 4
5090         Y1(I)=Y1(I)*(10^(-PP))
5100         Y1(I)=(INT(Y1(I)*10))/10
5110     NEXT
5120     QX=87
5130     FOR I= 1 TO 4
5140         X1$(I)=STR$(X1(I))
5150         QX=QX+65
5160     NEXT
5170     QY=126
5180     FOR I= 1 TO 4
5190         Y1$(I)=STR$(Y1(I))
5200         QY=QY-40
5210     NEXT

```

```

5220 FOR I= 1 TO NO
5230 LINE (CX(I)-1,CY(I)-1) - (CX(I)+1,CY(I)+1),.B
5240 NEXT
5250 FOR I= 1 TO NO
5260 FX(I)=50+(ITAU(I)-XO)*IX
5270 FY(I)=170-(Y(I)-YO)*IY
5280 NEXT
5290 M=NO-1
5300 FOR I= 1 TO M
5310 LINE (FX(I),FY(I))-(FX(I+1),FY(I+1))
5320 NEXT
5330 YY=2*(ABS(SD))*(ABS(IY))
5340 LINE (600,100)-<600,100-YY)
5350 LINE (599,100-YY) - (601,100-YY)
5360 LINE (599,100) - (601,100)
5370 GO* = INKEY$
5380 IF GO* = "" THEN GOTO 5370
5390 SCREEN 0
5400 GOTO 5600
5410 REM -10700
5420 AX=0:AY=0
5430 FOR I= 1 TO NO
5440 AX=AX+ITAU(I):AY=AY+YL(I)
5450 NEXT I
5460 AX=AX/NO:AY=AY/NO
5470 A1=0:A2=0:A3=0
5480 FOR I= 1 TO NO
5490 A1=A1+(YL(I)-AY)^2
5500 A2=A2+(ITALK I)-AX)*(YL(I)-AY)
5510 A3=A3+(ITAU(I)-AX)^2
5520 NEXT
5530 S=(A1-(A2^2)/A3)/(NO-2)
5540 SB=S/(SQR(A3))
5550 PRINT "s = ";S;"sb = ";SB
5560 RR=ABS(SB*T1*T1)
5570 PRINT:PRINT "error in t1 =";RR
5580 SL = A2/A3 : SS = 1/SL : PRINT "t1 is ";SS
5590 RETURN
5600 CLS
5610 PRINT "YOU HAVE THE FOLLOWING OPTIONS TO CHOOSE FROM: " : PRINT
5620 PRINT " i. A HARD COPY OUTPUT OF THE T1 DATA " : PRINT
5630 PRINT " 2. MANIPULATION OF EXISTING DATA " : PRINT
5640 PRINT " 3. MODIFICATION OF THE EXPTL. PARAMETERS" : PRINT
5650 PRINT " 4.T1 FIT OF ENTIRE DATA SET " : PRINT
5660 PRINT " PLEASE ENTER THE APPROPRIATE NUMBER FOR " : PRINT
5670 PRINT " FOR THE OPTION YOU CHOOSE (1/2/3/4) " : PRINT
5680 INPUT OPT
5690 IF OPT = 1 THEN GOTO 5750
5700 IF OPT = 2 THEN GOTO 4160
5710 IF OPT = 3 THEN GOTO 3040
5720 IF OPT = 4 THEN GOTO 6380
5730 CLS : PRINT " GIVE THE APPROPRIATE NUMBER PLEASE (1/2/3/4) "
5740 PRINT : GOTO 5680
5750 D* = DATE* : T* = TIME$
5760 SAMPLE$ = " [NH4]3 Sb2 Br9 " : FREQ$ = "8"
5770 BOOK = 1
5780 INPUT " EMF(FINISH) = ", EMF2
5790 INPUT " TEMPERATURE . ",TEMPR
5800 INPUT " PAGE NO. : ",PAGE

```



```

5810 T1FILE$ = LEFT$(EXP1$,8)+".DAT"
5820 OPEN T1FILE$ FOR OUTPUT AS #1
5840 REM SUBROUTINE PRINT OUT
5850 REM - - - - -
5860 REM
5870 REM
5880 FOR J = 1 TO NO
5890 PRINT #1, SPC(10);J;TAB(15); ITAU(J) TAB(40) A(J)
5900 NEXT J
5910 PRINT #1, TAB(15) "Yo" TAB(40) YO
5920 PRINT #1,
5930 PRINT #1, SPC(10);"date = " ;D$;TAB(40);" time = " ;T$
5940 PRINT #1,
5950 PRINT #1, SPC(10) "SAMPLE IS "+SAMPLE$;TAB(40);"FREQ. = "+FREQ$+" MHz."
5960 PRINT #1,
5970 PRINT #1, SPC(10) "SET POINT = "+SETPT$; TAB(40);"VARIAC = "+VARIAC$;" VOLTS"
5980 PRINT #1,
5990 PRINT #1, SPC(10) "EMF1 = " ;EMF1;TAB(40);"EMF2 = " ;EMF2
6000 PRINT #1,
6010 PRINT #1, "
6020 PRINT #1, CHR$(27);CHR$(87);"1"
6030 PRINT #1, " LS - F I T D A T A "
6040 PRINT #1, CHR$(27);CHR$(87);"0"
6050 PRINT #1, "
6060 PRINT #1,
6070 PRINT #1, "X(i)"; TAB(10); "Ym(i)";TAB(25);"Yl(i)";TAB(40);"Y(i)";TAB(60);"E(i)
6080 PRINT #1,
6090 PRINT #1, "
6100 FOR I = 1 TO N
6110 PRINT #1, ITAU(I);TAB(10);A(I);TAB(25);YL(I);TAB(40);Y(I);TAB(60);E(I)
6120 NEXT I
6130 PRINT #1, "
6140 PRINT #1,
6150 PRINT #1, SPC(10) "corr. = " ;R TAB(40) "T1 = " ;(-T1)
6160 PRINT #1,
6170 PRINT #1, SPC(10) "ERR. IN T1 = " ;RR;TAB(40) ; "TEMP. = " ;TEMR;" C"
6180 PRINT #1,
6190 PRINT #1, SPC(10) "RMSD = " ;SD;TAB(49);(273+TEMR);" K" :PRINT #1
6200 PRINT #1, SPCUO) "1000/T = " ;1000/(273+TEMR);TAB(40);"ln T1 = " ;LOG(-T1)
6210 PRINT #1, "
6220 PRINT #1, SPCUO) ;" BOOK NO. = " ;BOOK;TAB(40);" PAGE NO. = " ;PAGE
6230 PRINT #1, "
6240 CLOSE #1
6250 REM . . . . . END OF SUBROUTINE PRINT OUT . . . . .
6260 REM - - - - -
6270 REM
6280 REM
6290 CLS : PRINT "IF YOU WANT TO DO THE EXPERIMENT AGAIN WITH THE "
6300 PRINT:PRINT "SAME PARAMETERS, ENTER C. "
6310 PRINT:PRINT " IF YOU WANT TO QUIT, ENTER Q"
6320 QUR$ = INKEY$
6330 IF (QUR$ = "") THEN GOTO 6320
6340 IF (QUR$ = "Q") OR (QUR$ = "q") THEN STOP
6350 IF (QUR$ = "C") OR (QUR$ = "c") THEN GOTO 6360 ELSE GOTO 6320
6360 AFLAG = 0
6370 GOTO 460
6380 FOR KAN = 1 TO TAU01
6390 ITAU(KAN) * KTAU(KAN)
6400 A(KAN) = IATAU(KAN)

```

6410    NEXT   KAN  
6420    GOTO   3570

## A P P E N D I X    I I I

This appendix provides names of some chosen programs which were developed in BASICA and ASYST languages alongwith a brief comment on their application. Sample listings of a few of these programs, used for non-linear least square fit of T data in different compounds, are also provided.

### L I S T    O F    P R O G R A M S    I N    B A S I C A (GENERAL PURPOSE)

PROGRAM NAME	DESCRIPTION
ANMINEA.BAS	To calculate E from minima position at different Larmor frequencies.
ANMINTEM.BAS	To calculate the minima formation temperature.
DATASORT.BAS	To sort a given set of data.
LST1JAR.BAS	To calculate T from (M vs T) data.
CWDECODE.BAS	To extract data set from CW spectra.
MOMENT.BAS	To calculate second moment from CW data.
PEAKFIND.BAS	To find the spin-echo amplitude.
STRGSORT.BAS	To sort a given set of strings.
TAUCGEN.BAS	To calculate T in a given range of temperature.
T1SLOPE.BAS	To calculate E from the slope of T data.

### L I S T    O F    P R O G R A M S    I N    B A S I C A (GRAPHICS)

CURVE1.BAS	To plot data set (X, Y) with Zoom facility.
CURVE2.BAS	To plot two sets of data ( $X_1, Y_1$ ) and ( $X_2, Y_2$ ).
CURVE3.BAS	To plot an arbitrary no of data sets.
CURVTEK1.BAS	To transfer waveform from TEKTRONIX 2230 digitizer and plot on enlarged screen.
CURVTEK2.BAS	To transfer waveform from TEKTRONIX 2230 digitizer and plot on reduced screen.
CURSLOT.BAS	To plot a digitized waveform and extract a reduced data set by marking with cursors.

## LIST OF PROGRAMS IN ASYST

M2CALC2.ASY	To calculate second moment from CW spectra.
FFTPLOT.ASY	To perform fourier transform of an array and plot.
BASGRF.ASY	To read a BASICA output file and plot.
TORREY.ASY	To fit $T_1$ data to Torrey's model.
CWINTPOL.ASY	To interpolate and find intermediate points in a digitized CW spectrum.
MULTEXP1.FIT	To fit the non-exponential magnetization recovery.

Programs were also developed to perform other useful tasks in connection with processing and display of the data (in BASICA and ASYST languages).

PROGRAM NO : 1

PROGRAM USED TO FIT T1 DATA OF TETRAMETHYLAMMONIUM COMPOUNDS.

```

10 CLS
15 REM *****
30 REM          SAMPLE NAME      :      [(CH3)4 N]3 Bi2 C19
35 REM          FREQUENCY       :      8 MHz AND 39.6 MHz
50 REM          SOURCE FILE      :      SA6FIT8.BAS
60 REM          DATA FILE       :      SA6DATx.THR
70 REM          SOURCE PATH      :      \RAJAN\ANALYSIS\TEMABICL.SA6\X
80 REM          DATA PATH       :      \RAJAN\DATA\TEMABICL.SA6\X
90 REM          FIVE CORRELATION TIMES FIT

115 KEY OFF*
120 SAMPLES = "TEMABICL.SA6"
125 GRAPHAT$ = "1"
130 FILE1A$ = "D:\rajan\data\temabicl.sa6\8\sa6dat8.THR"
131 FILE1A$ = "D:\rajan\data\temabicl.sa6\40\sa6dat40.lt"
132 ROUTE$ = "NONE"
150 REM *****
170 OPT$ = "d"
190 OPEN FILE1A$ FOR INPUT AS #1
210 INPUT tfl.N
230   DIM TEMP1(N),SLRT(N),FX(N),FY(N),TEMP(N)
250   FOR I = 1 TO N
270   INPUT #1,TEMP(I),SLRT(I)
290   NEXT I
310 CLOSE
330   FOR J = 1 TO N
350     AMAX = TEMP(J): K = J
370     FOR I = J TO N
390       IF TEMP(I) <= AMAX THEN GOTO 430
410       AMAX = TEMP(I): K = I
430     NEXT I
450     XTEMP = TEMP(K) : TEMP(K) = TEMP(J) : TEMP(J) = XTEMP
470     YTEMP = SLRT(K) : SLRT(K) = SLRT(J) : SLRT(J) = YTEMP'
490   NEXT J
510 M=10
520 NTAU = 5
530 DIM F1(N),F(N),SLRE(N),R(N),INA(M),CX(N),CY(N),A(M)
550 DIM X(N),Y(2,N),X1(N),SLRC(N),C(N),DMSD(M),GAMA(M)
570 DIM KK(5),LL(5),MM(5),K(5),ANEW(N),T$(30),XP(N),YP1(N),YP2(N)
575 DIM RHO(N,NTAU),GOMEGA(N,NTAU)
610 KK1=0
630 FOR I = 1 TO N
640 SLRT(I) = SLRT(I) * .001
650 SLRE(I) = 1/SLRT(I)
660 TEMP1(I) = 1000/TEMP(I)
670 NEXT I
675 A = 8.05E+09
680 B = 4.61E+09
685 F0 = 8000000!
686 'F0 = 3.98E+07
687 FOMANTISSA = F0 / 1000000!
690 OMEGA0= 2 * 22 * F0 / 7
700 R=8.3143

```

```

701 ' =+++++++ INEQUIVALENCE FACTORS ++++++=
705 FRACX = 1/12 ' CH3-I
707 FRACY = 1/12 ' CH3-II
710 FRACZ = 5/12 ' CH3-III
712 FRACP = 1/12 ' CH3-IV
715 '
717 '
729 ' =+++++++ INEQUIVALENCE FACTORS ++++++=
730 REM *****
750 IF OPT$ = "U" OR OPT$ = "u" THEN GOTO 930
770 PRINT:PRINT:PRINT
790 A(1) = 9.357999E-22 : A(2) = 8.33 ' CH3-I GROUP
800 A(3) = 3.45E-09 : A(4) = .477' CH3-II GROUP
810 A(5) = 1.39E-13 : A(6) = 1.96' CH3-III GROUP
820 A(7) = 3.97E-24 : A(8) = 3.83 ' CH3-IV GROUP
830 A(9) = 5.94E-14 : A(10) = 3.18 ' TEMA GROUP
840 '
842 '
844 '
850 FOR BB = 1 TO NTAU
860 A(2*BB-1) = 1/A(2*BB-1) : A(2*BB) = A(2*BB) * 4.19
872 NEXT BB
920 GOTO 1180
930 OPEN "SA6SHADO.8" FOR INPUT AS #3
940 INPUT #3,ROUTE$
950 FOR BB = 1 TO NTAU
960 INPUT #3,A(2*BB-1),A(2*BB)
975 A(2*BB-1) = 1/A(2*BB-1) : A(2*BB) = A(2*BB) * 4.19
980 NEXT BB
995 CLOSE #3
1005 FOR BB = 1 TO NTAU
1010 INA(2*BB-1) = A(2*BB-1)/100
1020 INA(2*BB) = A(2*BB)/100
1025 NEXT BB
1035 NM = 3
1040 NN = 10
1180 GOSUB 7420
1200 PRINT " FOLLOWING ARE THE INITIAL VALUES "
1220 FOR BB = 1 TO NTAU
1240 PRINT "T0-";(BB);1/A(2*BB-1);TAB(40);"Ea-";(BB);A(2*BB)/4.19
1270 NEXT BB
1280 PRINT" MSD - "; RMSD
1350 RMSDX=RMSD
1370 RMSD1=RMSD
1390 OPEN "SA5OUT8.ONE" FOR OUTPUT AS #1
1410 PRINT #1," *****
1430 PRINT #1, " FOLLOWING ARE THE INITIAL VALUES "
1450 FOR BB = 1 TO NTAU
1470 PRINT #1,"T0-";(BB);1/A(2*BB-1);TAB(40);"Ea";(BB);A(2*BB)/4.19
1490 NEXT BB
1510 PRINT #1, " *****
1530 PRINT #1,"MSD = ";RMSD
1550 CLOSE #1
1740 GOSUB 4750
1745 IF ROUTE$ = "BOTH" OR ROUTE$ = "both" THEN GOTO 5700
1750 IF ROUTE$ = "GRID" OR ROUTE$ = "grid" THEN GOTO 1860
1790 GRAPHAT$ = INKEY$
1795 IF GRAPHAT$ = "" THEN GOTO 1790
1810 IF GRAPHAT$ = "P" OR GRAPHAT$="p" OR GRAPHAT$ = "Z" OR GRAPHAT$ = '

```

```

THEN GOSUB 5120 ELSE GOTO 1820

1815 GOTO 1790
1820 PRINT " DO YOU WANT TO START GRID SEARCH OR GRADIENT SEARCH
OR NONE (R/A/N)

1825 B$ = INKEY$ : IF B$ = "" THEN GOTO 1840
1830 IF B$ = "R" OR B$ = "r" THEN GOTO 1860
1835 IF B$ = "A" OR B$ = "a" THEN GOTO 5700
1840 IF B$ = "N" OR B$ = "n" THEN GOTO 3430
1850 GOTO 1825
1855 _____S U B R O U T I N E  G R I D  S E A R C H  . . . . .
1860 IF OPT$ = "U" OR OPT$ = "u" THEN GOTO 2110
1890 PRINT:PRINT:PRINT
1910 PRINT "THEN PLEASE PROVIDE INCRIMENTS OF THE PARAMETERS "
1930 PRINT:PRINT:PRINT
1950 FOR BB = 1 TO NTAU
1970 PRINT"          INCRIMENT IN r0-";(BB);:INPUT "",INA(2*BB-1):PRINT
1990 PRINT"          INCRIMENT IN Ea-";(BB);:INPUT "",INA(2*BB):PRINT
2010 NEXT BB
2070 INPUT"  NUMBER OF REFINEMENTS REQUIRED =";MM : PRINT
2090 INPUT"  REDUCTION FACTOR IN INTERATIONS =";NN
2110 GOSUB 4750
2111 LOCATE 22 1
2115 FOR LCOUNT = 1 TO NTAU : PRINT 1/A(2*LCOUNT-1);A(2*LCOUNT)/4.19;
      : NEXT LCOUNT
2120 ROUTE$ = "GRID"
2130 OPEN "SA50UT8.0NE" FOR APPEND AS #1
2150 PRINT #1," *****"
2170 PRINT tfl," THE INCREMENTS ARE : "
2190 FOR BB = 1 TO NTAU
2210 PRINT #1,"DEL.R0-";(BB);INA(2*BB-1);TAB(40);"DEL.Ea";(BB);INA(2*BB)
2230 NEXT BB
2250 PRINT #1,
2270 CLOSE #1
2290 OPEN "SAGSHADO.INC" FOR OUTPUT AS #1
2310 FOR BB = 1 TO NTAU
2330 PRINT tfl,INA(2*BB-1),INA(2*BB)
2360 NEXT BB
2370 CLOSE #1
2390 LOCATE 3,20:PRINT "PLEASE WAIT "
2400 LOCATE 4,50 : PRINT " ITERATION NO : ";KK1
2410 REM PRINT " SEARCH FOR MINIMUM RMSD IS IN PROGRESS"
2450 FOR JK1=1 TO M
2470 A(JK1) = A(JK1)+INA(JK1)
2510 GOSUB 7420
2530 RMSD2=RMSD
2550 IF RMSD2<RMSD1 THEN GOTO 2590
2570 INA(JK1)= -INA(JK1)
2590 A(JK1)=A(JK1)+INA(JK1)
2610 GOSUB 7420
2630 RMSD3=RMSD
2650 IF RMSD3 >= RMSD2 THEN GOTO 2790
2690 RMSD1=RMSD2
2710 RMSD2=RMSD3
2730 GOTO 2590
2750 P=RMSD3-2*RMSD2+RMSD1
2770 Q=(RMSD3-RMSD2)/P+.5
2790 A(JK1)=A(JK1)-INA(JK1)
2830 RMSD1=RMSD2

```

```

2850 NEXT JK1
2930 GOSUB 7420
2950 RMSDY=RMSD
2970 IMPR=(RMSDX-RMSDY)/RMSDX
2990 GOSUB 4750
2991 LOCATE 22,1
2995 FOR LCOUNT = 1 TO NTAU : PRINT 1/A(2*LCOUNT-1);A(2*LCOUNT)/4.19; :NEXT LCOUNT
3030 IF IMPR<.001 THEN GOTO 3090
3050 RMSDX=RMSDY
3070 GOTO 2390
3090 OPEN "SA5OUT8.ONE" FOR APPEND AS #1
3110 PRINT #1," *****"
3130 PRINT #1, " FOLLOWING ARE THE FITTED VALUES "
3150 FOR BB = 1 TO NTAU
3170 PRINT tfl,"T0-";(BB);(1/A(2*BB-1));TAB(40);"Ea-";(BB);(A(2*BB)/4.19)
3190 NEXT BB
3210 PRINT tfl,"RMSD - ";RMSD
3230 PRINT #1, " *****"
3240 PRINT tfl." MSD HAS CONVERGED AND REFINEMENT COMPLETE "
3250 CLOSE #1
3270 OPEN "SA6SHADO.8" FOR OUTPUT AS #2
3280 PRINT #2,"BOTH"
3290 FOR BB = 1 TO NTAU
3310 PRINT #2,1/A(2*BB-1),A(2*BB)/4.19
3340 NEXT BB
3350 CLOSE #2
3370 PRINT:PRINT
3390 GOSUB 4450
3410 GOTO 2130
3420 '-----R O U T I N E  ENDS -----
3430 SCREEN 0,0,0
3450 'STOP
3455 'END
3460 '
3465 '=====
3470 ' E N D      O F      P R O G R A M M E
3470 '=====
3490 ' S U B R O U T I N E   TAUC -----
3491 ' ARRAYS USED HERE ARE ASSUMED TO BE PROPERLY DIMENSIONED ALREADY
3492 ' A(odd)'s ARE RHO-0 - PRE EXPONENTIAL FACTORS. A(even)s ARE Ea-s
3493 '
3495 FOR I1 = 1 TO N          ' N IS NO. OF TEMPERATURES
3500   FOR JK2 = 1 TO NTAU
3505     RHO(I1,JK2) = A(2*JK2-1)*EXP(-A(2*JK2)/(R*.001*TEMP(I1)))
3510     NEXT JK2
3515 NEXT I1
3516 ' ALL RHOS ARE CALCULATED ABOVE
3520 RETURN
3521 ' E N D OF ROUTINE -----
3522 '
3525 ' S U B R O U T I N E   GOMEGA -----
3526 ' G OF OMEGA FOR THE INDIVIDUAL RHOS ARE CALCULATED AND STROED IN AN ARRAY
3527 ' WITH THE SECOND INDEX REFERRING TO THE PARTICULAR RHO BEING USED.
3528 '
3530 ' GEE OMEGA FOR CH3 GROUPS
3531 ' GEE OF K1 AND K2
3535 FOR J1 = 1 TO N
3537   FOR KA = 1 TO 4
3540     NR = RHO(J1,KA)
3545     TERM1 = RHO(J1,KA) * RHO(J1,KA)

```



```

3550 TERM2 = OMEGA0^2
3555 TERM3 = 4 * TERM2
3560 DR1 = TERM1 + TERM2
3565 DR2 = TERM1 + TERM3
3570 GEE1 = (NR/DR1)+(NR*4)/DR2
3576 '
3610 GOMEGA(J1,KA) = A * (GEE1)
3611 NEXT KA
3612 ' GEE OMEGA FOR TEMA GROUPS
3613 '
3620 NR = RHO(J1,5)
3625 TERM1 = RHO(J1,5)*RHO(J1,5)
3630 TERM2 = OMEGA0^2
3635 TERM3 = 4*TERM2
3640 DR1 = TERM1+TERM2
3645 DR2 = TERM1+TERM3
3650 GEE3 = (NR/DR1) + ((NR*4)/DR2)
3655 GOMEGA(J1,5) = B * GEE3
3665 NEXT J1
3670 RETURN
3671 ' E N D OF ROUTINE .....
3672 ' E N D OF ROUTINE .....
3680 '
3685 ' S U B R O U T I N E TEEONE-INVERSE
3686 '
3700 GOSUB 3495
3705 GOSUB 3535
3707 'OPEN "RAJAN\DATA\GRAPHICS\SA6FIT8.DAT" FOR OUTPUT AS #3
3710 FOR JK3 = 1 TO N
3720 SLRC(JK3) = (FRACX * GOMEGA(JK3,1)) + (FRACY * GOMEGA(JK3,2)) + (FRACZ * GOMEGA
>) + (FRACP * GOMEGA(JK3,4)) +
GOMEGA(JK3,5)
3730 'PRINT #3,TEMP1(JK3),(1000!/SLRC(JK3))
3740 NEXT JK3
3745 CLOSE #3
3750 '
3751 ' E N D OF ROUTINE .....
3752 ' E N D OF ROUTINE .....
3800 RETURN
4430 REM ***** SUBROUTINE TEEONNE INVERSE END *****
4450 REM ***** SUBROUTINE REFINE tftft#utftft#W*Wtft#
4470 KK1 = KK1 + 1
4490 FOR J = 1 TO M
4510 IF KK1 = MM THEN GOTO 4610
4530 INA(J) = INA(J) / NN
4550 NEXT J
4570 RETURN
4590 REM ++++++ SUBROUTINE REFINE ENDS ++++++
4610 OPEN "SA5OUT8.ONE" FOR APPEND AS #1
4630 PRINT #1,"MSD HAS CONVERGED AND REFINEMENT COMPLETE"
4650 CLOSE #1
4670 GOSUB 4750
4671 LOCATE 22,1
4672 FOR LCOUNT = 1 TO NTAU : PRINT 1/A(2*LCOUNT-1);A(2*LCOUNT)/4.19;
:NEXT LCOUNT
4673 LPRINT " Frequency ";F0
4675 FOR BB = 1 TO NTAU : LPRINT (1/A(2*BB-1));(A(2*BB)/4.19) : NEXT BB
4677 LPRINT " MSD = ";RMSD
4680 FOR BB = 1 TO NTAU : PRINT (1/A(2*BB-1));(A(2*BB)/4.19) : NEXT BB
4705 GOTO 3450

```

```

4710 REM * * * * *
4750 ' * * * * * R O U T I N E   PLOT _____
4760   FOR TR = 1 TO N
4770     Y(1,TR) = LOG(SLRE(TR))
4780     Y(2,TR) = LOG(SLRC(TR))
4790     X(TR) = TEMP1(TR)
4800   NEXT TR
5000 XMAX = 0 : YMAX = 0 : XMIN = 0 : YMIN = 0
5010 FOR IJ = 1 TO N
5020   IF IJ > 1 GOTO 5050
5030   XMAX = X(1) : YMAX = Y(1,1)
5040   XMIN = X(1) : YMIN = Y(1,1)
5050   IF X(IJ) > XMAX THEN XMAX = X(IJ)
5060   IF Y(1,IJ) > YMAX THEN YMAX = Y(1,IJ)
5070   IF X(IJ) < XMIN THEN XMIN = X(IJ)
5080   IF Y(1,IJ) < YMIN THEN YMIN = Y(1,IJ)
5090 NEXT IJ
5100 XDEN = (XMAX - XMIN) : YDEN = (YMAX - YMIN)
5120 SCREEN 2 : VIEW :CLS
5140 IF GRAPHAT$ = "Z" OR GRAPHAT$ = "z" THEN VIEW (0,0) - (639,189),,1
5160 IF GRAPHAT$ = "P" OR GRAPHAT$ = "p" THEN VIEW (50,1)-(300,75),,1
5180 IF GRAPHAT$ = "P" OR GRAPHAT$ = "p" THEN GOTO 5215
5200 LOCATE 2,50 : PRINT "SAMPLE :";SAMPLE$
5205 LOCATE 3,50 : PRINT " FREQ : ";F0
5210 IF GRAPHAT$ = "Z" OR GRAPHAT$ = "z" THEN GOTO 5240
5215 LOCATE 2,25 : PRINT FOMANTISSA
5240 WINDOW (0,0)-(1,1)
5260 LINE (.1,0)-(1,1) ' Y-AXIS Line
5280 LINE (0,.05)-(1,.05) ' X-AXIS Line
5300 FOR TCK = 1 TO 5
5320   LINE (.1+(TCK*.2),.03)-(.1+(TCK*.2),.07) ' TICK MARKS ON X AXIS
5340   LINE (9.00001E-02,(TCK*.2)-.1)-(.11,0+(TCK*.2)-.1) ' TICK
MARKS ON Y AXIS
5360 NEXT TCK
5380 FOR L = 1 TO N
5400   XNR = X(L) - XMIN : IF XNR < 0 GOTO 5660
5420   YNR1 = YMAX - Y(1,L) : IF YNR < 0 GOTO 5680
5440   YNR2 = YMAX - Y(2,L) : IF YNR < 0 GOTO 5680
5460   XP(L) = (.9 * (XNR/XDEN))+.1
5480   YP1(L) = (.9 * (YNR1/YDEN))+.1
5500   YP2(L) = (.9 * (YNR2/YDEN))+.1
5520   CIRCLE ((XP(L),YP1(L)),.0075: IF L = 1 GOTO 5580
5540   PSET (XP(L),YP2(L)): IF L = 1 GOTO 5580
5560   LINE (XP(L),YP2(L)) - (XPP,YPP)
5580   XPP = XP(L)
5600   YPP = YP2(L)
5620 NEXT L
5640 RETURN
5660 PRINT "ERROR XNR = ";XNR : STOP
5680 PRINT "ERROR YNR = ";YNR : STOP
5700 REM + + + + + R O U T I N E   GRADIENT SEARCH_____
5720   SCREEN 0,0,0
5740   IF OPT$ = "U" OR OPT$ = "u" THEN GOTO 5880
5760   PRINT " THEN PLEASE PROVIDE INCREMENTS OF THE PARAMETERS "
5780   PRINT : PRINT : PRINT
5800   FOR BB = 1 TO NTAU
5820   PRINT "          INCRIMENT IN R0-" ;(BB):INPUT "",INA(2*BB-1):PRINT
5840   PRINT "          INCRIMENT IN Ea-" ;(2*BB):INPUT "",INA(2*BB):PRINT
5860 NEXT BB

```

```

5880   GOSUB 4750
5900 LOCATE 22,1
5905 FOR LCOUNT = 1 TO NTAU : PRINT 1/A(2*LCOUNT-1);A(2*LCOUNT)/4.19;
: NEXT LCOUNT

5920 ROUTES = "GRID"
5940 OPEN "SA50UT8.0NE" FOR APPEND AS #1
5960 PRINT #1," *****"
5980 PRINT #1, " THE INCREMENTS ARE : "
6000 FOR BB = 1 TO NTAU
6020 PRINT #1, "DEL.R0-";(BB);INA(2*BB-1);TAB(40);"DEL.Ea-";(2*BB);INA(2*BB)
6040 NEXT BB
6060 PRINT #1, " *****"
6080 CLOSE #1
6100 OPEN "SA6SHADO.INC" FOR OUTPUT AS #1
6120 FOR BB = 1 TO NTAU
6140 PRINT #1,INA(2*BB-1),INA(2*BB)
6160 NEXT BB
6180 CLOSE #1
6200   LOCATE 3,20 : PRINT "PLEASE WAIT"
6220   LOCATE 4,50 : PRINT " GRADIENT SEARCH"
6240   GOSUB 7420
6260   MSD0 = RMSD
6280   DSUM = 0
6300   FOR J = 1 TO M
6320     A(J) = A(J) + .1 * INA(J)
6340     GOSUB 7420
6360     DMSD(J) = (MSD0-RMSD)
6380     DSUM = DSUM + DMSD(J)^2
6400     A(J) = A(J) -.1*INA(J)
6420   NEXT J
6440   DSUM = SQR(DSUM)
6460   FOR J = 1 TO M
6480     GAMA(J) = DMSD(J)/DSUM
6500   NEXT J
6520   FOR J = 1 TO M
6540     A(J) = A(J) + GAMA(J) * INA(J)
6560   NEXT J
6580   GOSUB 7420
6600   MSD1 = RMSD
6620   GOSUB 4750
6640 LOCATE 22,1
6645 FOR LCOUNT = 1 TO NTAU : PRINT 1/A(2*LCOUNT-1);A(2*LCOUNT)/4.19;
: NEXT LCOUNT

6660   IF MSD1<MSD0 THEN GOTO 6780
6680   FOR J = 1 TO M
6700     A(J) = A(J) - (GAMA(J)*INA(J))
6720     GAMA(J) = GAMA(J) / 2
6740   NEXT J
6760   GOTO 6520
6780   FOR J = 1 TO M
6800     A(J) = A(J) + (GAMA(J)*INA(J))
6820   NEXT J
6840   GOSUB 7420
6860   MSD2 = RMSD
6880   IF MSD2 > MSD1 THEN GOTO 6960
6900   MSD0 = MSD1
6920   MSD1 = MSD2
6940   GOTO 6780

```

```

6960 OPEN "SA5OUT8.ONE" FOR APPEND AS 81
6980 PRINT 81,
7000 FOR BB = 1 TO NTAU
7020 PRINT 81, "T0-";(BB);1/A(2*BB-1);TAB(40);"Ea-";(BB);A(2*BB)/4.19
7040 NEXT BB
7060 PRINT #1,"RMSD = ";RMSD
7080 PRINT 81, " *****
7100 PRINT #1, "          GRADIENT SEARCH HAS CONVERGED TO 1% ACCURACY "
7120 CLOSE 81
7140 OPEN "SA6SHADO.8" FOR OUTPUT AS #2
7150 PRINT #2,"BOTH"
7160 FOR BB = 1 TO NTAU
7180 PRINT #2,1/A(2*BB-1),A(2*BB)/4.19
7200 NEXT BB
7220 CLOSE 82
7240   GOSUB 4750
7260 LOCATE 22,1
7265 FOR LCOUNT = 1 TO NTAU : PRINT 1/A(2*LCOUNT-1);A(2*LCOUNT)/4.19;
: NEXT LCOUNT

7280   IF ROUTES = "GRID" OR ROUTES$ = "grid" THEN GOTO 1860
7300   PRINT " DO YOU WANT TO START GRID SEARCH (Y/N) ?"
7320   PP$ = INKEY$ : IF PP$ = "Y" OR PP$ = "y" THEN GOTO 1860
7340   IF PP$ = "N" OR PP$ = "n" THEN GOTO 3430
7360   GOTO 7320
7380   REM      + + + + +      E N D   O F   R O U T I N E   I N C R E M E N T      + +
7400 ' ////////////////
7420 GOSUB 3700
7440   RMSD = 0
7460   FOR ABA = 1 TO N
7480       RMSD = RMSD + ((SLRC(ABA)-SLRE(ABA))/SLRE(ABA))^2
7500   NEXT ABA
7520   RMSD = RMSD / N
7540   RETURN
7560 REM      + + + + +      R O U T I N E   E N D S      + + + + +
7580 ' ////////////////

```

# PROGRAM NO : 2

PROGRAM TO FIT T1 DATA OF TRIMETHYLAMMONIUM COMPOUNDS ...

10 CLS

```

30 REM          SAMPLE NAME          [(CH3)3 NH]3 Bi2 C19
35 REM          FREQUENCY            8 MHz AND 39.6 MHz
50 REM          SOURCE FILE          SA5FITAL.FOR
60 REM          DATA FILE           SA5DATX.THR
70 REM          SOURCE PATH           \RAJAN\ANALYSIS\TMABICL.SA5\X
80 REM          DATA PATH            \RAJAN\DATA\TMABICL.SA5\X
90 REM                                     FOUR CORRELATION TIMES FIT
110 REM
115 KEY OFF
120 SAMPLE$ = "TMABICL.SA5"
125 GRAPHAT$ = "Z"
130 FILE1A$ = "D:\rajan\data\tmabicl.sa5\8\sa5dat8.lt"
131 FILE1A$ = "D:\rajan\data\tmabicl.sa5\40\sa5dat40.thr"
132 ROUTES = "NONE"
135 REM _____TIMER INTERRUPT _____
137 NTIME = 600
140          ON TIMER(NTIME) GOSUB 7600
145          TIMER ON
150 REM ++++++ ++++++ ++++++ ++++++ ++++++ ++++++ ++++++ ++++++ ++++++ ++++++
165 PRINT " DO YOU WANT THE PROGRAM TO START WITH THE DEFAULT VALUES "
170 OPT$ = "d"
190 OPEN FILE1A$ FOR INPUT AS #1
210 INPUT #1,N
230 DIM TEMP1(N),SLRT(N),FX(N),FY(N),TEMP(N)
250 FOR I = 1 TO N
270 INPUT #1,TEMP(I),SLRT(I)
290 NEXT I
310 CLOSE
330 FOR J = 1 TO N
350     AMAX = TEMP(J): K = J
370     FOR I = J TO N
390         IF TEMP(I) <= AMAX THEN GOTO 430
410         AMAX = TEMP(I): K = I
430     NEXT I
450     XTEMP = TEMP(K) : TEMP(K) = TEMP(J) : TEMP(J) = XTEMP
470     YTEMP = SLRT(K) : SLRT(K) = SLRT(J) : SLRT(J) = YTEMP
490     NEXT J
510 M=12
520 NTAU = 6
530 DIM F1(N),F(N),SLRE(N),R(N),INA(M),CX(N),CY(N),A(M)
550 DIM X(N),Y(2,N),X1(N),SLRC(N),C(N),DMSD(M),GAMA(M)
570 DIM KK(5),LL(5),MM(5),K(5),ANEW(N),T$(30),XP(N),YP1(N),YP2(N)
575 DIM RHO(N,NTAU),GOMEGA(N,NTAU)
580 FOR I = 1 TO 5
585 READ KK(I),MM(I),LL(I)
590 NEXT I
600 DATA 24.22,1.74,0.63,48.45,7.28,4.3,19.99,11.68,6.86,0,0,1.16,0,0,2.39
610 KK1=0
630 FOR I = 1 TO N

```

```

640 SLRT(I) = SLRT(I) * .001
650 SLRE(I) = 1/SLRT(I)
660 TEHPL(I) = 1000/TEMP(I)
670 NEXT I
675 A1 = (KK(1)+LL(1)+MM(1)+KK(2)+LL(2)+MM(2))
677 A2 = LL(4)+LL(5)
680 B = (KK(3)+LL(3)+MM(3))
685 F0 = 8000000!
686 'F0 = 3.96E+07
687 F0MANTISSA = F0 / 1000000!
690 OMEGA0 = 2 * 22 * F0 / 7
700 R=8.3143
701 ' ===== INEQUIVALENCE FACTORS =====
705 FRACX = 1/6 ' TMA-I
707 FRACY = 1/6 ' TMA-II
710 FRACZ = 4/6 ' TMA-III
712 FRACP = 1/6 ' CH3-I
715 FRACQ = 1/6 ' CH3-II
717 FRACR = 2/6 ' CH3-III
729 ' ===== INEQUIVALENCE FACTORS =====
730 REM *****
750 IF OPT$ = "U" OR OPT$ = "u" THEN GOTO 930
770 PRINT:PRINT:PRINT
790 A(1) = 9.4E-15 : A(2) = 6.46' TMA-A GROUP
800 A(3) = 1.96E-11 : A(4) = 2.41 ' TMA - B GROUP
810 A(5) = 3.13E-13 : A(6) = 2.88' TMA - C GROUP
820 A(7) = 5E-14 : A(8) = 2.68 ' CH3 - II GROUP
830 A(9) = 2.11E-13 : A(10) = 2.48 ' CH3 - II GROUP
840 A(11) = 8.93E-13 : A(12) = 1.6 ' CH3 - III GROUP
842 '
844 '
850 FOR BB = 1 TO NTAU
860 A(2*BB-1) = 1/A(2*BB-1) : A(2*BB) = A(2*BB) * 4.19
872 NEXT BB
920 GOTO 1045
930 OPEN "SA5SHADO.8" FOR INPUT AS #3
940 INPUT #3,ROUTE$
950 FOR BB = 1 TO NTAU
960 INPUT #3,A(2*BB-1),A(2*BB)
975 A(2*BB-1) = 1/A(2*BB-1) : A(2*BB) = A(2*BB) * 4.19
980 NEXT BB
995 CLOSE 83
1000 OPEN "SA5SHADO.INC" FOR INPUT AS #3
1005 FOR BB = 1 TO NTAU
1010 INPUT #3,INA(2*BB-1),INA(2*BB)
1025 NEXT BB
1030 CLOSE #3
1035 MM = 5
1040 NN = 10
1045 REM ALPHA = .91 ' { alpha is torsional averaging reduction factor }
1180 GOSUB 7420
1200 PRINT " FOLLOWING ARE THE INITIAL VALUES "
1220 FOR BB = 1 TO NTAU
1240 PRINT "T0-";(BB);1/A(2*BB-1);TAB(40);"Ea-";(BB);A(2*BB)/4.19
1270 NEXT BB
1280 PRINT" MSD = "; RMSD
1290 INPUT "--",LJDF$
1350 RMSDX=RMSD
1370 RMSD1=RMSD

```

```

1390 OPEN "SA5OUT8.ONE" FOR OUTPUT AS #1
1410 PRINT #1," *****"
1430 PRINT #1, " FOLLOWING ARE THE INITIAL VALUES "
1450 FOR BB = 1 TO NTAU
1470 PRINT #1, "T0-";(BB);1/A(2*BB-1);TAB(40);"Ea";(BB);A(2*BB)/4.19
1490 NEXT BB
1510 PRINT #1, " *****"
1530 PRINT #1,"MSD = ";RMSD
1550 CLOSE #1
1740 GOSUB 4750
1745 IF ROUTES$ = "BOTH" OR ROUTES$ = "both" THEN GOTO 5700
1750 IF ROUTES = "GRID" OR ROUTES = "grid" THEN GOTO 1860
1790 GRAPHATS$ s INKEY$
1795 IF GRAPHATS$ = "" THEN GOTO 1790
1810 IF GRAPHATS = "P" OR GRAPHATS$r"p" OR GRAPHATS$ = "Z" OR GRAPHATS = "z"
THEN GOSUB 5120 ELSE GOTO 1820
1815 GOTO 1790
1820 PRINT " DO YOU WANT TO START GRID SEARCH OR GRADIENT SEARCH
OR NONE (R/A/N)"

1825 B$ = INKEY$ : IF B$ = "" THEN GOTO 1840
1830 IF B$ = "R" OR B$ = "r" THEN GOTO 1860
1835 IF B$ = "A" OR B$ = "a" THEN GOTO 5700
1840 IF B$ = "N" OR B$ = "n" THEN GOTQ 3430
1850 GOTO 1825
1855 '-----S U B R O U T I N E GRID SEARCH .....
1860 IF OPT$ = "U" OR OPTS = "u" THEN GOTO 2110
1890 PRINT:PRINT:PRINT
1910 PRINT "THEN PLEASE PROVIDE INCRIMENTS OF THE PARAMETRS "
1930 PRINT:PRINT:PRINT
1950 FOR BB = 1 TO NTAU
1970 PRINT"          INCRIMENT IN r0-";(BB);:INPUT "",INA(2*BB-1):PRINT
1990 PRINT"          INCRIMENT IN Ea-";(BB);:INPUT "",INA(2*BB):PRINT
2010 NEXT BB
2070 INPUT"  NUMBER OF REFINEMENTS REQUIRED =";MM : PRINT
2090 INPUT"  REDUCTION FACTOR IN INTERATIONS =";NN
2110 GOSUB 4750
2111 LOCATE 22,1 :PRINT 1/A(1);A(2)/4.19;1/A(3);A(4)/4.19;1/A(5);A(6)/4.19;
1/A(7);A(8)/4.19;1/A(9);A(10)/4.19;1/A(11);A(12)
2120 ROUTES = "GRID"
2130 OPEN "SA5OUT8.ONE" FOR APPEND AS t1
2150 PRINT #1," *****"
2170 PRINT til, " THE INCREMENTS ARE : "
2190 FOR BB = 1 TO NTAU
2210 PRINT #1, "DEL.R0-";(BB);INA(2*BB-1);TAB(40);"DEL.Ea";(BB);INA(2*BB)
2230 NEXT BB
2250 PRINT til, " *****"
2270 CLOSE **1
2290 OPEN "SA5SHADO.INC" FOR OUTPUT AS t1
2310 FOR BB = 1 TO NTAU
2330 PRINT #1,INA(2*BB-1),INA(2*BB)
2360 NEXT BB
2370 CLOSE #1
2390 LOCATE 3,20:PRINT "PLEASE WAIT "
2400 LOCATE 4,50 : PRINT " ITERATION NO : ";KK1
2410 REM PRINT " SEARCH FOR MINIMUM RMSD IS IN PROGRESS"
2450 FOR JK1=1 TO M
2470 A(JK1) s A(JK1)+INA(JK1)
2510 GOSUB 7420

```

```

2530 RMSD2=RMSD
2550 IF RMSD2<RMSD1 THEN GOTO 2590
2570 INA(JK1)= -INA(JK1)
2590 A(JK1)=A(JK1)+INA(JK1)
2610 GOSUB 7420
2630 RMSD3=RMSD
2650 IF RMSD3 >= RMSD2 THEN GOTO 2790
2690 RMSD1=RMSD2
2710 RMSD2=RMSD3
2730 GOTO 2590
2750 P=RMSD3-2*RMSD2+RMSD1
2770 Q=(RMSD3-RMSD2)/P+.5
2790 A(JK1)=A(JK1)-INA(JK1)
2830 RMSD1=RMSD2
2850 NEXT JK1
2930 GOSUB 7420
2950 RMSDY=RMSD
2970 IMPR=(RMSDX-RMSDY)/RMSDX
2990 GOSUB 4750
2991 LOCATE 22,1 : PRINT 1/A(1);A(2)/4.19;1/A(3);A(4)/4.19;1/A(5);A(6)/4.19;
1/A(7);A(8)/4.19;1/A(9);A(10)/4.19;1/A(11);A(12)/4.19
3030 IF IMPR<.001 THEN GOTO 3090
3050 RMSDX=RMSDY
3070 GOTO 2390
3090 OPEN "SA5OUT8.ONE" FOR APPEND AS til
3110 PRINT til," *****"
3130 PRINT #1, " FOLLOWING ARE THE FITTED VALUES "
3150 FOR BB = 1 TO NTAU
3170 PRINT til,"T0-";(BB);(1/A(2*BB-1));TAB(40);"Ea-";(BB);(A(2*BB)/4.19)
3190 NEXT BB
3210 PRINT #1,"RMSD = ";RMSD
3230 PRINT til, " tt**WW*P&l&&&PVI^^
3240 PRINT #1," MSD HAS CONVERGED AND REFINEMENT COMPLETE "
3250 CLOSE til
3270 OPEN "SA5SHADO.8" FOR OUTPUT AS »2
3290 FOR BB = 1 TO NTAU
3310 PRINT #2,1/A(2*BB-1),A(2*BB)/4.19
3340 NEXT BB
3350 CLOSE #2
3370 PRINT:PRINT
3390 GOSUB 4450
3410 GOTO 2130
3420 '-----R O U T I N E   E N D S -----
3430 SCREEN 0.0.0
3450 STOP
3455 END
3460 '-----
3465 '                               E N D   O F   P R O G R A M M E
3470 ' =====
3490 ' S U B R O U T I N E   TAUC .....
3491 ' ARRAYS USED HERE ARE ASSUMED TO BE PROPERLY DIMENSIONED ALREADY
3492 ' A(odd)'s ARE RHO-0 - PRE EXPONENTIAL FACTORS. A(even)s ARE Ea-s
3493 '
3495 FOR I1 = 1 TO N           ' N IS NO. OF TEMPERATURES
3500   FOR JK2 = 1 TO NTAU
3505     RHO(I1,JK2) = A(2*JK2-1)*EXP(-A(2*JK2)/(R*.001*TEMP(I1)))
3510     NEXT JK2
3515 NEXT I1
3516 ' ALL RHOS ARE CALCULATED ABOVE

```



```

3520 RETURN
3521 ' E N D OF ROUTINE .....
3522 '
3525 ' S U B R O U T I N E   G O M E G A .....
3526 ' G OF OMEGA FOR THE INDIVIDUAL RHOS ARE CALCULATED AND STROED IN AN
ARRAY
3527 ' WITH THE SECOND INDEX REFERRING TO THE PARTICULAR RHO BEING USED.
3528 '
3530 ' GEE OMEGA FOR CH3 GROUPS
3531 ' GEE OF K1 AND K2
3535 FOR J1= 1 TO N
3537   FOR KA = 2 TO 4
3540     NR = RHO(J1,KA+2)
3545     TERM1 = RHO(J1,KA+2) * RHO(J1,KA+2)
3550     TERM2 = OMEGA0^2
3555     TERM3 = 4 * TERM2
3560     DR1 = TERM1 + TERM2
3565     DR2 = TERM1 + TERM3
3570     GEE1 = (NR/DR1)+((NR*4)/DR2)
3575     GEE2 = GEE1
3576 '
3577 ' GEE OF KA4 AND KA5
3580 NR = 2 * RHO(J1,KA+2)
3585 TERM1 = 4 * RHO(J1,KA+2)*RHO(J1,KA+2) ' k - 2r
3590 DR1 = TERM1 + TERM2
3595 DR2 = TERM1 + TERM3
3600 GEE4 = (NR/DR1) + ((4*NR)/DR2)
3605 GEE5 = GEE4
3610 GOMEGA(J1,KA+2) = A1 * (GEE1) + A2 * (GEE4)
3611 NEXT KA
3612 ' GEE OMEGA FOR TMA GROUPS
3613 '
3615   FOR KA = 1 TO 3
3620     NR = RHO(J1,KA)
3625     TERM = RHO(J1,KA)*RHO(J1,KA)
3630     TERM2 = OMEGA0^2
3635     TERM3 = 4*TERM2
3640     DR1 = TERM+TERM2
3645     DR2 = TERM1+TERM3
3650     GEE3 = (NR/DR1) + ((NR*4)/DR2)
3655     GOMEGA(J1,KA) = B * GEE3
3660   NEXT KA
3665 NEXT J1
3670 RETURN
3671 ' E N D   OF ROUTINE .....
3672 ' E N D   OF ROUTINE .....
3680 '
3685 ' S U B R O U T I N E   T E E O N E - I N V E R S E
3686 '
3700 GOSUB 3495
3705 GOSUB 3535
3710 'OPEN "\\RAJAN\data\GRAPHICS\dm\SA5FT8c.ch3" FOR OUTPUT AS #1
3715 FOR JK3 = 1 TO N
3720   SLRC(JK3) = (FRACX * GOMEGA(JK3,1)) + (FRACY * GOMEGA(JK3,2))
+ (FRACZ * GOMEGA(JK3,3)) + (FRACP * GOMEGA(JK3,4)) + (FRACQ * GOMEGA(JK3,5))
+ (FRACR * GOMEGA(JK3,6))
3730   SLRC(JK3) = SLRC(JK3) * 1E+08
3735 'PRINT #1, TEMP(JK3),(1000/SLRC(JK3))

```

```

3740 NEXT JK3
3745 'CLOSE #1
3750 '
3751 ' E N D OF ROUTINE .....
3752 ' E N D OF ROUTINE .....
3800 RETURN
4430 REM ***** SUBROUTINE TEEONNE INVERSE END *****
4450 REM ##### SUBROUTINE REFINE #####
4470 KK1 = KK1 + 1
4490 FOR J = 1 TO M
4510     IF KK1 = MM THEN GOTO 4610
4530 INA(J) = INA(J) / NN
4550 NEXT J
4570 RETURN
4590 REM ++++++ SUBROUTINE REFINE ENDS ++++++
4610 OPEN "SA5OUT8.ONE" FOR APPEND AS #1
4630 PRINT #1,"MSD HAS CONVERGED AND REFINEMENT COMPLETE"
4650 CLOSE #1
4670 GOSUB 4750
4671 LOCATE 22,1 : PRINT 1/A(1);A(2)/4.19;1/A(3);A(4)/4.19;1/A(5);A(6)/4.19
1/A(7);A(8)/4.19;1/A(9);A(10)/4.19;1/A(11);A(12)/4.19
4672 LPRINT " Frequency ";F0
4675 FOR BB = 1 TO NTAU : LPRINT (1/A(2*BB-1));(A(2*BB)/4.19) : NEXT BB
4677 LPRINT " MSD = ":RMSD
4680 FOR BB = 1 TO NTAU : PRINT (1/A(2*BB-1));(A(2*BB)/4.19) : NEXT BB
4685 PRINT " fitting complete ; enter Q or q "
4690 INPUT " --".AKDLK$
4705 GOTO 3450
4710 REM * * * * *
4750 ' * * * * * R O U T I N E   P L O T _____
4760 FOR TR = 1 TO N
4770     Y(1,TR) = LOG(SLRE(TR))
4780     Y(2,TR) = LOG(SLRC(TR))
4790     X(TR) = TEMP1(TR)
4800 NEXT TR
5000 XMAX = 0 :YMAX = 0 :XMIN = 0 :YMIN = 0
5010 FOR IJ = 1 TO N
5020 IF IJ > 1 GOTO 5050
5030 XMAX = X(1) :YMAX = Y(1,1)
5040 XMIN = X(1) :YMIN = Y(1,1)
5050 IF X(IJ) > XMAX THEN XMAX = X(IJ)
5060 IF Y(1,IJ) > YMAX THEN YMAX = Y(1,IJ)
5070 IF X(IJ) < XMIN THEN XMIN = X(IJ)
5080 IF Y(1,IJ) < YMIN THEN YMIN = Y(1,IJ)
5090 NEXT IJ
5100 XDEN = (XMAX - XMIN) : YDEN = (YMAX - YMIN)
5120 SCREEN 2 : VIEW :CLS
5140 IF GRAPHAT$ = "Z" OR GRAPHAT$ = "z" THEN VIEW (0,0) - (639,189),,1
5160 IF GRAPHAT$ = "P" OR GRAPHAT$ = "p" THEN VIEW (50,1)-(300,75),,1
5180 IF GRAPHAT$ = "P" OR GRAPHAT$ = "p" THEN GOTO 5215
5200 LOCATE 2,50 : PRINT "SAMPLE :";SAMPLE$
5205 LOCATE 3,50 : PRINT " FREQ : ";F0
5210 IF GRAPHAT$ = "Z" OR GRAPHAT$ = "z" THEN GOTO 5240
5215 LOCATE 2,25 : PRINT F0MANTISSA
5240 WINDOW (0,0)-(1,1)
5260 LINE (.1,0)-(.1,1) ' Y-AXIS Line
5280 LINE (0,.05)-(1,.05) ' X-AXIS Line
5300 FOR TCK = 1 TO 5
5320     LINE (.1+(TCK*.2),.03)-(.1+(TCK*.2),.07) ' TICK MARKS ON X AXIS

```

```

5340      LINE (9.000001E-02,(TCK*.2)-.1)-( .11,0+(TCK*.2)-.1) ' TICK
MARKS ON Y AXIS

5360 NEXT TCK
5380 FOR L = 1 TO N
5400 XNR = X(L) - XMIN : IF XNR < 0 GOTO 5660
5420 YNR1 = YMAX - Y(1,L) : IF YNR < 0 GOTO 5680
5440 YNR2 = YMAX - Y(2,L) : IF YNR < 0 GOTO 5680
5460 XP(L) = (.9 * (XNR/XDEN))+.1
5480 YP1(L) = (.9 * (YNR1/YDEN))+.1
5500 YP2(L) = (.9 * (YNR2/YDEN))+.1
5520 CIRCLE ((XP(L)),YP1(L)),.0075: IF L = 1 GOTO 5580
5540 PSET (XP(L),YP2(L)): IF L = 1 GOTO 5580
5560 LINE (XP(L),YP2(L)) - (XPP,YPP)
5580 XPP = XP(L)
5600 YPP = YP2(L)
5620 NEXT L
5640 RETURN
5660 PRINT "ERROR  XNR = ";XNR : STOP
5680 PRINT "ERROR  YNR = ";YNR : STOP
5700 REM  + + + + +  R O U T I N E  GRADIENT SEARCH_____
5720      SCREEN 0,0,0
5740      IF OPT$ = "U" OR OPT$ = "u" THEN GOTO 5880
5760      PRINT " THEN PLEASE PROVIDE INCREMENTS OF THE PARAMETERS  "
5780      PRINT : PRINT : PRINT
5800      FOR BB = 1 TO NTAU
5820      PRINT          INCREMENT IN R0-";(BB):INPUT"",INA(2*BB-1):PRINT
5840      PRINT          INCREMENT IN Ea-";(2*BB):INPUT "",INA(2*BB):PRINT
5860      NEXT BB
5880      GOSUB 4750
5900      LOCATE 22,1 : PRINT 1/A(1);A(2)/4.19;1/A(3);A(4)/4.19;1/A(5);A(6)/4.19
;1/A(7);A(8)/4.19;1/A(9);A(10)/4.19;1/A(11);A(12)/4.19
5920      ROUTES$ = "GRID"
5940      OPEN "SA5OUT8.ONE" FOR APPEND AS 81
5960      PRINT #1," *****"
5980      PRINT #1," THE INCREMENTS ARE : "
6000      FOR BB = 1 TO NTAU
6020      PRINT 81, "DEL.R0-";(BB);INA(2*BB-1);TAB(40);"DEL.Ea-";(2*BB);INA(2*BB)
6040      NEXT BB
6060      PRINT #1, " *****"
6080      CLOSE 81
6100      OPEN "SA5SHADO.INC" FOR OUTPUT AS 81
6120      FOR BB = 1 TO NTAU
6140      PRINT #1,INA(2*BB-1),INA(2*BB)
6160      NEXT BB
6180      CLOSE #1
6200      LOCATE 3,20 : PRINT "PLEASE WAIT"
6220      LOCATE 4,50 : PRINT " GRADIENT SEARCH"
6240      GOSUB 7420
6260      MSD0 = RMSD
6280      DSUM = 0
6300      FOR J = 1 TO M
6320      A(J) = A(J) + .1 * INA(J)
6340      GOSUB 7420
6360      DMSD(J) = (MSD0-RMSD)
6380      DSUM = DSUM + DMSD(J)^2
6400      A(J) = A(J) -.1*INA(J)
6420      NEXT J
6440      DSUM = SQR(DSUM)

```

```

6460   FOR J = 1 TO M
6480   GAMA(J) = DMSD(J)/DSUM
6500   NEXT J
6520   FOR J = 1 TO M
6540   A(J) = A(J) + GAMA(J) * INA(J)
6560   NEXT J
6580   GOSUB 7420
6600   MSD1 = RMSD
6620   GOSUB 4750
6640 LOCATE 22,1 : PRINT 1/A(1);A(2)/4.19;1/A(3);A(4)/4.19;1/A(5);A(6)/4.19
;1/A(7);A(8)/4.19;1/A(9);A(10)/4.19;1/A(11);A(12)

6660   IF MSD1<MSD0 THEN GOTO 6780
6680   FOR J = 1 TO M
6700   A(J) = A(J) - (GAMA(J)*INA(J))
6720   GAMA(J) = GAMA(J) / 2
6740   NEXT J
6760   GOTO 6520
6780   FOR J = 1 TO M
6800   A(J) = A(J) + (GAMA(J)*INA(J))
6820   NEXT J
6840   GOSUB 7420
6860   MSD2 = RMSD
6880   IF MSD2 > MSD1 THEN GOTO 6960
6900   MSD0 = MSD1
6920   MSD1 = MSD2
6940   GOTO 6780
6960 OPEN "SA5OUT8.ONE" FOR APPEND AS 81
6980 PRINT 81, " *****"
7000 FOR BB = 1 TO NTAU
7020 PRINT 81, "T0-";(BB);1/A(2*BB-1);TAB(40);"Ea-";(BB);A(2*BB)/4.19
7040 NEXT BB
7060 PRINT #1,"RMSD = ";RMSD
7080 PRINT 81, " *****"
7100 PRINT #1, "          GRADIENT SEARCH HAS CONVERGED TO 1% ACCURACY "
7120 CLOSE 81
7140 OPEN "SA5SHADO.8" FOR OUTPUT AS 82
7160 FOR BB = 1 TO NTAU
7180 PRINT 82,1/A(2*BB-1),A(2*BB)/4.19
7200 NEXT BB
7220 CLOSE 82
7240   GOSUB 4750
7260 LOCATE 22,1 : PRINT 1/A(1);A(2)/4.19;1/A(3);A(4)/4.19;1/A(5);A(6)/4.19
;1/A(7);A(8)/4.19;1/A(9);A(10)/4.19;1/A(11);A(12)/4.19

7280   IF ROUTE$ = "GRID" OR ROUTE$ = "grid" THEN GOTO 1860
7300   PRINT " DO YOU WANT TO START GRID SEARCH (Y/N) ?"
7320   PP$ = INKEY$: IF PP$ = "Y" OR PP$ = "y" THEN GOTO 1860
7340   IF PP$ = "N" OR PP$ = "n" THEN GOTO 3430
7360   GOTO 7320
7380   REM   + + + + + END OF ROUTINE INCREMENT
7400   ' ////////////////
7420 GOSUB 3700
7440   RMSD = 0
7460   FOR ABA = 1 TO N
7480   RMSD = RMSD + ((SLRC(ABA)-SLRE(ABA))/SLRE(ABA))^2
7500   NEXT ABA
7520   RMSD = RMSD / N
7540   RETURN
7560 REM   + + + + + ROUTINE ENDS + + + +

```

```

7580 '////////_///
7600 REM + + + + T I M E R   I N T E R R U P T   R O U T I N E   + +
7620 OPEN "SA5SHADO.8" FOR OUTPUT AS tt3
7640 PRINT #3,ROUTE$
7660 FOR BB = 1 TO NTAU
7680 PRINT #3,1/A(2*BB-1);A(2*BB)/4.19
7700 NEXT BB
7720 CLOSE #3
7740 OPEN "SA5SHADO.INC" FOR OUTPUT AS 83
7760 FOR BB = 1 TO NTAU
7780 PRINT #3,INA(2*BB-1);INA(2*BB)
7800 NEXT BB
7820 CLOSE #3
7840 ON TIMER(600) GOSUB 7600
7860 TIMER ON
7880 RETURN
7900 REM + + + + + R O U T I N E   E N D S   + + + + +

```

PROGRAM USED TO FIT T1 DATA OF AMMONIUM SUBSTITUTED COMPOUNDS...

10 CLS

```
30 REM          SAMPLE NAME      :      [NH4]3 Bi2 Br9
35 REM          FREQUENCY       :      8 MHz AND 39.6 MHz
50 REM          SOURCE FILE     :      SA2FIT8.BAS
60 REM          DATA FILE      :      SA2DATxx.THR
70 REM          SOURCE PATH     :      \RAJAN\ANALYSIS\NH4BIBR.SA2\XX
80 REM          DATA PATH      :      \RAJAN\DATA\NH4BIBR.SA2\XX
90 REM                                single CORRELATION TIME FIT
```

```
115 KEY OFF
120 SAMPLES = "NH4BIBR.SA2"
125 GRAPHAT$ = "Z"
130 FILE1A$ = "D:\rajan\data\nh4bibr.sa2\8\sa2dat8.thr"
131 FILE1A$ = "D:\rajan\data\nh4bibr.sa2\40\sa2dat40.two"
132 ROUTES = "NONE"
150 REM ++++++
170 OPT$ = "d"
190 OPEN FILE1A$ FOR INPUT AS #1
210 INPUT #1, N
230   DIM TEMP1(N),SLRT(N),FX(N),FY(N),TEMP(N)
250   FOR I = 1 TO N
270     INPUT #1,TEMP(I),SLRT(I)
290     NEXT I
310 CLOSE
330   FOR J = 1 TO N
350     AMAX = TEMP(J): K = J
370     FOR I = J TO N
390       IF TEMP(I) <= AMAX THEN GOTO 430
410       AMAX = TEMP(I): K = I
430     NEXT I
450     XTEMP = TEMP(K) : TEMP(K) = TEMP(J) : TEMP(J) = XTEMP
470     YTEMP = SLRT(K) : SLRT(K) = SLRT(J) : SLRT(J) = YTEMP
490     NEXT J
510 M=2
520 NTAU = 1
530 DIM F1(N),F(N),SLRE(N),R(N),INA(M),CX(N),CY(N),A(M)
550 DIM X(N),Y(2,N),X1(N),SLRC(N),C(N),DMSD(M),GAMA(M)
570 DIM KK(5),LL(5),MM(5),K(5),ANEW(N),T$(30),XP(N),YP1(N),YP2(N)
575 DIM RHO(N,NTAU),GOMEGA(N,NTAU)
630 FOR I = 1 TO N
640   SLRT(I) = SLRT(I) * .001
650   SLRE(I) = 1/SLRT(I)
660   TEMPl(I) = 1000/TEMP(I)
670 NEXT I
685 'F0 = 8000000!
686 F0 = 3.96E+07
687 F0MANTISSA = F0 / 1000000!
690 OMEGA0 = 2 * 22 * F0 / 7
695 B = 2.375E+10
700 R=8.3143
729 ' =+++++ INEQUIVALENCE FACTORS ++++++
730 REM *****
```

```

750 IF OPT$ = "U" OR OPT$ = "u" THEN GOTO 930
770 PRINT:PRINT:PRINT
790 A(1) - 2.58E-13 : A(2) = 2.05' NH4 GROUP
850 FOR BB = 1 TO NTAU
860 A(2*BB-1) = 1/A(2*BB-1) : A(2*BB) - A(2*BB) * 4.19
872 NEXT BB
920 GOTO 1180
930 OPEN "SA2SHADO.8" FOR INPUT AS #3
940 INPUT tf3, ROUTES
950 FOR BB = 1 TO NTAU
960 INPUT #3, A(2*BB-1), A(2*BB)
975 A(2*BB-1) = 1/A(2*BB-1) : A(2*BB) = A(2*BB) * 4.19
980 NEXT BB
995 CLOSE #3
1000 FOR BB = 1 TO NTAU
1005 INA(2*BB-1) = A(2*BB-1)/100
1010 INA(2*BB) = A(2*BB)/100
1025 NEXT BB
1035 MM = 5
1040 NN = 10
1180 GOSUB 7420
1200 PRINT " FOLLOWING ARE THE INITIAL VALUES "
1220 FOR BB = 1 TO NTAU
1240 PRINT "T0-";(BB);1/A(2*BB-1);TAB(40);"Ea-";(BB);A(2*BB)/4.19
1270 NEXT BB
1280 PRINT" MSD - ": RMSD
1350 RMSDX=RMSD
1370 RMSDI=RMSD
1390 OPEN "SA4OUT8.ONE" FOR OUTPUT AS #1
1410 PRINT #1, " *****"
1430 PRINT #1, " FOLLOWING ARE THE INITIAL VALUES "
1450 FOR BB = 1 TO NTAU
1470 PRINT #1, "T0-";(BB);1/A(2*BB-1);TAB(40);"Ea";(BB);A(2*BB)/4.19
1490 NEXT BB
1510 PRINT #1, " *****"
1530 PRINT #1, "MSD = ";RMSD
1550 CLOSE #1
1740 GOSUB 4750
1745 IF ROUTES = "BOTH" OR ROUTES$ = "both" THEN GOTO 5700
1750 IF ROUTES = "GRID" OR ROUTES$ = "grid" THEN GOTO 1860
1790 GRAPHAT$ = INKEY$
1795 IF GRAPHAT$ = "" THEN GOTO 1790
1810 IF GRAPHAT$ = "p" OR GRAPHAT$ = "P" OR GRAPHAT$ = "Z" OR GRAPHAT$ = "z"
THEN GOSUB 5120 ELSE GOTO 1820

1815 GOTO 1790
1820 PRINT " DO YOU WANT TO START GRID SEARCH OR GRADIENT SEARCH OR NONE (R/A/N)
1825 B$ = INKEY$ : IF B$ = "" THEN GOTO 1840
1830 IF B$ = "R" OR B$ = "r" THEN GOTO 1860
1835 IF B$ = "A" OR B$ = "a" THEN GOTO 5700
1840 IF B$ = "N" OR B$ = "n" THEN GOTO 3430
1850 GOTO 1825
1855 '-----S U B R O U T I N E GRID SEARCH -----
1860 IF OPT$ = "U" OR OPT$ = "u" THEN GOTO 2110
1890 PRINT:PRINT:PRINT
1910 PRINT "THEN PLEASE PROVIDE INCRIMENTS OF THE PARAMETRS "
1930 PRINT:PRINT:PRINT
1950 FOR BB = 1 TO NTAU
1970 PRINT" INCRIMENT IN r0-";(BB);:INPUT "", INA(2*BB-1):PRINT
1990 PRINT" INCRIMENT IN Ea-";(BB);:INPUT "", INA(2*BB):PRINT

```

```

2010 NEXT BB
2070 INPUT"  NUMBER OF REFINEMENTS REQUIRED =";MM : PRINT
2090 INPUT"  REDUCTION FACTOR IN INTERACTIONS =";NN
2110 GOSUB 4750
2111 LOCATE 22,1
2115 FOR PLOOP = 1 TO NTAU : PRINT 1/A(2*PLOOP-1);A(2*PLOOP)/4.19; :NEXT PLOOP
2120 ROUTES$ = "GRID"
2130 OPEN "SA4OUT8.ONE" FOR APPEND AS #1
2150 PRINT #1," *****"
2170 PRINT #1, " THE INCREMENTS ARE : "
2190 FOR BB = 1 TO NTAU
2210 PRINT 81, "DEL.R0-";(BB);INA(2*BB-1);TAB(40);"DEL.Ea";(BB);INA(2*BB)
2230 NEXT BB
2250 PRINT #1, " *****"
2270 CLOSE 81
2290 OPEN "SA4SHADO.INC" FOR OUTPUT AS 81
2310 FOR BB = 1 TO NTAU
2330 PRINT #1,INA(2*BB-1),INA(2*BB)
2360 NEXT BB
2370 CLOSE 81
2390 LOCATE 3,20:PRINT 'PLEASE WAIT "
2400 LOCATE 4,50 : PRINT " ITERATION NO : ";KK1
2450 FOR JK1= 1 TO M
2470 A(JK1) = A(JK1)+INA(JK1)
2510 GOSUB 7420
2530 RMSD2=RMSD
2550 IF RMSD2<RMSD1 THEN GOTO 2590
2570 INA(JK1)= -INA(JK1)
2590 A(JK1)=A(JK1)+INA(JK1)
2610 GOSUB 7420
2630 RMSD3=RMSD
2650 IF RMSD3 >= RMSD2 THEN GOTO 2790
2690 RMSD1=RMSD2
2710 RMSD2=RMSD3
2730 GOTO 2590
2750 P=RMSD3-2*RMSD2+RMSD1
2770 Q=(RMSD3-RMSD2)/P+.5
2790 A(JK1)=A(JK1)-INA(JK1)
2830 RMSD1=RMSD2
2850 NEXT JK1
2930 GOSUB 7420
2950 RMSDY=RMSD
2970 IMPR=(RMSDX-RMSDY)/RMSDX
2990 GOSUB 4750
2991 LOCATE 22,1
3000 FOR PLOOP = 1 TO NTAU
3010 PRINT (1/A(2*PLOOP-1));(A(2*PLOOP)/4.19);
3020 NEXT PLOOP
3030 IF IMPR<.001 THEN GOTO 3090
3050 RMSDX=RMSDY
3070 GOTO 2390
3090 OPEN "SA4OUT8.ONE" FOR APPEND AS 81
3110 PRINT #1," *****"
3130 PRINT #1, " FOLLOWING ARE THE FITTED VALUES "
3150 FOR BB = 1 TO NTAU
3170 PRINT 81, "T0-";(BB);(1/A(2*BB-1));TAB(40);"Ea-";(BB);(A(2*BB)/4.19)
3190 NEXT BB
3210 PRINT #1,"RMSD = ";RMSD
3230 PRINT 81, " *****"

```



```

3240 PRINT #1, " MSD HAS CONVERGED AND REFINEMENT COMPLETE
3250 CLOSE #1
3270 OPEN "SA2SHADO.8" FOR OUTPUT AS #2
3280 PRINT #2, "BOTH"
3290 FOR BB = 1 TO NTAU
3310 PRINT tt2, 1/A(2*BB-1), A(2*BB)/4.19
3340 NEXT BB
3350 CLOSE #2
3370 PRINT:PRINT
3390 GOSUB 4450
3410 GOTO 2130
3420 '-----ROUTINE ENDS .....
3430 SCREEN 0.0,0
3455 END
3460 '-----
3465 ' END OF PROGRAMME
3470 '-----
3490 ' SUBROUTINE TAUC .....
3491 ' ARRAYS USED HERE ARE ASSUMED TO BE PROPERLY DIMENSIONED ALREADY
3492 ' A(odd)'s ARE RHO-0 - PRE EXPONENTIAL FACTORS. A(even)'s ARE Ea-s
3493 '
3495 FOR I1 = 1 TO N ' N IS NO. OF TEMPERATURES
3500 FOR JK2 = 1 TO NTAU
3505 RHO(I1,JK2) = A(2*JK2-1)*EXP(-A(2*JK2)/(R*.001*TEMP(I1)))
3510 NEXT JK2
3515 NEXT I1
3516 ' ALL RHOS ARE CALCULATED ABOVE
3520 RETURN
3521 ' END OF ROUTINE .....
3522 '
3525 ' SUBROUTINE GOMEGA .....
3526 ' G OF OMEGA FOR THE INDIVIDUAL RHOS ARE CALCULATED AND STROED IN AN ARRAY
3527 ' WITH THE SECOND INDEX REFERRING TO THE PARTICULAR RHO BEING USED.
3528 '
3530 ' GEE OMEGA FOR NH4 GROUPS
3531 '
3535 FOR J1 = 1 TO N
3540 NR = RHO(J1,1)
3545 TERM1 = RHO(J1,1) * RHO(J1,1) ' k = r
3550 TERM2 = OMEGA0^2
3555 TERM3 = 4 * TERM2
3560 DR1 = TERM1 + TERM2
3565 DR2 = TERM1 + TERM3
3570 GEE1 = (NR/DR1)+(NR*4)/DR2)
3576 GOMEGA (J1,1) = B * GEE1
3665 NEXT J1
3670 RETURN
3671 ' END OF ROUTINE .....
3680 '
3685 ' SUBROUTINE TEEONE-INVERSE
3686 '
3700 GOSUB 3495
3705 GOSUB 3535
3710 FOR JK3 = 1 TO N
3720 SLRC(JK3) = GOMEGA(JK3,1)
3731 'PRINT TEMP1(JK3):(1000/SLRC(JK3))
3735 '
3740 NEXT JK3
3750 '

```

```

3751 ' E N D   O F   R O U T I N E .....
3752 ' E N D   O F   R O U T I N E .....
3800 RETURN
4430 REM ***** SUBROUTINE TEEONNE INVERSE END *****
4450 REM ##### SUBROUTINE REFINE #####
4470 KK1 = KK1 + 1
4490 FOR J = 1 TO M
4510     IF KK1 = MM THEN GOTO 4610
4530 INA(J) = INA(J) / NN
4550 NEXT J
4570 RETURN
4590 REM ++++++ SUBROUTINE REFINE ENDS ++++++
4610 OPEN "SA40UT8.ONE" FOR APPEND AS #1
4630 PRINT «1,"MSD HAS CONVERGED AND REFINEMENT COMPLETE"
4650 CLOSE #1
4670 GOSUB 4750
4671 LOCATE 22,1:FOR PLOOP = 1 TO NTAU : PRINT 1/(A*(PLOOP-1));A*(PLOOP)/4.19;
: NEXT PLOOP
4672 LPRINT " Frequency ";F0
4675 FOR BB = 1 TO NTAU : LPRINT (1/(A*(BB-1)));A*(BB)/4.19 : NEXT BB
4677 LPRINT " MSD = ";RMSD
4680 FOR BB = 1 TO NTAU : PRINT (1/(A*(BB-1)));A*(BB)/4.19 : NEXT BB
4705 GOTO 3455
4710     REM      * * * * *
4750 ' * * * * * R O U T I N E   P L O T   _____
4760 FOR TR = 1 TO N
4770     Y(1,TR) = LOG(SLRE(TR))
4780     Y(2,TR) = LOG(SLRC(TR))
4790     X(TR) = TEMP1(TR)
4800 NEXT TR
5000 XMAX = 0 : YMAX = 0 : XMIN = 0 : YMIN = 0
5010 FOR IJ = 1 TO N
5020 IF IJ > 1 GOTO 5050
5030 XMAX = X(1) : YMAX = Y(1,1)
5040 XMIN = X(1) : YMIN = Y(1,1)
5050 IF X(IJ) > XMAX THEN XMAX = X(IJ)
5060 IF Y(1,IJ) > YMAX THEN YMAX = Y(1,IJ)
5070 IF X(IJ) < XMIN THEN XMIN = X(IJ)
5080 IF Y(1,IJ) < YMIN THEN YMIN = Y(1,IJ)
5090 NEXT IJ
5100 XDEN = (XMAX - XMIN) : YDEN = (YMAX - YMIN)
5120 SCREEN 2 : VIEW :CLS
5140 IF GRAPHAT$ = "Z" OR GRAPHAT$ = "z" THEN VIEW (0,0) - (639,189),,1
5160 IF GRAPHAT$ = "P" OR GRAPHAT$ = "p" THEN VIEW (50,1)-(300,75),,1
5180 IF GRAPHAT$ = "P" OR GRAPHAT$ = "p" THEN GOTO 5215
5200 LOCATE 2,50 : PRINT "SAMPLE :";SAMPLE$
5205 LOCATE 3,50 : PRINT " FREQ : ";F0
5210 IF GRAPHAT$ = "Z" OR GRAPHAT$ = "z" THEN GOTO 5240
5215 LOCATE 2,25 : PRINT FOMANTISSA
5240 WINDOW (0,0)-(1,1)
5260 LINE (.1,0)-(.1,1) ' Y-AXIS Line
5280 LINE (0,.05)-(1,.05) ' X-AXIS Line
5300 FOR TCK = 1 TO 5
5320     LINE (.1+(TCK*.2),.03)-(.1+(TCK*.2),.07) ' TICK MARKS ON X AXIS
5340     LINE (9.000001E-02,(TCK*.2)-.1)-(.11,0+(TCK*.2)-.1) ' TICK MARKS
ON Y AXIS
5360 NEXT TCK
5380 FOR L = 1 TO N

```

```

5400 XNR = X(L) - XMIN : IF XNR < 0 GOTO 5660
5420 YNR1 = YMAX - Y(1,L) : IF YNR < 0 GOTO 5680
5440 YNR2 = YMAX - Y(2,L) : IF YNR < 0 GOTO 5680
5460 XP(L) = (.9 * (XNR/XDEN))+.1
5480 YP1(L) = (.9 * (YNR1/YDEN))+.1
5500 YP2(L) = (.9 * (YNR2/YDEN))+.1
5520 CIRCLE ((XP(L)),YP1(L)),.0075: IF L = 1 GOTO 5580
5540 PSET (XP(L),YP2(L)): IF L = 1 GOTO 5580
5560 LINE (XP(L),YP2(L)) - (XPP,YPP)
5580 XPP = XP(L)
5600 YPP = YP2(L)
5620 NEXT L
5640 RETURN
5660 PRINT "ERROR XNR = ";XNR : STOP
5680 PRINT "ERROR YNR = ";YNR : STOP
5700 REM + + + + + R O U T I N E   G R A D I E N T   S E A R C H _____
5720 SCREEN 0,0,0
5740 IF OPTS = "U" OR OPT$ = "u" THEN GOTO 5880
5760 PRINT " THEN PLEASE PROVIDE INCREMENTS OF THE PARAMETERS "
5780 PRINT : PRINT : PRINT
5800 FOR BB = 1 TO NTAU
5820 PRINT"          INCRIMENT IN R0-";(BB):INPUT"",INA(2*BB-1):PRINT
5840 PRINT"          INCRIMENT IN Ea-";(2*BB):INPUT "",INA(2*BB):PRINT
5860 NEXT BB
5880 GOSUB 4750
5900 LOCATE 22,1
5905 FOR PLOOP = 1 TO NTAU
5910 PRINT 1/A(2*PLOOP-1);A(2*PLOOP)/4.19;
5915 NEXT PLOOP
5920 ROUTES$ = "GRID"
5940 OPEN "SA4OUT8.ONE" FOR APPEND AS #1
5960 PRINT #1," *****"
5980 PRINT #1," THE INCREMENTS ARE : "
6000 FOR BB = 1 TO NTAU
6020 PRINT #1,"DEL.R0-";(BB);INA(2*BB-1);TAB(40);"DEL.Ea-";(2*BB);INA(2*BB)
6040 NEXT BB
6060 PRINT #1," *****"
6080 CLOSE #1
6100 OPEN "SA4SHADO.INC" FOR OUTPUT AS #1
6120 FOR BB = 1 TO NTAU
6140 PRINT #1,INA(2*BB-1),INA(2*BB)
6160 NEXT BB
6180 CLOSE #1
6200 LOCATE 3,20 : PRINT "PLEASE WAIT"
6220 LOCATE 4,50 : PRINT " GRADIENT SEARCH"
6240 GOSUB 7420
6260 MSD0 = RMSD
6280 DSUM = 0
6300 FOR J = 1 TO M
6320 A(J) = A(J) + .1 * INA(J)
6340 GOSUB 7420
6360 DMSD(J) = (MSD0-RMSD)
6380 DSUM = DSUM + DMSD(J)
6400 A(J) = A(J) -.1*INA(J)
6420 NEXT J
6440 DSUM = SQR(DSUM)
6460 FOR J = 1 TO M
6480 GAMA(J) = DMSD(J)/DSUM
6500 NEXT J

```

```

6520   FOR J = 1 TO M
6540   A(.T) r A(J) + GAMA(J) * INA(J)
6560   NEXT J
6580   GOSUB 7420
6600   MSD1 = RMSD
6620   GOSUB 4750
6640   LOCATE 22,1
6645   FOR PLOOP = 1 TO NTAU
6650   PRINT 1/A(2*PLOOP-1):A(2*PLOOP)/4.19;
6655   NEXT PLOOP
6660   IF MSD1<MSD0 THEN GOTO 6780
6680   FOR J = 1 TO M
6700   A(J) = A(J) - (GAMA(J)*INA(J))
6720   GAMA(J) = GAMA(J) / 2
6740   NEXT J
6760   GOTO 6520
6780   FOR J = 1 TO M
6800   A(J) = A(J) + (GAMA(J)*INA(J))
6820   NEXT J
6840   GOSUB 7420
6860   MSD2 = RMSD
6880   IF MSD2 > MSD1 THEN GOTO 6960
6900   MSD0 = MSD1
6920   MSD1 = MSD2
6940   GOTO 6780
6960   OPEN "SA4OUT8.ONE" FOR APPEND AS #1
6980   PRINT #1," *****"
7000   FOR BB = 1 TO NTAU
7020   PRINT 81, "T0-":(BB);1/A(2*BB-1);TAB(40);"Ea-";(BB);A(2*BB)/4.19
7040   NEXT BB
7060   PRINT #1,"RMSD = ":RMSD
7080   PRINT #1, " *****"
7100   PRINT 81, "          GRADIENT SEARCH HAS CONVERGED TO 1% ACCURACY "
7120   CLOSE 81
7140   OPEN "SA2SHADO.8" FOR OUTPUT AS 82
7150   PRINT #2,"BOTH"
7160   FOR BB = 1 TO NTAU
7180   PRINT #2,1/A(2*BB-1),A(2*BB)/4.19
7200   NEXT BB
7220   CLOSE 82
7240   GOSUB 4750
7260   LOCATE 22,1
7265   FOR PLOOP = 1 TO NTAU
7270   PRINT 1/A(2*PLOOP-1):A(2*PLOOP)/4.19;
7275   NEXT PLOOP
7280   IF ROUTES = "GRID" OR ROUTES$ = "grid" THEN GOTO 1860
7300   PRINT " DO YOU WANT TO START GRID SEARCH (Y/N) ?"
7320   PP$ = INKEY$: IF PP$ = "Y" OR PP$ = "y" THEN GOTO 1860
7340   IF PP$ = "N" OR PP$ = "n" THEN GOTO 3430
7360   GOTO 7320
7380   REM      + + + + +      E N D   O F   R O U T I N E   I N C R E M E N T      + + +
7400   ' ////////////////
7420   GOSUB 3700
7440   RMSD = 0
7460   FOR ABA = 1 TO N
7480       RMSD = RMSD + ((SLRC(ABA)-SLRE(ABA))/SLRE(ABA))^2
7500   NEXT ABA
7520   RMSD = RMSD / N
7540   RETURN

```

PROGRAM NO : 4

```

1 CLEAR ,60000! : IBINIT1=60000! : IBINIT2=IBINIT1+3 : BLOAD "C:\GPIB\bib.m".
IBINIT1
2 CALL IBINIT1(IBFIND,IBTRG,IBCLR,IBPCT,IBSIC,IBLOC,IBPPC,IBBNA,IBONL,IBRSC,
IBSRRE,IBRSV,IBPAD,IBSAD,IBIST,IBDMA,IBEOS,IBTMO,IBEOT,IBROF,IBWRTF,IBTRAP)
3 CALL IBINIT2(IBGTS,IBCAC,IBWAIT,IBPOKE,IBWRT,IBWRTA,IBCMD,IBCMDA,IBRD,
IBRDA,IBSTOP,IBRPP,IBRSP,IBDIAG,IBXTRC,IBRDI,IBWRTI,IBRDTA,IBWRTIA,IBSTA%,IBERR%,
IBCNT%)
10 BOARDS = "GPIB0" : CALL IBFIND(BOARD$,BRD%)
15 SCOPE$ = "TEKSCOP" : CALL IBFIND(SCOPE$,TEK%)
20 DELAYS = "DELAY" : CALL IBFIND(DELAY$,DELAY%)
25 CLS
100 REM X X X X X X X X X X X X X X PROGRAM ECHO FEAK X X X X X X X X X X
110 REM HAHN ECHO SEQUENCE
115 REM X X X X X X X X X X X X X X X X X X X X X X X X X X X X X X
120 REM * * * * PART ONE * * * *
130 REM
140 REM THIS PART OF THE PROGRAM DOES THE FOLLOWING
150 REM
160 REM 1. ASKS THE USER FOR TAU VALUES IN MILLI SECONDS.
170 REM
180 REM 2. ASKS FOR THE REPETITION RATE i.e. 5T1
190 REM
200 REM 3. ASKS FOR THE NO. OF AVERAGES TO BE DONE.
210 REM
220 REM 4. ASKS FOR THE FILE NAME IN WHICH THE WAVEFORM IS TO BE
230 REM STORED.
240 REM * * * - - - - * * * *
250 REM + + + + +PART ONE BEGINS ++ + + + +
260 REM <=====> DECLARATIONS <=====>
270 REM
280 DIM TAU(200),A(200),B(200),ITAU(200),IATAU(200),X(200)
290 DIM Y(200),YL(200),YM(200),E(200),PX(1500),PY(1500)
300 DIM CX(200),CY(200),FX(200),FY(200),Ts(200)
310 DIM JTAU(200),KTAU(200),OFFTEMP(20),SLOPE(20)
320 AFLAG = 0
330 REM
340 REM
350 REM <=====>_____<=====>
360 REM
370 REM ?????????????????????? QUERIES ??????????????????????
380 CLS:INPUT " DO YOU NEED INTERNAL GENERATION OF TAU VALUES ? (Y/N)";INTG$
390 IF (INTG$ = "Y") OR (INTG$ = "y") THEN GOSUB 6520
400 CLS:INPUT "INPUT VALUES FROM KEYBOARD OR FILE ? ENTER CHOICE (K/F) " .KF$
410 IF (KF$ = "K") OR (KF$ = "k") THEN GOTO 510
420 OPEN "ECHOSET1" FOR INPUT AS #3
430 INPUT #3,TAU0 : TAU01 = TAU0
440 FOR T = 1 TO TAU0
450 INPUT #3,TAU(T) : ITAU(T) = TAU(T)
460 NEXT T
470 INPUT #3, AVERAGE
480 INPUT #3, WEIGHT
490 CLOSE #3
500 GOTO 730
510 OPEN "ECHOSET1" FOR OUTPUT AS #3

```

```

520 CLS:INPUT "HOW MANY TAU VALUES DO YOU HAVE "; TAU0 : TAU01 = TAU0
530 PRINT #3,SPC(5) TAU0
540 CLS:PRINT "GIVE THE TAU VALUES IN MILLI SECONDS "
550 FOR J = 1 TO TAU0
560 PRINT "TAU"+STR$(J)+" = ": INPUT TAU(J): PRINT
570 PRINT #3, SPC(10),TAU(J)
580 NEXT J
590 CLS:PRINT "THESE ARE THE TAU VALUES YOU GAVE " : PRINT
600 FOR K = 1 TO TAU0
610 PRINT "TAU"+STR$(K),TAB(20),TAU(K)
620 NEXT K
630 PRINT -ENTER TO PROCEED"
640 INPUT:QUES$
650 FOR LK = 1 TO TAU0 : ITAU(LK) = TAU(LK)
660 NEXT LK
670 CLS:INPUT "HOW MANY NO. OF AVERAGES DO YOU NEED ":AVERAGE
690 PRINT #3, SPC(5).AVERAGE
690 PRINT
700 CLS:INPUT "GIVE THE WEIGHT FOR AVERAGING ";WEIGHT
710 PRINT #3, SPC(5).WEIGHT
720 CLOSE #3
730 CLS:INPUT "WHAT IS THE REPETITION RATE (GIVE IN SECONDS PLEASE)";RATE
740 CLS:PRINT " GIVE THE FILE NAME TO SAVE DATA PTS. [tau,A(tau)] "
750 PRINT:INPUT EXP1$
760 REM ?????????????????? QUERIES END ??????????????????????????????
770 WORD1$ = "P@132000000" : CALL IBWRT(DELAY%,WORD1$)
780 WORD2$ = "Q@131000000" : CALL IBWRT(DELAY%,WORD2$)
790 WORD3$ = "R@123000000" : CALL IBWRT(DELAY%,WORD3$)
800 WORD4$ = "S@113000000" : CALL IBWRT(DELAY%,WORD4$)
810 WORD5$ = "T@133000000" : CALL IBWRT(DELAY%,WORD5$)
820 REM
830 REM
840 REM MASTER-----LOOP
850 REM LPRINTSPC(15) "TAU (m.sec)"SPC(15)"DELTA V (volts)"
860 OPEN EXP1$ FOR OUTPUT AS #2
870 LAB1 = 65 : LAB2 = 0
880 FOR JK = 1 TO TAU0
890 REM
900 IF TAU(JK) <= 9.998999 GOTO 950
910 IF TAU(JK) <= 99.999 GOTO 960
920 IF TAU(JK) <= 999.99 GOTO 970
930 IF TAU(JK) <= 9999.901 GOTO 980
940 IF TAU(JK) <= 99999! GOTO 990
950 GOSUB 1160 : GOTO 1000
960 GOSUB 1310 : GOTO 1000
970 GOSUB 1460 : GOTO 1000
980 GOSUB 1610 : GOTO 1000
990 GOSUB 1760 : GOTO 1000
1000 NEXT JK
1010 IF AFLAG = 1 THEN GOTO 1030
1020 CLOSE 32 : LAB1 = 65 : LAB2 = 0
1030 GOSUB 6200
1040 GOTO 1120
1050 D4 = EXTR * 10 : D41$ = STR$(D4)
1060 PART1$ s "S"
1070 PART2$ = "D"
1080 PART3$ = MID$(D41$,2) : PART4$ = "1"
1090 WORDS1$ = PART1$+PART2$+PART3$+PART4$
1100 CALL IBWRT(DELAY%.WORDS1$)

```

```

1110 CALL IBWRT(DELAY%,WORD4$)
1120 CMD$ - "ACQ REP:SAM,HSR:SAM,LSR:SAM,SCAN:SAM,NUM:0 "
1130 CALL IBWRT(TEK%,CMD$)
1140 IF AFLAG = 1 THEN GOTO 2810 ELSE GOTO 2520
1150 REM + + + + +
1160 REM SUBROUTINE RANGE 1
1170 REM
1180 D1 = TAU(JK) * 10000 : D11$ = STR$(D1)
1190 PART1$ = "P"
1200 PART2$ = CHR$(74-LEN(D11$))
1210 PART3$ = MID$(D11$,2) : PART4$ = "!"
1220 WORDP1$ = PART1$+PART2$+PART3$+PART4$
1230 CALL IBWRT(DELAY%,WORDP1$)
1240 CALL IBWRT(DELAY%,WORD1$)
1250 GOSUB 1940
1260 RETURN
1270 REM + + + + +
1280 REM SUBROUTINE WORKING PROPERLY.
1290 REM WWW SAVED IN THE NAME C:\GPIB-PC\T1R1.BAS AS AN ASCII FILE IN PC 1
1300 REM
1310 REM SUBROUTINE RANGE 2
1320 REM
1330 D2 = TAU(JK) * 1000 : D21$ = STR$(D2)
1340 PART1$ = "Q"
1350 PART2$ = "D"
1360 PART3$ = MID$(D21$,2) : PART4$ = "!"
1370 WORDQ1$ = PART1$+PART2$+PART3$+PART4$
1380 CALL IBWRT(DELAY%,WORDQ1$)
1390 CALL IBWRT(DELAY%,WORD2$)
1400 GOSUB 1940
1410 RETURN
1420 REM + + + + +
1430 REM WWW SUBROUTINE IS WORKING PROPERLY
1440 REM \\\\\\\ SAVED IN THE NAME C:\GPIB-PC\T1R2.BAS IN PC1 AS AN ASCII FILE
1450 REM
1460 REM SUBROUTINE RANGE 3
1470 REM
1480 D3 = TAU(JK) * 100 : D31$ = STR$(D3)
1490 PART1$ = "R"
1500 PART2$ = "D"
1510 PART3$ = MID$(D31$,2) : PART4$ = "!"
1520 WORDR1$ = PART1$+PART2$+PART3$+PART4$
1530 CALL IBWRT(DELAY%,WORDR1$)
1540 CALL IBWRT(DELAY%,WORD3$)
1550 GOSUB 1940
1560 RETURN
1570 REM + + + + +
1580 REM W\W SUBROUTINE IS WORKING PROPERLY
1590 REM WW\ SAVED IN THE NAME C:\GPIB-PC\T1R3.BAS IN PC1 AS AN ASCII FILE
1600 REM
1610 REM SUBROUTINE RANGE 4
1620 REM
1630 D4 = TAU(JK) * 10 : D41$ = STR$(D4)
1640 PART1$ = "S"
1650 PART2$ = "D"
1660 PART3$ = MID$(D41$,2) : PART4$ = "!"
1670 WORDS1$ = PART1$+PART2$+PART3$+PART4$
1680 CALL IBWRT(DELAY%,WORDS1$)
1690 CALL IBWRT(DELAY%,WORD4$)

```

```

1700 GOSUB 1940
1710 RETURN
1720 REM + + + + +
1730 REM \\\\\\ SUBROUTINE IS WORKING PROPERLY
1740 REM \\\\\\ SAVED IN THE NAME C:\GPIB-PC\T1R4.BAS IN PC1 AS AN ASCII FILE
1750 REM
1760 REM SUBROUTINE RANGE 5
1770 REM
1780 D5 = TAU(JK) : D51$ = STR$(D5)
1790 PART1$ = "T"
1800 PART2$ = "D"
1810 PART3$ = MID$(D51$,2) : PART4$ = "!"
1820 WORDT1$ = PART1$+PART2$+PART3$+PART4$
1830 CALL IBWRT(DELAY%,WORDT1$)
1840 CALL IBWRT(DELAY%,WORD5$)
1850 GOSUB 1940
1860 RETURN
1870 REM + + + + +
1880 REM \\\\\\ SUBROUTINE IS WORKING PROPERLY
1890 REM \\\\\\ SAVED IN THE NAME C:\GPIB-PC\T1R5.BAS IN PC1 AS AN ASCII FILE
1900 REM
1910 REM
1920 REM SUBROUTINE WAVE TRANS
1930 REM
1940 CMD$ = "ACQ REP:SAM,HSR:SAM,LSR:SAM,SCA:SAM": CALL IBWRT(TEK%,CMD$)
1950 SWEEP% = AVERAGE - 1
1960 MASK% = &H4000 : WAIT1% = 11
1970 CALL IBTMO(BRD%,WAIT1%) : CALL IBWAIT(BRD%,MASK%)
1980 QUERY$ = "ACQ? SWP" : CALL IBWRT(TEK%,QUERY$)
1990 ANSS = SPACES(30) : CALL IBRD(TEK%,ANS$)
2000 IF VAL(MID$(ANS$,22)) < 1 THEN GOSUB 2180 ELSE GOTO 2020
2010 GOTO 1980
2020 CMD$ = "ACQ REP:AVE,HSR:AVE,LSR:AVE,SCA:AVE,SMO:ON,VEC:ON,NUM:"
2030 VER$ = STR$(AVERAGE):CMD1$ = CMD$ + MID$(VER$,2)
2040 WEIT$ = ",WEI:" + MID$(STR$(WEIGHT),2)
2050 CMD2$ = CMD1$ + WEIT$
2060 CALL IBWRT(TEK%,CMD2$)
2070 SWEEP% = 0
2080 GOSUB 2180
2090 QUERY$ = "ACQ? SWP" : CALL IBWRT(TEK%,QUERY$)
2100 ANSS = SPACES(30) : CALL IBRD(TEK%,ANS$) : SWEEP% = VAL(MID$(ANS$,22))
2110 IF SWEEP% = AVERAGE THEN GOTO 2140
2120 GOSUB 2180
2130 GOTO 2090
2140 REM ~ . . . . . ECHOPEAK TRANSFER DETAILS . . . . .
2150 REM
2160 GOSUB 5980
2170 RETURN
2180 REM DDDDDDDDDDDD SUBROUTINE DELAY DDDDDDDDDDDD
2190 REM
2200 SWEEP1% = AVERAGE - SWEEP%
2210 TME = SWEEP1% * (TAU(JK)*.001 + RATE )
2220 AA = .001 : BB = .003
2230 FOR N = 5 TO 17
2240 IF (TME >= AA) AND (TME < BB) THEN GOTO 2310
2250 AA = AA * 10
2260 CC = AA
2270 AA = BB
2280 BB = CC

```



[illegible]

```

2820   FOR M = 1 TO TAU0
2830       FOR L = 1 TO TAU01
2840           IF ITAUCL) <> JTAU(M) THEN GOTO 2870
2850               ACL) = BOO
2860               GOTO 2910
2870       NEXT L
2880       KOUNT = KOUNT + 1
2890       ITAU(KOUNT) = JTAU(M)
2900   AC KOUNT) = BOO
2910   NEXT M
2920   TAU01 = KOUNT : AFLAG = 0
2930   FOR KAN - 1 TO TAU01
2940       KTAUCKAN) = ITAUCKAN)
2950   IATAU(KAN) = ACKAN)
2960   NEXT KAN
2970       REM LPRINT SPC(15) "TAU(m.sec)" SPC(15) "M(tau)(volts)"
2980   FOR N - 1 TO TAU01
2990       REM LPRINT SPCC20) ITAUCN) TAB(45) A(N)
3000   NEXT N
3010   OPEN "ECHOSET1" FOR OUTPUT AS #3
3020   OPEN EXP1$ FOR OUTPUT AS #2
3030       FOR J = 1 TO TAU01
3040           AMIN = ITAU(J) : K = J
3050           AAMIN = A(J)
3060           FOR I = J TO TAU01
3070               IF ITALIC I) >= AMIN THEN GOTO 3100
3080               AMIN = ITAU(I) : K = I
3090               AAMIN = A(I)
3100           NEXT I
3110       ATEMP = ITAUCJ)
3120       ITAUCJ) = AMIN
3130       ITAU(K) = ATEMP
3140       AATEMP = ACJ)
3150       ACJ) = AAMIN
3160       A(K) = AATEMP
3170       NEXT J
3180   PRINT #3,TAU01
3190   CLS:PRINT SPC(15) "TAU(m.sec)" SPC(15) "A(TAU)(volts)"
3200   FOR S = 1 TO TAU01
3210       PRINT SPC(5) S SPC(10)ITAU(S)TAB(45)A(S)
3220       PRINT #3, ITAU(S)
3230       PRINT #2, SPC(10)ITAUCS)TAB(45)ACS)
3240   NEXT S : PRINT
3250   PRINT #3,AVERAGE
3260   PRINT #3,WEIGHT
3270   CLOSE #3,#2
3280   GOTO 2520
3290   FOR TT = 1 TO TAU01
3300       XCTT) = ITAUCTT)
3310       YMCTT) = ACTT)
3320   PRINT SPC(10) XCTT) TAB(40) YMCTT)
3330   NEXT TT
3340   REM
3350   PRINT:PRINT:PRINT:PRINT"LS-FIT AND PLOT OF T1 DATA ":PRINT:PRINT
3360   PRINT:PRINT:PRINT:PRINT
3370   REM ***** PROGRAM FOR LS-FIT AND PLOT /T1 DATA *****
3380   PRINT:PRINT:PRINT:PRINT
3390   INPUT"NO. OF POINTS PLEASE";N
3400   READ SAMPLE$,FREQ$,STPT$,VARIAC$,EMF1,EMF2,TEMP

```

```

3410      S1=0:S2=0:S3=0:S4=0:S5=0
3420      FOR I = 1 TO N
3430          YL(I)=LOG(YM(I))
3440          S1=S1+X(I):S2=S2+YL(I):S3=S3+X(I)^2
3450          S4=S4+X(I)*YL(I):S5=S5+YL(I)^2
3460      NEXT I
3470      D=S3-(S1^2)/N
3480      A=(S4-S1*S2/N)/D
3490      B=(S2*S3-S1*S4)/(D*N)
3500      D1=SQR((S3-(S1^2)/N)*(S5-(S2^2)/N)):R=(S4-(S1*S2)/N)/D1
3510      S6=0:S7=0
3520      FOR I=1 TO N
3530          Y(I)=A*X(I)+B
3540          E(I)=Y(I)-YL(I)
3550          S6=S6+E(I)^2
3560          S7=S7+(E(I)/Y(I))^2
3570      NEXT I
3580      PRINT "x(i)";TAB(10);"ym(i)";TAB(20);"yl(i)";TAB(40);"y(i)";TAB(60);"e(i)"
3590      FOR I=1 TO N
3600          YL(I)=(INT(YL(I)*1000))/1000
3610          Y(I)=(INT(Y(I)*1000))/1000
3620          PRINT X(I);TAB(10);YM(I);TAB(20);YL(I);TAB(40);Y(I);TAB(60);E(I)
3630      NEXT I
3640      SD=SQR(S6/N)
3650      DY=SQR(S7/N)
3660      T1=1/A
3670      DT=DY*T1:PRINT:PRINT
3680      PRINT "t1=";T1:TAB(50);"error=";DT:PRINT:PRINT
3690      PRINT"rmsd=";SD:TAB(50);"corr.=";R
3700      GOSUB 5180
3710      FOR I=1 TO N
3720          CX(I)=X(I):CY(I)=YL(I):NEXT I
3730      GOSUB 3960
3740      SCREEN 0
3750      IF (BB$ = "P") OR (BB$ = "p") THEN GOSUB 5400
3760      IF (BB$ = "E")OR (BB$ = "e") THEN GOTO 2520
3770      IF (BB$ = "Q") OR (BB$ = "q") THEN GOTO 5130
3780      INPUT "how many bad data points do you have";M
3790      PRINT:PRINT:PRINT "type the x(i)'s of the bad points"
3800      FOR I=1 TO M
3810          INPUT";X1(I)
3820      FOR J=1 TO N
3830          IF X(J)<>X1(I) THEN 3890
3840          IF J=N THEN 3880
3850          FOR K=J TO N-1
3860              X(K)=X(K+1):YM(K)=YM(K+1)
3870          NEXT K
3880          N=N-1
3890      NEXT J
3900      NEXT I
3910      GOTO 3410
3920      DATA "[TEA]6 Bi8 C130",20,3.30(COLD),140,-3.663,-3.657,-103.4
3960      REM + + + + + + + + + + + + + + +
3970      REM ***** SUBROUTINE PLOT *****
3980      REM + + + + + + + + + + + + + + +
3990      PRINT:PRINT
4000      INPUT"      ":QS
4010      TQ=1
4020      PRINT:PRINT:PRINT

```

```

4030  X9=CX(1):X0=CX(1):Y9=C*Y(1):Y0=C*Y(1)
4040  FOR I= 1 TO N
4050  IF CX(I)>X9 THEN X9=CX(I)
4060  IF CX(I)<X0 THEN X0=CX(I)
4070  IF CY(I)>Y9 THEN Y9=C*Y(I)
4080  IF CY(I)<Y0 THEN Y0=C*Y(I)
4090  NEXT
4100  DX=(X9-X0)/10:DY=(Y9-Y0)/10
4110  X9=X9+DX:Y9=Y9+DY
4120  X0=X0-DX:Y0=Y0-DY
4130  IX=570/(X9-X0):IY=160/(Y9-Y0)
4140  FOR I=1 TO N
4150  CX(I)=50+(CX(I)-X0)*IX
4160  CY(I)=170-(CY(I)-Y0)*IY
4170  NEXT
4180  CLS
4190  SCREEN 2
4200  LINE (10,5) - (630,190),,B
4210  LINE (35,170)-(620,170)
4220  LINE (50,10) -(50,185)
4230  XL=107
4240  FOR I= 1 TO 10
4250  LINE (XL,168) - (XL,172)
4260  XL=XL+57
4270  NEXT
4280  YL=10
4290  FOR I=1 TO 10
4300  LINE(48,YL)-(52,YL)
4310  YL=YL+16
4320  NEXT
4330  REM TEXT SCREEN 0,0,1,10
4340  XL=107:YK=20
4350  FOR I= 1 TO 4
4360  XC(I)=X0+(XL-50)/IX
4370  XL=XL+65
4380  NEXT
4390  YK=10
4400  FOR I= 4 TO 1 STEP -1
4410  YC(I)=Y0+(170-YK)/IY
4420  YK=YK+40
4430  NEXT
4440  FOR I= 1 TO 4
4450  X1(I)=XC(I)
4460  NEXT
4470  I=1
4480  XQ(I)=INT(ABS(XC(I)))
4490  X1(I)=XC(I)
4500  L=0:K=0
4510  IF XQ(I)=0 THEN XC(I)=XC(I)*10:L=L+1:XQ(I)=INT(ABS(XC(I))):GOTO 4510
4520  IF XQ(I) > 10 THEN XC(I)=XC(I)/10:K=K+1:XQ(I)=INT(ABS(XC(I))):GOTO 4520
4530  IF L=0 THEN PP=K
4540  IF K=0 THEN PP=-L
4550  IF L=0 AND K=0 THEN PP=0
4560  PP$=STR$(PP)
4570  FOR I= 1 TO 4
4580  X1(I)=X1(I)*(10^(-PP))
4590  X1(I)=(INT(X1(I)*100))/100
4600  NEXT
4610  REM TEXT 240,190,"x10",1,1,8

```

```

4620 REM TEXT 260,186,PP$,1,1.8
4630 FOR I= 1 TO 4
4640 Y1(I)=YC(I)
4650 NEXT
4660 I=1
4670 YQ(I)=INT(ABS(YC(I)))
4680 Y1(I)=YC(I)
4690 L=0:K=0
4700 IF YQ(I)=0 THEN YC(I)=YC(I)*10:L=L+1:YQ(I)=INT(ABS(YC(I))):GOTO 4700
4710 IF YQ(I)>10 THEN YC(I)=YC(I)/10:K=K+1:YQ(I)=INT(ABS(YC(I))):GOTO 4710
4720 IF L=0 THEN PP=K
4730 IF K=0 THEN PP=-L
4740 IF L=0 AND K=0 THEN PP=0
4750 PP$=STR$(PP)
4760 FOR I=1 TO 4
4770 Y1(I)=Y1(I)*(10^(-PP))
4780 Y1(I)=(INT(Y1(I)*10))/10
4790 NEXT
4800 REM TEXT2,165,"x10",1,1,8
4810 REM TEXT 25,160,PP$,1,1,8
4820 QX=87
4830 FOR I= 1 TO 4
4840 X1$(I)=STR$(X1(I))
4850 REM TEXT QX,182,X1$(I),1,1,8
4860 QX=QX+65
4870 NEXT
4880 QY=126
4890 FOR I= 1 TO 4
4900 Y1$(I)=STR$(Y1(I))
4910 REM TEXT1,QY.Y1$(I),1,1,8
4920 QY=QY-40
4930 NEXT
4940 FOR I= 1 TO N
4950 LINE (CX(I)-1,CY(I)-1) - (CX(I)+1,CY(I)+1),,B
4960 NEXT
4970 IF TQ=1 THEN GOTO 4990
4980 GOTO 5110
4990 FOR I= 1 TO N
5000 FX(I)=50+(X(I)-X0)*IX
5010 FY(I)=170-(Y(I)-Y0)*IY
5020 NEXT
5030 M=N-1
5040 FOR I= 1 TO M
5050 LINE (FX(I),FY(I))-(FX(I+1),FY(I+1))
5060 NEXT
5070 YY=2*(ABS(SD))*(ABS(IY))
5080 LINE (600,100)-(600,100-YY)
5090 LINE (599,100-YY) - (601,100-YY)
5100 LINE (599,100) - (601,100)
5110 BB$ = INKEY$:IF BB$="" GOTO 5110
5120 RETURN
5130 SCREEN 0.0
5140 as
5150 END
5160 SCREEN 0
5170 END
5180 REM + + + + + SUBROUTINE ERROR ESTIMATE + + + + +
5190 REM + + + + + + + + + + + + + + + +
5200 AX=0:AY=0

```

```

5210 FOR I= 1 TO N
5220   AX=AX+X(I):AY=AY+YL(I)
5230   NEXT I
5240   AX=AX/N:AY=AY/N
5250   A1=0:A2=0:A3=0
5260   FOR I= 1 TO N
5270     A1=A1+(YL(I)-AY)^2
5280     A2=A2+(X(I)-AX)*(YL(I)-AY)
5290     A3=A3+(X(I)-AX)^2
5300   NEXT I
5310   S=(A1-(A2^2)/A3)/(N-2)
5320   SB=S/(SQR(A3))
5330   PRINT "s=";S;"sb=";SB
5340   RR=ABS(SB*T1*T1)
5350   PRINT:PRINT "error in t1 =" ;RR
5360   SL=A2/A3:SS=1/SL:PRINT"t1 is ";SS
5370   RETURN
5380 REM _____END OF SUBROUTINE ERROR ESTIMATE_____
5390 REM - - - - -
5400 REM - - - - - SUBROUTINE PRINT OUT - - - - -
5410 REM - - - - -
5420 REM - - - - -
5430 REM
5440 OPEN EXP1$ FOR APPEND AS 1*2
5450 FOR J = 1 TO TAU01
5460   REM LPRINT SPC(10) ITAU(J) TAB(40) A(J)
5470   NEXT J
5480   PRINT #2 : REM LPRINT
5490   REM LPRINT SPC(10) "SAMPLE IS "+SAMPLE$;TAB(40);"FREQ. = "+FREQ$+" MHz."
5500   PRINT #2 SPC(10) "SAMPLE IS "+SAMPLE$;TAB(40);"FREQ. = "+FREQ$+" MHz."
5510   REM LPRINT
5520   PRINT #2
5530   REM LPRINT SPC(10) "SET POINT - "+STPT$;TAB(40);"VARIAC = "+VARIAC$;" VOLTS"
5540   PRINT #2 SPC(10) "SET POINT = "+STPT$;TAB(40);"VARIAC = "+VARIAC$;" VOLTS"
5550   REM LPRINT
5560   PRINT #2
5570   REM LPRINT SPC(10) "EMF1 - ";EMF1;TAB(40);"EMF2 = ";EMF2
5580   PRINT #2 SPC(10) "EMF1 = ";EMF1;TAB(40);"EMF2 = ";EMF2
5590   REM LPRINT
5600   PRINT #2
5610   REM LPRINT " _____
5620   PRINT #2 " _____
5630   REM REM LPRINT " L S - F I T D A T A "
5640   PRINT #2 " L S - F I T D A T A "
5650   REM LPRINT " _____
5660   PRINT #2
5670   REM LPRINT
5680   PRINT #2
5690   REM LPRINT "X(i)"; TAB(10); "Ym(i)";TAB(25);"Yl(i)";TAB(40);"Y(i)";TAB(60);"E(i)
5700   PRINT #2 "X(i)"; TAB(10); "Ym(i)";TAB(25);"Yl(i)";TAB(40);"Y(i)";TAB(60);"E(i)"
5710   REM LPRINT
5720   PRINT #2
5730   REM LPRINT " _____
5740   PRINT #2 " _____
5750   FOR I = 1 TO N
5760     REM LPRINT X(I);TAB(10);YM(I);TAB(20);YL(I);TAB(35);Y(I);TAB(50);E(I)
5770     PRINT #2 X(I);TAB(10);YM(I);TAB(20);YL(I);TAB(35);Y(I);TAB(50);E(I)
5780   NEXT I
5790   REM LPRINT " _____

```

```

5800 PRINT #2 "
5810 REM LPRINT
5820 PRINT #2
5830 REM LPRINT SPC(10) "corr. = ";R TAB(40) "T1 = " ;(-T1)
5840 PRINT #2 SPC(10) "corr. = ";R TAB(40) "T1 = " ;(-T1)
5850 REM LPRINT
5860 PRINT #2
5870 REM LPRINT SPC(10) "ERR. IN T1 = ";RR;TAB(40);"TEMP. = ";TEMPR;" C"
5880 PRINT #2 SPC(10) "ERR. IN T1 = ";RR;TAB(40);"TEMP. = ";TEMPR;" C"
5890 REM LPRINT
5900 PRINT #2
5910 REM LPRINT SPC(10) "RMSD = ";SD;TAB(40);(273+TEMPR);" K" :REM LPRINT
5920 PRINT #2 SPC(10) "RMSD = ";SD;TAB(40);(273+TEMPR);" K" :REM LPRINT
5930 REM LPRINT SPC(10) "1000/T = ";1000/(273+TEMPR);TAB(40);"ln T1 = ";LOG(-T1)
5940 PRINT #2 SPC(10) "1000/T = ";1000/(273+TEMPR);TAB(40);"ln T1 = ";LOG(-T1)
5950 CLOSE #2
5960 RETURN
5970 REM + + + + + END OF SUBROUTINE PRINT OUT + + + + +
5980 REM EEEEEEEEEEEEEEE SUBROUTINE ECHO PEAK P P P P P P P P P P P P
5990 REM
6000 IF (JK <> 1) OR (AFLAG <> 0) THEN GOTO 6050
6010 INPUT " POSITION THE CURSOR AND ENTER ",JDJ
6020 CMD$ = "CURS? POS" : ANSS = SPACES(30)
6030 CALL IBWRT(TEK%,CMD$) : CALL IBRD(TEK%,ANSS)
6040 CURS = VAL(MID$(ANSS,17))
6050 CMD$ = "REFF ACQ:SAV REF1" : CALL IBWRT(TEK%,CMD$)
6060 CMD$ = "DATA SOU:REF1,ENC:HEX,CHA:CH2" : CALL IBWRT(TEK%,CMD$)
6070 CMD$ = "WFMPRE? YMULT" : ANSS = SPACES(80)
6080 CALL IBWRT(TEK%,CMD$) : CALL IBRD(TEK%,ANSS)
6090 YMULT = VAL(MID$(ANSS,14))
6100 CMD$ = "WFMPRE? XINCR" : ANSS = SPACES(80)
6110 CALL IBWRT(TEK%,CMD$) : CALL IBRD(TEK%,ANSS)
6120 XMULT = VAL(MID$(ANSS,14))
6130 LAB2 = LAB2 + 1 : IF LAB2 <= 99 THEN GOTO 6150
6140 LAB1 = LAB1 + 1 : LAB2 = 1
6150 LABELS = "."+CHR$(LAB2)+MID$(STR$(LAB2),2)
6160 DUMP$ = "ECHOWAVE"+LABEL$
6170 CMD$ = "WAVFRM?"
6180 CALL IBWRT(TEK%,CMD$) : CALL IBRDF(TEK%,DUMP$)
6190 RETURN
6200 REM * * * * *
6210 REM P E A K D E T E C T
6220 REM
6230 LAB2 = LAB2 + 1 : IF LAB2 <= 99 THEN GOTO 6250
6240 LAB1 = LAB1 + 1 : LAB2 = 1
6250 LABELS = "."+CHR$(LAB1)+MID$(STR$(LAB2+1))
6260 DUMP$ = "ECHOWAVE"+LABEL$
6270 OPEN "R",1,DUMP$,4
6280 FIELD 1,2 AS M1$,2 AS M2$
6290 GET 1,1024
6300 F1$ = "&H"+M1$: F2$ = "&H"+M2$
6310 FIRST = (VAL(F1$) * 256 + VAL(F2$)) * YMULT
6320 FOR LM = (CURS+4) TO 1027
6330 GET 1,LM
6340 Y1$ = "&H"+M1$:Y2$ = "&H"+M2$
6350 PY(LM-3) = (<VAL(Y1$)*256 + VAL(Y2$))*YMULT) - FIRST
6360 PY(LM-3) = ABS(PY(LM-3))
6370 PX(LM-3) = (LM - 3)
6380 NEXT LM

```

```

6390 Pxmax = Px(CURS+1) : Pymax = Py(CURS+1)
6400 FOR KM = CURS + 2 TO 1024
6410     IF Py(KM) < Pymax THEN GOTO 6430
6420     Pymax = Py(KM) : Pxmax = Px(KM)
6430 NEXT KM
6440 CLOSE 1
6450 IF AFLAG = 1 THEN B(JK) = Pymax
6460 IF AFLAG = 0 THEN A(JK) = Pymax
6470 IF AFLAG - 1 THEN GOTO 6490
6480 PRINT #2,SPC(20) TAU(JK) TAB(45) Pymax
6490 PRINT SPC(20) TAU(JK) TAB(45) Pymax
6500 RETURN
6510 REM * * * * * END OF ROUTINE ECHO-PEAK * * * * *
6520 REM + + + + + SUBROUTINE TAUINT + + + + +
6530 REM -----
6540 CLS:INPUT " INPUT VALUES FROM KEYBOARD OR FILE ? (K/F) ", K$
6550 IF (K$ = "K") OR (K$ = "k") THEN GOTO 6590
6560 OPEN "ECHOSET2" FOR INPUT AS #3
6570 INPUT #3, AINTAU,AFITAU,GRID
6580 GOTO 6620
6590 CLS:INPUT " INITIAL TAU, FINAL TAU, GRID PLEASE ",AINTAU,AFITAU,GRID
6600 OPEN "ECHOSET2" FOR OUTPUT AS #3
6610 PRINT #3 ,AINTAU,AFITAU,GRID
6620 TAU0 = INT((AFITAU-AINTAU)/GRID)
6630 TAU01 = TAU0
6640 FOR D = 1 TO TAU0
6650     TAU(D) = AINTAU + (D-1)*GRID
6660     ITAU(D) = TAU(D)
6670 NEXT D
6680 IF (K$ = "K") OR (K$ = "k") THEN RETURN 670
6690 RETURN 470
6700 REM * * * * * DATA-----P L O T * * * * *
6710 REM -----
6720 FOR TT = 1 TO TAU01
6730     X(TT) = ITAU(TT)
6740     Y(TT) = A(TT)
6750 NEXT TT
6760 XMAX = 0 :YMAX = 0 :XMIN = 0 :YMIN = 0
6770 FOR IJ = 1 TO TAU01
6780 IF IJ > 1 GOTO 6810
6790 XMAX = X(1) :YMAX = Y(1)
6800 XMIN = X(1) :YMIN = Y(1)
6810 IF X(IJ) > XMAX THEN XMAX = X(IJ)
6820 IF Y(IJ) > YMAX THEN YMAX = Y(IJ)
6830 IF X(IJ) < XMIN THEN XMIN = X(IJ)
6840 IF Y(IJ) < YMIN THEN YMIN = Y(IJ)
6850 NEXT IJ
6860 XDEN = (XMAX - XMIN) : YDEN = (YMAX - YMIN)
6870 KEY OFF : CLS : SCREEN 2
6880 LINE (10,10) - (600,190),,B
6890 FOR L = 1 TO TAU01
6900 XNR = X(L) - XMIN : IF XNR < 0 GOTO 6990
6910 YNR = YMAX - Y(L) : IF YNR < 0 GOTO 7000
6920 XP = 40 + 540 * (XNR/XDEN)
6930 YP = 15 + 155 * (YNR/YDEN)
6940 PSET (XP,YP) : IF L = 1 GOTO 6960
6950 LINE (XP,YP) - (XPP,YPP)
6960 XPP = XP
6970 YPP = YP

```



```

6980 NEXT L : GOTO 7010
6990 PRINT "ERROR XNR = ";XNR : STOP
7000 PRINT "ERROR YNR = ";YNR : STOP
7010 LINE (40,15) - (40,170)
7020 LINE (40,170) - (580,170)
7030 COEX1 = 40 : STEPX =110
7040 COWHY1 = 15 : STEPY = 32
7050 STEPVALX = XDEN/5
7060 FOR SDS = 1 TO 5
7070 LINE (COEX1,168) - (COEX1,172)
7080 LINE (38,COWHY1) - (42,COWHY1)
7090 COEFF = INT(COEX1/8)
7100 COEX1 = COEX1 + STEPX
7110 COWHY1 = COWHY1 + STEPY
7120 MESX = XMIN + (SDS-1) * STEPVALX
7130 LOCATE 23,COEFF
7140 PRINT MESX
7150 NEXT SDS
7180 LOCATE 5,55
7190 PRINT " tau vs echo ampl."
7200 LOCATE 23,68
7210 PRINT " m.sec "
7220 JARJ$ = INKEY$ : IF JARJ$ = "" THEN GOTO 7220
7230 SCREEN 0,0,0
7240 GOTO 2520

```

ECHO.OFF

+++++

\ This programme attempts to fit a five Lorentzian model to the experimental  
 \ T1 values IN TEACB. We assume four inequivalent methyl groups to be present  
 \ here. x , y , z and p are weightages of the four inequivalent methyl groups  
 \ respectively. User is prompted at the time of running the programme to  
 \ provide these four values.

\ L A R M O R F R E Q U E N C Y ; 10 M H z .

gd sd

FORGET ALL

CLEAR.TOKENS

\ load.overlay c:\asyst\matfit.sov

\ load programs\newskrn.asy

-1 4 sci.format

1e-20 fit.tolerance :=

1000 max.#.iterations :=

\ VARIABLE DECLARATIONS

real dim[ 5 ] array t0 dim[ 5 , 49 ] array tc

real dim[ 5 , 49 ] array gomega

real dim[ 5 ] array slope

real scalar x scalar y scalar z scalar freq

real scalar omega scalar a real scalar deviation

real scalar b scalar c scalar dev1 scalar dev2

real scalar delta scalar p

integer scalar dum integer scalar jk

integer scalar m scalar n scalar d scalar kount

integer scalar erno scalar outer.kount

50 string file 10 string myflag

12 string file1 12 string date1 12 string time1

5 string dummy 5 string catch

token temp token tlfitrate token tlexpval

token tlexprate token tlfitval token tempi

\.

\ C O L O N D E F I N I T I O N S

: tauc

slope [ 1 ] swap / exp t0 [ 1 ] \* tc xsect[ 1 , ! ] :=

slope [ 2 ] temp / exp t0 [ 2 ] \* tc xsect[ 2 , ! ] :=

slope [ 3 ] temp / exp t0 [ 3 ] \* tc xsect[ 3 , ! ] :=

slope [ 4 ] temp / exp t0 [ 4 ] \* tc xsect[ 4 , ! ] :=

slope [ 5 ] temp / exp t0 [ 5 ] \* tc xsect[ 5 , J ] :=

```

: tauc1
  slope [ 1 ] temp / exp t0 [ 1 ] * tc xsect[ 1 , 1 ] :=
  slope [ 2 ] temp / exp t0 [ 2 ] * tc xsect[ 2 , ! ] :=
  slope [ 3 ] temp / exp t0 [ 3 ] * tc xsect[ 3 , 1 ] :=
  slope [ 4 ] temp / exp t0 [ 4 ] * tc xsect[ 4 , ! ] :=
  slope [ 5 ] temp / exp t0 [ 5 ] * tc xsect[ 5 , ! ] :=
;

: gofom
  6 1 do
    tc xsect[ i , ! ]
    omega 2 ** tc xsect[ i , ! ] 2 ** * 1 +
    /
    tc xsect[ i , ! ] 4 *
    omega 2 ** tc xsect[ i , ! ] 2 ** * 4 * 1 +
    /
    +
    gomega xsect[ i , ! ] :=
  loop
;

: curve.plot
  gd
  " x " symbol
  1 temp1 / tlexpval 1e3 * ln xyyap
  solid 1 temp1 / tlfital 1e3 * ln xydap
;

: full.plot
  gd
  go
  " x " symbol
  1 temp1 / tlexpval 1e3 * ln xyyap
  solid 1 temp1 / tlfital 1e3 * ln xydap
;

: msd
  0 deviation :=
  tlexpval tlfital - dup *
  []sum deviation :=
  deviation n / deviation :=
;

: tlinverse
  tauc
  gofom
  a p * gomega xsect[ 5 , ! ] *
  a z * gomega xsect[ 4 , ! ] *
  +
  a y * gomega xsect[ 3 , ! ] *
  +
  a x * gomega xsect[ 2 , ! ] *
  +
  b gomega xsect[ 1 , ! ] *
  +
  tlfital :=
  tlfital inv tlfital :=
  tlfital 1 /
;

```

```

: tlinverse1
  taucl
  gofom
  a p * gomega xsect[ 5 , ! ] *
  a z * gomega xsect[ 4 , ! ] *
  +
  a y * gomega xsect[ 3 , ! ] *
  +
  a x * gomega xsect[ 2 , ! ] *
  +
  b gomega xsect[ 1 , ! ] *
  +
  tlfitrates :=
  tlfitrates inv tlfitrates :=

```

```

\ COLONS END
\ -----

```

```

: submain
  hybrid.fit
  curve.fit[ temp , tlexprates ; tlinverse ; t0 [ 1 ] , t0 [ 2 ] ,
t0 [ 3 ] , t0 [ 4 ] , t0 [ 5 ] , slope [ 1 ] , slope [ 2 ] , slope [ 3 ]
, slope [ 4 ] , slope [ 5 ] ]
  curve.plot
  msd
;

```

```

\ ** ** ** ** SUB MAIN ENDS ** ** ** **

```

```

: MAIN

```

```

CLEAR.TOKENS
CONSOLE.OFF OUT>PRINTER

```

```

CR

```

```

cr ." *****

```

```

cr ." FREQUENCY : 10 MHz. "

```

```

cr ." *****

```

```

CONSOLE

```

```

sd

```

```

real n ramp becomes> tlfitrates

```

```

real n ramp becomes> tlfitrates

```

```

real n ramp becomes> tlexprates

```

```

real n ramp becomes> tlexprates

```

```

real n ramp becomes> temp

```

```

real n ramp becomes> temp1

```

```

0 tlfitrates :=

```

```

0 tlfitrates :=

```

```

0 tlexprates :=

```

```

0 tlexprates :=

```

```

0 temp :=

```

```

0 temp1 :=

```

```

1.00e7 freq :=

```

```

freq 2 * pi * omega :=

```

```

8.05e8 a :=

```

```

3.382e8 b :=

```

```

5.1842e-12 t0 [ 1 ] :=

```

```

2.1067e-13      t0 [ 2 ] :=
2.0554e-13      t0 [ 3 ] :=
1.8735e-12      t0 [ 4 ] :=
6.2855e-13      t0 [ 5 ] :=
2.1687e3        slope [ 1 ] :=
1.4243e3        slope [ 2 ] :=
9.3092e2        slope [ 3 ] :=
7.163e2         slope [ 4 ] :=
1.0192e3        slope [ 5 ] :=
0 kount :=

```

```

" \rajan\data\teacb\sa210c.dat" file " :=

```

```

file defer> basic.open

```

```

n 1 + 1 do

```

```

    basic.read

```

```

    dum :=

```

```

    tlexpval [ i ] :=

```

```

    temp [ i ] :=

```

```

loop

```

```

tlexpval 1e-3 * tlexpval :=

```

```

tlexpval inv tlexprate :=

```

```

temp 1e-3 * temp1 :=

```

```

basic.close

```

```

T1INVERSE1 curve.plot

```

```

BEGIN

```

```

cr ." DO YOU NEED CHANGE OF INITIAL PARAMETERS? IF SO ENTER Y "

```

```

CR ." ELSE ENTER ANY OTHER KEY "

```

```

"INPUT dummy " := dummy " Y" "= dummy " y" "= OR

```

```

IF

```

```

sd

```

```

cr ." x = " #input x :=

```

```

cr ." y = " #input y :=

```

```

cr ." z = " #input z :=

```

```

cr ." p = " #input p :=

```

```

cr ." If you want to assume default values for t0 and s "

```

```

    ." enter d " #input catch " :=

```

```

catch " D" "= catch " d" "= OR NOT

```

```

IF

```

```

cr ." t0 [ 1 ] " #input t0 [ 1 ] :=

```

```

cr ." t0 [ 2 ] " #input t0 [ 2 ] :=

```

```

cr ." t0 [ 3 ] " #input t0 [ 3 ] :=

```

```

cr ." t0 [ 4 ] " #input t0 [ 4 ] :=

```

```

cr ." t0 [ 5 ] " #input t0 [ 5 ] :=

```

```

cr ." slope [ 1 ] " #input slope [ 1 ] :=

```

```

cr ." slope [ 2 ] " #input slope [ 2 ] :=

```

```

cr ." slope [ 3 ] " #input slope [ 3 ] :=

```

```

cr ." slope [ 4 ] " #input slope [ 4 ] :=

```

```

cr ." slope [ 5 ] " #input slope [ 5 ] :=

```

```

THEN

```

```

THEN

```

```

T1INVERSE1

```

```

curve.plot

```

```

dummy " Y" "= dummy " y" "= OR NOT

```

```

UNTIL

```

```

CONSOLE.OFF OUT>PRINTER

```

```

cr ."      tau1 = " t0 [ 1 ] . ."      s1 = " slope [ 1 ] .

```

```

cr ."      tau2 = " t0 [ 2 ] . ."      s2 = " slope [ 2 ] .

```

```

cr ."      tau3 = " t0 [ 3 ] . ."      s3 = " slope [ 3 ] .

```

```

cr ."      tau4 = " t0 [ 4 ] . ."      s4 = " slope [ 4 ] .

```

```

cr ."      tau5 = " t0 [ 5 ] . ."      s5 = " slope [ 5 ] .
CONSOLE
-1 4 sci.format
cr ." PROGRAM IS RUNNING ..... PLEASE DO NOT DISTURB OR STOP "
      submain
CONSOLE.OFF OUT>PRINTER
CR ." THE FINAL SET OF VALUES ARE THE FOLLOWING "
CR
cr ." ***** "
cr ."      tau1 = " t0 [ 1 ] . ."      s1 = " slope [ 1 ] .
cr ."      tau2 = " t0 [ 2 ] . ."      s2 = " slope [ 2 ] .
cr ."      tau3 = " t0 [ 3 ] . ."      s3 = " slope [ 3 ] .
cr ."      tau4 = " t0 [ 4 ] . ."      s4 = " slope [ 4 ] .
cr ."      tau5 = " t0 [ 5 ] . ."      s5 = " slope [ 5 ] .
cr ."      msd = " deviation .
cr ." ***** "
"DATE DATE1 " := "TIME TIME1 " :=
cr 5 spaces ." DATE : " DATE1 "TYPE 20 spaces ." TIME : " time1 "type
cr ." ***** "
CR
;
\ + + + + + MAIN ENDS HERE + + + + +
: SUPER.MAIN

49 N :=
cr ." x = " #input x :=
cr ." y = " #input y :=
cr ." z = " #input z :=
cr ." p = " #input p :=
main
cr ." ***** "
cr 5 spaces ." X = " x . 15 spaces ." FREQUENCY = " FREQ .
cr ." ***** "
CONSOLE
;

```